THE UNIVERSITY OF
WARWICK

University of Warwick institutional repository: http://go.warwick.ac.uk/wrap

A Thesis Submitted for the Degree of PhD at the University of Warwick

http://go.warwick.ac.uk/wrap/62903

This thesis is made available online and is protected by original copyright.

Please scroll down to view the document itself.

Please refer to the repository record for this item for information to help you to cite it. Our policy information is available from the repository home page.

The effect of SUMOylation on DELLA proteins and abiotic stress responses in *Arabidopsis thaliana*

Ailidh Catherine Woodcock
BSc (Hons)

Thesis
Submitted to the University of Warwick
For the degree of
Doctor of Philosophy

Supervisors: Professor Richard Napier[1] and Dr Ari Sadanandom[2]
[1]School of Life Sciences, University of Warwick
[2]School of Biological and Biomedical Sciences, University of Durham

School of Life Sciences
May 2014

Contents

Acknowledgements

First and foremost I would like to thank my supervisors Dr Ari Sadanandom and Professor Richard Napier for their help and assistance during my PhD studies. Without their advice, flexibility, scientific knowledge and empathy I would not have made it this far. I would also like to thank all members of the Sadanandom and Napier research groups, past and present, for all the support they have given me. I would especially like to thank Dr Cunjin Zhang from the Sadanandom group for the technical advice and help he gave on many occasions, and Stuart Nelis also from the Sadanandom group for providing expressed and purified proteins for SPR work in chapter 5.

Second, I must say thank you to Dr Lucio Conti, for mentoring me through the early stages of this project and generously allowing me to work with him for a month in his lab. I appreciate the support of his research group, Dr Massimo Galbiati and all at the Fondiazione Filarete and University of Milan for their help during my time working there.

Thank you to the Department of Life Sciences at the University of Warwick for funding and supporting my research project.

I would like to acknowledge my advisory panel Dr Stephen Jackson, Dr Volkan Cevik and Dr Hendrik Schafer for their guidance and suggestions during my

research. In addition I would like to thank Dr Miriam Gifford for help with root analyses, Dr Christian Craddock and Dr Sarah Thornber for help with the early stages of confocal microscopy and later Ian Hands-Portman for further support, Dr Steve Footit and Charlotte Carroll for advice on germination and establishment assays, Dr Siobhan Talbott for critical reading of many of my pieces of writing and Dr Julie Jones for statistical support. I extend thanks to all those from horticultural services, controlled environment/glasshouse services, stores and the prep room who have supported this work and answered many of my stupid questions.

I could not have completed my research without the colleagues and friends I have worked alongside who I have celebrated with when experiments have gone well, talked to when they have not and had support from with both work and personal matters. These include the old HRI crew, whom I started my PhD with, and those in labs C30 and C10 whom I have become close to at Gibbet Hill. In addition, my friends outside of science have given me endless support both before and during my studies, for which I will be forever thankful.

I would like to thank Sean, who has been a very positive, understanding, and supportive influence in my life and research for the last 18 months, and whose encouragement has pushed me on to reach the finish line.

I do not think I could have reached this point without the support of my family. I complete my thesis with those of my family who are not with me today in mind,

and hope they would be proud. Thank you to my younger brother Liam for his inspiration in me writing my ‘essay’ and for bringing much humour into my life, and my Gran for her kindness, generosity and care, which I appreciate very deeply. Most of all I would like to thank my Mum, who has looked after and supported me through every endeavour and dream I have had. Her never-ending belief, support and love have been irreplaceable to me during the last 28 years.

I would like to dedicate this thesis to the memory of my father, Stephen Woodcock, whom I miss dearly every day.

Declaration

This thesis is presented in accordance with the regulations for the degree of Doctor of Philosophy. It has been composed by myself and has not been submitted in any previous application for any degree unless otherwise stated. The work presented in this thesis has been undertaken by myself, except where otherwise stated.

Abbreviations

A.thaliana – Arabidopsis thaliana

CAPS - Cleavage Amplified Polymorphic Sequences

D - aspartate

D8 – Dwarf 8

DNA – Deoxyribonucleic acid

E – glutamate

ECL – Enhanced Chemiluminescence

GA – Gibberellin/Gibberellic acid

GAI – Gibberellic acid-insensitive

GFP – Green fluorescent protein

GID1 – GA Insensitive Dwarf 1

GRAS – GAI, RGA and SCARECROW

IP - Immunoprecipitation

K or ^{K} – lysine

$^{K/R}$ – lysine to arginine mutation

NaCl – Sodium Chloride

O-GlcNAc - *O*-linked *N*-acetylglucosamine transferase

OTS – Overly Tolerant to Salt

p35S – Cauliflower Mosaic Virus 35S Promoter

PAC – Paclobutrazol

PCR – polymerase chain reaction

PEG – Polyethylene glycol

R - Arginine

RGA – Repressor of GA1-3

RGL – RGA-like

Rht – Reduced height

RNA – Ribonucleic acid

RT-PCR – reverse transcriptase polymerase chain reaction

SAE – SUMO-activating enzyme

SCE - SUMO-conjugating enzyme

SCF - Skp, Cullin, F-box-containing protein

SDS-PAGE – Sodium dodecyl sulphate polyacrylamide gel electrophoresis

SIM – SUMO binding motif

SLN – Slender

SLR – Slender rice

SLY – Sleepy

SPR – Surface Plasmon Resonance

SPY - Spindly

SUMO – Small Ubiquitin-like Modifier

Ub – Ubiquitin

Ubl – Ubiquitin-like protein

UIM – Ubiquitin interaction motif

ULP – Ubiquitin-like protease

X – any amino acid

Ψ – large hydrophobic amino acid

Abstract

Post-translational modifications are an essential process in all levels of eukaryotic life. Some of these post-translational modifications, such as Ubiquitination, have been researched in great detail whereas the process of SUMOylation was only discovered in the late 1990's and is less well understood. The DELLA repressors of plant elongation growth have been shown to undergo modification with both Ubiquitin and SUMO, and both the SUMOylation process and DELLA proteins have been linked to responses to abiotic stress in plants. In this project, putative SUMO sites on DELLA proteins RGA and GAI have been mutated to create transgenic lines in which each DELLA becomes non-SUMOylatable. While results for RGA overexpressing lines may require some further investigation, the results for GAI^{K} versus $GAI^{K/R}$ have proven very interesting. With reduced levels of SUMOylation ($GAI^{K/R}$), there is less restriction of growth in terms of bolting phenotype. In addition, SUMOylation of GAI was demonstrated to have an important role in abiotic stress responses, in terms of primary root growth in *Arabidopsis thaliana*. Binding data indicates interaction of SUMO with both RGA and GID1a, and although these interactions do not seem to be dependent on GA, they may have influence in preventing degradation of DELLA proteins. Analysis of OTS SUMO protease mutants demonstrates that SUMOylation and deSUMOylation through the OTS protease are necessary for the seed germination process in *Arabidopsis*, although only at moderate levels. The OTS protease is also demonstrated to have involvement in the seedling establishment process. Overall, this data further reinforces the assertion that SUMOylation is an essential process in plants, and that

SUMOylation of DELLA proteins, and many other proteins, is integral to their response to abiotic stress.

1 Introduction

1.1 Background

1.1.1 Protein Post-translational Modifications and their Context in Plants

All living organisms must react to the changing environment around them and in order to do this they have evolved rapid, efficient, and highly selective signalling processes. In plants, many signals are carried by the phytohormones, and of these gibberellins will be mentioned in detail. Phytohormone activity is translated by a number of mechanisms and amongst the most frequent and well known is post-translational modification of proteins.

There are numerous and diverse means by which the function of proteins are modulated. These include the regulation of protein levels through the management of expression levels and turnover, and the regulation of protein activity and interactions via post-translational modifications. These modifications are most commonly applied through enzymatic reactions (Melchior, 2000) and are essential to all eukaryotes. For example, it has been demonstrated that protein post-translational modifications alter the role of transcription factors by influencing their localisation, conformation and stability (Spoel, Tada & Loake, 2010). Indeed, they are a means to alter the function, activity and localisation of a wide range of proteins after synthesis (Müller *et al.*, 2001). These modifications are responsible for diversifying the proteome, in order to control complex regulatory processes

that are essential for eukaryotic cell function. Amongst the most widespread post-translational modifications is the addition of ubiquitin (Ub), as a consequence of which many proteins are targeted for breakdown in the proteasome. Protein modifications by ubiquitin and ubiquitin-like proteins (Ubls) are critical to a multitude of cellular and developmental processes and for the reactions to many stimuli such as that of hormones, pathogens and the environment (Miura & Hasegawa, 2010).

Of the ubiquitin-like proteins (Ubls), ubiquitin is the best known and has been extensively studied since its discovery in 1987 (Bonifacino & Weissman, 1998; Hershko & Ciechanover, 1998). It has been demonstrated to have numerous different functions in eukaryotic life, particularly in targeting protein substrates for proteasomal degradation (Konstantinova, Tsimokha & Mittenberg, 2008). The Ubls vary in size from 72 to 186 amino acids and all have a canonical structure known as the Ub fold, which is made up of one α-helix and four β-sheets (Hochstrasser, 2009; Kerscher, Felberbaum & Hochstrasser, 2006).

Small Ubiquitin-like Modifier, (SUMO) and the process of SUMOylation has only come to the fore of research in very recent years and while not as often found as Ubiquitination, it has great relevance in all eukaryotes.

1.1.2 SUMOylation

The process of SUMOylation is integral to all eukaryotes. In animals, research has shown it to be necessary in many cellular processes (Watts, 2007) and has a role to play in common human diseases (Sarge & Park-Sarge, 2009; Yang *et al.*, 2008). Many essential proteins including cofactors, chromatin-modifying enzymes and promoter-specific transcription factors have been found to be modified by SUMO (Gill, 2005). SUMOylation is involved in stress responses in neurones, where both SUMO conjugation to substrate proteins and levels of SUMO protease SENP-1 are found to be upregulated following oxygen and glucose deprivation (Cimarosti *et al.*, 2012). Change in patterns of SUMOylation are detectable in models of Alzheimer's disease (McMillan *et al.*, 2011), while SUMO modification is implicated in BRCA1 response to genotoxic stress, with mutations in *BRCA1* having connection with high risk of certain forms of cancer (Morris *et al.*, 2009).

In plants the story is similar, in that SUMOylation is found to be involved in many ways in the cell. This includes many stress responses (Elrouby & Coupland, 2010), and SUMO paralogues have been found to have functions in plant development and defence through salicylic acid-controlled defence responses (van den Burg *et al.*, 2010). Indeed, the SUMO E3 ligase SIZ1 confers regulation on salicylic acid-mediated innate immunity in *Arabidopsis*, and this same E3 ligase also has a role in a wide range of processes such as cell growth and plant development through salicylic acid (Miura & Hasegawa, 2010), phosphate deficiency responses (Miura et al., 2005) and gene regulation following drought stress (Catala et al., 2007). Control of flowering time in *Arabidopsis* is in part attributed to Early in Short Days 4

(ESD4), a SUMO protease (Reeves *et al.*, 2002; Murtas *et al.*, 2003). Genetic studies of SUMO conjugation mutants has shown that SUMOylation of proteins, and with SUMO1 and SUMO2 in particular, is essential for *Arabidopsis* viability, Indeed, where SUMO-activating and conjugating enzymes (SAE2 and SCE1) are missing in null mutants, embryo lethality is seen (Saracco *et al.*, 2007). Finally, increase in SUMOylation levels inhibit abscisic acid (ABA)-governed inhibition of growth and enhance the induction of ABA- and stress-responsive genes like *RD29A* (Lois, Lima & Chua, 2003).

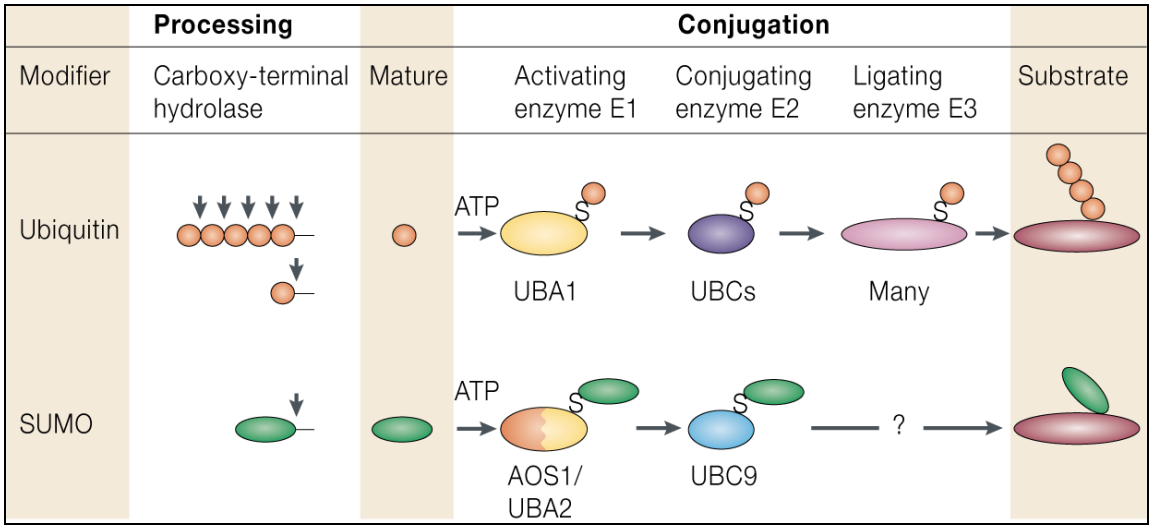

Figure 1-1 - Ubiquitin and SUMO are synthesised as precursors and processed by hydrolases/proteases (vertical arrows) to yield mature peptides. Ub and SUMO conjugation involves activating (E1) and conjugating (E2) enzymes that form thioesters (S) before ligation to target substrates by E3-type activities. Ubiquitination and SUMOylation are reversible, ATP-dependent processes (Geiss-Friedlander & Melchior, 2007). Taken from 'Sumo, ubiquitin's mysterious cousin' (Müller et al.*, 2001).*

While ubiquitination and SUMOylation have numerous similarities, there are also some clear differences (Figure 1-1). Like ubiquitin, SUMO is found in all eukaryotic kingdoms (Hanania *et al.*, 1999) and reputedly, both systems have common

ancestry, which may date back to ancient biosynthetic pathways of prokaryotes (Hochstrasser, 2000). SUMO is highly conserved in all species from yeast to humans (Müller *et al.*, 2001). SUMO and ubiquitin have approximately 18% sequence identity even though they do share similar 3D structures with the characteristic Ub fold (Bayer *et al.*, 1998) present in both.

SUMO has a number of paralogues in both humans and plants, with at least three in mammalian cells (SUMO1, 2, 3) and only one in *Saccharomyces cerevisiae* (Smt3) (Johnson, 2004; Kerscher, 2007). In humans, SUMO1 and SUMO2/3 seem to function with some distinction from each other, as they conjugate with differing substrates, and SUMO 2/3 have been demonstrated to have a role in SUMOylation in situations where proteins have become damaged, such as environmental stress (Saitoh & Hinchey, 2000). So far 8 SUMO isoforms have been identified in *Arabidopsis* (Kurepa *et al.*, 2003; Colby *et al.*, 2006), however only four of these have been identified thus far as having post-translational modification function, SUMO 1, 2, 3 and 5 (Colby *et al.*, 2006; Budhiraja *et al.*, 2009). Studies have shown that AtSUMO1 and AtSUMO2 are well conserved in sites on the SUMO protein governing E1-activating enzyme recognition, and E2-conjugating enzyme and SIM (SUMO interacting-motif) non-covalent interactions, where AtSUMO3 is less conserved, and AtSUMO5 shows the highest degree of divergence. In addition, AtSUMO1/2 are thought to be essential paralogues, as they are the most efficiently conjugated isoforms, with AtSUMO3 less efficiently conjugated, and AtSUMO5 even less so (Castaño-Miquel, Seguí & Lois, 2011).

SUMOylation has its own classes of E1 (activating), E2 (conjugating) and E3 (ligating) enzymes (Figure 1-2). However, during SUMOylation the E3 enzyme does not appear to be as important as in ubiquitination. SUMOylation can take place *in vitro* without any E3 enzyme activity, although the relevance of E3-independent ligation is yet to be identified (Geiss-Friedlander & Melchior, 2007). E3s seem to be a lot more important *in vivo* (Johnson, 2004) thus specificity might be dependent on the SUMO E3 ligases.

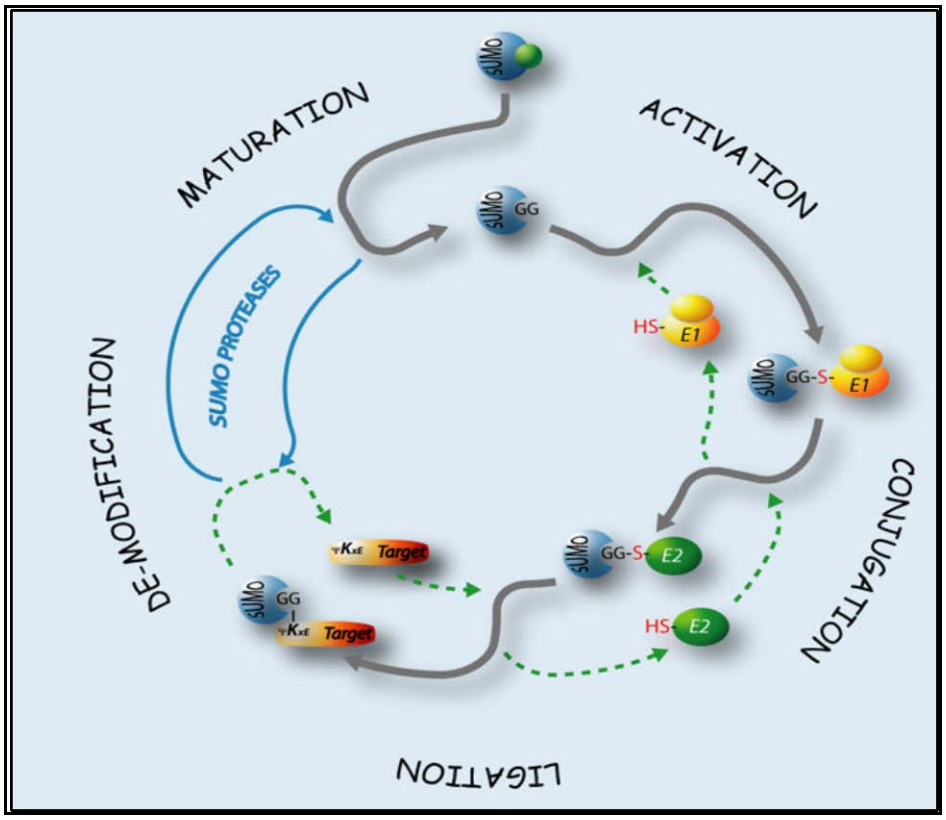

Figure 1-2 - The SUMOylation cycle. The different stages of the SUMOylation process (solid arrows) and recycling (dashed arrows) are shown. SUMO = Small Ubiquitin-Like Modifier, E1 = SUMO activating enzyme and E2 = SUMO conjugating enzyme. Taken from GAM1 and the SUMO pathway (Boggio & Chiocca, 2005).

SUMO is created from SUMO precursor proteins by cysteine-type SUMO peptidases, that target newly synthesised pro-SUMO, cleaving off a section to leave an active

SUMO protein (Johnson, 2004). These SUMO proteases (termed ubiquitin-like proteases or Ulp's) (Miura, Jin & Hasegawa, 2007) process precursor SUMO molecules at the C-terminal tail creating a mature SUMO with a Gly-Gly motif at the C-terminus (Dye & Schulman, 2007; Mukhopadhyay & Dasso, 2007). SUMO proteases are responsible for both the generation of mature SUMO and the cleavage of SUMO from protein targets at completion of the cycle (Miura & Hasegawa, 2010) (Figure 1-2). As SUMOylation is a reversible process, SUMO is cleaved from target proteins following completion of its function as a post-translational modification. Isopeptidase activity is used by the protease to elicit this recycling function (Miura, Jin & Hasegawa, 2007).

Following the cleavage to create mature SUMO the molecule is activated by SUMO-specific E1 activating enzymes, which catalyse ATP-dependent thioesterification of a cysteine residue in the E1 enzyme to SUMO (Johnson, 2004; Geiss-Friedlander & Melchior, 2007). The active SUMO molecule is subsequently moved from E1 to a C residue in the E2 conjugating enzyme by a transesterification reaction to create a SUMO-E2 complex (Johnson, 2004). Following this, SUMO is transferred onto a substrate protein by way of an isopeptide bond between the SUMO carboxyl-terminal G and the E amino group of lysine (K) in the SUMO consensus motif ΨKXE/D (Ψ, large hydrophobic residue; K, acceptor lysine; X, any amino acid; E/D, glutamate or aspartate) of the substrate (Miura *et al.*, 2007). By contrast, in the ubiquitination process, the consensus motif only consists of a lysine reside, (Peng *et al.*, 2003; Pickart & Fushman, 2004; Hochstrasser, 2006), allowing selectivity for these two separate post-translational modifications.

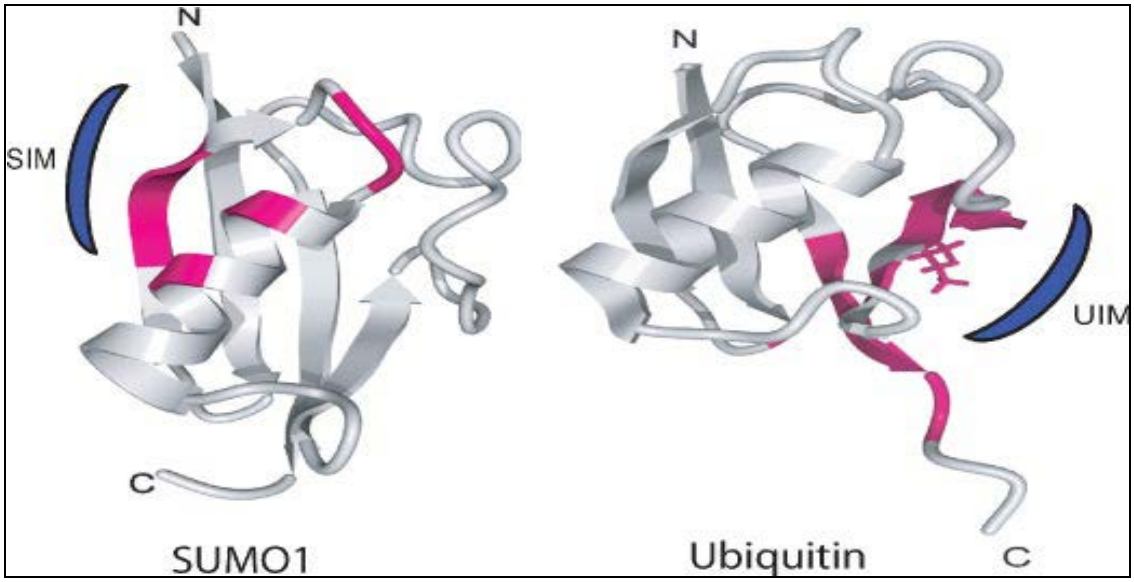

*Figure 1-3 - Comparison of the SIM-binding site on SUMO1 and the UIM-binding site on Ubiquitin. The SIM (*blue*) binds to an area specified to the second β-strand and the α-helix of SUMO, and by comparison the UIM (*blue*) binds to a group of amino acids of the third and fourth β-strands of Ub. The structures used in the figure are SUMO1 (Protein Data Bank accession code 1A5R) and UIM-Ubiquitin structure (Protein Data Bank accession code 1Q0W) (Swanson* et al.*, 2003). Adapted from (Hecker* et al.*, 2006).*

In addition to their being a consensus motif available on target proteins for either ubiquitin or SUMO, which is the point at which the molecule is attached onto the target, both of these molecules have specific sites at which they interact with a target protein, known as a ubiquitin interaction motif (UIM) or SUMO binding motif (SIM). More detail on SIM motifs is covered in 5.1, however, these are motifs that were first discovered a number of years ago (Minty *et al.*, 2000), and interact non-covalently with SUMO molecules. Either canonical or non-canonical SIM's are found in many proteins that interact with SUMO. The essential part of the SIM motif has since been found to be the hydrophobic core, often flanked by a group of negatively charged amino acid residues (Hannich *et al.*, 2005; Hecker *et al.*, 2006).

So far only few SIM's have been elucidated, whereas many UIM's have been

identified. The position at which the SUMO and ubiquitin molecules interact with these domains has been identified and marked on the secondary structure of the proteins (Figure 1-3) (Hecker *et al.*, 2006). SUMO-SIM recognition seems to be quite specific, based on the finding that while all SIMs found so far bind only to SUMO isoforms, and not to any ubiquitin or ubiquitin-like molecules, UIMs have been found to bind to the ubiquitin-like proteins NEDD8 and FAT10, although not to SUMO (Tanaka *et al.*, 2003; Hipp *et al.*, 2004; Hecker *et al.*, 2006).

In plants, SUMO is activated by SUMO-specific E1 activating enzymes (SAE1 and SAE2), and is transferred to SCE1 (SUMO E2 conjugating enzyme) to create a SUMO-SCE1 complex (Johnson, 2004), from where the SUMO is attached to the target protein. SUMO E3 ligases are yet to be properly investigated but are known to be SCE1-interacting proteins required for transfer of SUMO from SCE1 to the substrate protein *in vivo* (Johnson, 2004).

The fate of SUMOylated proteins is less well defined and some SUMO conjugates are recycled from the substrate protein by SUMO proteases (Mukhopadhyay & Dasso, 2007). Two specific SUMO proteases of particular interest in plants are Overly Tolerant to SALT1 (OTS1) and OTS2, which are localised to the nucleus and function redundantly to manage salt stress responses in *Arabidopsis* (Conti *et al.*, 2008). ESD4 is another SUMO protease which has been characterized and has an integral role in flowering in *Arabidopsis* (Reeves *et al.*, 2002; Murtas *et al.*, 2003).

1.1.3 DELLA proteins

The Green Revolution was a term coined due to the massive increases in global grain yields which began in the 1960s (Dyson, 1996; Conway, 1998; Evans, 1996; Gale, Youssefian & Russell, 1985). These increases were in part due to the introduction of new high-yielding varieties of wheat and rice into agriculture, twinned with the application of enhanced levels of fertilizers and pesticides (Hedden, 2003). This was in addition to new cultivation methods in agriculture (Peng *et al.*, 1999). Introduction of dwarfing genes into these varieties of cereal crops was integral to this revolution as the weightier grain of these new varieties led to plants becoming vulnerable and more prone to lodging in challenging weather conditions.

Norman Borlaug initiated the use of dwarfing genes in wheat, which provided the plants with a shorter, stronger stem that was more robust against lodging (Hedden, 2003) (*Figure 1-4*). These genes originated from Japan (Gale, Youssefian & Russell, 1985), and Norman Borlaug began their use after being sent the Norin 10-Brevor 14 cross from Japan, where it was bred with varieties of wheat tailored to grow in tropical and subtropical climates (Hedden, 2003). The Norin 10-Brevor 14 cross was the start of dwarfing genes used in many wheat cultivars appropriate to temperate climates, and the Norin 10 dwarfing genes exist in >70% of contemporary wheat cultivars in the world today (Evans, 1996). There were seen to be clear benefits to the use of dwarfing genes in partnership with high-yielding varieties of wheat and other crop plants, and most commercial varieties have now been bred selectively to include such genes. Indeed, these varieties of wheat are

able to allocate more energy toward grain yields rather than shoot elongation.

Figure 1-4 - Example of dwarfing alleles in use (left side) compared with wild-type wheat crops (right side) (Hedden, 2003).

The Norin 10 wheat cultivar contains two dwarfing genes, which are semi-dominant (change of function) alleles of homologous genes on two of the wheat chromosomes. These dwarfing genes are called *Rht-B1b* and *Rht-D1b* (Börner *et al.*, 1996). While there are numerous genes associated with a semi-dwarf growth habit in wheat (Ellis *et al.*, 2005) the most important are the *Reduced height (Rht*) genes. A large proportion of these genes are dominant/semi-dominant, and thus they actively inhibit growth. The *Rht–B1b* and *Rht–D1b alleles* are used in many commercial wheat varieties (Hedden, 2003). The wild-type alleles of *Rht–B1b* and *Rht–D1b* were isolated and demonstrated to encode putative transcription factors dubbed as DELLA proteins (Peng *et al.*, 1999). DELLA proteins are part of a subfamily of the GRAS (GAI, RGA and SCARECROW) family of transcriptional regulator proteins that have a part in regulating many facets of plant development

(Pysh *et al.*, 1999; Tian *et al.*, 2004). GRAS proteins are generally made up of between 400 and 770 amino acid residues and display substantial sequence homology to each other in their C-termini (Bolle, 2004) (Figure 1-5).

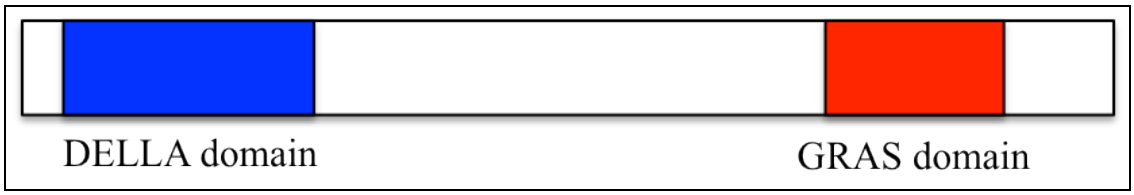

Figure 1-5 - Schematic of DELLA protein with N-terminal DELLA domain, conserved in the DELLA subfamily of GA response proteins but not found in all GRAS proteins, and the C-terminal GRAS domain. Not to scale.

The molecular basis for the dominant behaviour of DELLA's such as RhtB1b and RhtD1b, suggested by Peng et al. (1999) was that the dwarfing alleles each had a point mutation, or nucleotide substitution, that converted a codon into a translational stop codon in the DELLA domain of the protein (Figure 1-5). It is possible to speculate that the similarity of the mutations conferred in Rht-B1b and Rht-D1b are why they lead to comparable severities of dwarfism (Gale, Youssefian & Russell, 1985). Genetic analysis has shown that although both Rht-B1b and Rht-D1b confer a severely dwarf phenotype, they still produce active products (Gale & Marshall, 1976). One possibility for how this occurs is that the short N-terminal peptide fragments encoded by Rht-B1b and Rht-D1b result in plants with the mutant phenotype. A second possibility is that the process of ribosomal scanning after translational termination at the stop codon in Rht-B1b/Rht-D1b allows the translation process to restart at one of several downstream methionine residues that follow soon after the stop codon. This would lead to production of an N-

terminally truncated protein which demonstrates the mutant phenotype (Peng *et al.*, 1999). While neither of these possibilities has been experimentally validated, the latter suggestion seems to be more likely, considering that the D8-Mpl allele also encodes an N-terminally truncated product. Therefore, it seems to be the case that Rht-B1b and Rht-D1b, as with D8-Mpl, encode N-terminally truncated products that lack region I, one of the conserved regions among DELLA proteins (Peng *et al.*, 1999).

It has been demonstrated from work with *Arabidopsis* that in the scenario where the DELLA domain of the protein had been deleted, the protein accrued in the plant even following the application of gibberellins (GAs). In addition, the DELLA domain does not seem to be required for the growth-inhibiting activity of the protein, thus accumulation of mutant DELLA protein leads to plants to be dwarfed (Peng *et al.*, 1999; Hedden, 2003). Indeed, the DELLA domain is important for binding of GID1 and DELLA degradation, rather than transcriptional regulation (Willige *et al.*, 2007).

Following discovery of the DELLA proteins RhtB1b and RhtD1b in wheat, and implementation of their dwarfing effect on wheat crops, further DELLA proteins were discovered in other crop species. These have been covered further in Chapter 3 (3.1.1).

DELLAs are growth repressors. In *Arabidopsis* there are 5 different DELLA protein genes: Gibberellic Acid Insensitive (GAI), Repressor of GA1 – 3 (RGA), RGA – like 1 (RGL1), RGA – like 2 (RGL2) and RGA – like 3 (RGL3). These have been

demonstrated, with the exception of RGL3, to share partially overlapping functions in repressing GA-regulated plant growth and development (Thomas & Sun, 2004), although they do have some unique functions, such as RGL1, which is demonstrated to have a role in mediating GA-dependent germination of seeds, leaf expansion, flowering, and floral development (Wen & Chang, 2002), and RGL2, shown to have involvement in seed germination (Lee *et al.*, 2002). Overall there is a clear interplay between DELLA proteins and GA in order to regulate plant growth.

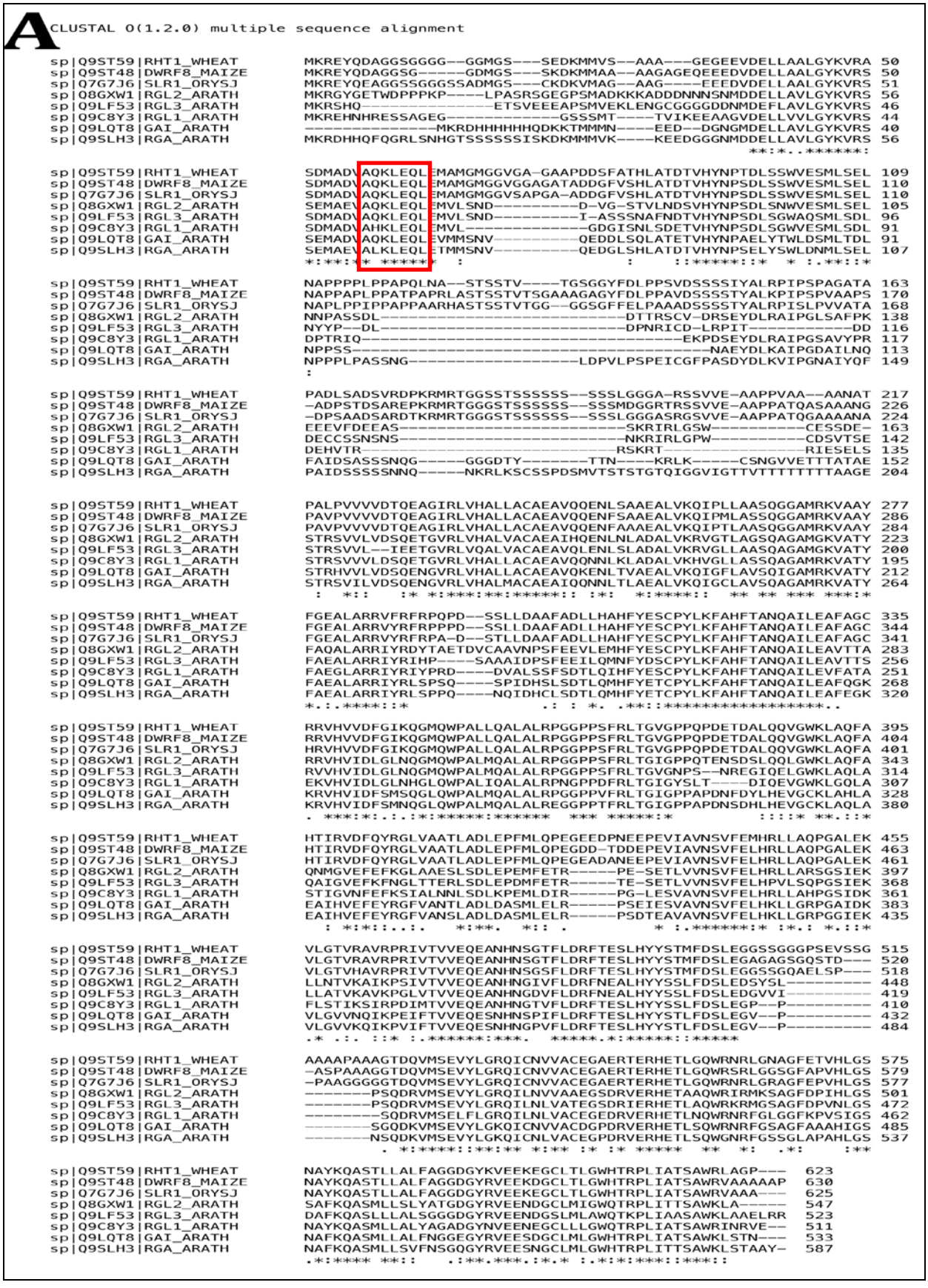
CLUSTAL O(1.2.0) multiple sequence alignment
sp|Q9ST59|RHT1_WHEAT
sp|Q9ST48|DWRF8_MAIZE
sp|Q7G7J6|SLR1_ORYSJ
sp|Q8GXW1|RGL2_ARATH
sp|Q9LF53|RGL3_ARATH
sp|Q9C8Y3|RGL1_ARATH
sp|Q9LQT8|GAI_ARATH
sp|Q9SLH3|RGA_ARATH

B

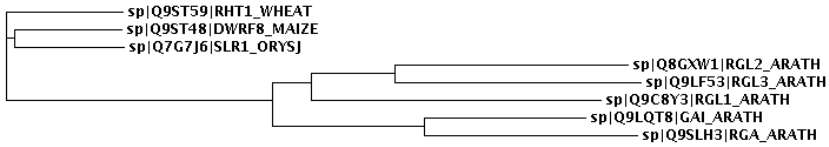

C

		% Sequence Identity							
DELLA Protein	Plant Species	RHT1	DWRF8 (D8)	SLR1	GAI	RGA	RGL1	RGL2	RGL3
RHT1	wheat	100	86.97	86.81	61.95	56.74	59.6	57.49	58.27
DWRF8 (D8)	maize	86.97	100	87.72	61.79	57.57	59.37	58.02	57.36
SLR1	rice	86.81	87.72	100	60.84	56.37	60.32	58.61	57.76
GAI	*Arabidopsis*	61.95	61.79	60.84	100	78.8	63.37	61.19	60.12
RGA	*Arabidopsis*	56.74	57.57	56.37	78.8	100	61.06	60.89	58.95
RGL1	*Arabidopsis*	59.6	59.37	60.32	63.37	61.06	100	65.81	64.66
RGL2	*Arabidopsis*	57.49	58.02	58.61	61.19	60.89	65.81	100	72.87
RGL3	*Arabidopsis*	58.27	57.36	57.76	60.12	58.95	64.66	72.87	100

Figure 1-6 – Protein alignment of DELLA proteins in both Arabidopsis and crop species. The actual alignment of full-length proteins is shown, with the consensus site of SUMOylation indicated by a red outline (A), a phylogram of the same proteins constructed using the neighbour-joining method (B) and a table showing % sequence identity between proteins (C) (Goujon et al.*, 2010; Sievers* et al.*, 2011).*

Comparison of the *Arabidopsis* DELLA proteins to DELLA's from crop species is important, so that we can to compare exactly how similar they are (Figure 1-6) with the consensus motif for SUMOylation marked by a red outline (Figure 1-6A). The most similar of the *Arabidopsis* proteins to wheat, rice and maize is GAI, which has the most orthology, measured by sequence identity to these crop species (Figure 1-6C). While RGA and GAI do have high levels of similarity, at 78.8%, and have shared divergence from crop species and RGL1, 2 and 3 on a phylogram

(Figure 1-6B) this analysis does show significant difference between the proteins. It may be the case that this difference in sequence identity could lead to divergent behavior of the proteins in *Arabidopsis* as is yet to be discovered. In addition, the GAI protein has greater similarity to crop species DELLA proteins in the consensus SUMOylation motif (ΨKXE/D) (Figure 1-7). All of these DELLA proteins have a lysine, leucine, and glutamic acid residue in the second, third and fourth positions of the motif. However, the first residue differs, with RGA having a leucine residue, with hydrophobic properties, where GAI, RGL2 and RGL3, and the crop DELLA proteins analysed have a glutamine residue with an amide group attached. These differences in the SUMO consensus motif could prove essential in the interactions of these DELLA proteins with SUMO and SUMOylation machinery.

DELLA proteins are degraded upon application of GA through the action of the Gibberellin Insensitive Dwarf (GID1)-GA complex (Dill et al., 2001). The interaction with this complex stimulates association with the SCF^{SLY1} complex, prompting attachment of ubiquitin to the DELLA protein and subsequent signalling for degradation. DELLA proteins are localized to the nucleus and their levels are quickly reduced following GA application (Silverstone *et al.*, 2001; Itoh *et al.*, 2002). Furthermore, the disappearance of DELLAs induced by GA requires a working 26S proteasome (Fu *et al.*, 2002).

Both GAI and RGA, like the Rht proteins, have had alleles discovered which are dominant mutations resistant to GA treatment. The *gai* and *rga-Δ17* alleles have similarity to the *Rht-B1* and *Rht-D1.* They are both lacking a stretch of amino acids

in the DELLA domain, making the proteins unable to be degraded, and therefore conferring a dominant mutation insensitive to gibberellin treatment (Koorneef *et al.*, 1985; Peng & Harberd, 1993; Peng *et al.*, 1997; Silverstone *et al.*, 2001).

Figure 1-7 – Alignment of Arabidopsis and non-Arabidopsis DELLA proteins in the consensus SUMOylation motif within the DELLA domain of the protein shows divergence in this site, when RGA is compared with both GAI, and DELLA proteins from crop species. RGA, GAI and RGL1, 2, and 3 from Arabidopsis; D8 from maize; SLR1 from rice; Rht-1 from wheat; and SLN1 from barley.

In terms of dwarf mutants, there were two major classes discovered (Figure 1-8); those whose phenotype can be restored by GA application (GA-sensitive), such as the gai-t6 mutant where the protein has the majority of the GRAS domain deleted and as a result is degraded (Peng *et al.*, 1997; Dill & Sun, 2001; Dill *et al.*, 2004) and those whose phenotype is not restored (GA-insensitive/resistant) such as the gai mutant, where deletion of the protein leads to the protein not being degraded by the proteasome (Koorneef *et al.*, 1985; Peng & Harberd, 1993; Peng *et al.*, 1997) and having an added repressive effect (Koornneef & Veen, 1980; Fujioka *et al.*, 1988; Wilson & Somerville, 1995). The second class represents the dominant

alleles of DELLA (Sun & Gubler, 2004).

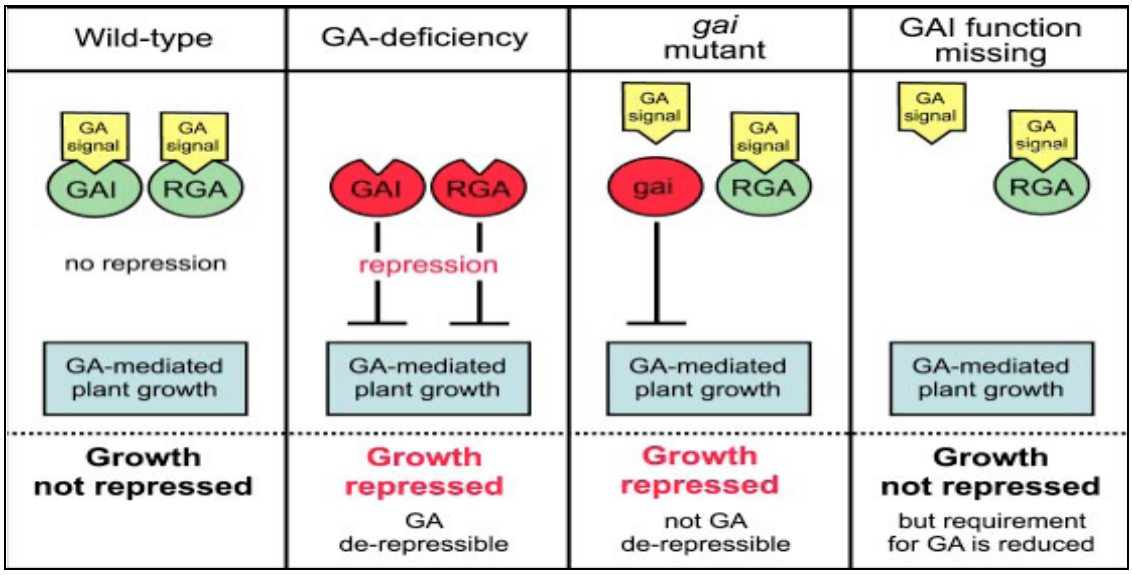

Figure 1-8 – Illustration of factors in interaction of GA and DELLA proteins. Including wild-type function, GA deficiency, gai mutant and lack of GAI function (i.e. gai-t6 mutant). Taken from (Richards et al.*, 2001).*

Further mutants affecting DELLA function are GA-deficiency mutants, which are repressed in growth as there is little or no GA produced by these mutants to give relief of repression (Figure 1-8). These mutants, such as the *ga1-3* mutant are reviewed further in 1.1.4 and Chapter 3 (3.1.1).

1.1.4 Gibberellins

The discovery of Gibberellins occurred in the early 20th Century, although what was described to have the characteristics of gibberellins was not named as such until the 1930's. In 1912, a researcher called Sawada published a paper in the Formosan Agricultural Review entitled "The Diseases of Crops in Taiwan". In this paper he proposed that elongation in rice seedlings infected with bakanae fungus could be as a result of a stimulus derived from fungal hyphae. Bakanae fungus was known to

cause a serious disease in rice named “foolish seedling disease” by Japanese farmers (Eckardt, 2002).

Following this, in the 1920’s it was noted that culture filtrates from dried rice seedlings conferred marked elongation in rice and other sub-tropical grasses, and that this was likely die to bakanae fungus secreting a chemical that which promoted shoot elongation, while suppressing root growth and preventing chlorophyll formation in parallel (Kurosawa, 1926). The bakanae fungus imperfect stage was named *Fusarium moniliforme* (Sheldon) and the perfect stage, *Gibberella fujikuroi* (Saw.) Wr. by the researcher H.W. Wollenweber.

Gibberellin itself was first isolated in Japan in the 1930s from the bakanae fungus. This followed work by the scientist Teijiro Yabuta to isolate the active component, that gave this effect of plant growth promotion, derived from fungal strains provided by his predecessor Kurosawa. A non-crystalline solid was obtained that stimulated the growth of rice seedlings. This compound was named gibberellin by Yabuta in 1935, which was the first use of the term "gibberellin" in the scientific literature (Yabuta, 1938).

Gibberellin or Gibberellic acid (GA) was later discovered to have an effect on shoot growth in pea seedlings in the 1950’s, elongating the stems of these plants (Brian & Hemming, 1955; Vlitos & Meudt, 1957). From this point a great deal of research has been carried out on gibberellins and today they are known to be a group of tetracyclic diterpenoid acids, which hormonally control a range of developmental processes in the plant life cycle and are essential to normal plant growth (Hooley,

1994; Yamaguchi, 2008). Studies have shown over 23 GA derivatives exist in *Arabidopsis thaliana* (Talon, Koornneef & Zeevaart, 1990; Derkx, Vermeer & Karssen, 1994) and over 130 in plant, fungal and bacterial species combined, but only few of these such as GA_1, GA_3 and GA_4 actively function biologically (MacMillan, 2001; Davies, 2004). The key structural feature that seems to be essential for GA function is 3β-hydroxlation. GA_4 is 3β-hydroxylated, and is a functioning GA, whereas its direct precursor GA_9, which is not 3β-hydroxylated, is not biologically active. In addition, 3β-hydroxylated GA can be inactivated by hydroxylation at the 2β position (ChandlerRobertson, 1999). These structural findings suggest that the interaction of GA with a receptor is likely to be highly specific (Richards *et al.*, 2001).

Study of GA biosynthesis mutants has revealed a lot about how GA's work as a group of phytohormones, and the interactions they are involved in to elicit their effects. GA deficient mutants including the *ga1-3* mutant in *Arabidopsis,* exhibit a classical dwarf phenotype, with bushier stature (reduced apical dominance) and darker green leaves, compared to wild-type plants. The *ga1-3* mutant also produces seeds which do not germinate, flowering in this mutant is delayed and flowers are male sterile (Koornneef & Veen, 1980; Zeevaart & Talon, 1992). Applying exogenous GA rescues all of these phenotypes (Koornneef & Veen, 1980). The *ga1-3* mutation is a sizeable loss, which prevents the function of the gene *GA1*, which encodes *ent*-CDP synthase, an enzyme that has a role in the early stages of GA

biosynthesis (Hedden & Kamiya, 1997; Koornneef & Veen, 1980; Sun, GoodmanAusubel, 1992; Sun & Kamiya, 1994; Zeevaart & Talon, 1992).

Endogenous GA levels can be enhanced or reduced, and doing this in plants leads to alterations in plant phenotype. GA signalling mutants have been identified that demonstrate these changes, but they are found to change the perception of GA, or GA signalling, instead of GA levels, leading to the mutant phenotype (Richards *et al.*, 2001). These mutants include the *gai* mutant in *Arabidopsis,* mutants similar to *gai* in DELLA proteins orthologous to GAI in other plant and crop species, and the loss-of-function *rga* allele, again in *Arabidopsis*.

SPY was the first GA signalling constituent to be cloned, and was discovered to be a product of the *SPINDLY* (*SPY*) gene of *Arabidopsis*. From investigations using knockout lines of *spy* it was discovered that *spy* was able to grown on concentrations of the GA biosynthesis inhibitor paclobutrazol (PAC) lethal to wild-type plants, and that these plants, when grown on no treatment looked like wild-type plants treated with exogenous GA (Jacobsen & Olszewski, 1993). Later SPY was shown to be a tetratricopeptide repeat (TPR) protein, with the TPR motif likely to be important in protein-protein interactions. SPY was also found to have homology to *O*-linked *N*-acetylglucosamine (*O*-GlcNAc) transferases (Jacobsen, Binkowski & Olszewski, 1996; Robertson *et al.*, 1998), which in animals have a function in signal transduction pathways in the dynamic modification of proteins, akin to protein phosphorylation (Hart, 1997; Hart *et al.*, 1989; Kreppel, Blomberg &

Hart, 1997). More recent analysis has shown SPY to be an *O*-GlcNAc transferase (Thornton *et al.*, 1999).

In *Arabidopsis*, GA lifts the repression on its signalling pathway imposed by DELLA proteins by provoking proteolysis of DELLA proteins such as RGA (Silverstone *et al.*, 2001). *SLEEPY 1* (*SLY1*) encodes an F-box inclusive protein, and the loss-of-function sly1 mutant is insensitive to GA and exhibits a dwarf phenotype (Steber, Cooney & McCourt, 1998; Sasaki *et al.*, 2003). This mutant is shown to accumulate a high quantity of RGA (McGinnis *et al.*, 2003; Sasaki *et al.*, 2003). Molecular studies have found that SLY1 interacts directly with RGA and GAI via the DELLA proteins C-terminal GRAS domain, and providing a model whereby SCF^{SLY1} targets these two DELLA proteins for degradation (Dill *et al.*, 2004).

GA has involvement and control in a wide range of developmental processes. GA's moderate the production of α-amylase by the cereal aleurone, providing nutrients that sustain the growing seedling. In this process GA regulates gene transcription of α-amylase, and secretion of this hydrolase from the aleurone cells (Zwar & Chandler, 1995). GA also plays major roles in floral induction (Langridge, 1957; Wilson, Heckman & Somerville, 1992) and seed germination (Peng & Harberd, 2002).

GID1 is the receptor of GA, and has three homologues in *Arabidopsis*; GID1a, GID1b and GID1c. All of these homologues are demonstrated to bind to GA, form stable

complexes with GA and demonstrate an overlap in function in regards to GA signalling (Griffiths *et al.*, 2006; Willige *et al.*, 2007). This overlap in function is reinforced by research showing that while single and double *gid1a*, *gid1b* and *gid1c* mutants have little or no effect on germination capability (Willige *et al.*, 2007), the *gid1a gid1b gid1c* mutant translates enhanced seed dormancy or lead to total lack of germination (Willige *et al.*, 2007). The GID1 protein has been shown to reduce DELLA repressors of GA signalling through proteolysis-dependent and independent mechanisms (Ariizumi *et al.*, 2008; Ueguchi-Tanaka *et al.*, 2008).

1.1.5 Gibberellin control of DELLAs

DELLA proteins are nuclear-localised transcriptional regulators, that regulate expression of GA-responsive genes (Silverstone, Ciampaglio & Sun, 1998). In interplay with GA, DELLA proteins are degraded in response to GA (McGinnis et al., 2003; Sasaki et al., 2003).

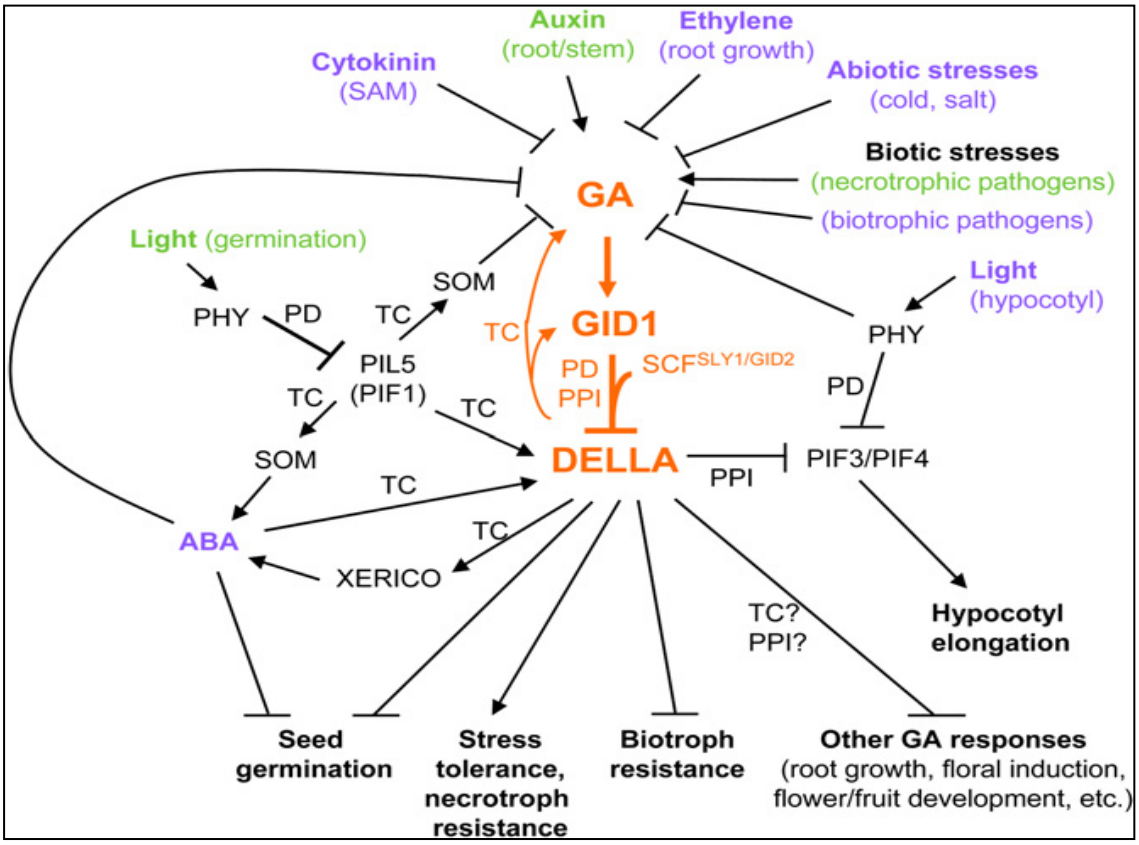

Figure 1-9 – Signalling network surrounding the interaction between DELLA proteins and the Gibberellin/GID1 signalling pathway. The GA-GID1-DELLA regulatory unit is seen in orange. Signals enhancing bioactive GA accumulation are labeled in green, and in contrast signals that reduce GA levels are highlighted in purple. Activation/ inhibition are possible by different modes of action. PD - Protein degradation; PPI - protein-protein interaction; TC - transcription; SAM - shoot apical meristem; PHY - PHYTOCHROME; SOM - SOMNUS. Taken from (Sun, 2010).

The central components of GA signalling are the growth-repressing DELLAs, and their interaction with gibberellin and GID1. However, this interaction and negative feedback mechanism is the central part of a very complex signaling network with many internal and external cues and outputs (*Figure 1-9*) (Sun, 2010). Their activity is mainly regulated at the post-translational level by changes in the level of

GA (Harberd, 2003). GA in turn negatively regulates DELLA proteins by binding to them via the GA receptor GID1. This leads to DELLA proteins interacting with the SLEEPY1 (SLY1) F-Box subunit of the SCF^{SLY1} E3 ubiquitin ligase complex (Ariizumi *et al.*, 2008) and becoming ubiquitinated. The result is degradation of DELLAs by the 26S proteasome and increased plant growth in the absence of DELLA proteins (Fu *et al.*, 2002) (Figure 1-10). This relief-of restraint effect whereby GA regulates DELLAs and thus promotes plant growth was proposed as a model by the Harberd laboratory (Harberd, 2003).

For an example of the interplay between GA and DELLA, it is seen that GA mediates the development and fertility of *Arabidopsis* flowers, and does this by contrasting the function of DELLA proteins RGA, RGL1 and RGL2 (Cheng *et al.*, 2004). DELLA proteins and GA are also observed to regulate seed development (Tyler *et al.*, 2004a).

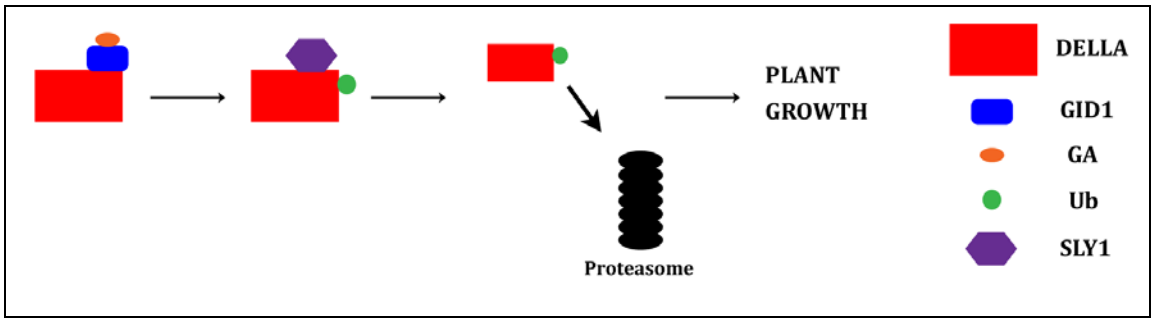

Figure 1-10 - Known mechanism by which DELLA proteins and Gibberellin (GA) interplay to regulate plant growth. DELLAs interact with GA via the GA receptor GID1 (Gibberellin Insensitive Dwarf 1) and are subsequently ubiquitinated by SLY1, the subunit of SCF^{SLY1}, leading to degradation of DELLAs and the promotion of plant growth/relief of growth repression.

1.1.6 SUMO, DELLAs, Environmental Stress and the OTS SUMO Proteases

The Sadanandom laboratory has discovered that a proportion of the cellular pool of DELLAs is SUMOylated *in vivo* (Conti *et al.*, 2014). Although DELLAs were earlier identified as being centrally involved in the GA signalling pathways, more recent publications have also identified DELLAs to be integral to plant growth and survival under stress, including cold, salt and pathogen stresses (Achard *et al.*, 2006; 2008a; Navarro *et al.*, 2008). This could be due to the fact that GA is highly modulated by the environment. Thus, changes in DELLAs in response to the environment are exerted via changes in GAs. Other explanations are possible, and the role of SUMOylation in DELLA function merits further investigation.

For example, mutant *Arabidopsis* plants deficient in 4 of 5 DELLAs are found to be less restricted in growth than wild-type plants when exposed to moderate salt stress. Nevertheless, these mutants die in extreme salt stress suggesting that the growth restraint implemented by functional DELLAs supports survival in high salinity by extending the vegetative growth phase (Achard *et al.*, 2006) and upregulating antioxidant defenses (Achard *et al.*, 2008b). Thus, it is clear that regulating DELLA function confers an advantage to plants and facilitates adaptable and suitable modulation of growth in reply to alterations in the environment.

The Sadanandom group has also demonstrated *ots1 ots2* double mutants are salt sensitive (Conti *et al.*, 2008) and that DELLA proteins are hyper-SUMOylated in the double mutant (Conti *et al.*, 2014) perhaps because these double mutants do not have the capacity to cleave SUMO off DELLAs. In wild-type plants, DELLA

SUMOylation as well as non-SUMOylated DELLAs increases rapidly in response to GA deficiency induced by paclobutrazol (PAC) treatment. It has been shown that the salt sensitive *ots1 ots2* double mutants exhibit hypersensitivity to the GA biosynthesis inhibitor PAC and this sensitivity can be reversed by application of GA, showing that this effect is DELLA dependent (Conti *et al.*, 2014). The data collected so far demonstrates that OTS1/2 SUMO protease activity and DELLA SUMOylation are functionally linked.

1.2 Hypothesis

These observations have facilitated the development of a model, which shows the compensatory roles of SUMO and Ub in DELLA function (*Figure 1-11*). By this model, SUMOylated DELLA stabilizes non SUMOylated DELLA by binding to and titrating away the GID1 and SCF^{SLY1} complexes. This would lead to less non-SUMOylated DELLA being degraded. What is intriguing is that the abundance of SUMOylated DELLA seems to follow the abundance of non-SUMOylated DELLA and it is not known which of the two forms of DELLA might be causal to the levels of the other, or whether they cycle with each other in terms of quantity. This would fit with the model that SUMOylated DELLA stabilizes non SUMOylated DELLA. While SUMOylated DELLA could interact with the SCF complex it is also degraded by ubiquitination, like non SUMOylated DELLA, so SUMO and ubiquitin are not in direct competition with each other for the fate of DELLA proteins. However this does not preclude the possibility that SUMOylated DELLA undergoes deSUMOylation before degradation. Nevertheless, from previous work (Conti *et al.*,

2014) it is clear that SUMO may directly disrupt the life cycle of DELLA, and it is essential to find out if this happens and why it happens.

As referred to above, the DELLA proteins GAI and RGA have different levels of protein sequence similarity to non-*Arabidopsis* crop DELLA's (Figure 1-6), and also have variation in their SUMOylation motif (Figure 1-7), therefore, it is important to carry out investigations of both of these proteins to allow assessment of integral DELLA proteins which are involved in a wide scope of growth and developmental functions in *Arabidopsis thaliana*.

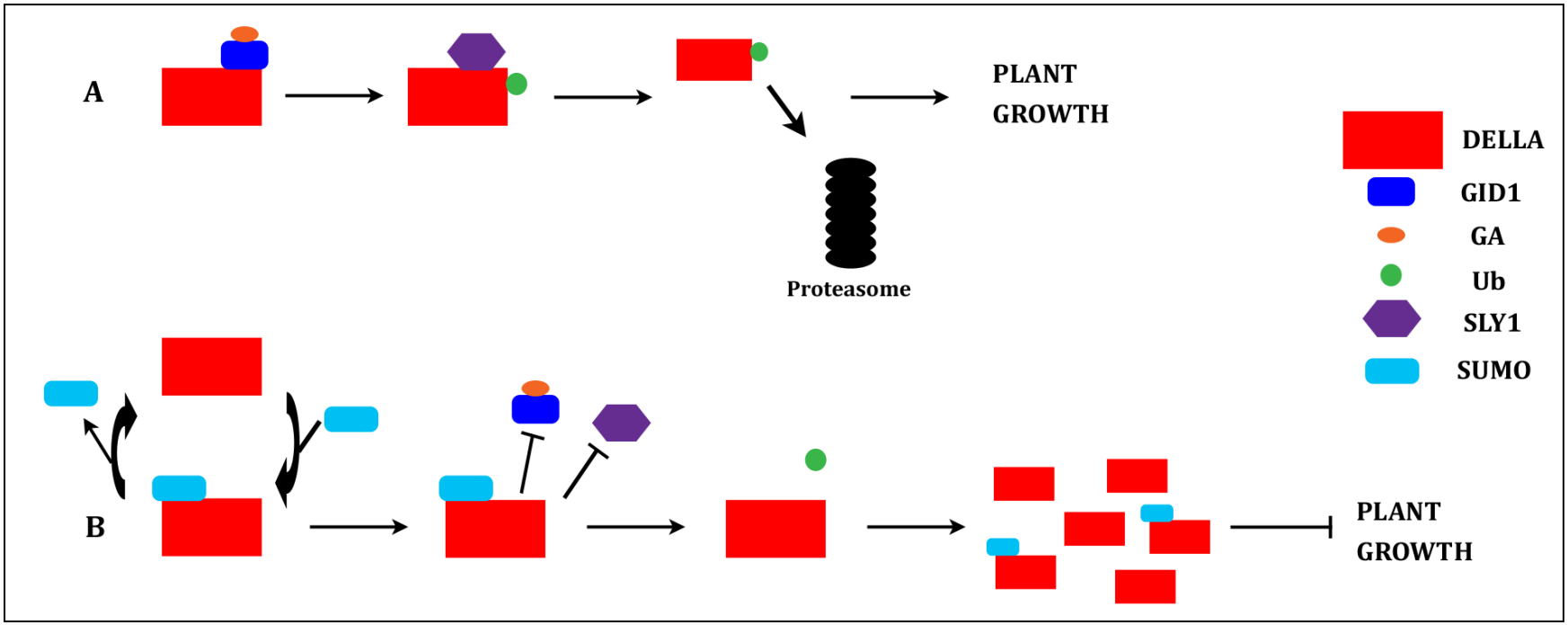

*Figure 1-11 - Proposed model of SUMOylated DELLA function. (A) Canonical DELLA degradation model (*Figure 1-10*) and (B) Mutants where the OTS SUMO protease has been knocked-out or PAC treatment causes SUMOylated DELLA levels to rise and this acts to stabilize non-SUMOylated DELLAs by binding and titrating away either GID1 or SLY1 or both. This antagonizes ubiquitinated turnover of non-SUMOylated DELLAs. Consequently non-SUMOylated DELLAs accumulate co-comitantly with SUMOylated DELLA and this leads to increased growth repression* (Conti *et al.*, 2014).

1.3 Aims

- To investigate the interaction of SUMO (via SUMOylation) with the Arabidopsis DELLA proteins RGA and GAI
- To analyse the connection between SUMOylation with abiotic stress, via the OTS protease, and of SUMOylation of DELLA proteins with abiotic stress
- To elucidate the binding interactions of the components of the GID1/GA/DELLA/SUMO signalling pathway.

2 Methods

2.1 General Plant Methods

2.1.1 Organism and Seed Ecotype

Arabidopsis thaliana ecotypes *Columbia-0* (Col-0) or *Landsberg erecta* (L-er) were used as appropriate. Wild-type seeds of these ecotypes and all other seed lines required were obtained from the National Arabidopsis Stock Centre (NASC) in Nottingham.

Table 2-1 - Vectors used to create Constructs for transformation of Arabidopsis thaliana

Vector	Features	Antibiotic Selection	Herbicide Selection	Genes cloned	Reference
pENTR/D-TOPO	None	Kanamycin	N/A	All	Invitrogen
pGBPGWG	35S promoter, GFP (C-terminal)	Kanamycin, Chloramphenicol	Glufosinate ammonium	RGA, RGAK65R, GAI, GAIK49R	Zhong et al. 2008
pLCG1/ntapi.289	35S promoter, TAP (N-terminal)	Chloramphenicol, Spectinomycin	Glufosinate ammonium	OTS1	Rohila el al. 2004

2.1.2 Constructs for Plant Transformation

All constructs were prepared by initial cloning of the gene of interest into the pENTR/D-TOPO plasmid to create an entry clone, followed by LR recombination into the vectors of choice (Table 2-1) for transformation into *Arabidopsis thaliana*. A full description of the cloning process can be found in 2.3.4.

Table 2-2 - Designed constructs used for transformation into Arabidopsis thaliana plants. p35S = 35S promoter, GFP = Green Fluorescent Protein, OTS = Overly Tolerant to Salt, K = lysine, R = arginine, RGA = Repressor of GA1-3, GAI = Gibberellic Acid Insensitive, Col0 = Columbia 0.

Construct	Background	Germplasm
p35S:RGA-GFP	Columbia	Col-0
p35S:RGA$^{K/R}$-GFP	Columbia	Col-0
p35S:GAI-GFP	Columbia	Col-0
p35S:GAI$^{K/R}$-GFP	Columbia	Col-0
p35S:GFP	Columbia	Col-0
p35S:NTAP-OTS1	Columbia	Col-0
p35S:NTAP	Columbia	Col-0
ots1-1/2-1	Columbia	Col-0

Potential sites of SUMOylation on *Arabidopsis thaliana* RGA and GAI were identified using knowledge of the known consensus motif for SUMOylation of a protein (ΨKXE/D) and using the web programme SUMOsp (Xue et al., 2006). The proteins were then aligned with non-*Arabidopsis* DELLA proteins to identify SUMOylation motifs conserved across DELLA proteins in a wide range of plant species (*Figure 1-6*, *Figure 1-7*). Following this, as a proof of concept the SUMOylation motif identified on the RGA protein was confirmed using an *in-*

vitro SUMOylation system in *E.coli (Okada* et al*., 2009)*, demonstrating that where the consensus motif was mutated, their was a disappearance of SUMOylation of the RGA protein *(Conti* et al*., 2014)*.

The $^{K/R}$ Mutant constructs (*Table 2-2*) were prepared initially by site-directed mutagenesis of the pGBPGWG plasmid (Table 2-1) (Zhong et al., 2008), an adaptation of the pGreen plasmid (Hellens et al., 2000), containing the relevant DELLA to mutagenise the bases representing either lysine 65 for an arginine (RGA) or lysine 49 for an arginine (GAI). Transformations were carried out in the Col-0 backgrounds. These pGreen constructs are fusions of DELLA genes RGA and GAI to a C-terminal GFP tag under the control of the constitutive 35S promoter. The GFP fusion was made to facilitate the detection and localisation of the fusion protein as well as its efficient immunoprecipitation. For the OTS overexpressors, the transformation was with the ntapi.289 plasmid (Table 2-1) (*Figure 2-1*) (Rohila et al., 2004) with an insert of the OTS gene and including a constitutive 35S promoter and n-terminal TAP tag (*Table 2-2*).

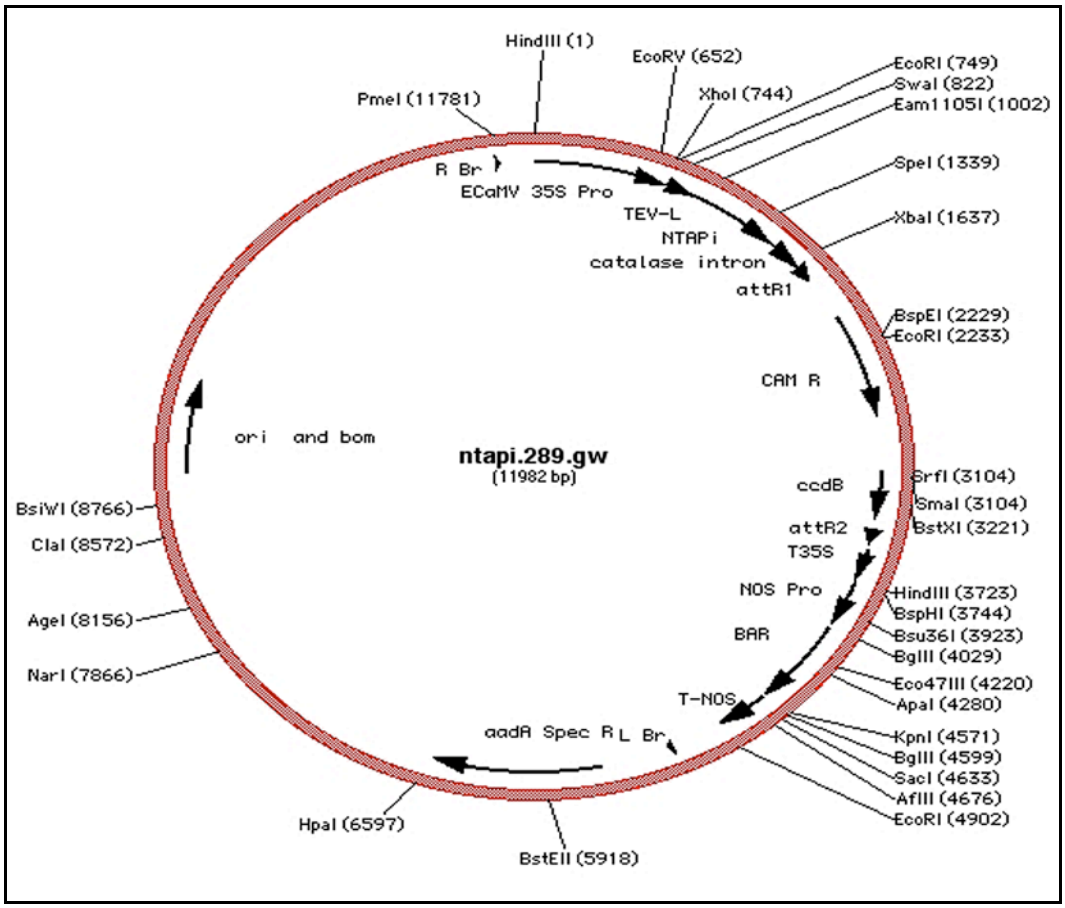

Figure 2-1 - The ntapi.289 vector used for design of the 35S-TAP:OTS1 construct.

2.1.3 Transformation of wild type *Arabidopsis thaliana* with *Agrobacterium*

Transformation was carried out by Lucio Conti of the Sadanandom research group using a protocol from Clough and Bent (Clough & Bent, 1998) for floral dipping. 200 ml of LB media containing the appropriate antibiotics was inoculated with *Agrobacterium tumefaciens* Strain GV3101 transformed with the appropriate construct and grown for 2 days at 28°C. The culture was centrifuged and the pellet resuspend in 5 % sucrose to an OD_{600} 0.8. Silwet L-77 was added to a concentration of 0.05 % and mixed well. Flowering *Arabidopsis* had the primary inflorescence cut off and the secondary inflorescence stems were immersed in the solution at bud break (4 weeks old). Plants were returned

to normal growth conditions and covered by a dome for 1 day. *Arabidopsis* plants were dipped again as above one week after the initial dipping.

The T1 generation seeds were grown on glufosinate ammonium (20μg/ml) to identify T1 plants that had at least one copy of the relevant transgene. After the transformation process and this initial selection in the T1 stage I received the T2 seeds from Cunjin Zhang of the Sadanandom research group.

These T2 seeds were subsequently plated on glufosinate ammonium at the same concentration and the ratio of sick:healthy plants used to select lines that were segregating for the transgene. Healthy seedlings were noted as having light/dark green cotyledons and seedling growth comparable to the negative control seedlings grown without any treatment. By comparison, sick seedlings had pale yellow/white, opaque cotyledons, and were stunted in growth. Some T2 plants, either homozygous or hemizygous for the transgene, were transferred to soil. From these plants, T3 seeds were kept to establish whether the transgene was in a homozygous/hemizygous state and to collect tissue samples to test for transgene-derived expression using RT-PCR and western blotting.

2.1.4 Seed Storage

Seeds were stored in eppendorf tubes at room temperature in the dark, having been dried overnight at 37^{o}C prior to storage.

2.1.5 Seed Sterilisation, Treatment and Vernalisation

Seed sterilisation was carried out using vapour-phase sterilisation method, sterilising approximately 20µg seed per eppendorf tube. 3ml 37% hydrochloric acid was added to 100ml sodium hypochlorite in a beaker in an airtight box, all carried out in a fume hood for 3-4 hours. Following sterilisation, seeds were left to aerate for 10 minutes in a flow hood before being plated on media.

Seeds were plated on ½ strength MSO (2.15g/l Murashige & Skoog medium-Duchefa), 0.5% sucrose, 1% agar pH5.8. For selection of transgenic seed lines, glufosinate ammonium at a final concentration of 20µg/ml was used, with *Columbia-0* as a negative control seed line. Plates were subsequently stratified at 4^{o}C for 48 hours to achieve uniform germination, and then placed in controlled environment conditions, at 22^{o}C in constant light.

2.1.6 Seedling Growth on Soil

Seedlings were transferred to soil after 7-14 days. Following this they were grown up for phenotyping (2.2.1) or for bulking up of seed stocks. Once on soil seeds or seedlings were grown in glasshouse conditions, at 22^{o}C, in long day (16 hours light, 8 hours dark) with 400W bulbs and no humidity control. Plants were grown in Levingtons F2 compost containing 6 parts compost, 1 part sand and 1 part vermiculite.

2.1.7 Seed Collection

Following bolting, plants were put into aracons/bags and allowed to flower. After flowering was complete and the siliques had begun to yellow, water was withheld and the plants allowed to dry out. Individual dried plants were cut from the rosette, placed in labelled bags and left for 3-4 days in a dark, dry environment at room temperature, before being threshed and seeds stored in eppendorf tubes.

2.2 Plant Phenotyping and Stress Assays

2.2.1 Phenotyping Parameters

Several rounds of phenotypic analysis of the T2 and T3 generations were completed in either controlled environments or glasshouse conditions. This included seedling observations such as zygosity scoring (using glufosinate ammonium), and growth on high salt (100mM sodium chloride), Gibberellin (100μM) and Paclobutrazol (0.5μM) to observe the stimulated phenotype, confocal imaging of transgenic lines containing the GFP-linked DELLA protein and scoring of bolting/flowering. Phenotypes were compared to the known/expected phenotypes for specific transgenes. This work was combined with assays such as RT-PCR and Western blotting to check if the observed phenotypes correlated with a biochemical difference in gene/protein levels.

OTS overexpressing lines were analysed by zygosity scoring with glufosinate ammonium, growth on high salt, and using stress-inducing assays; germination

under osmotic stress (0 to -0.8MPa pressure with PEG 8000), establishment under osmotic stress (0-600mM mannitol) and drought stress.

2.2.1.1 Statistical Analysis

Where necessary, randomisation of plants for phenotyping, and data analysis using Genstat were performed (Payne, Harding & Murray, 2008).

The aim of statistical analysis was to identify significance to attach to the data collected. Due to the data being normal and because we wanted to analyse the variance and means, we used one-way Analysis of variance (ANOVA) statistical test. Factors used in the analysis were always the line, and in some cases treatment. The analysis involved checking the values of least significant difference, degrees of freedom, residuals and residual plots, and if the distribution of data was not normal, data was transformed with a natural log transformation (stated where required).

In the case of the germination assay used (2.2.4), non-linear regression analysis was required to estimate parameters attributed to a curve in the data. The logistic equation (sigmoidal function):

$$\% = A+C/(1+\exp(-B(t-M)))$$

Following identification of values for parameters C, A+C, B and M; attributable to each individual germination event of a seed line at all replicates of each treatment, they were used for further statistical analysis with ANOVA.

2.2.2 Bolting Scoring

Scoring of the bolting phenotype of *Arabidopsis* mutant plants included recording the number of days for the plant to bolt, the rosette diameter of the plant at bolting, the number of vegetative leaves at bolting and measurement of plant height at weekly intervals. For these purposes, bolting was defined as an inflorescence stem of 1cm or greater.

2.2.3 Root Phenotyping

Seeds were suspended in 0.1% agarose and 10-15 seeds applied onto each square petri dish in a straight line at the top of the petri dish using a pipette to assist in handing seeds. Seeds were stratified at 4^{o}C for 48 hours and then plates arranged vertically in constant light. Scans of the plates were taken at 7, 10, 14 and 21 days using an HP office scanner and the images analysed using ImageJ software, obtained from the National Institute of Health (USA) website (www. http://rsb.info.nih.gov).

2.2.4 Germination Assay

Sterilised seeds were resuspended in distilled water. Germination boxes (12cm x 7.5cm) were arranged with a filter paper (Whatman) on the bottom. This filter paper was soaked in 5ml of distilled water and a nylon mesh (Clarcor UK) of 125µm placed on top. Seeds were pipetted onto each mesh in a 10 x 5 arrangement. Lids were placed on the boxes and put into the incubator at 4^{o}C for 3 days, with constant light.

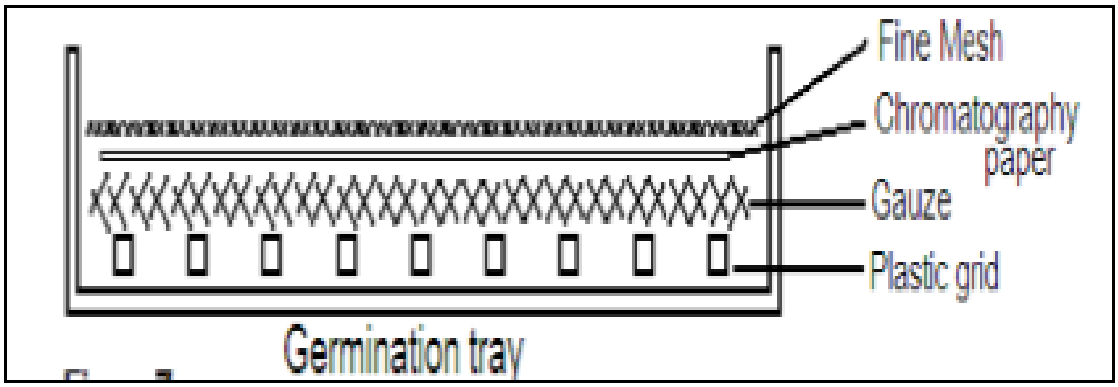

Figure 2-2- Germination box set-up following cold-treatment. The order of layers from the top is: - fine mesh, chromatography (filter) paper, gauze and plastic grid in the germination tray.

Following cold treatment, mesh/filter paper layers were carefully removed from the boxes and transferred to another box, prepared with a gauze layer and plastic grid (Figure 2-2). Variable concentrations of polyethylene glycol (PEG) were made related to the weight of PEG 8000 in g 400^{-1} determined using the required formula ($\Psi = 1.29[PEG]^2T - 140[PEG]^2 - 4.0[PEG]$), where Ψ = water potential and T = temperature in Celsius (Table 2-3) (Michel, 1983). 25ml PEG solution was pipetted into duplicate boxes. Boxes were placed in constant light at 15^{o}C for approximately 20 days, or until the majority of seeds had germinated. Germination was scored once per day, with germination defined as the emergence of radicle from the seed coat (Müller, Tintelnot & Leubner-Metzger, 2006).

Table 2-3 - Gradient of Water Potential and Equivalent Weight of Polyethylene Glycol (PEG) 8000 in 400g^{-1} volume (Michel, 1983)

Nominal Water Potential (MPa)	Polyethylene Glycol 8000 (g)
0	0
-0.2	45.3
-0.4	66.5
-0.6	82.8
-0.8	96.6

After scoring germination under stress, non-homozygous lines were moved onto ½ MSO plates with glufosinate ammonium selection, in constant light, for 7 days, and seedlings survival status recorded. Where not all seeds had germinated by the end of the stress experiment, the seeds were moved onto ½ MSO media plates in constant light with no ammonium glufosinate for 3 days in order to identify non-germinants from non-viable seed, and then moved onto plates with 20µg/ml ammonium glufosinate subsequently. Non-viable seeds were not included in experimental analysis.

2.2.5 Establishment Assay

Seeds from OTS overexpressing lines and controls were suspended in 0.1% agarose solution and applied to mesh strips on ½ MS media plates. Following cold treatment (4^{o}C) for 48 hours, seeds were allowed to germinate for 3 days in constant light before the mesh strips were transferred onto ½ MS media plates with 0, 100, 200, 300, 400 or 600mM mannitol and returned to constant light. Scans were taken at regular intervals up to a period of 28 days, and results

analysed with Image J software, obtained from the National Institute of Health (USA) website (www. http://rsb.info.nih.gov).

2.3 Molecular Biology and Biochemistry

2.3.1 RNA Extraction, DNase Treatment and RT-PCR

RNA extraction from *Arabidopsis* used the Spectrum Plant Total RNA Method (Sigma-Aldrich). Plant tissue (maximum 100mg) was ground under liquid nitrogen, using a 1.5ml Dremel 3000 rotary tool workstation (Dremel) and lysis buffer including 2-mercaptoethanol added. The samples were vortexed and then incubated at 56^{o}C for 5 minutes to lyse plant cells. Cellular debris was removed by centrifugation and then the resulting lysate filtered. The resultant RNA was bound onto a column and impurities and residual genomic DNA washed from the column before the RNA sample was eluted.

From the extracted RNA, analysis of total RNA was carried out with a Nanodrop ND-1000 Spectophotometer (Nanodrop Instruments, Software version 3.6.0) measuring at 260nm for nucleic acid, and 280nm to assess the level of protein contamination. Following calculation, 1µg RNA was treated with DNAse I (Fermentas – Dnase I, RNAse-free) for 30 minutes at 37^{o}C. The reaction was terminated by heating at 65^{o}C for 10 minutes, after the addition of 50mM EDTA. RNA samples were checked for the presence of any remaining genomic DNA using PCR with primers for actin and running the products on agarose gel electrophoresis. 0.5µg of the RNA samples was used for the reverse-transcription polymerase chain reaction (RT-PCR) using SuperScript First-

Strand Synthesis System for RT-PCR (Invitrogen). The PCR reaction was carried out using the desired cycle in a DNA Engine Tetrad 2 (MJ Research).

PCR products were analysed using agarose gel electrophoresis, using a 1% agarose gel made with 1 x TAE buffer (40mM Tris-acetate, 1mM EDTA pH8.3) and 1x SYBR safe DNA gel stain (Invitrogen), run at 100 Volts for 30 minutes.

2.3.2 Genomic DNA Extraction

Genomic DNA was extracted using the Qiagen DNeasy Plant Mini Kit, which is a silica-based DNA purification method. Plant tissue (maximum 100mg) was ground under liquid nitrogen using a 1.5ml Dremel 3000 rotary tool workstation (Dremel) and then chemically lysed using lysis buffer including 1mg/ml RNase A to digest RNA, at 65^{o}C. Following termination of the RNAse activity, cell debris, proteins and polysaccharides were removed and the sample homogenised by centrifugation through a column. DNA was then bound onto a spin column where genomic DNA is selectively bound to a silica membrane. Further contaminants were removed through centrifugation, and purified DNA eluted.

2.3.3 PCR

The DNA for PCR was obtained following genomic DNA extraction (2.3.5). PCR reactions were set up using 2 x Reddymix PCR mastermix with 1.5mM MgCl2 (Thermo Scientific). The reactions were carried out in 20µl volume, as described in the protocol for the 2 x Reddymix. The PCR reaction sequence was altered

dependent on the primers used (Table 2-4), as detailed, however the standard PCR cycle was – 95°C for 5 minutes (initialisation), 95°C for 1 minute (denaturation), 60°C for 1 minute (annealing), 72°C for 1 minute (elongation), 29 further cycles of denaturation, annealing then elongation, and then final elongation at 72°C for 10 minutes. The PCR reaction was carried out using the desired cycle in a DNA Engine Tetrad 2 (MJ Research).

PCR products were analysed using agarose gel electrophoresis, using a 1% agarose gel made with 1 x TAE buffer (40mM Tris-acetate, 1mM EDTA pH8.3) and 1x SYBR safe DNA gel stain (Invitrogen), run at 100 Volts for 30 minutes. Images of the banding pattern on the agarose gel were captured using the SynGene imager (SynGene G:Box, with GeneSnap for SynGene software) on the transilluminator setting with variable exposure time dependent on the level of gene expression.

Table 2-4 – Primer pairs used for PCR, RT-PCR and CAPS marker analysis

Gene of Interest	F Primer	R Primer	Details	Additional cycle details
RGA	CCGTCGGAGCTTTATTCTTG	TCGTTCCTATGACTCCACCA	RT-PCR	2 rounds of PCR of 25 cycles (using 1µl of product from round 1 for second round)
GAI	CACCATGAAGAGAGATCATCATCATCATC	CTAATTGGTGGAGAGTTTCCAAGC	RT-PCR	2 rounds of PCR of 25 cycles (using 1µl of product from round 1 for second round), 2 min extension time
GFP	GACGTAAACGGCCACAAGTT	GAACTCCAGCAGGACCATGT	RT-PCR	35 cycles
Actin	GTTGGGATGAACCAGAAGGA	CTTACAATTTCCCGCTCTGC	RT-PCR	
RGA	CACCATGAAGAGAGATCATCACC	AGTATCCGTCGCGAGATGAG	CAPS Sequencing	annealing temperature 55^{o}C, 35 cycles
GAI	CACCATGAAGAGAGATCATCATC	CTCCGCCGGATTATAGTGAA	CAPS Sequencing	annealing temperature 55^{o}C, 35 cycles

2.3.4 Cloning, Ligation and Transformation

Cloning was carried out using Gateway Cloning Technology (Invitrogen), following isolation of the relevant DNA insert amplified by PCR and ligation into the entry vector pENTR/D-TOPO (Table 2-5), to form an entry clone. Following formation of an entry clone, sequencing was carried out to ensure that cloning had been carried out successfully. The LR reaction allowed the DNA insert to be moved from entry clone to destination vectors (pDEST15 or pDEST17), shown in Table 2-5. In order to do this, the enzyme LR Clonase II was used to catalyse in vitro recombination reaction in TE buffer (10mM Tris-HCl 1mM EDTA pH8.0) between an entry clone containing the gene of interest, which was flanked by sticky attL sites, that match up with the sticky attR sites of the destination vector.

This was followed by transformation of the vector into either Dh5α (initial cloning) or BL21-AI (protein expression) *Escherichia coli* cells using heat-shock at 42^{o}C for 30 seconds and then growth in nutrient-rich S.O.C medium in an orbital incubator at 220rpm at 37^{o}C for 1 hour. Successful transformants were selected by overnight growth on Luria-Bertani (LB) agar plates with the antibiotic appropriate for selection (Table 2-5).

Table 2-5 - Vectors for Cloning and Protein Expression

Vector	Tag	Supplier	Antibiotic Selection	Genes cloned
pDEST15	GST	Invitrogen	Ampicillin 100µg/ml	GID1a
pDEST17	6 x His	Invitrogen	Ampicillin 100µg/ml	RGA, SUMO1, SUMO3
pENTR/D-TOPO	None	Invitrogen	Kanamycin 50µg/ml	All

2.3.5 Protein Expression and Purification

Proteins were expressed by growing a 5ml overnight culture, set up with 5ml Luria-Bertani (LB) broth. To this broth, a stab of the relevant glycerol stock was added (vector with insert in BL21 AI cells) (pre-prepared using 820µl of an overnight culture and 180µl of an 80% glycerol solution, flash-frozen in liquid nitrogen and stored at -80^{o}C) along with the antibiotic required for the vector being used (Table 2-5). This culture was grown in a New Brunswick Scientific (Innova 44) orbital incubator overnight at 37^{o}C at 220rpm.

The subsequent day, part of the culture was diluted 1:100 in LB broth and relevant antibiotic for protein expression. The culture was grown up at 37^{o}C in a New Brunswick Scientific (Innova 44) orbital incubator at 220rpm to an optical density (OD) between 0.5 and 0.7, at a wavelength of 595nm. The OD was tested once per hour, until it was over 0.2, after which it was tested every 20-30 minutes. Following growth to OD>0.5, protein expression was induced by addition of IPTG (0.1mM) and arabinose (0.2%) for 3 hours at 37^{o}C, or overnight at 16^{o}C.

Following expression, cultures were transferred to centrifuge tubes and spun down at 5000rpm for 20 minutes, supernatant discarded and pellets frozen at -20°C.

1ml aliquots were taken before induction and upon completion as pre- and post-induction. These were prepared for analysis for analysis by SDS-PAGE by being spun for 1 minute at 13000rpm and the supernatant discarded. A total protein extract sample was prepared with 30µl distilled water and 10µl 4x SDS loading dye. Soluble and insoluble protein was obtained by adding 50µl Bugbuster (Novagen) and vortexing every 5 minutes for 15 minutes. The sample was then centrifuged 1 minute at 13000rpm. To the supernatant, 16.67µl 4x SDS loading dye was added, and to the pellet 30µl distilled water and 10µl 4x SDS loading dye were added. The total, insoluble and soluble samples were heated at 95°C before being loaded onto a gel for SDS-PAGE.

Proteins were purified using fast protein liquid chromatography (FPLC) with an AKTA system (GE Healthcare). Prior to FPLC protein was extracted by applying 1ml Bugbuster (Novagen) to each pellet and vortexing every 5 minutes for 15 minutes. Protein was applied to a HisTrap HP 1ml nickel column (GE Healthcare) with 1 x TBS pH8, and detected by collecting fractions where a peak in absorbance was evident at 280nm, following application of Imidazole at a gradient up to 200mM (1 x TBS 200mM Imidazole pH8). Following FPLC, the protein fractions of interest were applied to a gel for SDS-PAGE analysis to confirm the presence of pure protein at the correct molecular weight.

2.3.6 CAPS Marker Analysis

Sequencing of *Arabidopsis thaliana* lines, both from seed and seedling material, began with extraction of genomic DNA (2.3.2). PCR was carried out with primers for CAPS sequencing (Table 2-4) to amplify up the relevant DNA fragments. PCR products were cleaned up using a PCR purification kit (Qiagen), and then, following quantification using a Nanodrop ND-1000 Spectrophotometer (Nanodrop Instruments, Software version 3.6.0) measuring at 260nm for nucleic acid, and 280nm to assess the level of protein contamination, 1µg/µl PCR product digested with HinfI (10U/µl) (Promega) for 4 hours. Following this, products were analysed using a 2.5% agarose gel, made with 1 x TAE buffer (40mM Tris-acetate, 1mM EDTA pH8.3) and 1 x SYBR Safe DNA gel stain (Invitrogen), run at 100V for 2-3 hours.

2.3.7 Protein Extraction

Protein extraction from *Arabidopsis* tissue samples was achieved obtaining *Arabidopsis* total protein extracts (Martinez-Garcia et al., 1999), using leaf tissue ground under liquid nitrogen. The extraction buffer was: 125mM Tris-HCl, 1% (w/v) SDS (sodium dodecyl sulphate), 10% (v/v) glycerol, 50mM sodium metabisulfite, pH 8.8 and a protease inhibitor tablet (cOmplete, Mini, EDTA-free Protease Inhibitor Cocktail Tablets - Roche) per 10ml of buffer. After clarification by centrifugation the protein was quantified using a Bradford assay (Sigma). Equal protein was loaded in all samples.

2.3.8 Sodium Dodecyl Sulphate Polyacrylamide Gel Electrophoresis (SDS-PAGE)

Samples for SDS-PAGE were prepared in 4x SDS buffer and heated at 95^{o}C for 10 minutes. The Acrylamide percentage was based on the molecular weight of the protein(s) of interest. The apparatus used was the Invitrogen NuPAGE system, with Bis-Tris 4-12% gradient gels and 1x MES running buffer (50mM MES, 50mM Tris, 0.1% SDS, 1mM EDTA, pH7.3) made up for the gel tank fresh from a 10x stock. Alternatively protein samples were frozen at -20^{o}C to be used at a later time.

2.3.9 Western Blotting

For western blotting, proteins separated on a Bis-Tris protein gel were transferred onto a PVDF membrane overnight at 25 Volts, using Biorad Western blot system, in Transfer buffer (25mM Bicine, 25mM Bis-Tris, 1mM EDTA, 0.05mM Chlorobutanol, 10% methanol).

Table 2-6 - Primary antibodies utilised in Western Blotting

Antibody	Details	Dilution	Supplier
anti-GST	Rabbit polyclonal	1/5000	Sigma
anti-His	Mouse monoclonal	1/2000	Millipore
anti-SUMO1	Rabbit polyclonal	1/10000	Agrisera
anti-SUMO3	Rabbit polyclonal	1/10000	Agrisera
anti-GFP	Rabbit polyclonal	1/5000	AbCam
anti-RGA	Sheep	1/5000	Agrisera
anti-GAI	Sheep	1/5000	Agrisera

Following transfer, the membrane was washed in 15 ml 1 x phosphate buffered saline (137mM NaCl, 2.7mM KCl, 10mM Na_2HPO_4, 1.8mM KH_2PO_4 pH7.4) and 0.1% Tween 20 (PBST) pH 7.3, for approximately 5 minutes. The membrane was blocked with 20ml 5% dried milk powder in 1 x PBST for one hour then incubated with the primary antibody at a dilution appropriate for the antibody (Table 2-6) in 1% milk in 1 x PBST for 1 hour. After three washes in 1 x PBST the secondary antibody (Table 2-7) was incubated in 1% milk in 1 x PBST for 1 hour before three washes in 1x PBST.

Table 2-7 - Secondary antibodies utilised in Western Blotting

Antibody	Details	Dilution	Supplier
anti-Rabbit	IgG HRP conjugate	1/10000	Promega
anti-Sheep	IgG Peroxidase produced in Donkey	1/15000	Sigma
anti-Mouse	HRP conjugate raised in Goat	1/10000	Novagen

This was the initial method used for Western Blotting, however this method was modified depending on the protein of interest, in terms of antibody and block concentrations and times for different stages of the protocol.

2.3.10 Enhanced Chemiluminescence (ECL)

To develop the PVDF membrane following western blotting protocol, the ECL method was used, where the secondary antibody in western blotting includes a horseradish peroxidase enzyme, which reacts with ECL solutions applied onto the PVDF membrane, leading to light being emitted in proximity to the HRP enzyme, which is tethered to the protein of interest on the membrane through the primary and secondary antibody. Equal quantities of the two ECL reagents (GE Healthcare) were mixed and applied to the PVDF membrane for one minute. Excess liquid was taken off the membrane and it was placed in an X-ray film cassette for an appropriate exposure time. Development was carried out using a Hyperprocessor (AGFA Curix 60).

2.3.11 Protein Extraction and Immunoprecipitation

Arabidopsis seedlings between 5-7 days old, from the T3 generation, were weighed and then frozen in liquid nitrogen. Seedling material was ground in a pestle and mortar under liquid nitrogen and extraction buffer (50mM NaCl, 1% Tween 20, 0.5% sodium deoxycholate, 0.1% SDS, 50mM Tris HCl (pH 8.0), 1mM EDTA, 10mM NEM and protease inhibitor cocktail (NEM and protease inhibitor (cOmplete, Mini, EDTA-free Protease Inhibitor Cocktail Tablets - Roche) freshly added) added followed by homogenisation of the sample. The resulting

homogenate was filtered through a layer of miracloth, clarified by centrifugation and the supernatant recovered. A reference total protein sample was collected from each extract. Following a protein assay around 3-4mg of protein was added for each immunoprecipitation.

Immunoprecipitation (IP) followed the Miltenyi method using magnetic beads (Miltenyi Biotech). Magnetic beads and protein sample were incubated together for approximately 45 minutes on ice. After this, the mixture was applied to a Miltenyi column and allowed to flow through. The column was washed several times to remove any debris and non-affinity tagged proteins. Bound protein was then eluted using a hot elution 2 x SDS buffer for SDS-PAGE/Western blotting analysis.

2.3.12 SUMOylation Assay

Carrying out a SUMOylation assay is a modified protocol originating from Protein extraction and Immunoprecipitation (2.3.11). Within the extraction protocol, a greater quantity of seedling material was required, approximately 500mg. There was the addition of MG132 (Sigma) into the extraction buffer at a final concentration of 10μM. The Miltenyi beads used for the Immunoprecipitation were α-GFP beads. Within the Western blotting protocol, the SUMO1 antibody, and relevant secondary antibody are used at described dilutions (2.3.9). A second membrane was exposed to an anti-GFP or anti-RGA/GAI antibody to confirm the presence of the transgene corresponding to the SUMOylation pattern.

2.3.13 Binding Assays of Protein Interaction

Binding assays were carried out with Glutathione Sepharose 4B Beads (GE Healthcare) using the GID1a receptor and SUMO1, with GID1a-GST (SLY1-GST and GST alone were used as controls) and SUMO1-His. Increasing concentrations of GA, from 0-100μM (0μM, 1μM, 10μM and 100μM) were used as appropriate. The Glutathione beads were equilibrated using 1 x Binding buffer (50mM Tris pH7.5, 0.15M NaCl, 1mM DTT, 0.1% Triton). The purified GID1-GST (10μg/ml) (bait) and other controls were then applied onto samples of the equilibrated beads and left overnight at 4^{o}C.

The following day, beads were washed three times with binding buffer and the SUMO1 (20μg/ml) and GA were added in appropriate concentrations and mixtures were incubated at room temperature on a rotormixer for 1.5 hours. The bead mixtures were then washed a further three times with binding buffer before 2 x SDS loading dye was added to them for analysis by SDS-PAGE/western blotting.

2.3.14 Surface Plasmon Resonance (SPR)

SPR was carried out with a Biacore 2000 machine (GE Healthcare) using a CM5 Sensor CHIP (GE Healthcare) with four channels. The software for this work was BIACORE 2000 control software for main operations and BIAevaluation for data analysis. Proteins for this process were obtained from Stuart Nelis (Sadanandom group, University of Durham).

Previous data for GID1a-GST indicated that the preferred buffer for coupling to the CHIP was 10mM sodium acetate pH5.5. pH scouting was carried out using SUMO1-His and RGA-His proteins (40µg/ml) in 10mM sodium acetate buffers between pH 3.5-5.5. 50mM NaOH (pH10) was used for regeneration of the CHIP surface.

GID1a-GST 25µg/ml, GST 55µg/ml, SUMO1-His 25µg/ml and RGA-His 20µg/ml in 10mM sodium acetate buffer (pH determined by pH scouting) were coupled at a flow rate of 5µl/min for 10 minutes using 0.4M 1-ethyl-3-(3-dimethylaminopropyl)carbodiimide hydrochloride (EDC) and 0.1M N-hydroxysuccinimide (NHS). Ethanolamine (pH8.5) was used to block remaining sites.

Two different buffers were used, HBS-EP buffer (GE healthcare) (0.01M HEPES pH7.4, 0.15M NaCl, 3mM EDTA, 0.005% v/v Surfactant P20) with 1mM DTT, or 25mM phosphate (sodium) pH7 0.005% Surfactant P20 (Hecker et al., 2006). Analysis was carried out using the 'direct binding' method in the application wizard. Proteins were injected for 3 minutes at a flow rate of 20µl/min. Regeneration of the CHIP following each cycle of binding analysis was 10mM glycine-HCl pH2.2.

2.4 Imaging

2.4.1 Confocal Microscopy and Gibberellin Treatment

Microscopy was carried out using 5-10 day old transgenic *Arabidopsis* seedlings from the T3 generation, using both the cotyledon and root tissues in different experiments. Seedlings were grown on ½ MS Media (2.15g/l MS, 1% Agar, 0.5% Sucrose) with 0.1µM Paclobutrazol (PAC).

Seedlings being treated with Gibberellin (GA) were sprayed with 100mM GA in 70% Ethanol and left for 3 hours prior to microscopy. Control seedlings were treated with 70% Ethanol.

Transgenic *Arabidopsis* leaves and root tissue were mounted for microscopy in water under glass coverslips. The tissue samples were examined using a Zeiss LSM 710 laser-microscope. The Argon laser excitation wavelength was 488 nm, and EGFP emission was detected with the filter set for FITC (505–530 nm). Images were taken at 400x magnification using a water immersion lens. The fluorescence of the images was assessed using the Zeiss Zen 2009 software.

3 Phenotypic and Genotypic Characterisation of GAI^{K} and $GAI^{K/R}$ overexpression lines

3.1 Introduction

3.1.1 DELLA Proteins and GAI

GIBBERELLIN INSENSITIVE (GAI) was discovered through studying the dwarf mutant line *gai* present in *Arabidopsis thaliana* (Koorneef *et al.*, 1985). The *gai* allele has similarity to the *Rht-B1* and *Rht-D1* reduced height varieties of wheat discovered in the 'Green Revolution' (Dyson, 1996; Conway, 1998; Evans, 1996; Gale, Youssefian & Russell, 1985), which present decreased GA sensitivity and lower height than wild-type plants. Cloning of the *gai* allele has shown that it differs from the wild-type *GAI* gene by a 17 amino acid in-frame deletion toward the N-terminus in the DELLA domain of the GAI protein (Peng & Harberd, 1993; Peng *et al.*, 1997). The semi-dwarf phenotype and diminished GA response (Figure 3-1) was not rescued by GA treatment (Koorneef *et al.*, 1985). The semi-dominant *gai* mutation, converts the GAI protein into a constitutive repressor of plant growth (Hussain & Peng, 2003) (Figure 3-4).

Figure 3-1 – Plants with the gai allele demonstrate a dwarf phenotype compared to the wild-type GAI. From left to right: - GAI/GAI (homozygous), gai/GAI (heterozygous), and gai/gai (homozygous) plants segregating in the progeny of a self-pollinated gai/GAI plant (Peng & Harberd, 1993).

Following further study, it has become clear that the *gai* allele is not gibberellin-insensitive, however plants with this allele have elevated levels of bioactive GA's, as the lack of GAI degradation leads to GA production via a feedback loop. As GAI in the form of the gai allele is not being broken down, the plants with this allele are dwarf (Koorneef *et al.*, 1985; Talon, Koornneef & Zeevaart, 1990). The *gai/ga1-1* mutant has a more severe dwarf phenotype than *gai,* due to the presence of the other DELLA proteins in the mutant. This mutant can be partially rescued by addition of exogenous GA to produce a semi-dwarf phenotype (Koorneef *et al.*, 1985).

Another mutant allele of GAI, the transposon-tagged null allele line *gai-t6*, helped elucidate the function and importance of the GAI protein in plant growth

regulation (Figure 3-2). This mutant exhibits a wild-type phenotype, with lower endogenous GA levels (Peng *et al.*, 1997), and early flowering due to a shorter juvenile phase (Dill & Sun, 2001). This mutant has the same 17 amino acid deletion from the N-terminal of the GAI protein as in the *gai* allele, and a Ds transposon insertion resulting in a C-terminal deletion in the GRAS domain (Dill *et al.*, 2004).These features lead to the knockout of the GAI gene in the gai-t6 mutant, meaning that it exhibits a wild-type phenotype as it lacks GAI but still has the other DELLA proteins functioning. The characteristics of the *gai* and *gai-t6* alleles indicate that GAI is a negative regulator of gibberellin in plant growth (Peng & Harberd, 1993; Wilson & Somerville, 1995; Peng *et al.*, 1997).

Figure 3-2 - The gai-t6 mutant contains a transposon that results in a null-allele. From left to right – homozygous GAI, gai and gai-t6. GAI and gai-t6 display a phenotype that is taller, while the gai plant is severely repressed in growth. The lack of a functional DELLA domain in gai leads to accumulation of GAI and repression of growth. In gai-t6 the DELLA domain is also faulty but the insertion in the GRAS domain renders the protein inactive, hence full growth (Peng et al.*, 1997).*

Despite belief that GAI was a regulator of GA response, lack of phenotype in the *gai-t6* mutant implicated another gene functioning alongside *GAI*. Indeed, shortly after *GAI,* a gene first assigned as *GRS* (GAI RELATED SEQUENCE) was

reported as a repressor of the *ga1-3* phenotype and renamed *RGA* (REPRESSOR OF ga1-3) (Peng *et al.*, 1997; Silverstone, Ciampaglio & Sun, 1998).

Figure 3-3 - Loss of GAI and RGA function reduces the reliance on GA for stem elongation. Image demonstrating some of the different mutant backgrounds used to elucidate gibberellin and DELLA protein function in Arabidopsis. Plants from left to right: - ga1-3; gai-t6 ga1-3; rga-24 ga1-3; gai-t6 rga-24 ga1-3; and wild type (Col0). Plants were grown for 57 days in standard greenhouse conditions (King, Moritz & Harberd, 2001).

An *Arabidopsis* mutant lacking a GA biosynthetic enzyme (*GA1*), *ga1-3,* results in very low endogenous gibberellin and a phenotype of severe dwarfism, dark green leaves, non-germinant seeds, decreased apical dominance and male sterility (Koornneef & Veen, 1980). Although these phenotypes are extreme, they can be rescued by application of exogenous GA. Studies of double mutants of *ga1-3* with either DELLA null-allele have found that while *rga-24* inhibits many elements of the *ga1-3* phenotype, the *gai-t6* allele has lower suppression (King, Moritz & Harberd, 2001; Dill & Sun, 2001). However, the triple mutant *gai-t6 rga-24 ga1-3* exhibits a GA-overdose phenotype (Figure 3-3), with full rescue of both late flowering and restricted elongation growth, and even early

flowering in mutant plants (Dill & Sun, 2001; King, Moritz & Harberd, 2001; Cheng *et al.*, 2004). The lack of both RGA and GAI de-represses the GA response and over-compensates for the absence of *GA1*. This suggests that RGA and GAI are the main repressors of GA responses, and have a role in negative feedback regulation of the biosynthesis of GA, through association with *GA1* (Dill & Sun, 2001) as demonstrated in Figure 3-4.

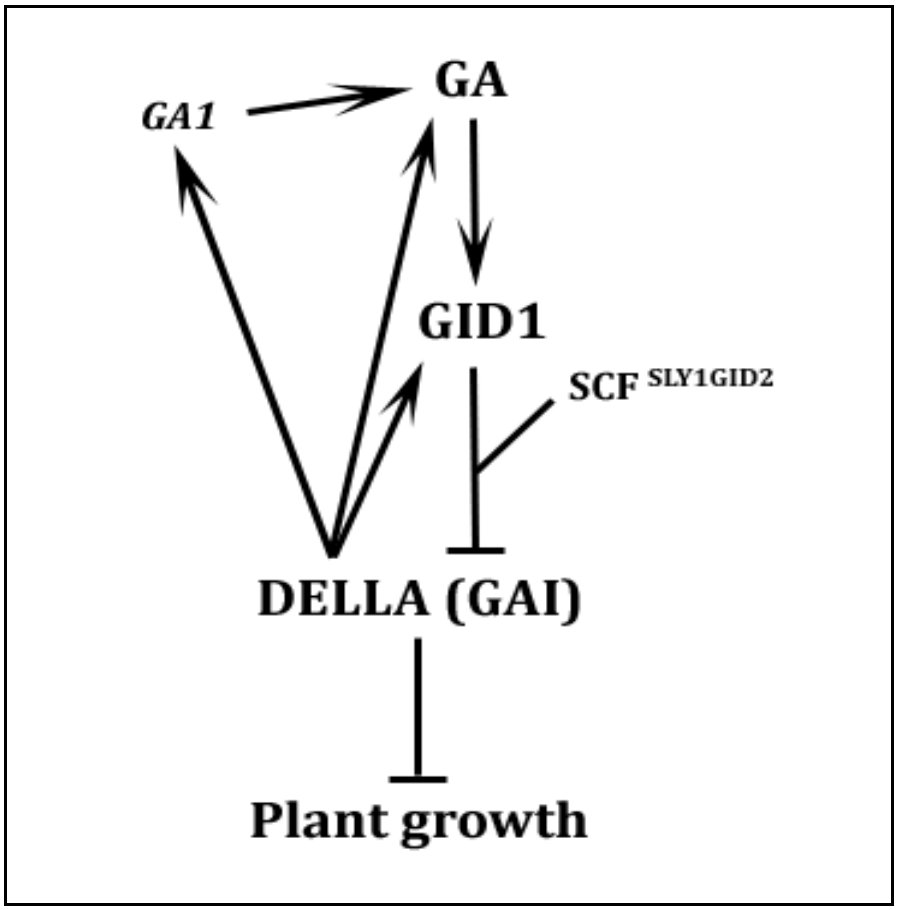

Figure 3-4 – Schematic representation of the interaction of gibberellin, and its receptor GID1a, with DELLA proteins GAI (and RGA, not shown). Negative feedback from DELLA proteins regulates gibberellin activity and gibberellin biosynthesis via GA1. Figure adapted from Sun, 2010 (Sun, 2010).

Research in *Arabidopsis* DELLA proteins has demonstrated the importance of RGA and GAI, and infers that RGA and GAI functions are redundant in the main,

and that both genes negatively regulate the GA response (Peng *et al.*, 1997; Harberd *et al.*, 1998; Dill & Sun, 2001).

Along with GAI and RGA, there are three further DELLA proteins in *Arabidopsis,* RGL (RGA-like) 1, 2 and 3. DELLA proteins have also been characterised and annotated in a wide range of plant species, including Rht-1 (wheat), D8 (maize) (Peng *et al.*, 1999), SLN1 in barley and SLR1 in rice (Ikeda *et al.*, 2001; ChandlerRobertson, 1999; Chandler *et al.*, 2002), along with VvGAI1 in grapevine (Boss & Thomas, 2002). The genes corresponding to these proteins form an orthologous gene family, spanning a range of plant species with diverse importance. Mutations in both *Rht-1* and *D8* within the DELLA domain, lead to dwarf phenotype with decreased GA responses and a constitutive inhibition of plant growth, similar to the *gai* or *rga-Δ17* mutations (Peng *et al.*, 1999). This homology in functionality means DELLA genes from different plant species can be interchanged. *Arabidopsis* GAI and gai proteins transgenically expressed in rice influence GA responses (Fu *et al.*, 2001; Peng *et al.*, 1999). It has been found that the stereotypical green revolution genes *Rht-D1a* and *d8* appear to be more closely related to *GAI* than *RGA*, with percentage amino acid identity of 62% for GAI with Rht, compared with 58% for RGA, and identity of 62% for GAI with d8, against 59% for RGA with d8 (Peng *et al.*, 1999).

Both RGA and GAI proteins carry putative nuclear localisation signals and have been shown to be nuclear localised (Silverstone, Ciampaglio & Sun, 1998; Fleck & Harberd, 2002). However, while RGA is seen to disappear from the nucleus of cells treated with exogenous GA (Silverstone *et al.*, 2001), this is not necessarily

the case for GAI. Using confocal microscopy, Fleck and Harberd observed that both GAI-GFP and gai-GFP fusion proteins localise to the nucleus, but that their localisation is not altered by treatment with gibberellin. In addition, they noted that localisation of GAI-GFP is unaltered in mutants that do not have sequences homologous to typical nuclear localisation sequences (NLS's) (Fleck & Harberd, 2002). However, genetic approaches and immunoblot analysis found the opposite, that GA does stimulate degradation of exogenous GA, and a mutant deficient in the F-box protein SLY1, *sly1-10*, builds up a greater quantity of GAI than the wild-type (Dill *et al.*, 2004). Therefore, it would seem that GA does signal for degradation of the GAI protein, like RGA.

3.1.2 SUMOylation

SUMOylation is essential for both plants and other eukaryotes. In animals, it has been demonstrated to be integral in processes such as chromosome segregation (Watts, 2007) and implicated in human diseases such as cancer, neurodegenerative diseases, heart disease (Sarge & Park-Sarge, 2009) and cerebral ischemia (Yang *et al.*, 2008). In *Arabidopsis*, the SUMO E3 ligase SIZ1 contributes to salicylic-acid-mediated innate immunity (Lee *et al.*, 2007). Indeed SIZ1 is also involved in regulation of cell growth and plant development (Miura & Hasegawa, 2010), is important in gene regulation in response to drought stress (Catala *et al.*, 2007) and controls phosphate deficiency responses (Miura *et al.*, 2005). In addition the SUMO protease Early in Short Days4 (ESD4) has been found to be essential as a regulator of flowering time in *Arabidopsis* (Reeves *et al.*, 2002; Murtas *et al.*, 2003).

SUMO proteases are responsible for maturation of the SUMO protein and also cleaving it from target proteins to allow them to be recycled (Miura & Hasegawa, 2010). Following work carried out studying salt tolerant lines overexpressing the OTS1 and OTS2 proteases, it was discovered that the OTS proteins were SUMO proteases (Conti *et al.*, 2008). Overexpression of these OTS proteases demonstrated a clear growth phenotype, and therefore it was decided to investigate the relationship between SUMOylation and growth control further. The DELLA protein family was an ideal target for this investigation due to their key role in plant growth regulation in *Arabidopsis thaliana*.

Further investigation showed that both RGA and GAI proteins contained a single consensus SUMOylation motif, ΨKXE/D (Conti *et al.*, 2014). Transgenic *Arabidopsis* lines were designed for overexpression of DELLA genes (via a 35S promoter) with either presence or absence (wild-type) of a point mutation in the SUMOylation motif. In the mutants the lysine residue that is essential for SUMOylation was changed into an arginine residue, creating $DELLA^{K/R}$ lines to compare with $DELLA^{K}$ lines (Table 2-2). The reason for changing the lysine residue to an arginine was that both residues are basic in nature, so this mutation should not lead to disruption in protein structure or folding, however the lysine residue includes an ε-amino group which is the acceptor for the glycine residue of ubiquitin in the ubiquitination reaction, whereas the arginine residue does not have the ε-amino group, therefore the interaction of the site with the glycine residue does not occur, due to lack of association of glycine and arginine (Pickart, 2001). The constructs used for these transgenic lines included

a C-terminal GFP tag, to create a convenient, multipurpose fusion protein when expressed to ascertain the effects of the mutation on the DELLA proteins.

3.2 Objectives

For this chapter the main objective is to obtain better understanding of SUMOylation of GAI. The aims are:

- To use *Arabidopsis* lines in which the GAI SUMOylation site is disrupted by mutagenesis (K49R) in order to quantify the importance of SUMOylation in plant growth and in the GA response pathway
- To elucidate any difference in behaviour of the $GAI^{K/R}$-GFP fusion protein from GAI^{K}-GFP, and deduce whether these are likely to be due to lack of SUMOylation

3.3 Strategy

The strategy for achieving the above objectives is to use transgenic *Arabidopsis* lines that have been constructed, along with the relevant controls.

The first part of the investigation will be to characterise the phenotype of transgenic p35S:GAI^{K}-GFP and p35S:$GAI^{K/R}$-GFP lines, particularly looking for classical DELLA phenotypes, most of which have been described in the introduction to this chapter. Prior to characterising the phenotype plants have been selected to be homozygous in the T3 generation.

Secondly, having identified phenotypes, the genotype of these plant lines will be assessed, primarily through molecular techniques such as RT-PCR, western blotting and immunoprecipitation, to understand levels of both gene construct and fusion protein in the lines, and also using techniques such as confocal microscopy to ascertain whether the behaviour of the GAI protein has been altered by lack of SUMOylation.

3.4 Results

3.4.1 Line Selection

Independent transgenic lines as described in the Methods section (2.1.3) and Introduction to the chapter (3.1) were brought through to T2 generation with BASTA selection to select those homozygous or at least heterozygous for the transgene (Table 3-1). Homozygous T3 lines were used for phenotypic and genotypic studies (Table 3-2). Further information can be found in the Appendix 1 (9).

It should be noted that, due to the numbers of T2 seeds collected from plant lines in the T1 generation, between 235 and 382 seeds per each line in the T2 generation were analysed by BASTA selection (Table 3-1). While it would be highly unlikely to find a double insertion event of the transgene when using these numbers of seeds, it would still be possible to get two insertion events very close together rather than a single insertion. If it had been possible, the ideal protocol would have been to screen approximately 1000 seeds per line

with BASTA, to make this part of the process more stringent and ensure that all transgene insertions were a single insertion.

Table 3-1 –BASTA selection (20µg/ml glufosinate ammonium) of T2 independent transgenic lines.

	Number of Seeds				
Line	**Healthy**	**Sick**	**Non-Germinant**	**Ratio of Healthy : Sick**	**Homozygous/Heterozygous**
p35S:RGA^{K}-GFP a	174	61	14	2.85:1	Heterozygous
p35S:RGA^{K}-GFP b	291	91	0	3.2:1	Heterozygous
p35S:RGA$^{K/R}$-GFP	251	72	0	3.49:1	Heterozygous
p35S:GAI^{K}-GFP	253	75	1	3.37:1	Heterozygous
p35S:GAI$^{K/R}$-GFP a	247	58	1	4.26:1	Heterozygous
p35S:GAI $^{K/R}$ –GFP b	294	86	10	3.42:1	Heterozygous
p35S:GFP b	218	62	1	3.52:1	Heterozygous
Col-0	0	All	12	N/A	N/A

Table 3-2 – T3 independent transgenic lines identified as homozygous by BASTA selection (20µg/ml glufosinate ammonium) and used for phenotypic and genotypic studies.

	Number of Seeds			
Line	**Healthy**	**Sick**	**Non-germinants**	**Homozygous**
p35S:RGA^{K}-GFP 1.0	96	0	12	✓
p35S:RGA^{K}-GFP 2.0	101	0	15	✓
p35S:RGA$^{K/R}$-GFP 1.0	54	0	12	✓
p35S:GAI^{K}-GFP 1.0	25	0	10	✓
p35S:GAI$^{K/R}$-GFP 1.0	57	0	4	✓
p35S:GAI$^{K/R}$-GFP 2.0	61	0	12	✓
p35S:GFP 1.0	78	0	12	✓
Col-0	0	176	4	Not applicable

Confirming the genotype of the lines studied was essential, so CAPS marker analysis was carried out to ascertain whether these lines did indeed have the lysine to arginine mutation in position 49 in the amino acid sequence in *GAI* following mutagenesis and transformation of *Arabidopsis* plants. The mutated transgene would hold the sequence 5'-GACTC-3' (rather than 5'-AACTC-3'), within which the restriction enzyme HinfI cuts between guanine and adenine bases. PCR primers were used to amplify genomic DNA from the respective transgenic lines. Following digestion of the PCR products, two DNA products would be seen on an agarose gel in the successfully mutagenized coding sequence, rather than one product present within the non-mutagenised form (Figure 3-5) confirming the genotypes of the lines.

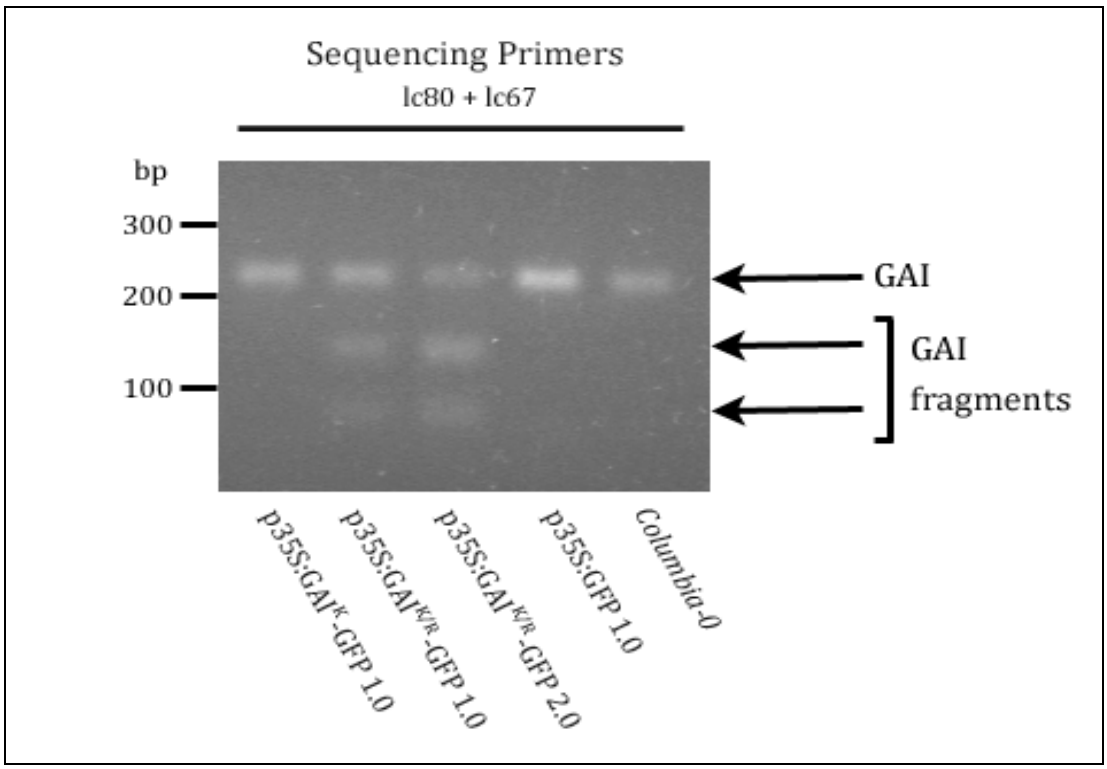

Figure 3-5 – CAPS marker analysis of p35S:GAI^{K}-GFP and p35S:GAI$^{K/R}$-GFP transgenic Arabidopsis thaliana lines. Primers were lc80 and lc67 for PCR amplification. Genomic DNA from 5-day old T3 seedlings was amplified before digestion with Hinf1. Products were separated on 2.5% agarose gels.

3.4.2 Phenotyping

Having brought the p35S:GAI^{K}-GFP, p35S:GAI$^{K/R}$-GFP and p35S:GFP control transgenic lines to the T3 generation, the first stage of analysis was to quantify aspects of the phenotypes of these plants in the T3 generation. In two pairs of distinct independent transgenic lines with single insertion, GAI$^{K/R}$-GFP plants bolt earlier than the transgenic plants carrying the copy of the GAI^{K}-GFP fusion protein (Figure 3-6). The GAI$^{K/R}$-GFP plants are similar to the Col-0 and GFP control lines in this characteristic. Compared to the GAI$^{K/R}$-GFP mutant plants, GAI^{K}-GFP plants exhibit less vegetative growth (Figure 3-6B and D) and delayed phase transition from the vegetative growth phase (Figure 3-6A and C), meaning delayed bolting.

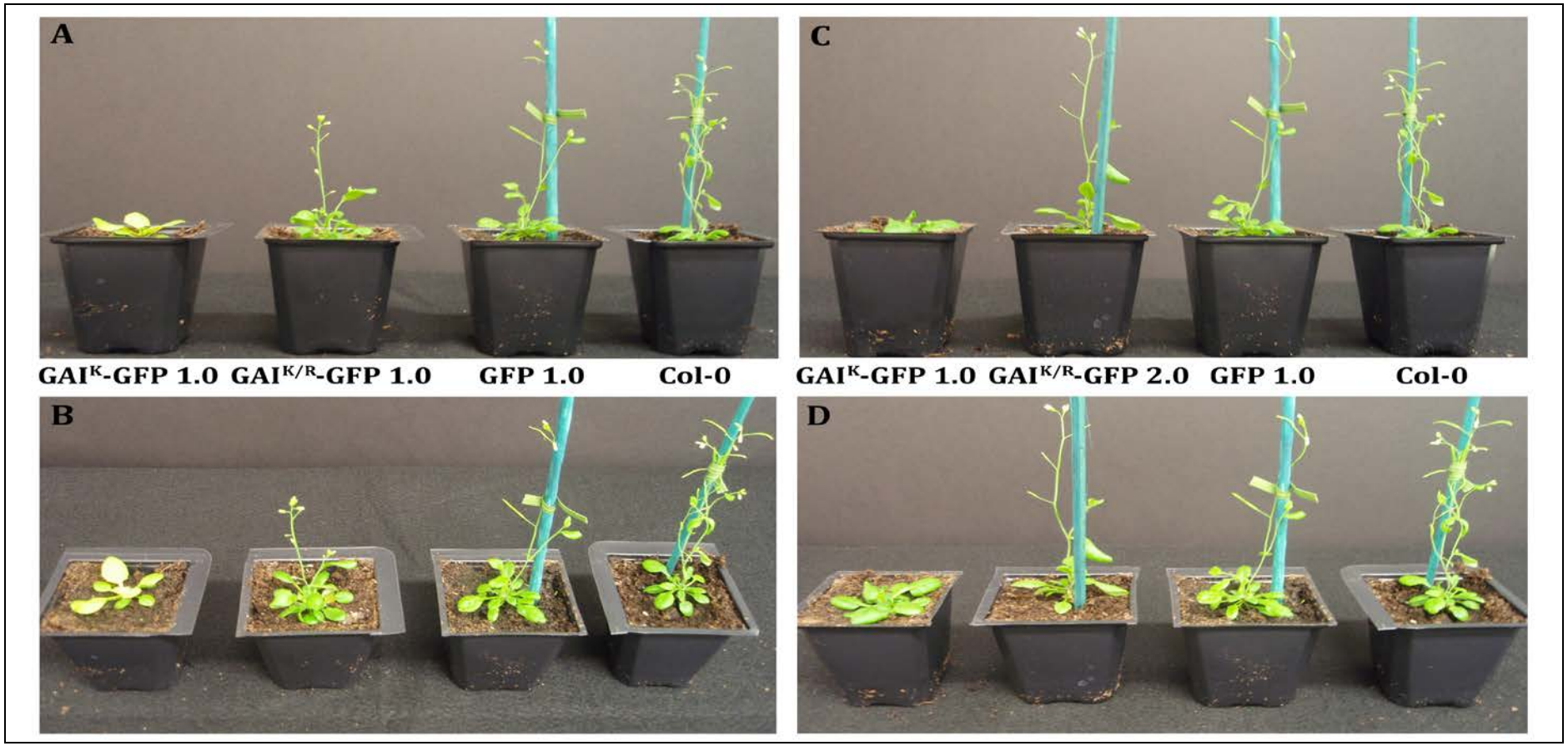

Figure 3-6 – Comparing the phenotypes of p35S:GAI^{K}-GFP and p35S:GAI$^{K/R}$-GFP overexpressing lines. Two sets of independent transgenic GAI$^{K/R}$ lines (A/B and C/D) are shown. Each pair is shown from the side (A and C) and above (B and D). From left to right: - p35S:GAI^{K}-GFP, p35S:GAI$^{K/R}$-GFP, p35S:GFP, Columbia-0. Plants were grown in controlled environment up to 14 days old, and subsequently grown in glasshouse conditions

.

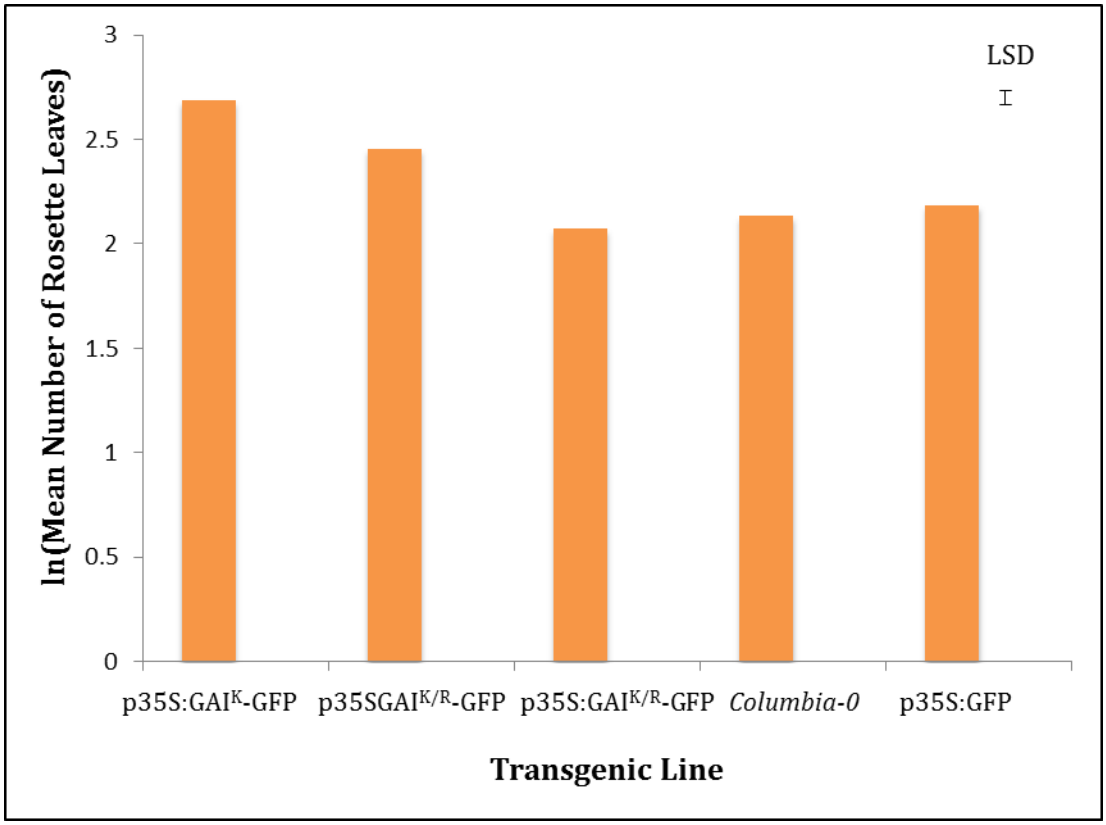

Figure 3-7 – The p35S:GAI$^{K/R}$-GFP mutant has fewer leaves at bolting than the p35S:GAI^{K}-GFP line. Comparison of the natural log transformation of mean number of rosette leaves, counted at the point of a 1cm bolt, of T3 GAI^{K}-GFP against GAI$^{K/R}$-GFP lines, with control lines included. Plants were grown in controlled environment up to 14 days old, and subsequently in glasshouse conditions. General ANOVA found P<0.001, LSD (P<0.05) – 0.066, d.f. – 61. n=12-24 with two biological replicates carried out of the experiment.

Number of rosette leaves at bolting has been one of the phenotypic measurements used to assess growth. Comparison of the lines (data transformed with natural log) shows that consistent with known phenotypes of DELLA overexpressing lines (Fleck & Harberd, 2002), the GAI^{K}-GFP line accumulates more leaves than the controls and two independent GAI$^{K/R}$-GFP lines 1.0 and 2.0 (Figure 3-7). Rosette leaf number between the two independent GAI$^{K/R}$-GFP lines did vary (see discussion on protein expression levels alongside *Figure 3-11*) with the second line (GAI$^{K/R}$-GFP 2.0) having mean

number of rosette leaves closer to the control Col-0 and GFP lines. However, in each case these values were lower than the GAI^{K}-GFP 1.0 line.

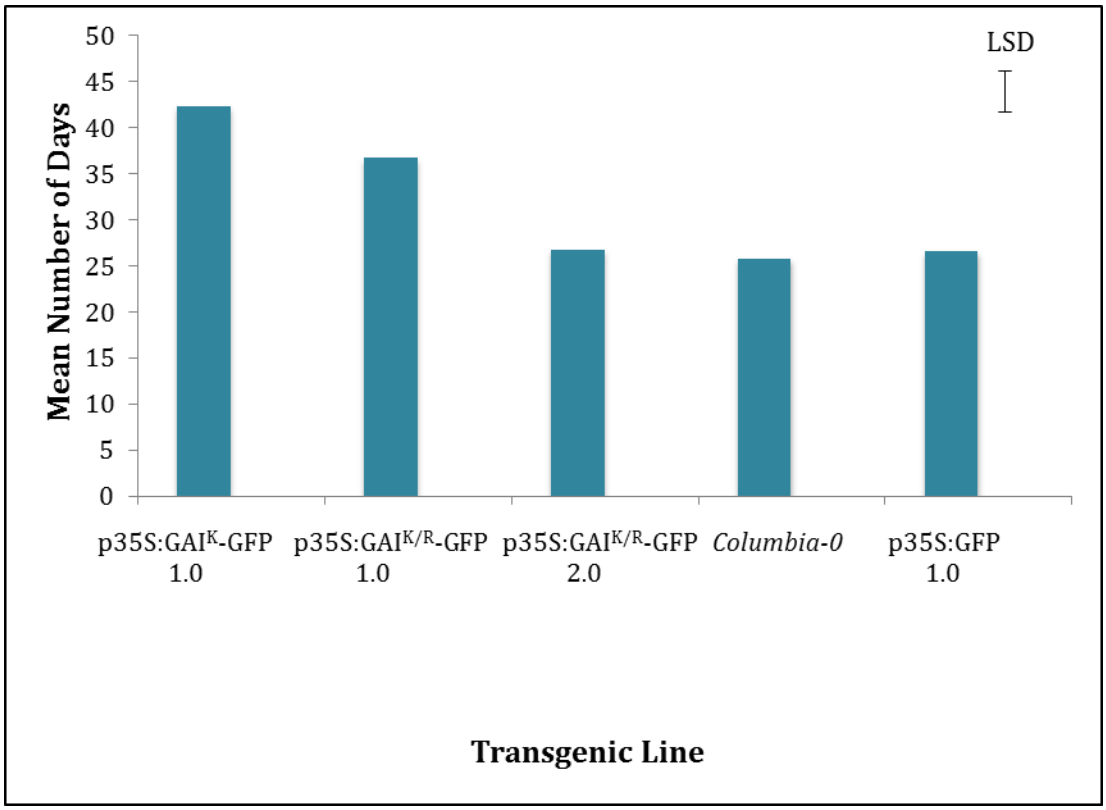

Figure 3-8 – p35S:GAI$^{K/R}$-GFP transgenic lines bolt sooner than p35S:GAI^{K}-GFP lines. Bolting defined as a 1cm inflorescence stem. Plants were grown in controlled environment up to 14 days old, and subsequently grown in glasshouse conditions. General ANOVA found P<0.001, LSD (P<0.05) - 4.442, d.f. - 95. n=12-24 with two biological replicates carried out of the experiment.

A second measure of growth rate was the number of days for plants to reach a 1cm inflorescence stem, as slower bolting signifies delay in phase transition. As with rosette leaf number above, the GAI^{K}-GFP line bolts later, whereas the GAI$^{K/R}$-GFP lines both bolt sooner, and GAI$^{K/R}$-GFP line 2.0 again behaves like the wild-type Col-0 (Figure 3-8).

As detailed above, previous work in the group has shown that SUMO proteases OTS1 and OTS2 moderate growth in response to salt (NaCl) stress (Conti *et al.*,

2008) and part of this action is through regulating the pool of DELLA proteins. Hence, it was important to test the growth responses of p35S:DELLA^{K} and DELLA$^{K/R}$-GFP lines under salt stress. For comparison, GA treatment is expected to remove DELLA proteins, while paclobutrazol should enhance the inhibitory effect of DELLA's by inhibiting GA synthesis (Griffiths *et al.*, 2006). Taking these together an experiment was set up to test the root phenotypes of the overexpressing lines, growing plants vertically on plates to allow analysis of the root architecture. A root growth assay was chosen because GAI is considered to play a more distinctive role in root growth (Busov *et al.*, 2006; Ubeda-Tomás *et al.*, 2008; 2009) compared with other *Arabidopsis* DELLA proteins.

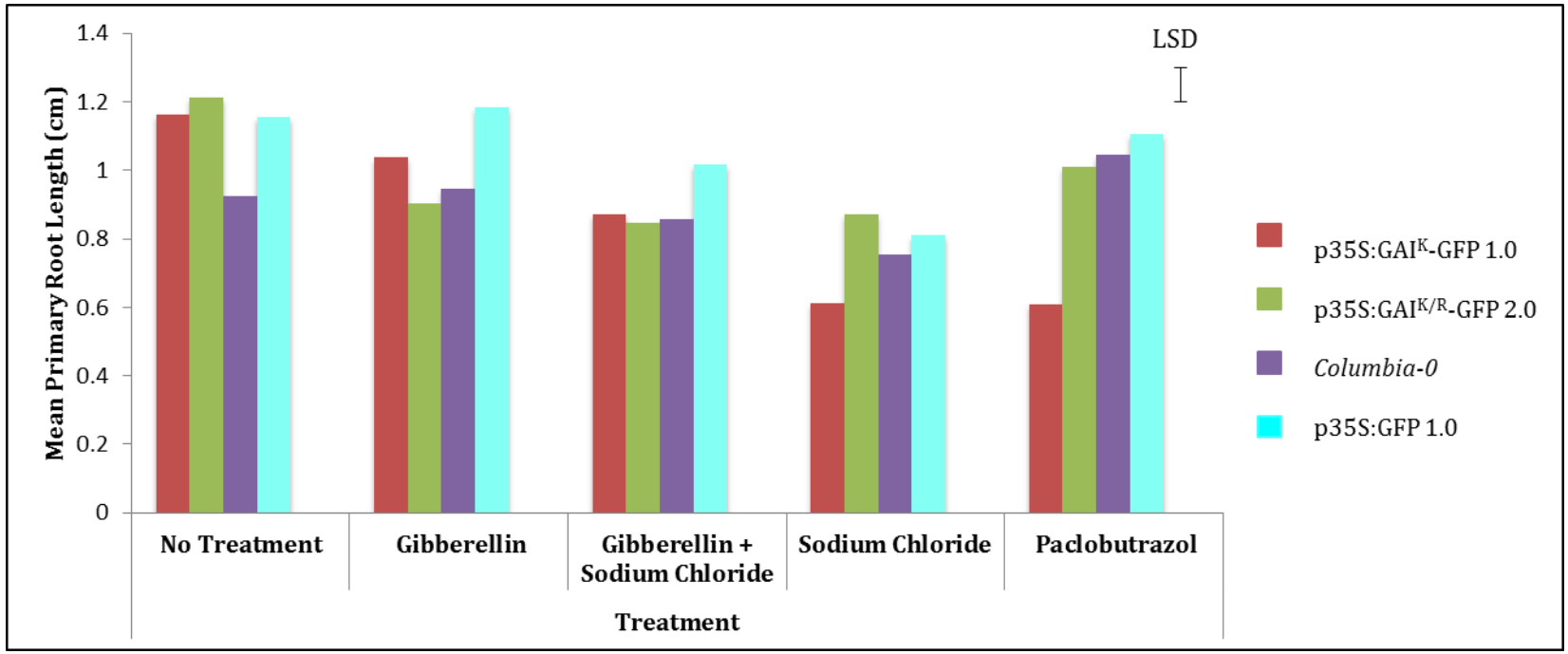

Figure 3-9 – The p35S:GAI$^{K/R}$-GFP mutant line root architecture is less affected by abiotic stress than the p35S:GAI^{K} line. T3 seeds from the transgenic lines were germinated and grown vertically in constant light and controlled environment conditions on ½ MS media plates containing different treatments (no treatment, 100µM gibberellin, 100µM gibberellin and 100mM sodium chloride, 100mM sodium chloride and 0.5µM paclobutrazol) for 10 days before data was collected. Plates were scanned and primary root length measured with Image J software. General ANOVA found P<0.001, LSD (P<0.05) - 0.09973, d.f. - 549. n = 21-30, with two technical replicates of each variable and one biological replicate making up the experiment.

Root length does not differ between the GAI^{K}-GFP 1.0 and GAI$^{K/R}$-GFP 2.0 lines in the absence of stress (Figure 3-9), which suggests that perhaps SUMOylation is not in play when there is no stress effect on plant growth. However, the phenotypes observed for bolting differ between the GAI^{K}-GFP and GAI$^{K/R}$-GFP lines (Figure 3-6, Figure 3-7, Figure 3-8) and there is also no stress induced on plants in this situation. These findings do tell us that the GAI$^{K/R}$-GFP line differs more from the GAI^{K}-GFP in regards to bolting time than root growth in non-stress conditions, suggesting that mutation of the GAI SUMOylation site confers more influence on bolting time in these circumstances. It is noted that the GFP vector-only control line consistently grew longer primary roots than Col-0. No difference in response was seen between these controls with any of the treatments and so the data are presented as a set of comparisons between responses from GAI^{K} and $^{K/R}$-GFP lines.

Treatment with GA induced some reduction in root length for both GAI^{K}-GFP and GAI$^{K/R}$-GFP lines, somewhat more in the latter, but no change in the controls.

Growth in 100mM sodium chloride induced a clear reduction in primary root length in all lines. The strongest effect was on the GAI^{K}-GFP line and although the GAI$^{K/R}$-GFP line was also affected its response was comparatively low. The difference in effect of high salinity between the two lines was found to be statistically significant by ANOVA analysis. This result shows that high salinity has an effect on root growth, in interplay with DELLA SUMOylation.

The use of 100mM sodium chloride and 100μm gibberellin in combination was designed to stimulate relief from repression of GAI overexpression, but induce abiotic stress with high salinity. The results support the interpretation of the experiment in that both 35S lines overexpressing GAI were indistinguishable from each other and from Col-0. This result supports the idea that the changes in root length in response to salt stress and salinity were indeed due to the effects of the transgenes.

While there is reduction in mean root length with the GAI^{K}-GFP and control lines between the gibberellin treatment, and gibberellin/sodium chloride treatment, there is little change in the measurement for the $GAI^{K/R}$-GFP line. The GAI^{K}-GFP line has a higher root length than $GAI^{K/R}$-GFP with gibberellin treatment, but greater reduction in length with addition of sodium chloride. Considering sodium chloride treatment alone, the value for mean primary root length of GAI^{K}-GFP reduces significantly again, while the $GAI^{K/R}$-GFP line increases slightly in mean primary root length. The control lines show the same pattern as the GAI^{K}-GFP line, reducing from the values for the gibberellin/sodium chloride treatment.

Paclobutrazol is an inhibitor of gibberellin biosynthesis, therefore is likely to enhance the phenotypes of the overexpressing lines because DELLA removal by GA will be impaired, in addition to overexpression of DELLA by the 35S promoter. As above, this hypothesis was confirmed in that the GAI^{K}-GFP plant roots were more severely inhibited than all the other lines. The $GAI^{K/R}$-GFP line

behaved just like Col-0 with slightly more elongation than after GA treatment and similar extension to no treatment.

3.4.3 Assessment of Gene Expression

It was important to ascertain the levels of transgene expression at T3 in order to allow comparison of phenotype with transgene expression. The housekeeping gene actin was used as an indicator for overall cDNA amount for RT-PCR of all lines (Figure 3-10A). After these RT-PCR reactions were run using primers for *GFP* and *GAI*, to ascertain expression levels (Figure 3-10B,C).

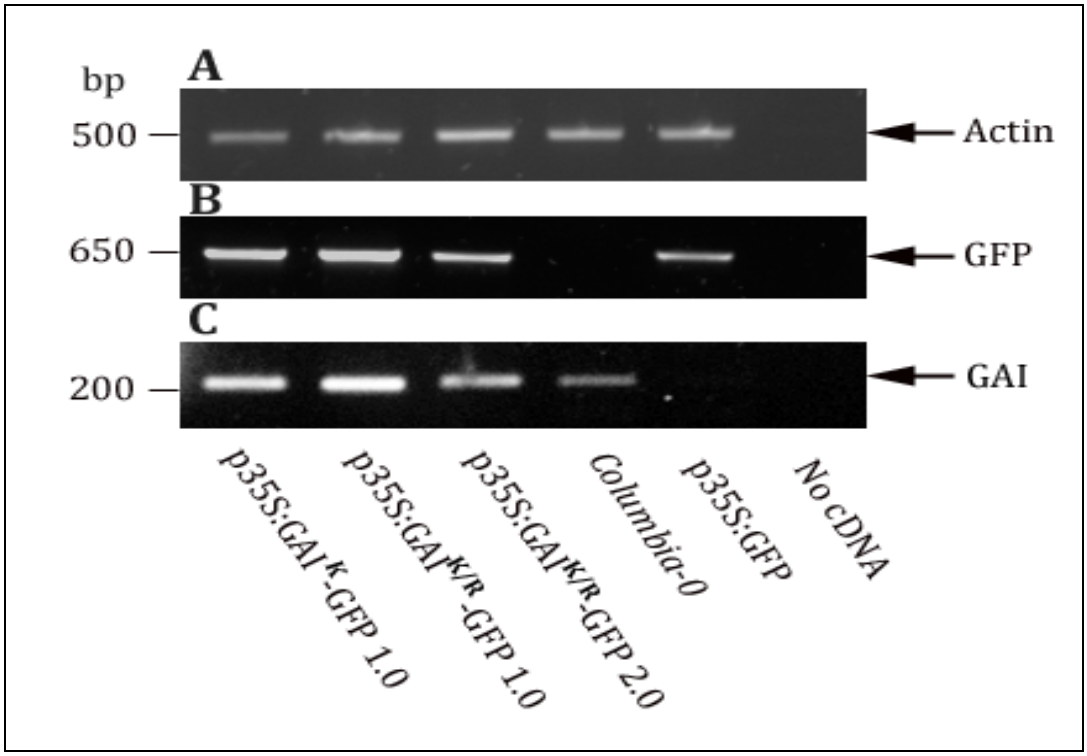

Figure 3-10 – RT-PCR to show expression levels of each transgene. Data are shown after gel electrophoresis of RT-PCR products on a 1% agarose gel. Actin levels in cDNA samples were used as an indicator for total cDNA (A) after which PCR was carried out with GFP primers (B) and GAI primers (C). RNA was extracted from 7 day-old Arabidopsis thaliana whole seedlings.

Using primers for the transgene GFP expression, a band corresponding to the anticipated product size of 650 base pairs was seen in all lines except Col-0

(Figure 3-10B). GAI$^{K/R}$-GFP 1.0 has the visibly highest level of expression, with seemingly less expression in the GAI^{K}-GFP 1.0 line. GAI$^{K/R}$-GFP 2.0 has noticeably lower expression. No band was seen in the negative control where no cDNA was added to the PCR reaction. When the GAI primers were used a PCR product at 200 base pairs indicated that the reactions were working. Reassuringly, this corresponded to the size of the fragment for Col-0, which is considered the positive control. Once again, the highest expression seemed to be GAI$^{K/R}$-GFP 1.0 (Figure 3-10C). The GAI^{K}-GFP 1.0 and GAI$^{K/R}$-GFP 2.0 lines both appeared to have a lower level of expression. The control wild-type *Columbia-0* had much lower expression as would be anticipated, and very little expression at all was seen in the GFP line (which might help explain the longer root phenotype in this line; Figure 3-9). No product was seen in the negative control lane.

While these results are open to some degree of speculation, it was important to keep in mind that caution should be exercised in interpreting or analysing the results too extensively, as RT-PCR is not a quantifiable technique. If there had been more time available, quantitative PCR (qPCR) could have been utilised, giving scope for comparable gene expression levels rather than the more basic presence or absence of gene expression inferred from RT-PCR.

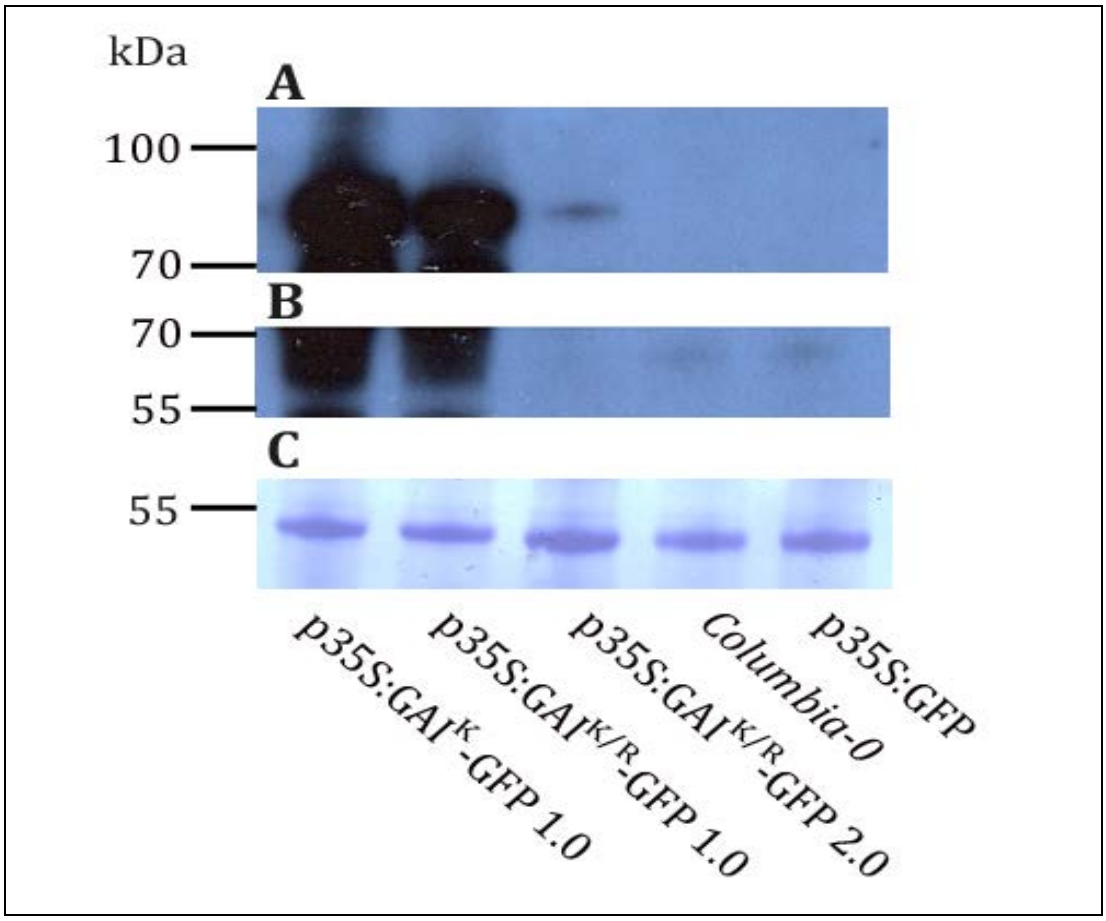

Figure 3-11 - Western blot of protein expression in p35S:GAI^{K}-GFP and p35S:GAI$^{K/R}$-GFP lines. Protein was extracted from 7 day-old Arabidopsis thaliana seedlings and applied to a 4-12% polyacrylamide gel for SDS-PAGE gel electrophoresis. Transfer to PVDF membrane ran overnight, and the blot was developed with sheep anti-GAI as the primary antibody and ECL detection. The figure shows the developed western blot (A and B) and coomassie blue-stained PVDF membrane as a loading register (C).

Western blotting was used to assess the level of fusion protein present for each transgenic line (*Figure 3-11*). Loading of the gel was equalised using protein assay and verified by post-staining the PVDF membrane with Coomassie Blue, as shown in *Figure 3-11*C. The protein was detected using a polyclonal antibody for GAI. There is considerable variation in the quantity of fusion protein evident. The GAI^{K}-GFP transgenic line has a high level of protein present at a molecular weight corresponding to the fusion protein (*Figure 3-11*A). The two GAI$^{K/R}$-GFP lines have variable quantities of the fusion protein, with line 1.0 displaying high levels of the protein, and much less in line 2.0, although there is a clear

overexpression signal. There are no bands at this molecular weight in either the Col-0 or vector–only control, which would be expected, as they are not expressing fusion protein. Detection of endogenous GAI is difficult, but there is a band in these lines (both overexpressing lines and controls) corresponding to GAI, between 55 and 70kDa (*Figure 3-11*B), However this band is faint in the vector only and Col-0 controls and almost undetectable in $GAI^{K/R}$-GFP 2.0, which has low levels of the fusion protein, and seems to have low levels of expression for GAI proteins in this case, perhaps due to co-suppression.

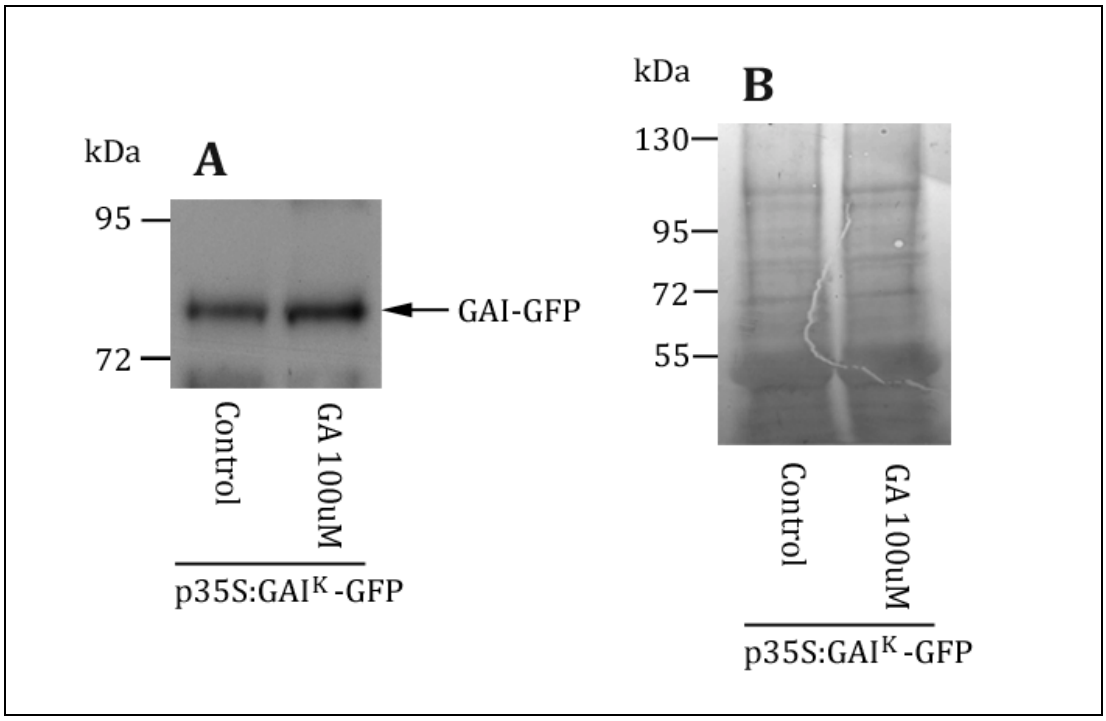

Figure 3-12 – p35S:GAI^{K}-GFP protein continues to be expressed strongly after overnight treatment with 100μM gibberellin overnight. Western blot showing protein extracts taken from 10 day-old A. thaliana seedlings were incubated with 100μM overnight prior to extraction. Following extraction, samples were immunoprecipitated on αGFP beads. Immunoprecipitated samples were run on SDS-PAGE for western blot and probed with an anti-GAI antibody raised in sheep (A). Protein was assessed for equal loading by coomassie stain (B).

Assessing the stability of the DELLA-GFP fusion protein was an integral part of the hypothesis for this thesis. Through immunoprecipitation, it was demonstrated that there is no loss of GAI^{K}-GFP fusion protein following

overnight treatment with 100μM gibberellin (Figure 3-12). It is still possible to see a significant quantity of the fusion protein at the same molecular weight as the control line after treatment (Figure 3-12A). Short-term changes in GAI^{K}-GFP along with GAI$^{K/R}$-GFP abundance are studied below.

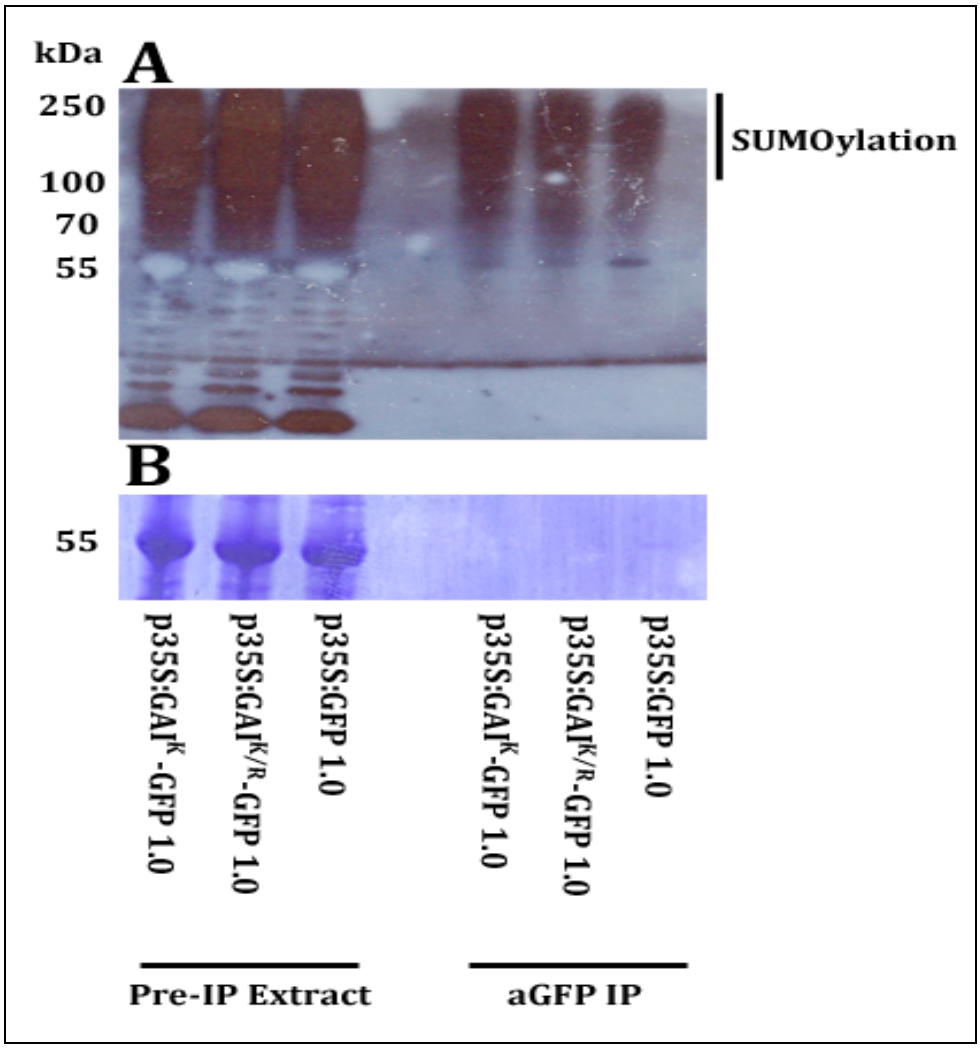

Figure 3-13 – SUMOylation assay of GAI transgenic lines. Western blot following immunoprecipitation with αGFP beads demonstrating SUMOylation of p35S:GAI^{K}-GFP and p35S:GAI$^{K/R}$-GFP proteins. Protein was extracted from 7 day-old A. thaliana seedlings. The PVDF membrane was probed with an anti-SUMO antibody raised in rabbit, following immunoprecipitation of protein samples with αGFP beads (A). Total protein levels were equalised by use of equivalent seedling homogenate was used for each IP, and checked with pre-IP protein controls (B).

The SUMOylation assay was an essential part of the chapter, in ascertaining whether mutation of GAI from GAI^{K} to GAI$^{K/R}$ had lead to a reduction in

SUMOylation of the protein (Figure 3-13). Above approximately 100kDa a marked reduction in SUMOylation could be seen for the $GAI^{K/R}$-GFP line compared to the GAI^{K}-GFP line, with less of a heavy banding pattern. In addition, less of a SUMOylation pattern compared to both overexpressing lines of GAI could be seen in the vector only control, which is not surprising as this line had no overexpression of DELLA protein.

3.4.4 Microscopy

The transgenes are designed to translate as GFP fusion proteins. This has allowed confocal microscopy of the transgenic lines, to observe the localisation and behaviour of the GAI protein, both in mutant and non-mutant forms.

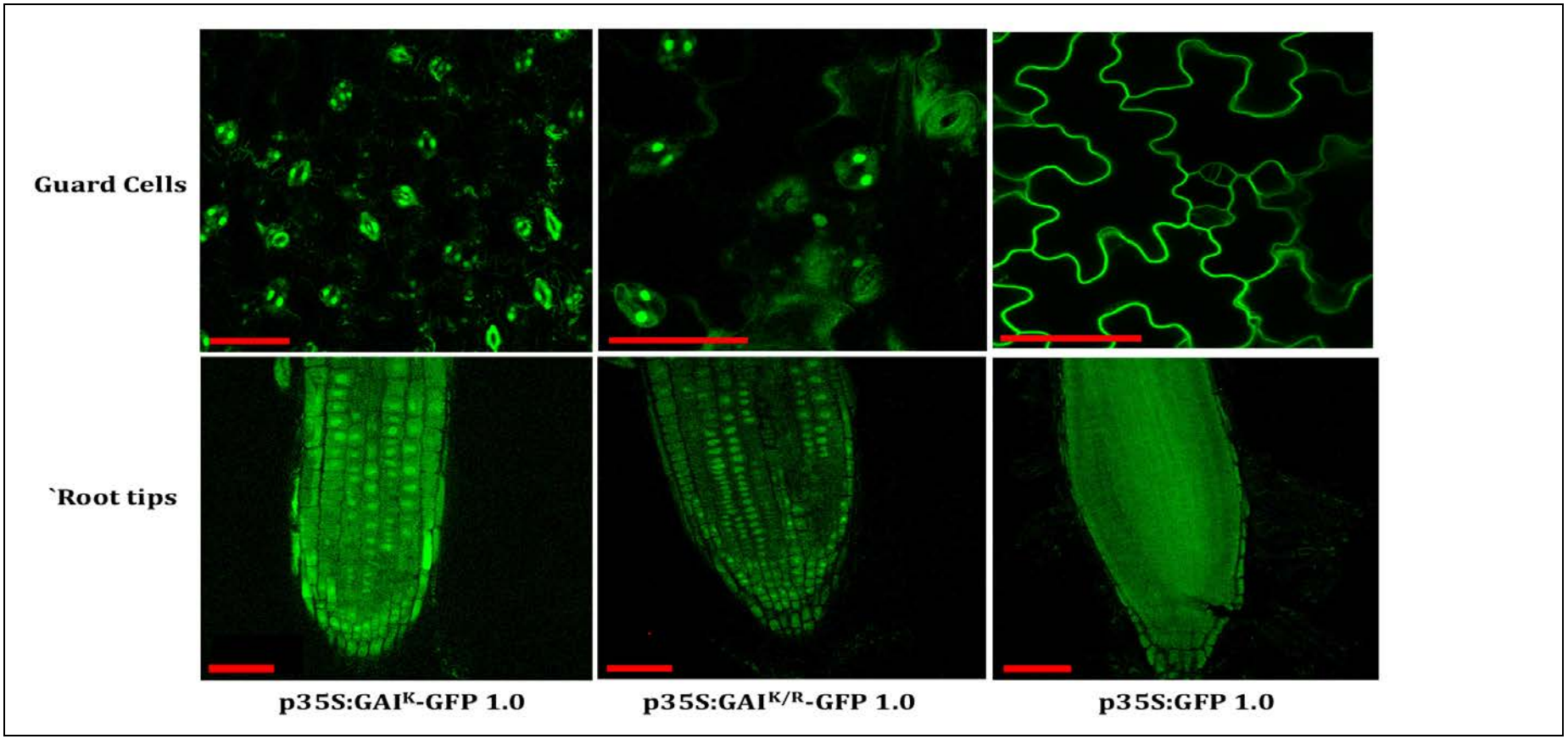

Figure 3-14 – The p35S:GAI^{K}-GFP and p35S:GAI$^{K/R}$-GFP fusion proteins are nuclear localised in two cell types. Confocal microscopy showing localisation of GAI^{K}-GFP and GAI$^{K/R}$-GFP fusion proteins, along with the GFP control, in both guard cells from the epidermis of the cotyledon, and root cap/root tip cells from Arabidopsis root tissue. Material used for confocal imaging was 10 day-old seedlings. Scale bar in red equal to 50μM. n = 8.

Both the GAI^{K}-GFP and GAI$^{K/R}$-GFP proteins localise to the nuclei of stomatal cells (*Figure 3-14*). The GFP signal in the control line 35S:GFP is also present in guard cells, but is dispersed within the cells and around the edge of the cells where the cytoplasm is compressed. Nuclear expression of the GAI^{K}-GFP and GAI$^{K/R}$-GFP proteins is also evident in root tissue (*Figure 3-14*). The control line overexpressing GFP shows some expression in root tissue, again dispersed within the cells in the root cap.

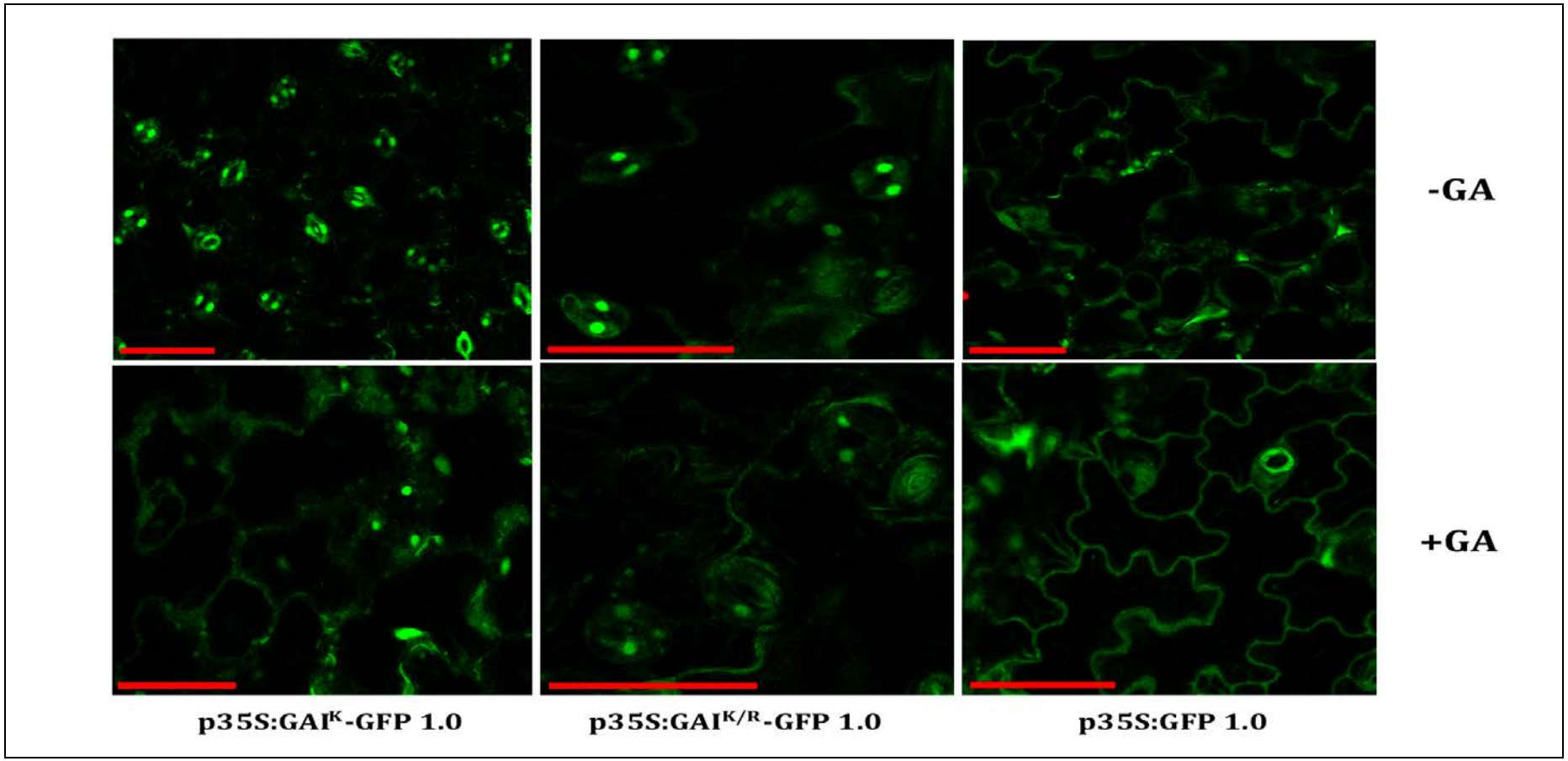

Figure 3-15 - Both the p35S:GAI^{K}-GFP and p35S:GAI$^{K/R}$-GFP proteins are degraded within 3 hours of gibberellin application. Where GAI is present after treatment it remains in the nucleus. Confocal microscopy showing localisation of GAI^{K}-GFP and GAI$^{K/R}$-GFP fusion proteins, along with the GFP control in guard cells from the epidermis of the cotyledon, with and without treatment with 100µM gibberellin for 3 hours. Material used was 10 day-old Arabidopsis seedlings. Scale bar in red equal to 50µM. n = 5.

Confocal microscopy carried out following treatment of *Arabidopsis* seedlings with gibberellin or controls with solvent only (*Figure 3-15*). Gibberellin reduced the GFP signal in both GAI overexpression lines, but not the control GFP line. Loss appeared greater in the GAI$^{K/R}$-GFP mutant line than the non-mutant, after 10 experimental replicates were taken into account. However, nuclear localisation did not fully disappear for either of the GAI transgenic lines.

3.5 Discussion

3.5.1 Phenotyping and comparison of the p35S:GAI^{K}-GFP and p35S:GAI$^{K/R}$-GFP lines

Having confirmed that the transgenic lines were either GAI^{K}-GFP or GAI$^{K/R}$-GFP (Figure 3-5) the next stage was to describe the phenotypes. From published data, p35S:GAI-GFP or p35S:GAI transgenic lines show late bolting and delay in phase transition (exit from vegetative growth) and reduced growth (Dill *et al.*, 2004). The p35S:GAI^{K}-GFP phenotype is in full agreement, with delayed bolting and less vegetative growth (Figure 3-6). In contrast, the GAI$^{K/R}$-GFP lines bolt earlier (Figure 3-8) and have fewer rosette leaves at bolting (Figure 3-7). Indeed, GAI$^{K/R}$-GFP plants behave more like wild-type plants than GAI^{K}-GFP plants, inferring that the $^{K/R}$ mutation does affect the function of the GAI protein.

GAI is known to be a DELLA protein highly expressed in *Arabidopsis* root tissue (Busov *et al.*, 2006; Ubeda-Tomás *et al.*, 2008; 2009). As demonstrated in Figure 3-9, there is little difference in mean primary root length between ^{K} and $^{K/R}$ lines in the absence of stress. There was a slight decrease in mean primary root

length for both the GAI^{K}-GFP and GAI$^{K/R}$-GFP lines following gibberellin application, but gibberellin application has little impact on the control lines suggesting that gibberellin may not have a large influence on root growth. While gibberellin has a role in promoting stem elongation (Koornneef & Veen, 1980), perhaps it does not have such fundamental involvement in promotion of root growth.

Recent publications have confirmed that gibberellins are present in roots and collect in the endodermal cells of the root elongation zone (Shani *et al.*, 2013). It was noted that gibberellins are required by embryos for emergence and establishment of a full root primordia, but are inhibitory to the early initiation stage of primary root development (in interplay with auxin) (Niu *et al.*, 2013). As these transgenic lines in Figure 3-9 were grown on gibberellin from germination, this may have been inhibitory to their growth, explaining these results, however, as a similar pattern of inhibition was not seen in the control lines this explanation is unlikely. A second possibility is that gibberellin has little effect on the GAI protein, compared with other DELLA proteins. This point has been debated by researchers, with some reports that GAI is resistant to GA-induced degradation (Fleck & Harberd, 2002), where others have found it to be degraded (Dill *et al.*, 2004). We have found GAI to be degraded in the presence of GA during confocal microscopy (*Figure 3-15*) but complete disappearance is not seen in the longer term following GA treatment (Figure 3-12). As previously stated GAI is considered to play a more distinctive role in root growth compared with other *Arabidopsis* DELLA proteins (Busov *et al.*, 2006; Ubeda-Tomás *et al.*, 2008; 2009), especially RGA, so it may be that gibberellin treatment in the long-

term leads to greater stimulation of GAI expression in those lines already overexpressing GAI, leading to greater DELLA growth repressive effects.

Gibberellin does have some bearing on the fate of these plant lines, as it rescues the GAI^{K}-GFP transgenic line when the line is under abiotic stress with sodium chloride treatment. The same pattern is demonstrated in the control GFP line to some extent, which also has capability of SUMOylation of endogenous GAI and other DELLA proteins. The loss of root length over the majority of lines when gibberellin is applied could be due to the fact that the system is already primed with gibberellin from exogenous treatment and this has lead to a reduction in endogenous gibberellin and slightly shorter root lengths. Increase in salt stress has a stimulatory effect on the OTS1 and OTS 2 SUMO proteases (Conti *et al.*, 2008), which facilitate plant growth at high salinity through their function of recycling SUMO from target proteins (Conti *et al.*, 2008). Sodium chloride treatment has little effect on the GAI$^{K/R}$-GFP transgenic line, in terms of primary root growth, which would be expected, as the GAI$^{K/R}$-GFP protein is not SUMOylated. Therefore there is no requirement for the deSUMOylation function of the OTS proteases. In contrast, there is a big difference in the primary root length of the GAI^{K}-GFP line between no treatment and sodium chloride treatment. This line is affected by high salinity due to its capacity for SUMOylation of GAI. The diverse effects of sodium chloride, and the fact that there is little change in the phenotype of the GAI$^{K/R}$-GFP line under this stress condition suggests that SUMOylation is an important process in responses to abiotic stress, and that SUMOylation is enforcing repression of plant growth by maintaining GAI protein levels during increased stress, perhaps to support the

plant in this environment. Indeed, over SUMOylation of target proteins can impair plant growth, and it has been proposed from previous publication that in environmental stress conditions hyperSUMOylation of certain target proteins work to restrict growth to enhance survival in stress periods (Conti *et al.*, 2009).

Overall, there are many other proteins which are modified by SUMOylation and which the OTS protease cleaves SUMO from, meaning that this is only one small part of the network of interactions through which this process plays a role in abiotic stress responses.

Another interesting comparison is looking at the data for the gibberellin, gibberellin/sodium chloride and sodium chloride treatments. While the GAI^{K}-GFP transgenic line and control lines demonstrate a general downward trend in primary root length, from gibberellin, decreasing gibberellin combined with sodium chloride, and the lowest root measurement with high salinity treatment alone, the same is not observed for the $GAI^{K/R}$-GFP line. For these three treatments the mean root length stays relatively constant, suggesting that these plants are able to combat abiotic stress such as high salinity better than the GAI^{K}-GFP line, perhaps with some bearing of SUMOylation. It would be interesting to treat $GAI^{K/R}$-GFP plant lines on serial dilutions of abiotic stress treatments such as high salinity, to gauge at what point these type of abiotic stress becomes apparent in $GAI^{K/R}$-GFP mutant plants.

While high levels of abiotic stress such as high salinity, or growth repression stimulated by paclobutrazol incite clear reduction in mean primary root length

of the GAI^{K}-GFP line, this is not the case for the GAI$^{K/R}$-GFP line, which stays fairly consistent from measurements with gibberellin when sodium chloride is applied, and has a mean root length when paclobutrazol is applied, not much shorter than with no treatment. Particularly true with paclobutrazol treatment, is that the mutant line behaves very similarly to the control lines. It seems to be the case that the mutant GAI$^{K/R}$-GFP line has the ability to combat stress conditions more effectively than the GAI^{K}-GFP line. Extension of this experiment to include more iterations and further concentrations of the treatments would improve this understanding.

We must consider what the impact of SUMOylation is, in relation to DELLA proteins, and what conclusions we can draw from phenotypic data from these transgenic lines. In comparison with plants expressing GAI^{K}-GFP, those expressing GAI$^{K/R}$-GFP bolt earlier, have lower levels of vegetative growth at bolting, and combat abiotic stress differently. By preventing SUMOylation, GAI is no longer active, as a DELLA protein and plant growth is similar to the wild-type in the GAI$^{K/R}$-GFP mutant. Growth can be modulated by gibberellin, at least partially in the GAI^{K}-GFP overexpressing line, perhaps less so in the GAI$^{K/R}$-GFP lines. The effect of SUMOylation on GAI is not due to localisation of the GAI protein, as both the GAI ^{K} and $^{K/R}$ -GFP fusion proteins remain nuclear localised after GA treatment, although the majority of protein is degraded (*Figure 3-15*). It is not due to GA-dependent proteolysis as all evidence suggests that both GAI ^{K} and $^{K/R}$ -GFP fusion proteins are degraded. SUMOylation of GAI affects the proteins activity, but we have yet to establish how it does this.

3.5.2 Genotyping and comparison of the p35S:GAI^{K}-GFP and p35S:GAI$^{K/R}$-GFP lines

It was essential to ascertain the gene and protein expression profiles of these lines. The transgenic lines were all shown to have detectable levels of cDNA for both GAI and GFP (Figure 3-10B,C), although slightly variable. There was a notable difference in the perceived expression level between GAI and GFP but expression of GFP takes into account solely the transgene whereas GAI expression is a combination of the transgene and endogenous GAI. However the disparity if anything favours the GFP expression with higher levels. The pattern in expression for the three transgenic lines is the same for both GAI and GFP, with the GAI$^{K/R}$-GFP 1.0 seemingly the most high in expression of both elements of the transgene. GAI^{K}-GFP 1.0 appeared to be the second highest in expression, and GAI$^{K/R}$-GFP 2.0 exhibiting the lowest expression for both GAI and GFP. While the Col-0 shows weak expression of GAI, attributable to endogenous GAI expression, the levels of GAI in the control GFP line 1.0 are not detectable from RT-PCR. Through these investigations it has been challenging to detect endogenous DELLA protein, and unsurprisingly much easier to detect both GAI and RGA when overexpressed with the 35S promoter, so this result was not surprising.

As previously referred to (3.4.3), it was hard to make more than basic inferences using the results of the gene expression profiling, as RT-PCR is not a quantifiable technique. To compare expression levels more closely, qPCR would have been a more appropriate technique to use.

There is some disparity in protein levels when comparing these through a western blot (*Figure 3-11*). There is vastly more protein present for the GAI^{K}-GFP line and the GAI$^{K/R}$-GFP 1.0, than 2.0, which has a low level of fusion protein expression by comparison. When the samples were equalised for total protein it was difficult to get a meaningful comparison of levels of the fusion protein as this led to overexposure of the samples with higher expression.

While the protein expression level of GAI$^{K/R}$-GFP 2.0 was low, there was clear expression of the transgene within this independent transgenic line. Of the three transgenic lines this one did have the lowest level of both GAI and GFP, although not with the noticeable difference evident when comparing protein expression. This shows that the process within the plant of converting transgene to fusion protein could have lead to disparity in expression from what might be anticipated. Indeed, when comparing protein expression, GAI^{K}-GFP 1.0 had the highest level of expression, while GAI-GFP$^{K/R}$ 1.0 was lesser, but based on GFP as a measure of transgene expression, the mutant line had higher expression than the non-mutant line.

The result of overnight incubation of the GAI^{K}-GFP fusion protein with gibberellin, show that GAI confers some resistance to degradation (Figure 3-12). It was predicted that SUMOylation of the fusion protein perhaps conferred increased resistance to degradation, via signalling by gibberellin. Previous data from publication has found GAI to be more resistant to degradation than RGA had been shown to be (Silverstone *et al.*, 2001; Fleck & Harberd, 2002; Dill, Jung & Sun, 2001), although the resistance of GAI to degradation has been disputed

(Dill *et al.*, 2004). The lack of overnight degradation of GAI to be due to the 35S promoter continuing to drive expression of the GAI protein following GA application in seedlings, meaning that GAI is degraded but more is also produced. One way to test this would be to include addition of the protein biosynthesis inhibitor cycloheximide, to see if this would yield results showing GAI degradation. In addition, another DELLA protein in *Arabidopsis*, RGL1, was found to be resistant to degradation when part of the GFP-RGL1 fusion protein (Wen & Chang, 2002) suggesting that there are clear differences in the behaviour of DELLA proteins and their interactions with gibberellin. The results obtained here allow some further debate about the effectiveness of gibberellin at signalling for degradation of the DELLA protein. Indeed it can be noted that the effects of gibberellin on the transgenic *Arabidopsis* lines was also not as predicted in phenotypic experiments (Figure 3-9), with it seeming to have some inhibitory effect on growth of lines with the GAI^{K}-GFP and $GAI^{K/R}$-GFP transgenes.

An integral finding is that there is a reduction in level of SUMOylation when the $GAI^{K/R}$ mutation is introduced into *Arabidopsis thaliana* (Figure 3-13). This confirms that the difference in the phenotype and genotype of these transgenic lines is linked to the capacity for the GAI protein to be SUMOylated.

3.5.3 Microscopy and comparison of the p35S:GAI^{K}-GFP and p35S:GAI$^{K/R}$-GFP lines

Previous data demonstrated that GAI localised to the nucleus of *Arabidopsis* cells (Fleck & Harberd, 2002). My results confirmed this and use of the p35SS:GAI$^{K/R}$-GFP protein showed that we can now discount the hypothesis that SUMOyation alters the localisation of the GAI protein.

Incorporating gibberellin into the hypothesis, it was found that the GAI^{K}-GFP fusion protein seems to be more resistant to degradation by gibberellin than the GAI$^{K/R}$-GFP protein. When carrying out confocal microscopy, more nuclear localisation of the fusion protein is evident in the GAI^{K}-GFP cotyledon samples than the GAI$^{K/R}$-GFP. However, it was difficult to measure this quantitatively. Techniques such as differential centrifugation and western blotting would have allowed more quantitative measurement of the level of the ^{K} and $^{K/R}$ versions of the fusion protein in whole leaf samples, and additionally in individual organelles from plant cells.

What is clear from the results is that neither of the mutant or non-mutant fusion protein was fully degraded over a 3-hour period when 100μM gibberellin had been applied. This could be down to GAI being more resistant to degradation, as suggested by Figure 3-12, or that gibberellin does not have such a profound effect on degradation of GAI as it does on other DELLA proteins as noted above. It is also a possible conclusion that the GAI^{K}-GFP fusion protein is more resistant to degradation, and has greater stability, than the GAI$^{K/R}$-GFP fusion protein. This conclusion is drawn based on the presence of more nuclear

localisation of this protein still present following gibberellin treatment. This enhanced stability may well be due to the ability of the GAI protein to be SUMOylated as part of the GAI^{K}-GFP fusion protein, where it cannot in the GAI$^{K/R}$-GFP protein.

Figure 3-12 shows that the GAI^{K}-GFP fusion protein is resistant to degradation following overnight treatment with gibberellin, so evidence gathered here suggests that gibberellin may have a lesser effect on GAI than other *Arabidopsis* DELLA proteins. Results suggest that a single application leads to degradation of GAI by GA, through the GID1 receptor (*Figure 3-15*). When left for a longer time 35S promoter continues to carry out function and the either GA is not taken up efficiently, the GA response becomes damped, or plants are desensitised to GA or GA is degraded quicker (Figure 3-12).

3.5.4 Conclusions drawn from Phenotyping and Genotyping and effect of SUMOylation

A combination of the results from the phenotypic, genotypic and microscopy studies gives an interesting story. While phenotypic analysis shows that the GAI$^{K/R}$-GFP line is earlier to bolting, lower vegetative growth at bolting than GAI^{K}-GFP, and more tolerant to abiotic stresses, in terms of impairment of primary root length, confocal microscopy suggests that the GAI^{K}-GFP line is more resistant to destabilisation and degradation by gibberellin, reinforced by the fact that the GAI^{K}-GFP fusion protein is not degraded following overnight gibberellin treatment.

There is some difference between the two GAI$^{K/R}$-GFP lines studied, in terms of their gene and protein expression profiles. As GAI$^{K/R}$-GFP 2.0 has a low level of fusion protein, this may lead to it having less functionality as a subject for these studies. However, this line was used for the study of primary root phenotype (Figure 3-9) and although its phenotype compared with GAI$^{K/R}$-GFP 1.0 is somewhat variable (Figure 3-7, Figure 3-8), it does not behave like wild-type or vector only control plants, as demonstrated, suggesting that it does have a reasonable quantity of functional protein.

3.5.5 Future Work

Comparisons between GAI and RGA proteins will be presented in the final discussion section of the thesis.

Future work would include further analysis of the accumulation (or otherwise) of SUMOylated GAI protein and its responses to additional stress treatments. Experiments to further understand degradation of both the GAI^{K}-GFP and GAI$^{K/R}$-GFP fusion proteins with gibberellin treatment over a more detailed timescale would also be included.

4 Phenotypic and Genotypic Characterisation of RGA^{K} and RGA$^{K/R}$ overexpression lines

4.1 Introduction

4.1.1 DELLA Proteins and RGA

RGA (*repressor of ga1-3*) was discovered shortly after GAI, and originally termed the GAI-related sequence (GRS), due to its 83% homology in amino acid sequence with GAI. Having cloned the GRS gene, it was found to be a repressor of the *ga1*-3 phenotype and named RGA (Silverstone, Ciampaglio & Sun, 1998; Peng *et al.*, 1997). In addition, to *RGA* having homology to *GAI,* it was found to be orthologous to a number of other genes from a range of plant species such as wheat, maize (Peng *et al.*, 1999), barley, rice (Ikeda *et al.*, 2001; ChandlerRobertson, 1999; Chandler *et al.*, 2002) and grapevine (Boss & Thomas, 2002), as discussed in Chapter 3. As also previously referred to, it has been found through a number of studies of mutant plants that RGA and GAI have redundant, overlapping functions, shown by triple mutant *gai-t6, rga-24, ga1-3* plants. While neither of the individual DELLA alleles rescues the *ga1-3* phenotype, a mixture of the two alleles with *ga1-3* leads to a GA-overdose phenotype, with complete recovery of the restricted elongation growth and delayed flowering phenotypes of *ga1-3* (Dill & Sun, 2001; King, Moritz & Harberd, 2001).

While the *ga1-3* phenotype can be entirely rescued by a combination of the two DELLA null-alleles, singly the alleles have variable effects. RGA was named as the *repressor of ga1-3*, and this can be seen to be a true reflection as double

mutant (*ga1-3 rga-24*) plants are taller in stature, paler green and more apically dominant than *ga1-3* plants, although still more repressed in growth than the wild-type. However, these plants are still male sterile and seeds are not able to germinate, suggesting that RGA is not essential for these processes (Silverstone, Ciampaglio & Sun, 1998). Nonetheless, the *rga-24* allele does significantly restrict *ga1-3* phenotype, where the *gai-t6* allele is lesser in its suppressive effect (Dill & Sun, 2001; King, Moritz & Harberd, 2001). While both the double mutants flower earlier than *ga1-3*. The *rga-24 ga1-3* is alone in its ability to establish phase transition in *Arabidopsis* plants (Silverstone *et al.*, 1997; Dill & Sun, 2001).

In addition to the *rga-24* mutant, *rga-2* and *rga-3* null alleles partially complement the *ga1-3* phenotype, speeding up flowering in long and short-days in the *ga1-3* mutant background (Silverstone *et al.*, 1997; Dill & Sun, 2001; King, Moritz & Harberd, 2001). Absence of GA function also leads to limited reinstatement of trichome formation on leaves, and as a result the juvenile to adult transition is restored (Silverstone *et al.*, 1997).

RGA as a protein is known to have nuclear localisation, and it carries a nuclear localisation signal (Silverstone, Ciampaglio & Sun, 1998); (Silverstone *et al.*, 2001). In addition, when plants expressing the GFP-RGA protein were treated with gibberellin, fluorescent signal in the nucleus disappeared (Silverstone *et al.*, 2001), demonstrating the capacity of gibberellin to stimulate degradation of RGA. Further work using the DELLA domain deleted RGA mutant (rga-Δ17) (*Figure 4-1*), lacking the same amino acid sequence as gai-1, was found to be

resistant to degradation following GA application, highlighting the importance of the DELLA domain in GA control of growth. Indeed, similar results were found in work on mutant varieties of rice SLR1 and barley SLN1 proteins (Gubler *et al.*, 2002; Itoh *et al.*, 2002).

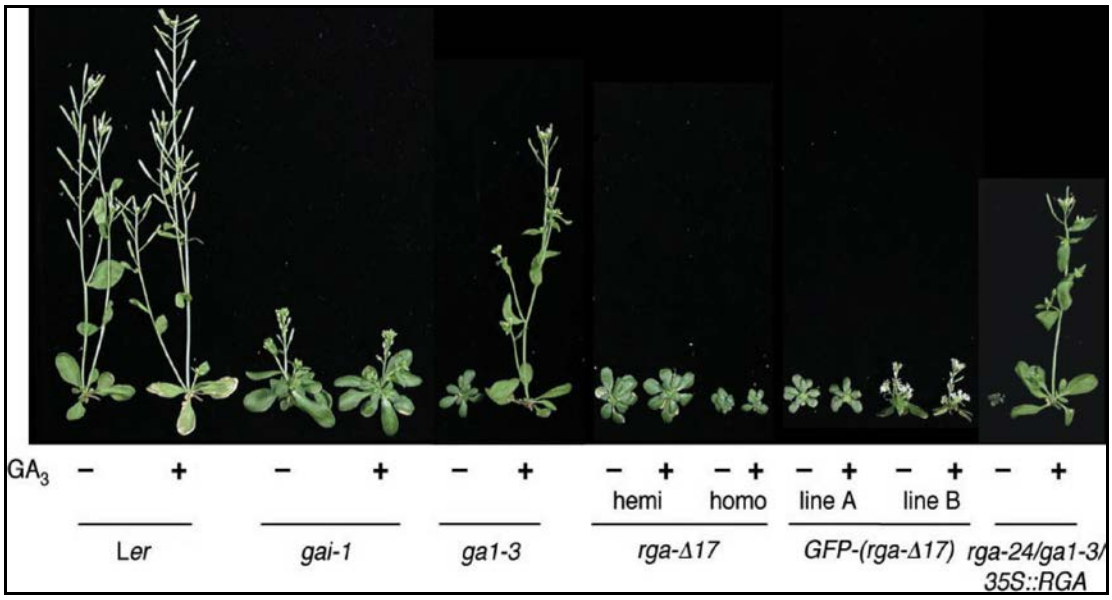

Figure 4-1 – The rga-Δ17 phenotype, whether hemizygous or homozygous, is not rescued by treatment with GA_3, while the ga1-3 mutant and rga-24/ga1-3/35S::RGA mutant is.. All lines are 36 days old and have been treated or not treated with GA_3 as indicated. All the lines except the hemizygous rga-Δ17 line are homozygous for the mutation and/or the transgene as labeled (Dill, Jung & Sun, 2001).

The *Arabidopsis* rga-Δ17 mutant has a semi-dominant dwarf phenotype, resistant to GA (*Figure 4-1*). Indeed, the protein is found to be resistant to GA-induced degradation, highlighting the essential need for the DELLA domain in the process of RGA degradation conferred by gibberellin signalling (Dill, Jung & Sun, 2001). In addition to the requirement for the DELLA domain, the GRAS domain at the C-terminal of RGA is also of high importance, emphasised by study of *rga-1* and *rga-22* mutants. The *rga-1* allele encodes a truncated protein with no GRAS domain, due to a premature stop codon, while *rga-22* has an amino-acid deletion in the GRAS domain (Dill *et al.*, 2004). These mutations

render both the mutant proteins inactive, but while the *rga-1 ga1-3* mutant has high levels of *rga* protein that is not responsive to GA treatment (i.e. no degradation of RGA), the *rga-22 ga1-3* mutant has high levels of protein but the protein is gibberellin sensitive and is degraded following GA treatment (Dill *et al.*, 2004). It is speculated that the insensitivity of *rga-1* to GA-induced degradation may be the result of the loss of the GRAS domain. It is not likely to be a result of protein inactivation as both rga-1 and rga-22 are inactive (Dill *et al.*, 2004). In addition to involvement in GA responses, RGA may also play a role in GA biosynthesis (Chiang, Hwang & Goodman, 1995); (Silverstone, Ciampaglio & Sun, 1998; Dill, Jung & Sun, 2001).

4.1.2 SUMOylation and RGA

As described in chapter 3, SUMOylation is an integral part of plant growth and development, and previous data suggested that DELLA proteins might be targets of SUMOylation. Transgenic lines were designed to test the hypothesis that SUMOylation of RGA protects RGA from degradation, so enhancing growth inhibition with or without GA. It should be noted that when supplied, the lines herein labelled as RGA^{K} and $RGA^{K/R}$ were incorrectly mislabelled as each other, which was confirmed using CAPS marker analysis (Figure 4-3). Hence, early work was led by the same hypothesis as previously discussed for GAI, namely that the RGA^{K}-GFP overexpressor would give dwarf plants and late bolting. As mentioned, CAPS markers later corrected this mistake and yielded somewhat interesting and surprising results.

Both of the *Arabidopsis* DELLA proteins RGA and GAI were analysed in this thesis, as there are differences in function between GAI and RGA; therefore we may expect that the pattern of SUMOylation differ. In addition, these two DELLA proteins have differences in their SUMOylation consensus motif and vary in similarity to non-Arabidopsis crop DELLA's (Figure 1-6). These reasons are why it is important to compare the RGA and GAI SUMOylation effects.

4.2 Objectives

- To obtain better understanding of the SUMOylation of RGA
- To elucidate any difference in behaviour of the $RGA^{K/R}$-GFP fusion protein from RGA^{K}-GFP, and deduce whether these are likely to be due to lack of SUMOylation
- Compare data with those gained with GAI, to identify differences in behaviour between DELLA proteins in *Arabidopsis thaliana*

4.3 Strategy

The first part of the investigation will be to characterise the phenotype of the transgenic p35S:RGA^{K}-GFP and p35S:$RGA^{K/R}$-GFP lines. Prior to characterising the phenotype plants have been selected to be homozygous in the T3 generation.

Secondly, having identified phenotypes, the genotype of these plant lines will be assessed, primarily through molecular techniques, but also using confocal

microscopy to ascertain whether the behaviour of the RGA protein has been altered by lack of SUMOylation.

4.4 Results

4.4.1 Line Selection

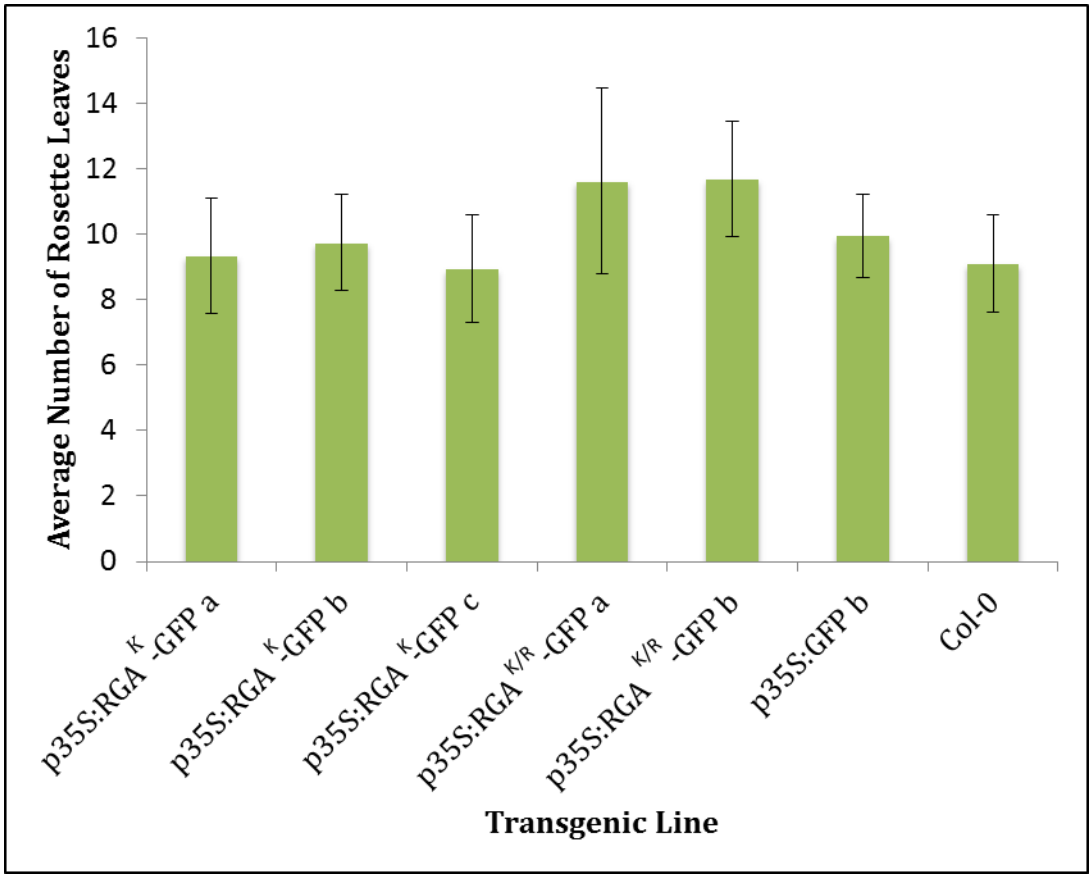

Figure 4-2 - The p35S:RGA$^{K/R}$-GFP overexpressor has more leaves at bolting than p35S:RGA^{K}-GFP lines. Comparison of mean number of rosette leaves, counted at the point of a 1cm bolt, of T2 RGA^{K}-GFP against RGA$^{K/R}$-GFP lines, with control lines included. Plants were grown in controlled environment up to 14 days old, and subsequently in glasshouse conditions. n = 18-20, with one biological replicate making up the experiment.

Transgenic lines were brought through the T2 generation and the phenotype assessed in order to decide which lines were preferable to be taken through to the T3 generation. Phenotypic analysis showed that the RGA^{K}-GFP transgenic

lines have a lower number of rosette leaves at bolting than RGA$^{K/R}$-GFP lines. The lines exhibiting the most clear divergent phenotype in this case were taken into the next generation, to see if these results were repeatable and carry out further phenotypic and genotypic analyses.

Following identification of preferable T2 lines, seeds were collected from these lines and growth up to produce the T3 generation. Independent homozygous lines at T3 identified using BASTA selection (Table 3-1, Table 3-2). Following selection, these lines were analysed by CAPS markers to confirm the transgene and confirm those lines carrying the RGA$^{K/R}$ mutation.

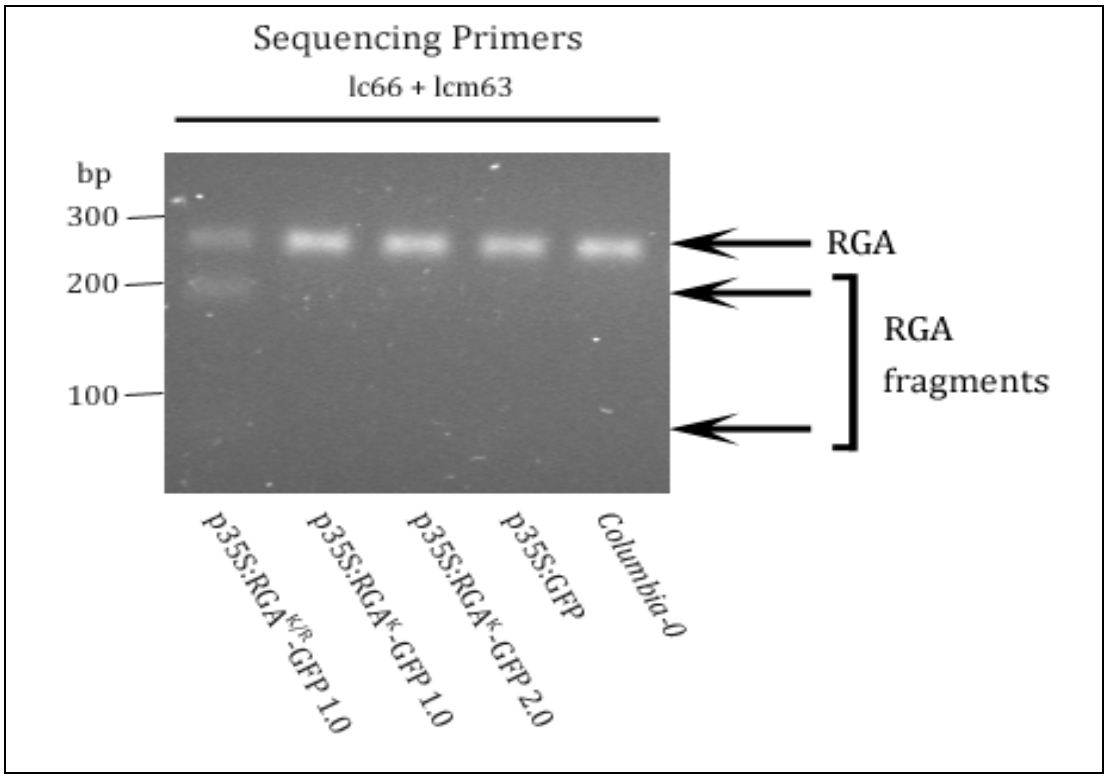

Figure 4-3 – CAPS marker analysis of p35S:RGA^{K}-GFP and p35S:RGA$^{K/R}$-GFP transgenic Arabidopsis thaliana lines. Primers were lc66 and lcm63 for PCR amplification. Genomic DNA from 5-day old representative T3 seedlings was amplified before digestion with Hinf1. Products were separated on 2.5% agarose gels.

CAPS analysis confirms the identity of the T3 transgenic lines (Figure 4-3), with the RGA$^{K/R}$-GFP line having nuclease digestion bands corresponding to the fragments cleaved at the mutation site, along with a band matching to RGA^{K}-GFP lines where there is no nuclease site and yielding one band the size of the whole amplicon for *RGA*.

4.4.2 Phenotyping

Having confirmed the sequence identity of the T3 transgenic lines, phenotypic analysis of transgenic lines was used to identify any divergence in phenotype between independent lines expressing the RGA^{K} and $^{K/R}$-GFP proteins.

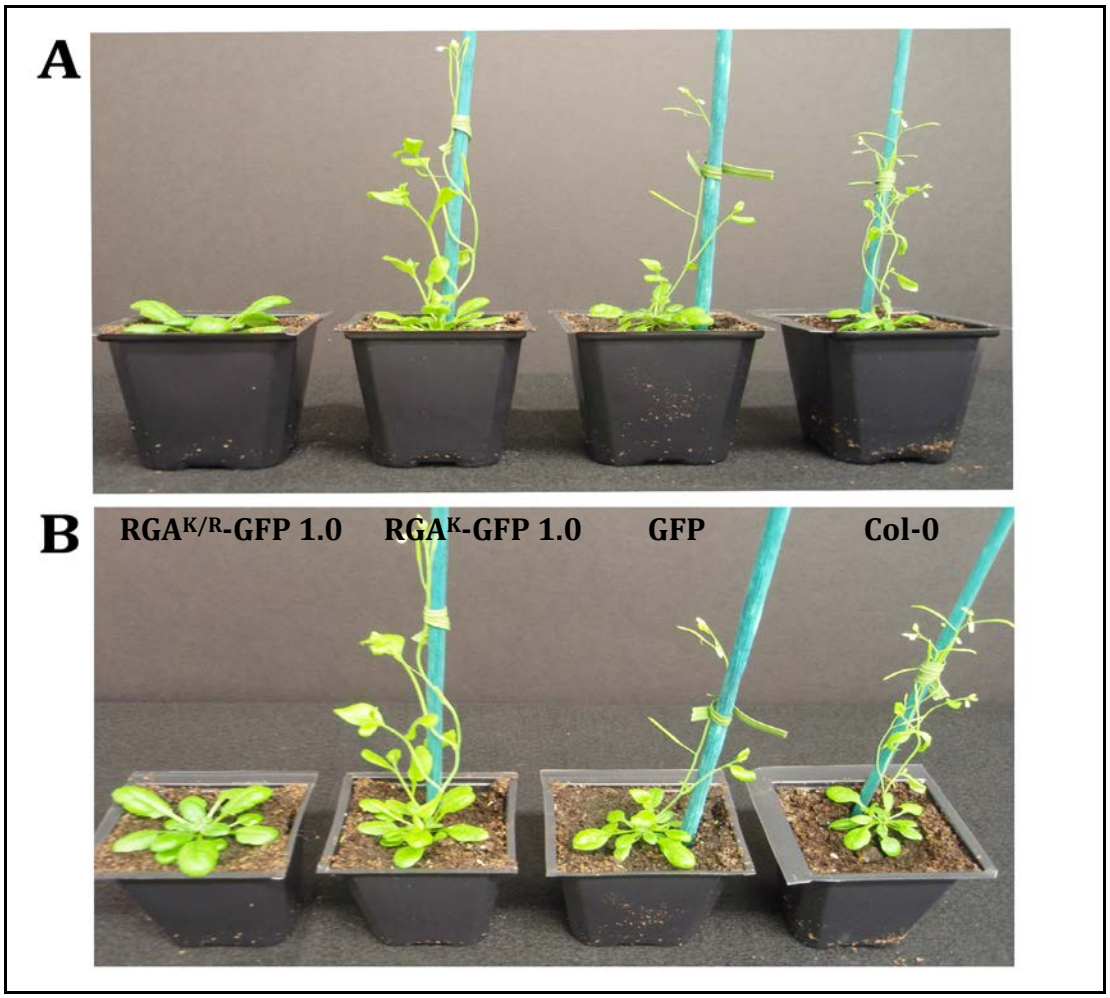

Figure 4-4 - Comparing the phenotypes of p35S:RGA^{K}-GFP and p35S:RGA$^{K/R}$-GFP overexpressing lines. One set of independent transgenic RGA^{K} and $^{K/R}$-GFP lines is shown from the side (A) and above (B). From left to right: - p35S:RGA$^{K/R}$-GFP, p35S:RGA^{K}-GFP, p35S:GFP, Columbia-0. Plants were grown in controlled environment up to 14 days old, and subsequently grown in glasshouse conditions.

From images of the plant lines overexpressing RGA^{K} or RGA$^{K/R}$-GFP, it is clear that there are some differences in the phenotype of the two plant lines (Figure 4-4). Most dramatically, the RGA$^{K/R}$-GFP plant demonstrates delayed bolting compared with the RGA^{K}-GFP line and controls. This is in marked contrast to the bolting phenotype of GAI^{K}-GFP and GAI$^{K/R}$-GFP lines (Figure 3-8).

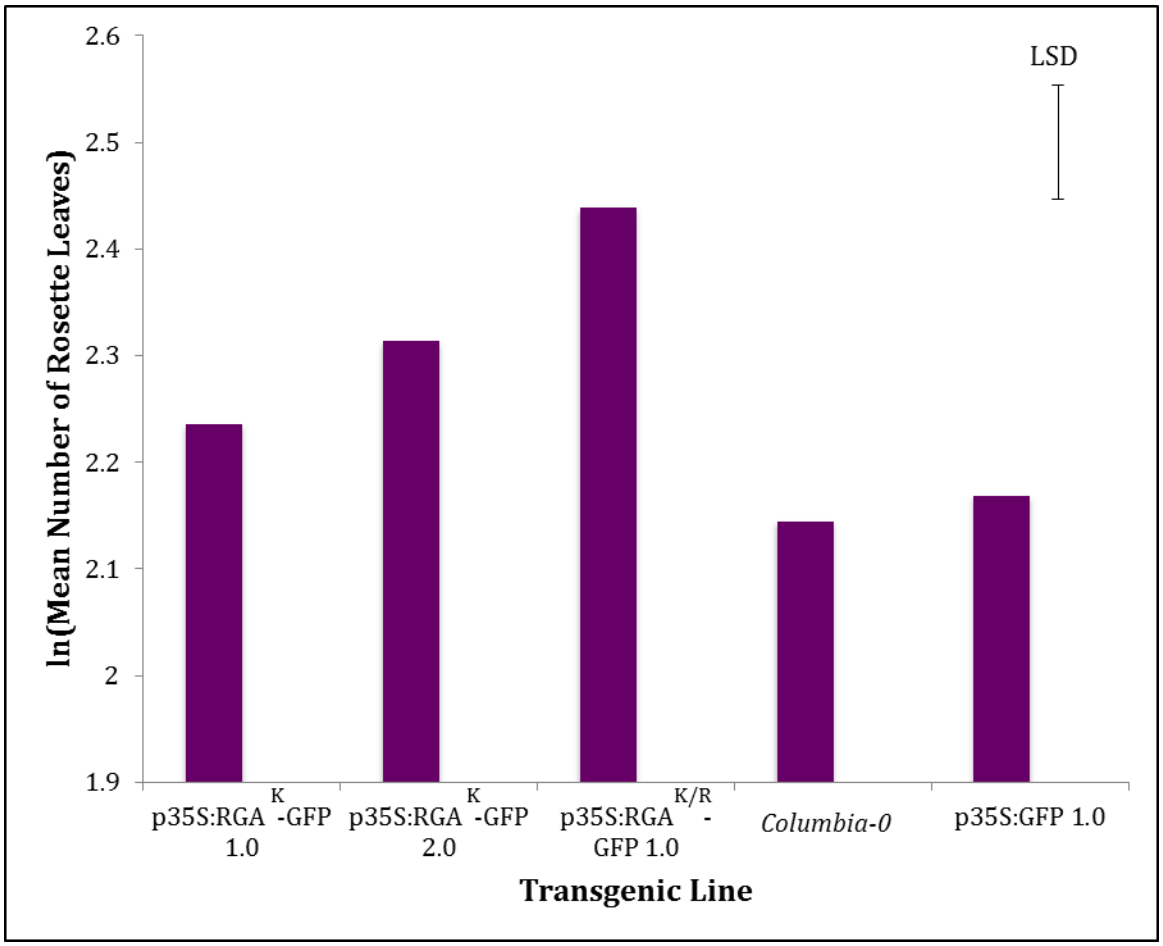

Figure 4-5 – The p35S:RGA$^{K/R}$-GFP overexpressor has more leaves at bolting than p35S:RGA^{K}-GFP lines. Comparison of the natural log transformation of mean number of rosette leaves, counted at the point of a 1cm bolt, of T3 RGA^{K}-GFP against RGA$^{K/R}$-GFP lines, with control lines included. Plants were grown in controlled environment up to 14 days old, and subsequently in glasshouse conditions. General ANOVA found P<0.001, LSD (P<0.05) – 0.1070, d.f. – 99. n = 12-24, with two biological replicates making up the experiment.

Data collected on the mean number of rosette leaves at bolting found that RGA$^{K/R}$-GFP 1.0 had a higher number of rosette leaves at the point of bolting than the RGA^{K}-GFP 1.0 and 2.0. Both the Col-0 and vector only controls had fewer rosette leaves at bolting than any RGA^{K} and $^{K/R}$-GFP lines, suggesting that overexpression of RGA promotes the number of rosette leaves. These results agree with T2 data (Figure 4-2), giving us further confidence that they are accurate.

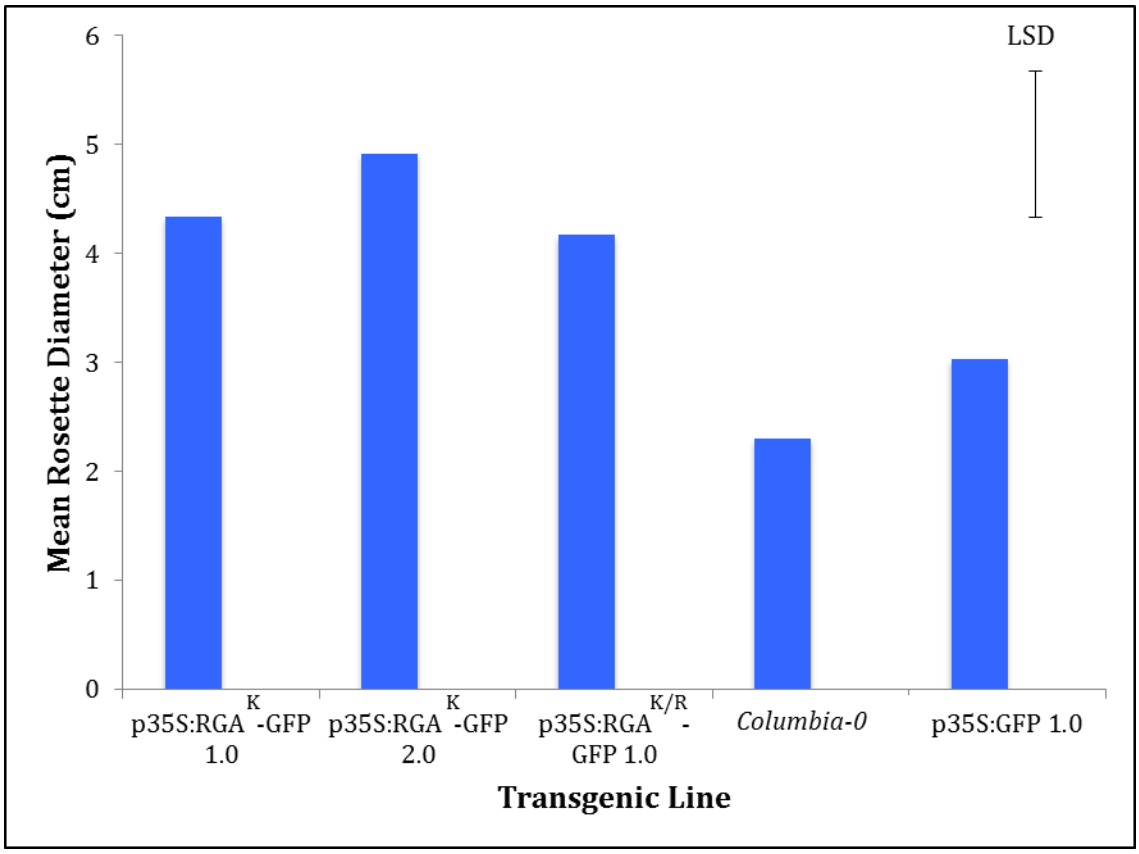

Figure 4-6 – Rosette diameters at bolting. Bolting defined as a 1cm inflorescence stem. Plants were grown in controlled environment up to 14 days old, and subsequently grown in glasshouse conditions. General ANOVA found P<0.01, LSD (P<0.05) – 1.340, d.f. - 53. n = 9-12, with one biological replicate making up the experiment.

Rosette diameter is another measure of bolting scoring when characterising DELLA mutants. For, while DELLA's often repress growth of the plant, this leads to a longer vegetative stage of growth and therefore generally more rosette leaves and a larger rosette size at bolting. It is noted that there is no significant difference between all the overexpressing lines, but again all overexpressing lines have larger rosettes than the controls.

As stated in Chapter 3, previous work in the group has shown that SUMO proteases OTS1 and OTS2 moderate growth in response to salt (NaCl) stress (Conti *et al.*, 2008) and part of this action is through regulating the pool of

DELLA proteins. Hence, it was important to test the growth responses of DELLA^{K} and DELLA$^{K/R}$-GFP lines under salt stress. As for GAI, this experiment was set up with RGA to test the root growth phenotypes of the overexpressing lines, so that GAI and RGA could be directly compared. As noted, GAI is found to play a specialised role in *Arabidopsis* root growth (Busov *et al.*, 2006; Ubeda-Tomás *et al.*, 2008; 2009), while RGA is known to be more involved in stem growth/hypocotyl elongation (King, Moritz & Harberd, 2001).

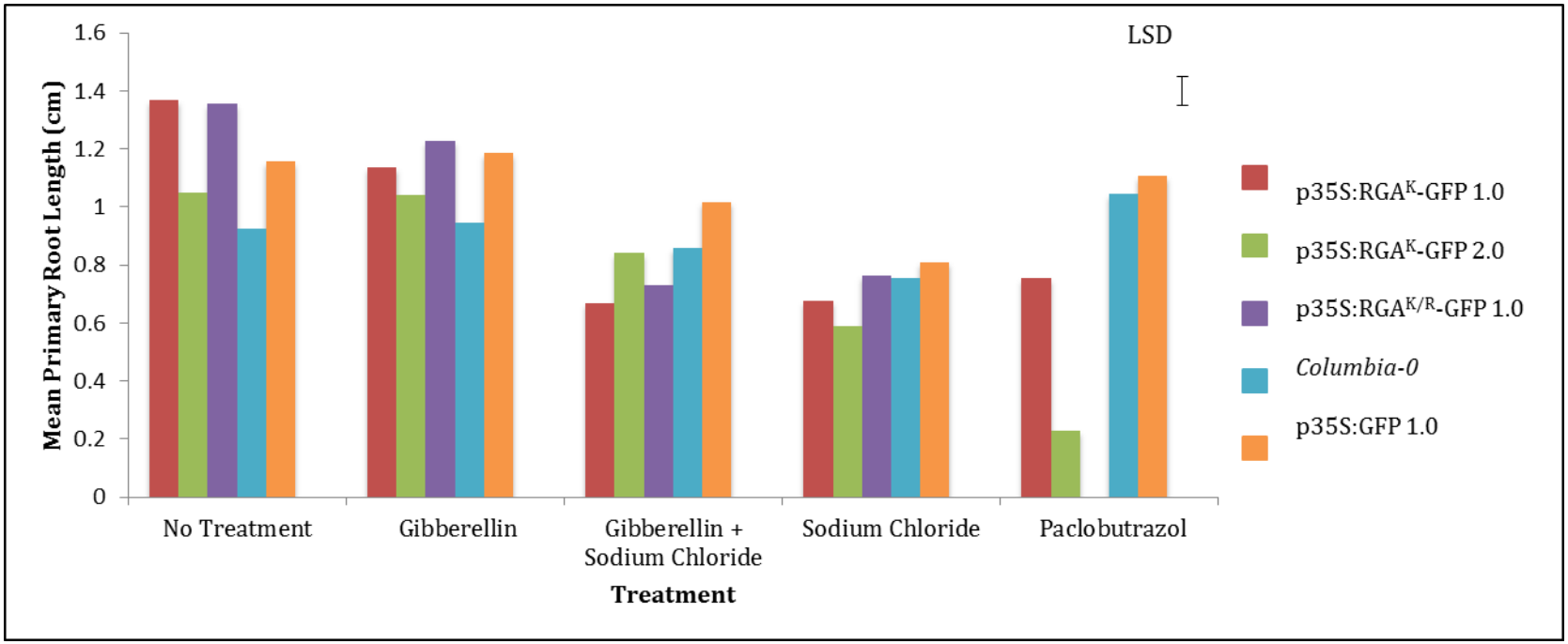

Figure 4-7 – Abiotic stress inhibits root growth, but does not induce differential responses between p35S:RGA^{K} and $^{K/R}$-GFP overexpressing lines, nor between these overexpressing lines and controls. T3 seeds from the transgenic lines were germinated and grown vertically in constant light and in controlled environment on ½ MS media plates containing different treatments (no treatment, 100µM gibberellin, 100µM gibberellin and 100mM sodium chloride, 100mM sodium chloride and 0.5µM paclobutrazol) for 10 days before data was collected. Plates were scanned and primary root length measured with Image J software. General ANOVA found P<0.001, LSD (P<0.05) - 0.09683, d.f. - 658. No root growth on paclobutrazol indicates no germination for line p35S:RGA$^{K/R}$-GFP 1.0. n= 27-30 with the experiment conducted in two technical replicates and one biological replicate.

Analysis of abiotic stress on primary root growth shows that there is no consistent difference between RGA^{K} and $RGA^{K/R}$-GFP lines (Figure 4-7). Line RGA^{K}-GFP 1.0 and $RGA^{K/R}$-GFP 1.0 give very similar data, while RGA^{K}-GFP 2.0 is consistently a little shorter. As before, the control lines Col-0 and GFP 1.0 respond consistently in their pattern of growth during different treatments.

When 100μM gibberellin is applied there is little response at all from any line, supporting the previous data showing that RGA affects growth mainly in shoot tissues. Abiotic stress in the shape of salt stress severely inhibits root growth in all lines and there is no pronounced effect of RGA overexpression with or without SUMOylation. If stress sometimes drives more or less SUMOylation of DELLA pools, it is clear that neither deSUMOylated nor wild-type RGA has a role in primary root elongation. Hence, compounding treatments will also reveal no further phenotype.

4.4.3 Assessment of Gene Expression

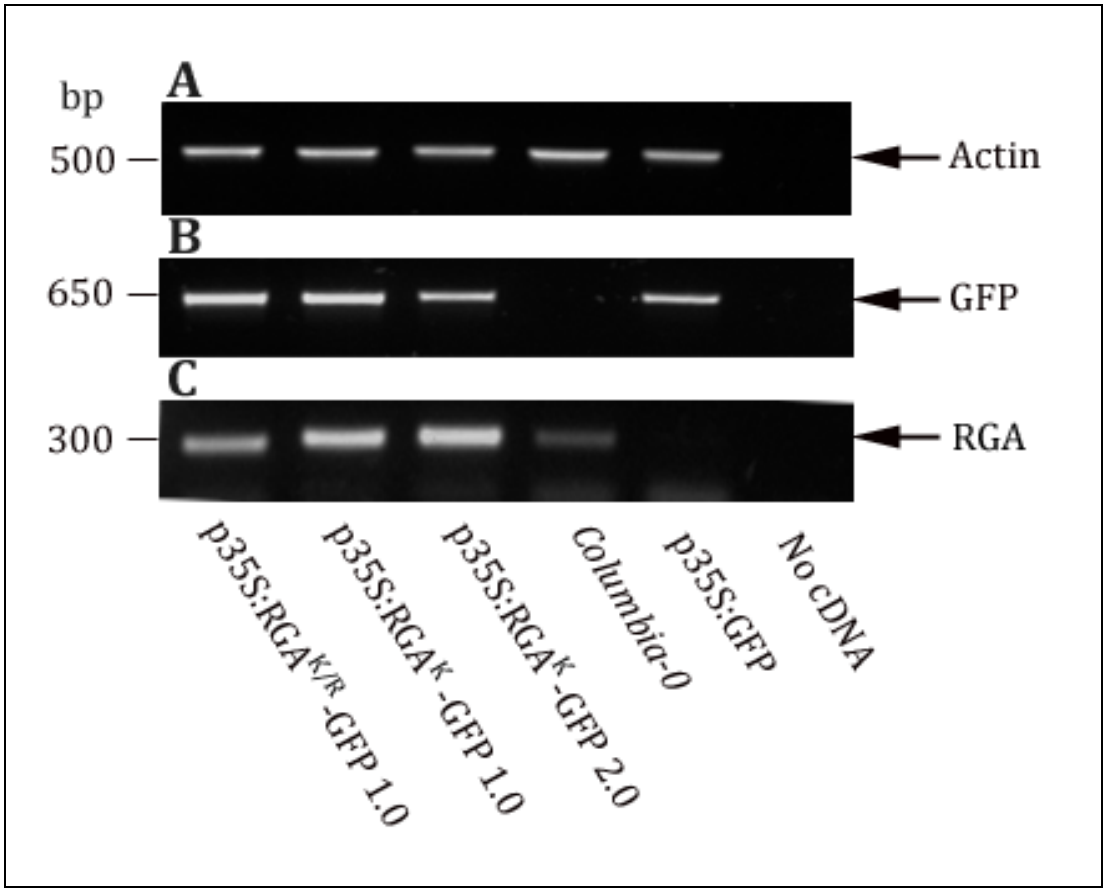

Figure 4-8 - RT-PCR to show expression levels in p35S:RGA^{K}-GFP and p35S:RGA$^{K/R}$-GFP lines and controls. RNA was extracted from 7 day-old Arabidopsis thaliana whole seedlings. Data are shown after gel electrophoresis of RT-PCR products on a 1% agarose gel. Actin PCR was used as an indicator for total cDNA in samples (A) after which PCR was carried out with GFP primers (B) and RGA primers (C).

Actin levels for the different cDNA samples are comparable (Figure 4-8A), meaning that some degree of comparison of samples for GFP and RGA levels was possible, although as referred to in Chapter 3 there was only limited scope for interpretation using RT-PCR, as it is not a quantitative technique. Analysing the levels of GFP expressed, expression could be interpreted as slightly higher in RGA^{K} and RGA$^{K/R}$-GFP 1.0 lines, compared to RGA^{K}-GFP 2.0 (Figure 4-8B). There is expression of GFP in the vector only control as would be expected in this positive control, and no expression of GFP in the Col-0 line. The results for RGA primers differ a little from those for GFP, perhaps due to the presence of both

endogenous and transgenic RGA (Figure 4-8C). RGA$^{K/R}$-GFP 1.0 has lower expression of RGA, where RGA^{K}-GFP 1.0 and 2.0 appear to have higher expression. RGA is detectable in the Col-0 line, representative only of endogenous RGA, although there is no RGA visible in the p35S:GFP control.

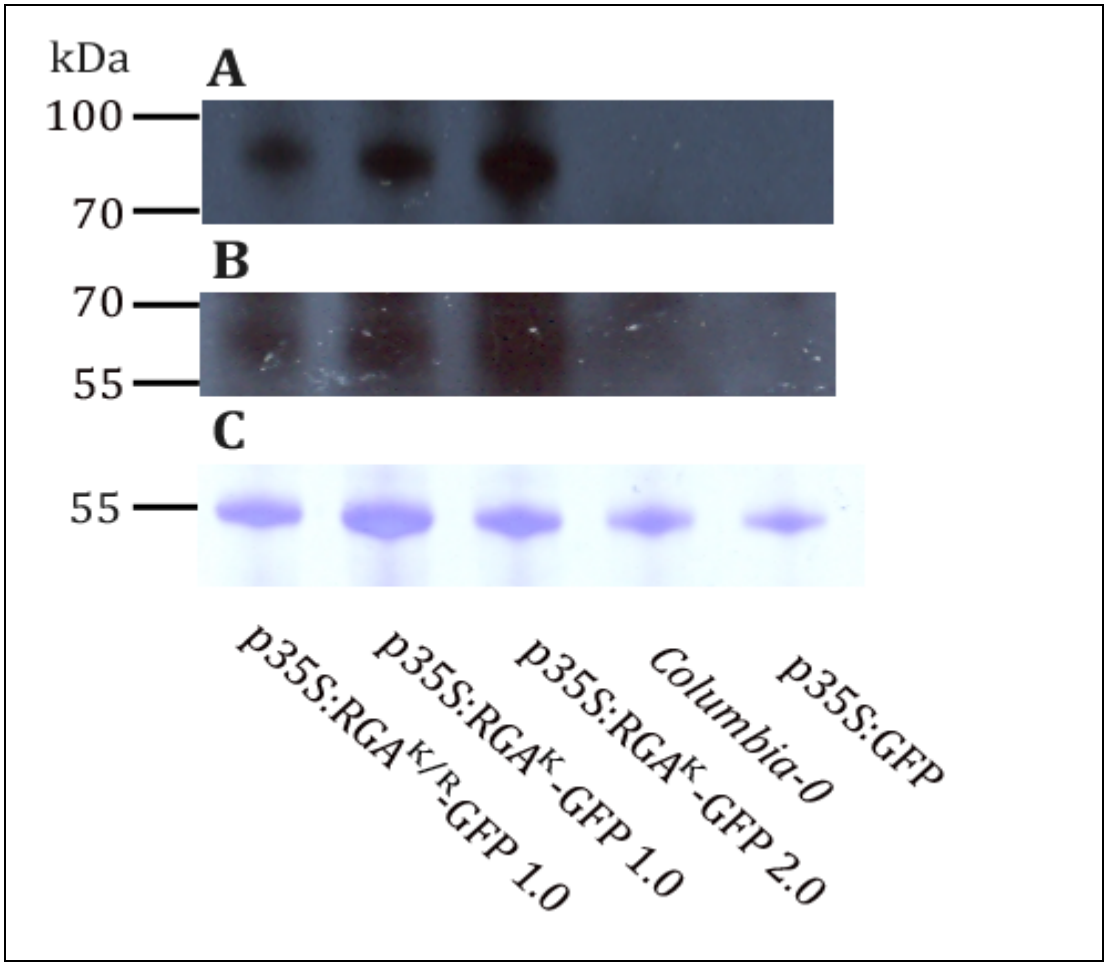

Figure 4-9 - Western blot of protein expression in p35S:RGA^{K}-GFP and p35S:RGA$^{K/R}$-GFP lines. Protein was extracted from 7 day-old Arabidopsis thaliana seedlings and applied to a 4-12% polyacrylamide gel for SDS-PAGE gel electrophoresis. Transfer to PVDF membrane ran overnight. Blots were developed with primary and secondary antibodies and ECL detection. The figure shows the developed western blot for primary antibody anti-RGA (A and B) and coomassie blue-stained PVDF membrane as a loading register (C).

Comparison of the transgene and protein levels was a key part of assessing the RGA overexpressing lines. The RGA-GFP (^{K} or $^{K/R}$) fusion protein was present in the three overexpressing lines in variable quantities (Figure 4-9). The lowest

level of protein was present in the RGA$^{K/R}$-GFP 1.0 line, with more protein expression in the RGA^{K}-GFP 1.0 line, and the most in RGA^{K}-GFP 2.0. However, there was slightly less total protein in the RGA$^{K/R}$-GFP line (Figure 4-9C), which may account for some of the differences in level of RGA detection in the immunoblot. No band is present corresponding to the size of the fusion protein in the GFP or Col-0 control lines, as expected. There is also a band matching the size of endogenous RGA (64kDa) for all of the overexpressing lines, although the overall signal in these experiments was always low. This may have been due to low levels of RGA accumulation, or to a weak antibody titre. The signal from endogenous RGA is similar to that of the fusion protein supporting the suggestion that even with overexpression, RGA (whether ^{K} or $^{K/R}$) does not accumulate greatly. There is some evidence of RGA in the Col-0 line, as you would expect as this control should still have endogenous RGA, although there is no such signal for vector only GFP 1.0.

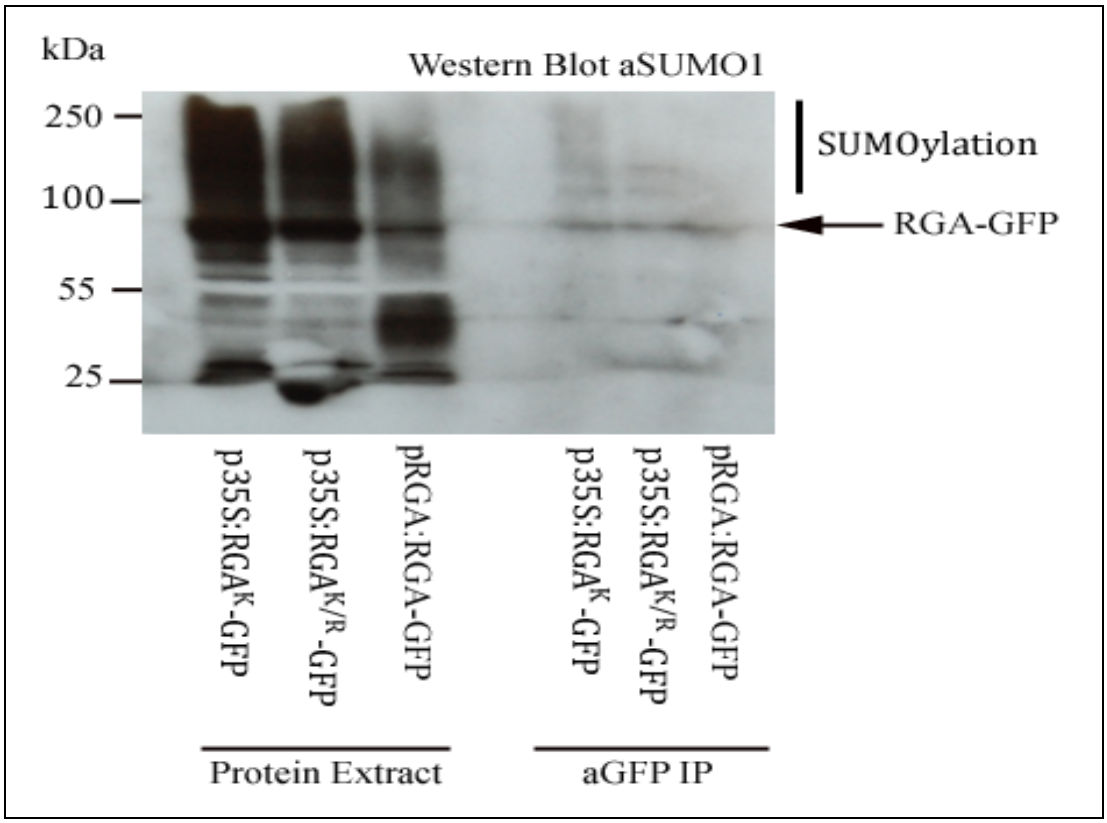

Figure 4-10 - SUMOylation assay. Western blot following immunoprecipitation with αGFP beads demonstrating SUMOylation of p35S:RGA^{K}-GFP and p35S:RGA$^{K/R}$-GFP fusion proteins. Protein was extracted from 7 day-old A. thaliana seedlings. The PVDF membrane was probed with an anti-SUMO antibody raised in rabbit, following immunoprecipitation of protein samples with αGFP beads. Equivalent seedling homogenate was used for each IP.

The direct way to confirm the presence or absence of SUMOylation capacity of the RGA^{K} and $^{K/R}$ proteins was to do a SUMOylation assay. This required using samples that had been homogenised and GFP-tagged protein selected through immunoprecipitation with αGFP beads, and carrying out a western blot on these with a primary antibody for SUMO1. Under a 35S promoter, it is evident that with immunoprecipitated samples you can see a greater level of SUMOylation (shown by the banding pattern upwards of 91kDa) in RGA^{K}-GFP samples compared to RGA$^{K/R}$-GFP samples. It appears that both RGA^{K}-GFP and RGA$^{K/R}$-GFP are SUMOylated, but the degree of SUMOylation in the RGA$^{K/R}$-GFP line is greatly reduced.

4.4.4 Microscopy

Confocal microscopy confirms the nuclear localisation of the RGA^{K}-GFP and RGA$^{K/R}$-GFP fusion proteins in both root cap and guard cells in the cotyledon (Figure 4-11). This result confirms previous work showing GFP-RGA to be nuclear localised (Silverstone *et al.*, 2001), and shows that absence or reduction in SUMOylation fails to alter this localisation in the mutant RGA$^{K/R}$-GFP line. The GFP in control GFP 1.0 is localised in the cytoplasm or at the cell membrane in cotyledon epithelial cells, and is diffuse in the root cap.

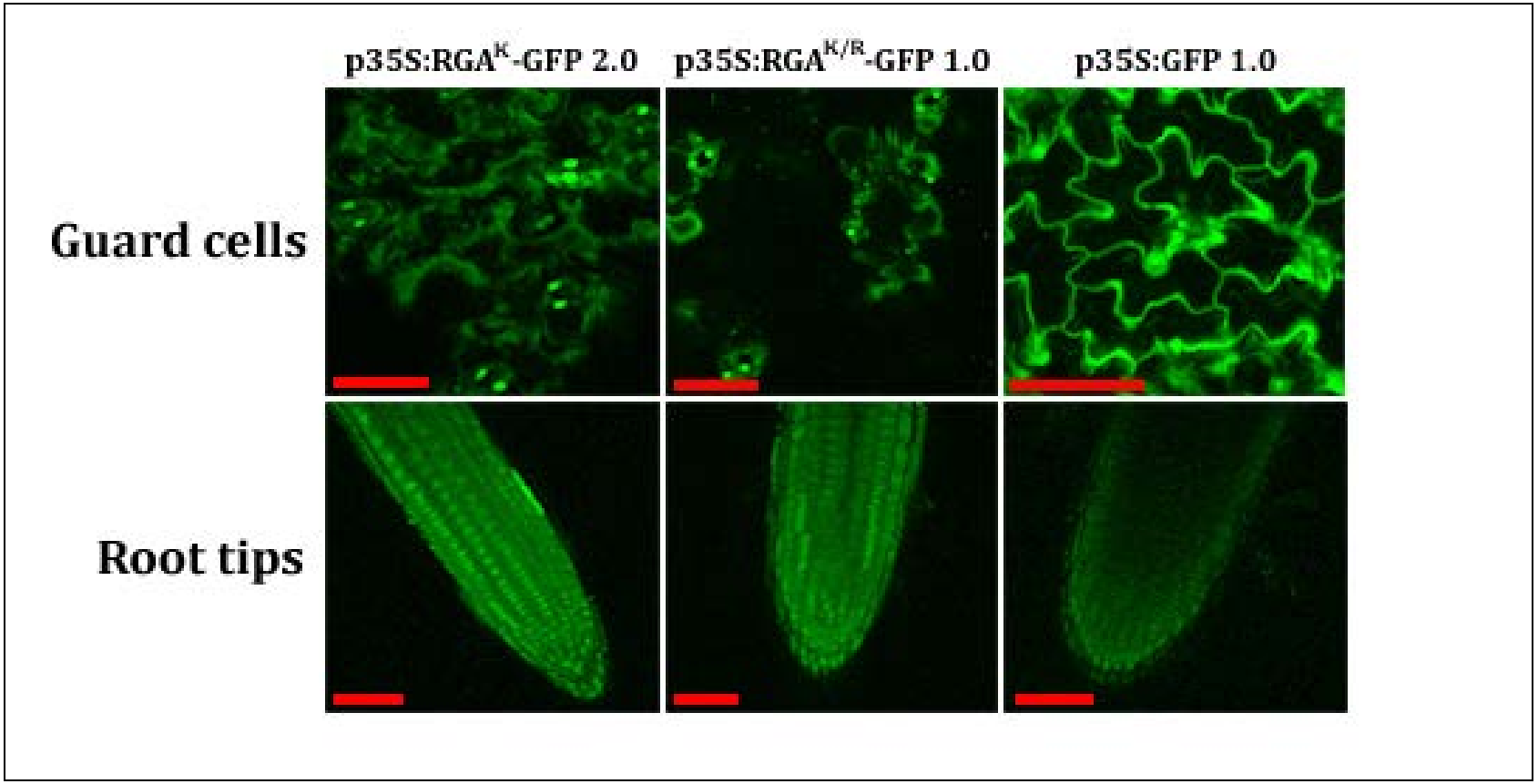

Figure 4-11 – Nuclear localisation of the p35S:RGA^{K}-GFP and p35S:RGA$^{K/R}$-GFP fusion proteins. Confocal microscopy showing localisation of RGA^{K}-GFP and RGA$^{K/R}$-GFP fusion proteins, plus the GFP control, in both guard cells from the epidermis of Arabidopsis cotyledons, and root cap/tip cells from Arabidopsis 10 day-old seedling root tissue. Scale bar in red equal to 50μM. n = 10 (Guard cells) n = 8 (Root tips).

Application of gibberellin to roots of RGA^{K}-GFP and $RGA^{K/R}$-GFP transgenic plants shows that gibberellin signalling does lead to degradation of the fusion protein, whether it includes RGA^{K} or $RGA^{K/R}$ (Figure 4-12). No distinction was found between the degradation rates of the two fusion proteins in the overexpressing lines. Interestingly, gibberellin application leads not only to degradation of the RGA proteins and loss of nuclear signal, some GFP signal appears diffusely throughout the cells. There is no disappearance of the GFP signal evident in the control GFP line 1.0 after GA treatment. The data suggest that GA treatment leads to RGA leakage or ejection from the nucleus, although SUMOylation is not involved in this relocation, but this requires further investigation.

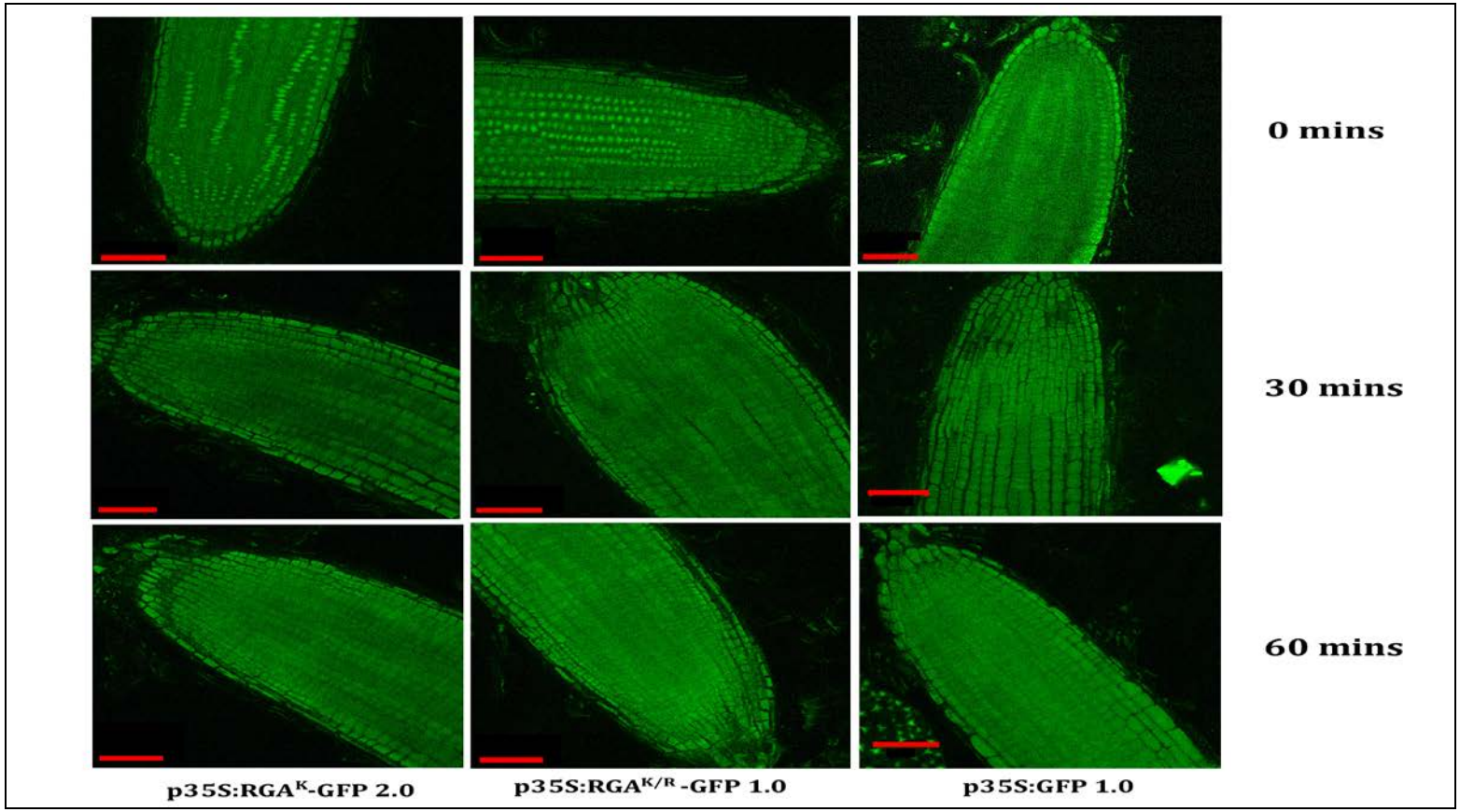

Figure 4-12 – Degradation of p35S:RGA^{K}-GFP and p35S:RGAI$^{K/R}$-GFP proteins within 1 hour of gibberellin application. Where RGA is present in root tip nuclei before treatment, after addition of GA it becomes reduces and becomes diffuse. Confocal microscopy showing localisation of RGA^{K}-GFP and RGA$^{K/R}$-GFP fusion proteins, along with the p35S:GFP control in root cap cells from the root tissue, with and without treatment with 100µM gibberellin for 0, 30 and 60 minutes using 14 day-old Arabidopsis seedlings. Scale bar in red equal to 50µM. n = 5.

One of the hypotheses of the project was that sodium chloride treatment, or other abiotic stress conditions, were involved in stimulating SUMOylation of proteins. Therefore this hypothesis extends to whether stresses such as sodium chloride have an effect on SUMOylation in the overexpressing lines. This is including consideration of the influence SUMOylation may have on DELLA proteins and whether this influence would translate to differences between the results for RGA^{K}-GFP and $RGA^{K/R}$-GFP overexpressing lines. Therefore, studying the reaction to high salinity treatment of these lines by confocal microscopy was an important experiment (Figure 4-13).

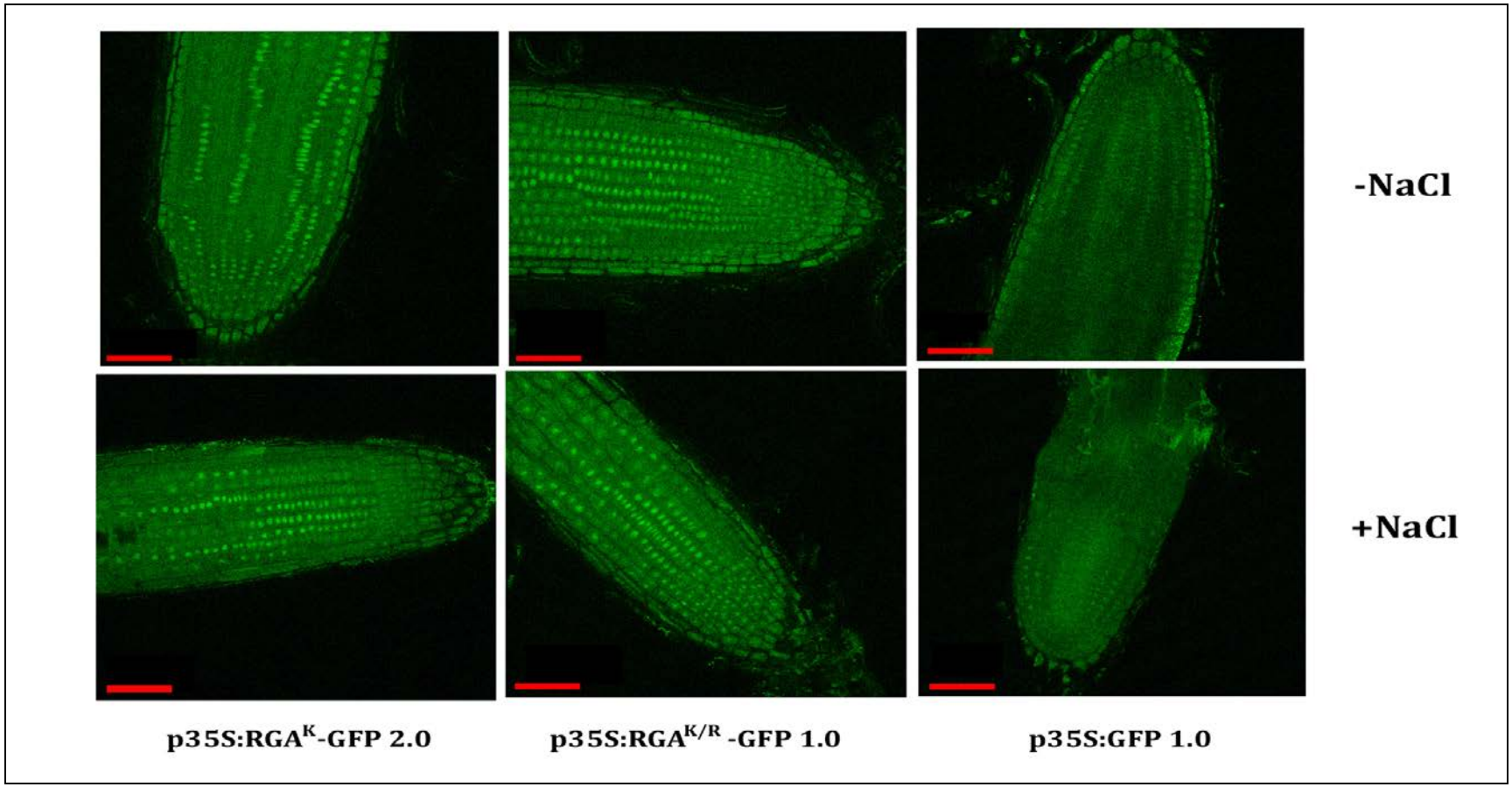

Figure 4-13 - Treatment of p35S:RGA^{K}-GFP and p35S:RGAI$^{K/R}$-GFP overexpressing lines with sodium chloride does not visibly stabilise the presence of RGA. Confocal microscopy showing localisation of RGA^{K}-GFP and RGA$^{K/R}$-GFP fusion proteins, along with the p35S:GFP control in root cap/tip cells from the root tissue. Seedlings used were 14 day-old Arabidopsis seedlings and were grown either in the presence or absence of 100mM sodium chloride. Scale bar in red equal to 50µM. n = 5.

Growth of lines on sodium chloride demonstrates that there is little difference in the presence of nuclear localised fusion protein, or the level of expression of the protein, between the RGA^{K} and $^{K/R}$-GFP lines. Thus, it seems that sodium chloride in these circumstances, may not stimulate any change in SUMOylation, conferring change in RGA protein expression, or localisation of RGA proteins.

4.5 Discussion

As stated in Chapter 3, comparison between results for RGA and GAI^{K} and $^{K/R}$-GFP transgenic lines will be made in the final thesis discussion.

4.5.1 Phenotyping and comparison of the p35S:RGA^{K}-GFP and p35S:RGA$^{K/R}$-GFP lines

The phenotype of lines with the RGA ^{K} and $^{K/R}$-GFP proteins can be explained by the genotypic characteristics of the overexpressing lines. Bolting scores show that the RGA$^{K/R}$-GFP overexpressor has delayed bolting and more rosette leaves at bolting compared with RGA^{K}-GFP lines and controls (Figure 4-4, *Figure 4-5*). This suggests that in RGA, loss of SUMOylation leads to late growth phase transition in plants, and therefore increased vegetative growth in terms of rosette leaves. In addition, it is found that RGA$^{K/R}$-GFP overexpressing plants had smaller rosette diameter at bolting than the RGA^{K}-GFP plants (Figure 4-6). This could be due to the build up of RGA$^{K/R}$-GFP protein leading to growth repression and therefore restriction in rosette size. However, this result is slightly against what one might have predicted, as usually delayed bolting leads to greater vegetative growth before the point of bolting, meaning that rosette

diameter should be larger by bolting. The image of transgenic lines (Figure 4-4) agrees with this line of reasoning, as it shows that the RGA$^{K/R}$-GFP 1.0 transgenic plant has a larger rosette than the RGA^{K}-GFP 1.0 plant. This plant was chosen as a good example of the phenotype of the RGA$^{K/R}$-GFP line, however, it seems from the statistical analysis, which was found to be significant through an ANOVA, that the majority of plants of RGA$^{K/R}$-GFP 1.0 had slightly smaller rosette size than RGA^{K} 1.0, and much smaller than RGA^{K} 2.0.

Results of the phenotyping experiments demonstrate the absence of both late flowering and dwarf phenotypes for the RGA^{K}-GFP line. This result is in direct contrast to what one might expect having analysed previous studies of plants which were either overexpressing RGA or where the RGA protein had been knocked out (Silverstone *et al.*, 1997; King, Moritz & Harberd, 2001; Dill, Jung & Sun, 2001). In this case, the RGA^{K}-GFP version confers a phenotype closer to what is anticipated for the wild-type, while RGA$^{K/R}$ has a more dwarf phenotype. Looking at the phenotyping data, these results could be due to the occurrence of cosuppression. This possibility will be proven or disproven by comparing the phenotyping data with gene and protein expression data later in the discussion. It is also possible that additional, unexpected mutations have been introduced into the construct that was transformed into the plant, leading to other effects in the plant and altering the observed phenotype. In order to ascertain whether the phenotypes recorded are an accurate reflection of the 35S:RGA^{K}-GFP and 35S:RGA$^{K/R}$-GFP constructs, the best solution would be to re-sequence the plasmids used for transformation of these transgenic lines.

Analysis of the primary root length under abiotic stress (Figure 4-7) was completed to give data comparable to those for GAI (Chapter 3). However, RGA was not found to confer any rooting phenotype in any of these lines and so these data will not be discussed further.

As already mentioned above, RGA is more important as a DELLA protein in the hypocotyl/plant shoot (King, Moritz & Harberd, 2001), so comparisons of RGA and GAI will rest primarily on shoot phenotype data (Discussion).

4.5.2 Genotyping and comparison of the p35S:RGA^{K}-GFP and p35S:RGA$^{K/R}$-GFP lines

Looking at the expression of the RGA and GFP gene fragments and the RGA protein in the overexpressing lines, there are some points that require further explanation. The level of expression of RGA in RT-PCR (endogenous and transgene) (Figure 4-8) correlates with the levels of RGA, both fusion protein and endogenous present in the transgenic plants (Figure 4-9). However, the results for GFP primers are not as definitive. Firstly, the levels of GFP originating from the transgene apparently do not match with the levels of RGA expression (Figure 4-8A/B). This can be explained by the fact that RGA expression encompasses both transgene and endogenous gene expression, whereas GFP expression is solely the transgene. Whilst protein detection shows that there is not total co-suppression of transcription, it is possible that the transgenes are affecting endogenous RGA expression to give variable translation. Secondly, the levels of GFP transgene expression (Figure 4-8B) appear to be the inverse of the translated fusion protein expression assessed by

western blots, with the lowest expression of the transgene in RGA^{K}-GFP 2.0 and the highest in RGA$^{K/R}$-GFP 1.0, where the opposite is the case for GFP fusion protein expression (Figure 4-9A). The fusion protein expressed in RGA^{K}-GFP 2.0 is visibly of greater abundance than the level of transcript suggests that it should be. One explanation for this difference in level of expression is that confusion in the translation process leads to alteration of the expression levels between gene and protein expression. It is possible that heat shock responses play some part in this notable difference between expected and actual level of protein expression.

The vector only control show a lack of detectable RGA expression, both at gene and protein level (Figure 4-8, Figure 4-9). This encompasses both the transgene/fusion protein and endogenous gene/protein. It may be that the levels of RGA are below detectable levels in this transgenic line, meaning that the Col-0 line may be a better comparison as a control. Overall the protein expression levels are suggest that the overexpressing lines are all expressing within a similar window, as the protein levels are all within the same detectable magnitude from immunoblotting (Figure 4-9).

In addition, the SUMOylation assay (Figure 4-10) confirms that the SUMOylation site identified around the lysine residue in position 65 of the RGA protein sequence is the correct site where RGA is modified by SUMO. This result also tells us that mutation of this lysine residue to an arginine to create the RGA$^{K/R}$ protein leads to reduction in the SUMOylation capacity of RGA.

4.5.3 Microscopy and comparison of the p35S:RGA^{K}-GFP and p35S:RGA$^{K/R}$-GFP lines

Nuclear localisation for RGA^{K} and $^{K/R}$-GFP is evident in both cell types analysed, showing that lack of SUMOylation does not alter localisation of this protein. In both RGA^{K} and $^{K/R}$-GFP lines gibberellin application leads to degradation of the fusion protein within 30 minutes, and no difference in time for degradation is notable between the mutant and non-mutant forms. In order to confirm this, real-time microscopy experiments would need to be carried out with the same seedling, and GFP expression visualised over a time-course to measure disappearance of the RGA^{K} or $^{K/R}$-GFP protein. In addition, using a nuclear stain such as DAPI would have allowed easier identification of the presence and subsequent loss (following GA application) of nuclear localisation. Sodium chloride does not appear to confer any difference in the expression of the RGA^{K} or $^{K/R}$-GFP fusion protein, which is in agreement with results from phenotypic experiments using sodium chloride treatment (Figure 4-7). In order to accurately confirm these results, seedlings of overexpressing lines would need to be grown on a range of sodium chloride concentrations, and the same root analysis and confocal experiments carried out for each one.

4.5.4 Conclusions drawn from Phenotyping and Genotyping and effect of SUMOylation

Overall, the phenotyping, genotyping and microscopy work carried out suggest that the RGA$^{K/R}$-GFP line has reduced levels of SUMOylation, which confers delayed bolting, more rosette leaves and a smaller rosette diameter at bolting, when compared with the RGA^{K}-GFP transgenic lines. The RGA$^{K/R}$-GFP

phenotype might be due to the mutation having some stabilising effect on this protein, but stabilisation that is not related to SUMOylation, as SUMOylation is reduced in RGA$^{K/R}$-GFP. As the GRAS domain of the RGA$^{K/R}$-GFP protein is present it still has the capacity to act like any other DELLA protein to repress growth.

As noted above, the absence of dwarfing and late-flowering phenotypes of the RGA^{K}-GFP line is the converse to expectation and other reports and this requires some consideration. It is extraordinary that the RGA^{K}-GFP version confers a phenotype closer to what is anticipated for the wild-type. Cosuppression is not a possible explanation because the immunoblot data shows that RGA is present. One possible method to elucidate the mechanisms behind this unexpected phenotype would be to re-sequence the plasmids used for transformation of these transgenic lines. A mutation in GRAS domain unrelated to the site of the $^{K/R}$ mutation would mean that RGA cannot bind DNA anymore, and would therefore lose its function as a transcriptional regulator, having numerous effects on the plants which could contribute to the overall phenotype and genotype.

Microscopy results demonstrate nuclear localisation of both the RGA^{K}-GFP and RGA$^{K/R}$-GFP proteins in root cap and guard cells. Gibberellin treatment in root cap cells leads to degradation of both forms of the protein after 30 minutes post-treatment, leaving a diffuse GFP signal in the cell, while growth on sodium chloride does not appear to confer any change in presence of the RGA^{K} or $^{K/R}$-GFP protein in cells of the root cap. This is interesting, because it shows that

the DELLA domain of RGA in both RGA^{K} and $^{K/R}$-GFP lines is functional and SUMOylation is not affecting GA-mediated interaction with GID1 and breakdown.

4.5.5 Future Work

Further work would include more extensive abiotic experiments to gather a wider picture of the responses of the RGA^{K} and $^{K/R}$-GFP proteins to different conditions. However to increase information from the work the $DELLA^{K}$ and $^{K/R}$-GFP lines would be crossed to *ots* double mutant lines and to OTS overexpressing lines to exaggerate possible SUMO phenotypes. Only shoot phenotypes would be recorded for RGA. In addition, further confocal microscopy using sodium chloride and gibberellin treatments would be useful in further elucidating the behaviour of each version of the protein within *Arabidopsis* plants, particularly the diffusion of DELLA proteins out of the nucleus after GA treatment (Figure 4-12).

One important factor is the line selection of RGA T3 lines. Further homozygous transgenic lines would need to be brought through to the T3 generation to give more scope for comparison between RGA^{K}-GFP and $RGA^{K/R}$-GFP. However, with this said, phenotype of a wider range of T2 lines incorporating both transgenes suggest that the phenotype is consistent, however these lines could not be brought forward to the T3 stage.

5 Analysis of the Binding Interactions of the SUMO1/GID1a/RGA Complex

5.1 Introduction

This chapter summarises investigations into the binding interactions between several proteins thought to have association with each other, some through previous publication and others through unpublished data.

One of these proteins is SUMO (Small Ubiquitin-Like Modifier). It is highly conserved in species from yeast to humans (Müller *et al.*, 2001), has eight isoforms in *Arabidopsis thaliana* (Kurepa *et al.*, 2003; Colby *et al.*, 2006), but is a molecule which has only come to the fore in recent years due to its similarity to ubiquitin. The SUMO structure has been solved using NMR (Bayer *et al.*, 1998) (Figure 5-1). There is only 18% sequence identity to ubiquitin, but there is a similarity in structure. Both molecules have two conserved glycine residues at the C-terminus required for isopeptide bond formation and the classic ββαββαβ fold common to the ubiquitin family (Figure 5-1A). However, while the hydrophobic core common to ubiquitin is maintained, the overall surface topology of the molecule is significantly different, suggesting that they have different potential partners in terms of substrates or modifying enzymes (Bayer *et al.*, 1998).

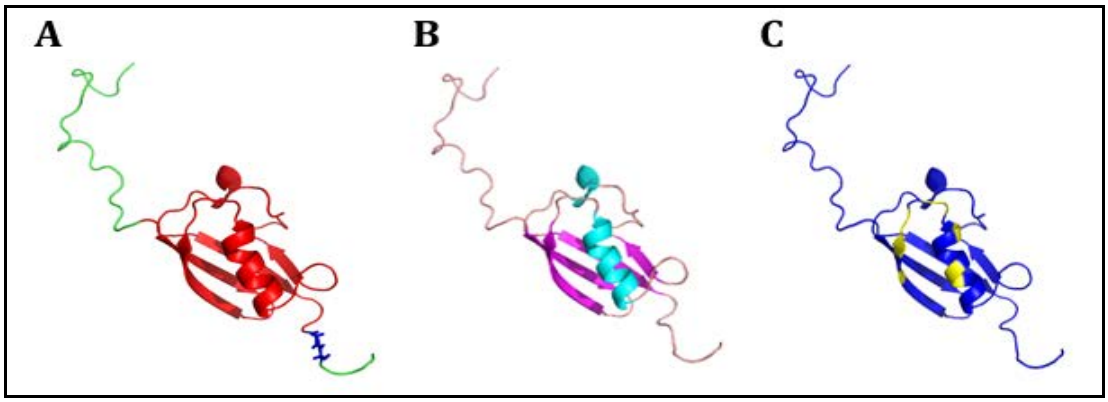

Figure 5-1 – Structural features of the SUMO1 molecule. Representations of SUMO1 showing the characteristic ubiquitin fold (red) and glycine residues (Gly96/Gly97) involved in isopeptide bond formation (blue) (A), secondary structure of the molecule; α-helix (turquoise), β-sheet (magenta) (B), and the SIM binding site on SUMO1 (yellow) (C). The structure used in the figure is SUMO1 (Protein Data Bank accession code 1A5R) (Bayer et al.*, 1998; Hecker* et al.*, 2006).*

A motif has been identified on a number of SUMO targets, which is believed to be the site at which SUMO interacts with the protein that is to be modified. This is known as a SUMO-interacting motif (SIM). The canonical and best described class of SIMs are made up of a hydrophobic core ([V/I]-X-[V/I]-[V/I]) flanked by a group of negatively charged amino acids (Song *et al.*, 2004; Kerscher, 2007), essentially a short hydrophobic β-strand, that has the ability to bind in parallel or antiparallel orientation to the β_2 strand of SUMO (Figure 5-1C) (Hecker *et al.*, 2006). The acidic residues around the core may be important for the orientation, affinity or paralogue specificity in the binding process (Hecker *et al.*, 2006; Meulmeester *et al.*, 2008). GID1 has been found to have two variant SIMs in its structure, something that could be integral in the binding interactions that are being studied in this thesis. The SIM identified in GID1 along with SIMs identified in other proteins have been presented below (Table 5-1).

Table 5-1 – SIM motifs discovered in different proteins from a range of different species including both the canonical SIM (Song et al*., 2004) and variant SIMs which have been shown to interact with SUMO1.*

Motif	Protein	Reference
[V/I]-X-[V/I]-[V/I]	RanBP2/Nup358	Song et al., 2004
K-X_{3-5}-[I/V]-[I/L]-[I/L]-X_3-[D/E/Q/N]-[D\E]-[D/E]	Sap1, Ris1, Nis1, Fir1	Hannich et al., 2005
h-h-x-[S]-[X]-[S/T]	p73α	Minty et al., 2000
[I/V/L]-[D/E]-[I/V/L]-[D/E]-[I/V/L]	CoREST1	Ouyang et al., 2009
KVDVIDLTIESSSDEEEDPPAKR	PIASX	Song et al., 2005
VVPLNTWVLISN	GID1	Unpublished data

GID1 proteins are known to be gibberellin receptors (Ueguchi-Tanaka *et al.*, 2005). GID1 from both *rice* and *Arabidopsis* has been found to be similar in consensus sequence to the hormone-sensitive lipases (HSL's) (Conti *et al.*, 2008; Ueguchi-Tanaka *et al.*, 2005; 2007a). The closest relative is AeCXE1, a plant carboxylesterase from *Actinidia eriantha* (Chosed *et al.*, 2006; Ileperuma *et al.*, 2007). Like the HSL's, GID1 has a catalytic triad (Ser, Val, Asp), a deep gibberellin-binding pocket corresponding to the substrate-binding site of HSL's, and an α/β-hydrolase fold (Mossessova & Lima, 2000; Shimada *et al.*, 2008; Li & Hochstrasser, 2003). However, in GID1, this fold also includes an amino-terminal lid, which covers GA that is buried in the binding pocket when bound onto GID1 (Conti *et al.*, 2008; Shimada *et al.*, 2008; Murase *et al.*, 2008).

Arabidopsis thaliana has three homologues of GID1: - GID1a, b and c (Gong & Yeh, 2006; Nakajima *et al.*, 2006). There is substantial evidence that indicates that these proteins work as GA receptors, including evidence from yeast-2 hybrid assays which show that all *Arabidopsis* GID1 proteins interact with the five *A. thaliana* DELLA proteins in a GA-dependent manner (Rajan *et al.*, 2005;

Griffiths *et al.*, 2006). The overlapping expression profiles of the GID1 proteins suggests a high level of functional redundancy (Gong & Yeh, 2006; Nakajima *et al.*, 2006). Indeed, the severe GA dwarf phenotype of the *gid1abc* triple mutant, demonstrated no detectable GA-dependent growth or transcriptional responses, indicating that the GID1 proteins are likely to be the predominant receptors regulating GA growth responses in *Arabidopsis* (Garvin *et al.*, 2013; Griffiths *et al.*, 2006).

Structural analysis of *Oryza sativa* GID1 bound to GA_3 show that GA_3 is embedded in the GID1 binding pocket (Li & Hochstrasser, 1999; Shimada *et al.*, 2008; Li & Hochstrasser, 2000), and the lid protects the GA molecule from solvent and prevents direct contact of GA with the DELLA protein (Taylor *et al.*, 2002; Murase *et al.*, 2008). The embedded molecule exhibits a high contact surface area by positioning the hydrophilic carboxylate toward the bottom of the binding pocket and hydrophobic aliphatic rings at the entrance (Roden *et al.*, 2004; Murase *et al.*, 2008). It has been shown through yeast-2 hybrid work that GA binding to GID1 enhances interaction with DELLA proteins such as SLR1 in rice. In contrast, studies using GA-insensitive mutants of rice and *Arabidopsis* have demonstrated that three components, GID1, DELLA protein and an F-box protein are necessary for GA perception, leading to formation of the GID1-GA-DELLA complex (Kurepa *et al.*, 2003; Ueguchi-Tanaka *et al.*, 2007b; Chosed *et al.*, 2006; Itoh, Ueguchi-Tanaka & Matsuoka, 2008; Colby *et al.*, 2006).

There are five DELLA proteins in *A.thaliana* with some redundancy in function (Lois, 2010; King, Moritz & Harberd, 2001; Dill & Sun, 2001; Lee *et al.*, 2002;

Cheng *et al.*, 2004; Tyler *et al.*, 2004b). DELLA proteins have two domains that are of significance. The GRAS domain is toward the C-terminal of the protein and is common between the GRAS family of regulatory proteins (Hermkes *et al.*, 2011; Pysh *et al.*, 1999). This domain is implicated in F-box protein binding (Colby *et al.*, 2006; Dill *et al.*, 2004). The other important domain is the N-terminal DELLA domain, which is integral for degradation of DELLA proteins in reply to gibberellin. This is highlighted by studies showing that deletion or missense mutations of conserved motifs in the domain lead to plants that exhibit a GA-insensitive dwarf phenotype (Li & Hochstrasser, 1999; Dill, Jung & Sun, 2001; Hermkes *et al.*, 2011; Gubler *et al.*, 2002; Itoh *et al.*, 2002).

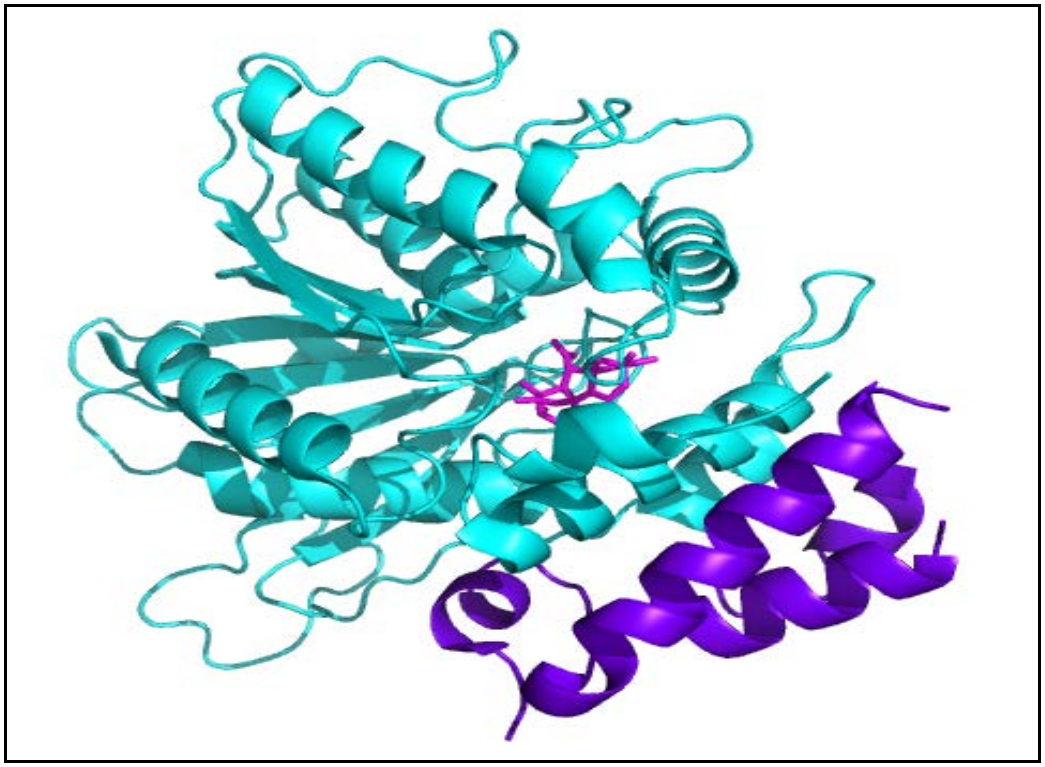

Figure 5-2 – Structural representation of the DELLA, GID1a and Gibberellin complex. The model represents GiD1a (light blue), gibberellin bound to GID1 (pink) and the DELLA domain of GAI (purple) in complex together. The structure used in the figure is GID1A, GAI (residues 11-113, the GAI DELLA domain) and ligand GA3 (Protein Data Bank accession code 2ZSH) (Murtas et al.*, 2003; Murase* et al.*, 2008).*

The DELLA domain of GAI and its interaction with GID1a were investigated with structural analysis carried out by Murase and co-workers (Figure 5-2). The DELLA domain was found to have four α-helices and a flat surface, bearing resemblance to a palm with helices B, C and D, and the fourth helix off plane like a thumb (A) (Figure 5-3A). The outside of the domain is negatively charged, where the inside forms a non-polar surface that interacts with GID1a (Reeves *et al.*, 2002; Murase *et al.*, 2008). The DELLA palm contacts GID1a via its N-terminal extension helices, and does so with non-polar interactions, whereas helix αA interacts with both the N-terminal and the core domain of GID1a. DELLA binding has a stabilising effect on the GID1a extension helices that cover the pocket trapping GA into GID1a (Murtas *et al.*, 2003; Nakajima *et al.*, 2006).

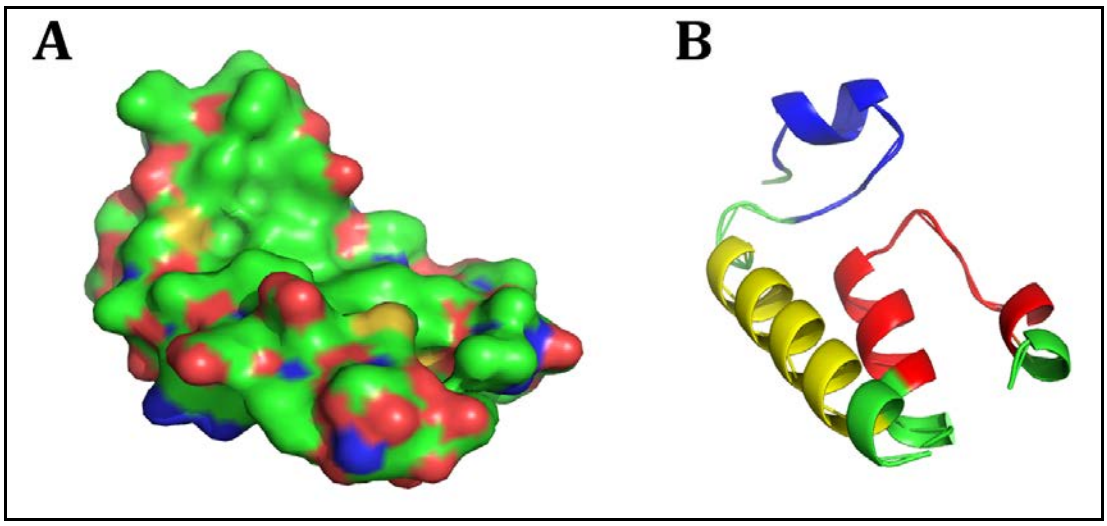

Figure 5-3 – GAI DELLA domain structure represented by two different means. The DELLA domain has a palm-like structure (αB-αD), with αA protruding upwards like a thumb (A), and has several important motifs for DELLA protein function; the DELLA motif (blue), VHYNP motif (red) and LExLE motif (yellow) (B). The structure used in the figure is GAI residues 11-113 (DELLA domain) (Protein Data Bank accession code 2ZSH) (Conti et al.*, 2008; Murase* et al.*, 2008).*

Within the DELLA domain there are three motifs that are of much importance for the interaction and direct contact with GID1a (Figure 5-3B). The first is the

DELLA motif, for GID1 recognition, within the αA helix, with sequence DeLLaΦLxYxV (where capital letters are residues that directly contact GID1, Φ represents a nonpolar residue, and lowercase letters are residues that do not have a role in direct contacts, where 'e' and 'a' represent Glu and Ala residues, and 'x' represents any residue) (Lois, 2010; Murase *et al.*, 2008). This domain has a distinct influence on binding affinity with GID1a, so much that deletion of this motif gives rise to a GA-insensitive phenotype (Mukhopadhyay & Dasso, 2007; Peng *et al.*, 1997; Dill, Jung & Sun, 2001; Itoh *et al.*, 2002). The second motif is the VHYNP motif, extending from the αC to αD loop. The HYN residues are essential for maintaining the αD helix, and subsequent loop conformation by their involvement in intra-domain interactions (Conti *et al.*, 2008; Murase *et al.*, 2008). The final motif in the DELLA domain that has a role in GID1 binding is the LExLE motif, found on helix αB. Mutations of key residues in this clearly decrease binding of the DELLA domain to the GA_3-bound GID1a (Conti *et al.*, 2009; Murase *et al.*, 2008). The N-terminal domain of DELLA proteins, inclusive of the conserved DELLA and VHYNP motifs, are found to be unstructured in the absence of any interaction with GID1. Binding-induced folding of N-terminal domains of DELLAs has been observed upon interaction with *Arabidopsis thaliana* GID1/GA (Sun *et al.*, 2010).

The work done in this chapter explores the interaction of the components GA, GID1a and DELLA with the newly identified interactor SUMO1.

5.2 Objectives

The main objectives of the analyses were to further understand binding interactions of GID1a with RGA and perhaps SUMO 1 to: -

1. Ascertain whether there was a specific interaction between GID1a and SUMO 1, and whether any GA dependency exists in this interaction
2. Demonstrate RGA binding onto GID1a

5.3 Strategy

Surface plasmon resonance (SPR) can be used to measure molecular interactions. The BIAcore is an optical apparatus that can record real-time alteration in refractive index near a gold surface. The gold chip surface is engineered with carboxy-methylated dextran over four flow cells, which can be addressed individually. Ligand is covalently attached to each flow cell by amine coupling (Conti *et al.*, 2009; Fivash, Towler & Fisher, 1998). The test protein, known as the analyte, is passed across one or more flow cells and protein binding to the chip surface results in a change in refractive index, recorded as a sensorgram (resonance units vs. time).

5.4 Results

5.4.1 Coupling to CHIP1

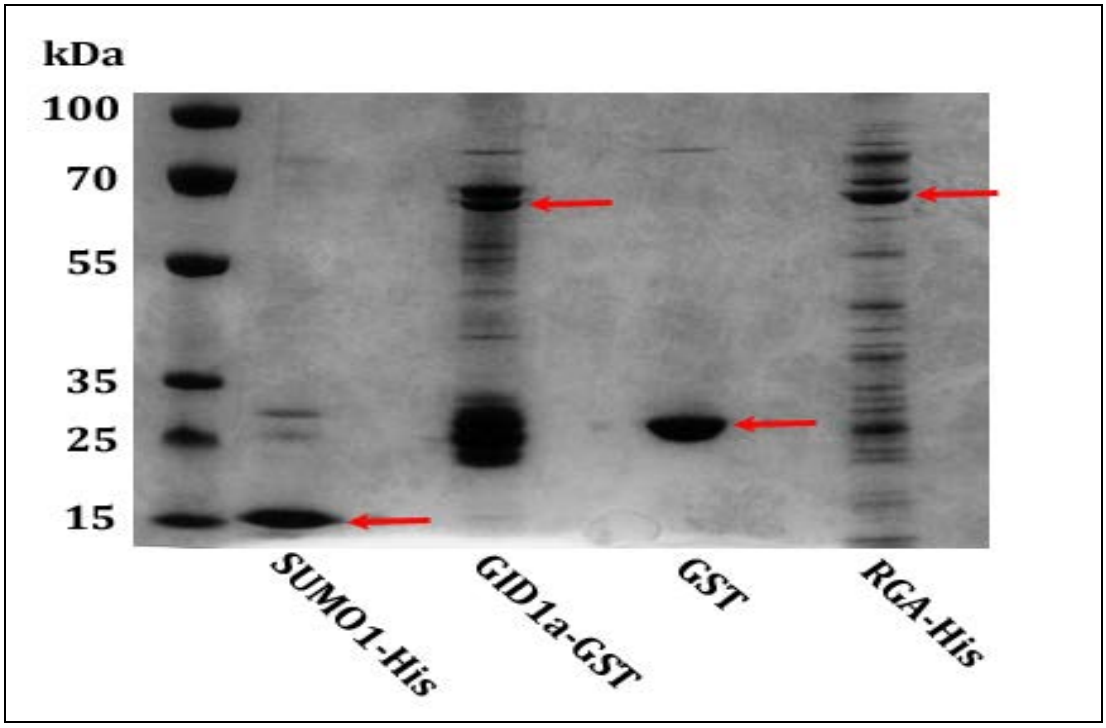

Figure 5-4 - 4-12% gradient Bis-Tris SDS-PAGE gel demonstrating the level of purity of the protein samples used for the subsequent experiments in this chapter. Gel electrophoresis run at 200 volts for 40 minutes and gel stained with Coomassie blue stain in order to visualise proteins. The proteins used were expressed and purified by Stuart Nelis (Sadanandom group, University of Durham).

The gel in Figure 5-4 demonstrates that the proteins used for SPR binding assays were all of reasonable purity and were identified at the correct molecular weight.

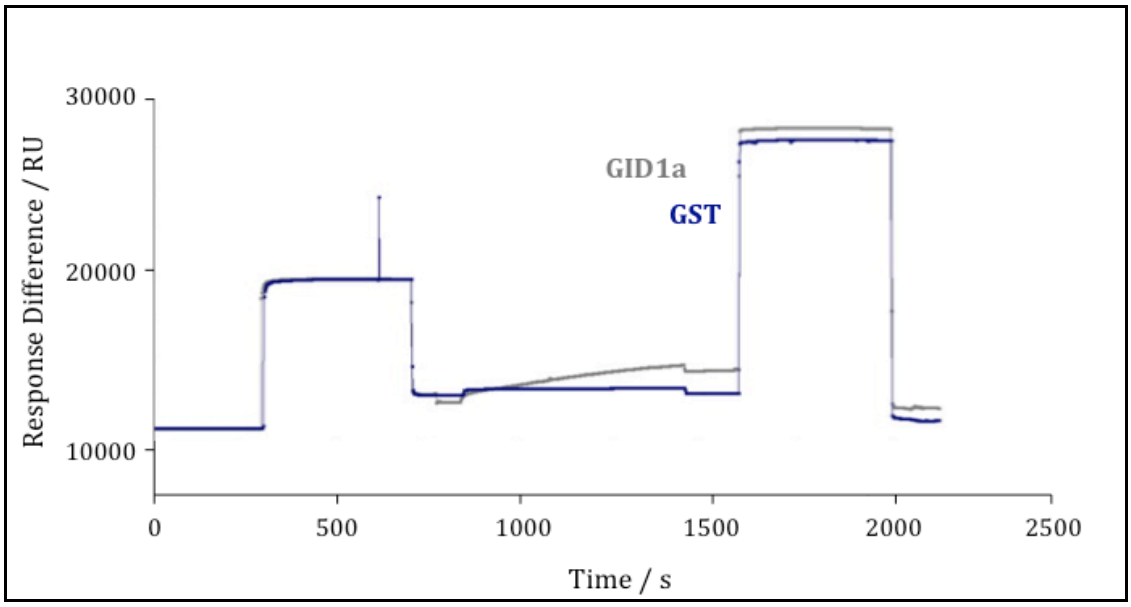

Figure 5-5 – GID1a-GST and GST binding onto a CM5 CHIP surface, in Sodium acetate buffer pH5.5, and using the reagents EDC and NHS, with Ethanolamine used for regeneration purposes. Resonance units bound onto the CHIP were ~1200 for GID1a-GST (channel 2; grey) and ~425 for GST (channel 3; blue). Each sensorgram shows data for test channel subtracting channel 1.

Channel 1 of each CM5 chip was used as a reference channel, activated and blocked using ethanolamine. From previous studies, it had been ascertained that GID1a bound optimally to the CM5 chip in a 10mM sodium acetate buffer of pH5.5. Therefore, this buffer was used to bind GID1a-GST onto the chip in channel 2 (Figure 5-5), or other channels as stated. As a control GST was coupled to channel 3. Approximately 1200 resonance units of GID1a-GST and 400 of GST were successfully bound.

5.4.2 CHIP1 Binding Experiments

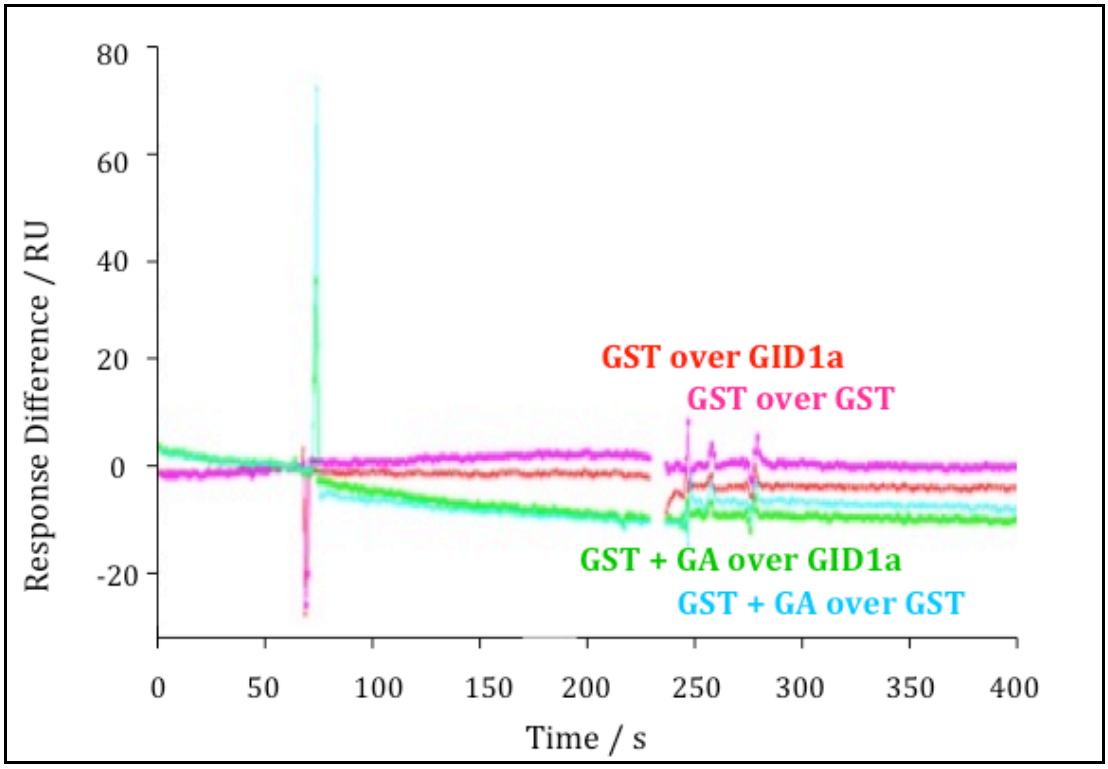

Figure 5-6 – GST does not bind to GID1a or GST. GID1a-GST and GST were passed as analyte in HBS-EP buffer +1mM DTT, in the presence and absence of 100μM GA. 10mM Glycine-HCl pH2.2 was used for chip regeneration between each run. Each sensorgram shows data for test channel subtracting ch1. Concentration of GST = 0.112mg/ml.

Having bound GID1a and GST successfully onto the CM5 chip GST was passed over GID1a and GST. In *Figure 5-6* the sensorgram traces remain flat suggesting little or no binding of GST to either GID1a-GST or GST in HBS-EP buffer.

As GST did not have interaction with GID1a, the next experiment was to study the binding of SUMO1 to GID1a, using variable GA concentration, instead of one concentration, to see if any selective binding of SUMO1 onto GID1a could be detected. The putative variant SIM on AtGID1a suggests that there would be binding of GID1a to SUMO1, independent of the presence of a DELLA protein (Table 5-1) and thus we might expect to see binding in this experiment.

Gibberellin at 1, 3, 10, 30 or 100μM was combined with SUMO1 in HBS-EP buffer in order to test these binding interactions.

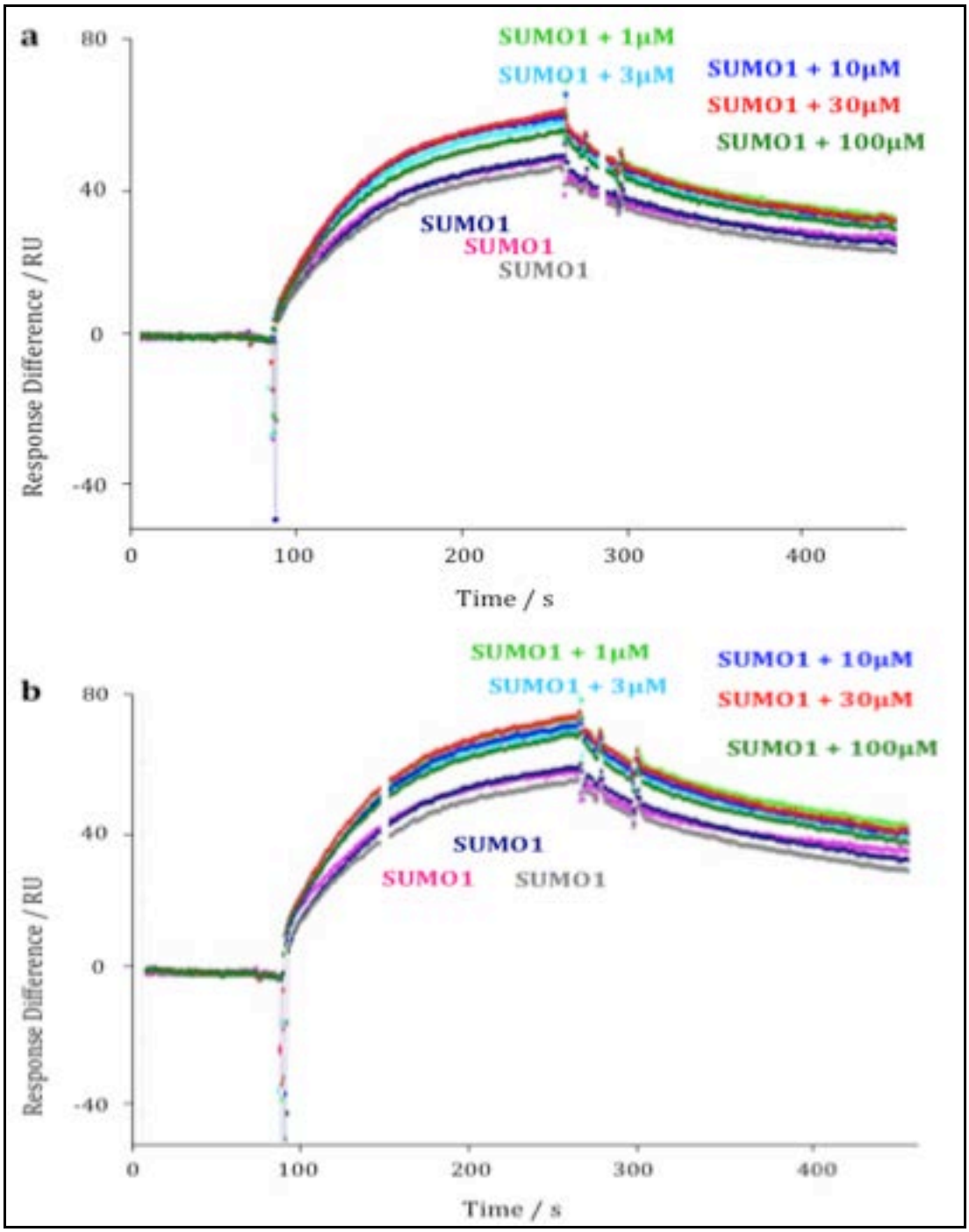

Figure 5-7 – SPR analysis of the gibberellin-dependent interaction between SUMO1 and GID1a, in HBS-EP buffer. The sensorgram shows effect without gibberellin and gibberellin at concentrations of 1, 3, 10, 30 and 100μM. The figure shows two sensorgrams, one for SUMO1 interacting with GID1a (a) and one for interaction with GST (b). 10mM Glycine-HCl pH2.2 was used for chip regeneration. Each sensorgram shows data for test channel subtracting ch1. Concentration of SUMO1 = 0.055mg/ml.

The sensorgram shows the interaction of SUMO1 with both GID1a-GST (a) and GST (b) (Figure 5-7). There is some binding of SUMO1 to both GID1 and GST, at a level of approximately 60-80 resonance units. Indeed, there is probably marginally more binding of SUMO1 to the negative control GST, which has binding to a level of almost 80 resonance units, where binding to GID1a is closer to 60 resonance units. This leads to the conclusion that there is no selective binding between SUMO1 and GID1a in HBS-EP buffer, something that fits with replicate data collected. Additionally, as all of the sensorgram traces for SUMO1 interacting with GID1 and GST were collected together, there is no clear GA dependence demonstrated in binding of SUMO1 to GID1a-GST or GST in HBS-EP buffer. Even the lowest GA concentration appeared to support a little extra binding, but this was a feature of both GID1a and GST sensorgrams. This GA effect may be associated with masking hydrophobicity.

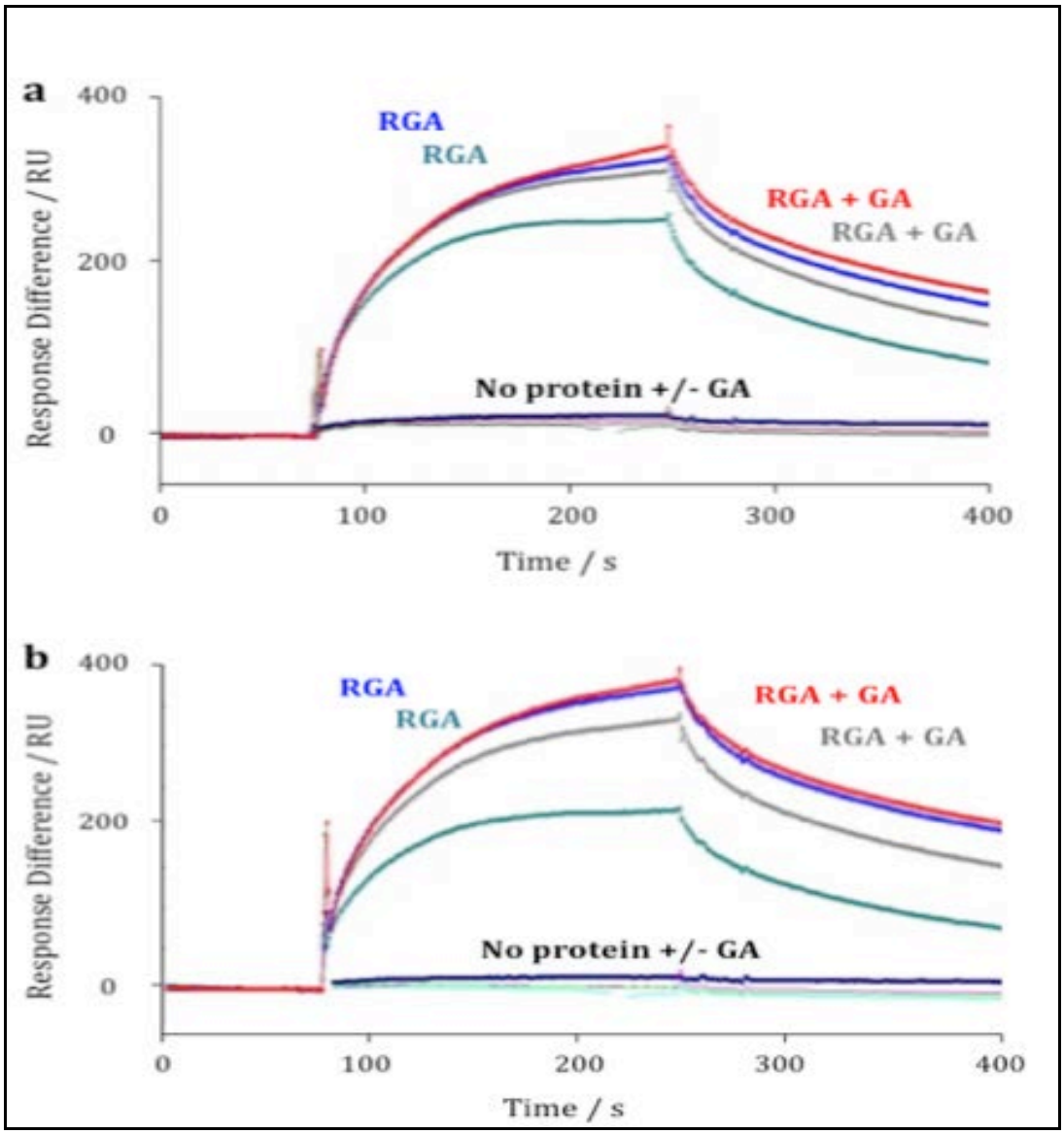

Figure 5-8 – RGA binds to both GID1a and GST. a) GID1a and b) GST, in HBS-EP buffer +1mM DTT, in the presence and absence of 100μM GA. 10mM Glycine-HCl pH2.2 was used for chip regeneration. Each sensorgram shows data for test channel subtracting ch1. Concentration of RGA = 0.045mg/ml.

The next stage was to try to demonstrate selective binding of RGA protein to GID1a-GST. Since the interaction of RGA with GID1a usually occurs when gibberellin is bound to GID1a, this experiment was carried out with and without GA present.

As can be seen, there is a binding interaction between GID1a and the analyte RGA, with between 250 and 350 units of the analyte protein bound onto the

ligand, with some variation between replicates (Figure 5-8*)*. Unfortunately this cannot be identified as selective binding, as a similar quantity of RGA was bound to the negative control GST. In addition, there was no GA dependence in this interaction, as both samples with and without GA lead to RGA binding to GID1a or the negative control in comparable amounts. It appears RGA is a 'sticky' protein, as it associated with both ligands on the chip surface, and did not appear to dissociate readily. These observations do not exclude the possibility of specific and GA-dependent binding, but the conditions of this experiment prevent further analysis.

5.4.3 Further Coupling to CHIP1

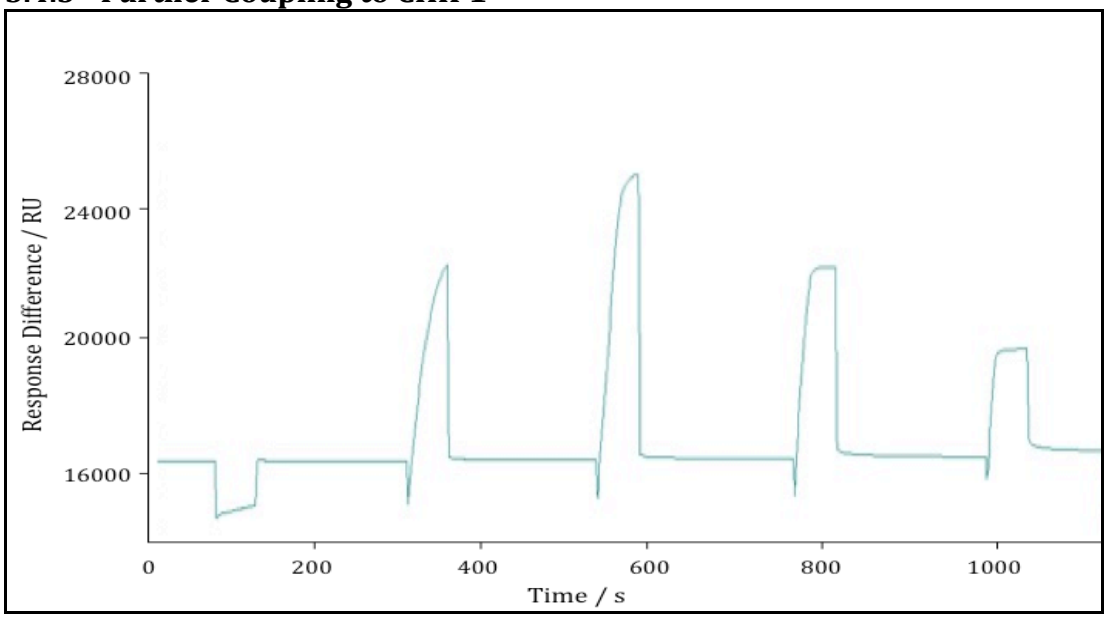

Figure 5-9 – pH scout for SUMO1 on CM5 chip. SUMO1 was diluted into 10mM sodium acetate buffers of pH3.5 to 5.5. 50mM NaOH pH 10 was used as the regeneration solution.

Having tried binding other proteins to GID1a-GST and GST on the chip as ligands, it seemed wise to try inverting the assay and coupling another of the proteins in the potential interaction. The protein selected was SUMO1. From the

pH scout (Figure 5-9) the optimal pH for association of SUMO1 with the chip surface was found to be pH5.0.

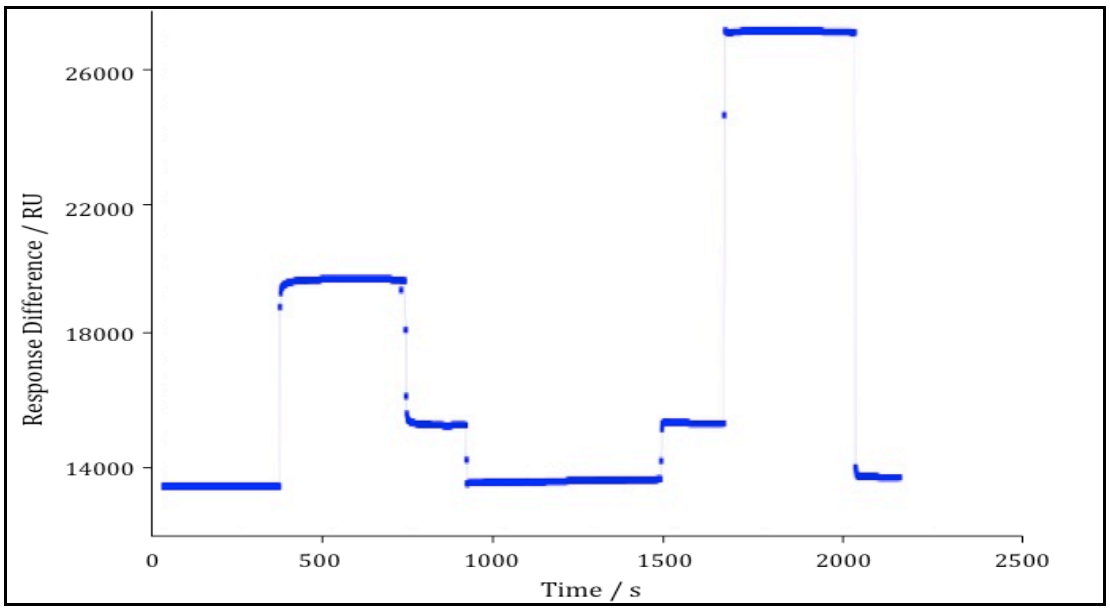

Figure 5-10 - SUMO1 coupling to a CM5 CHIP. SUMO1 was diluted in Sodium acetate buffer pH5.0 and amine coupling using the reagents EDC and NHS followed manufacturer's instructions (channel 4). Ethanolamine was used to block unreacted sites and for ch 1. Resonance units bound onto the CHIP were ~304 for SUMO1.

5.4.4 Further CHIP1 Binding Experiments

Following binding of SUMO1 onto the CM5 chip (*Figure 5-10*), the binding affinity for the ligand for the analytes GID1a-GST and GST were again tested, in the reverse of the experiment carried out in *Figure 5-7*.

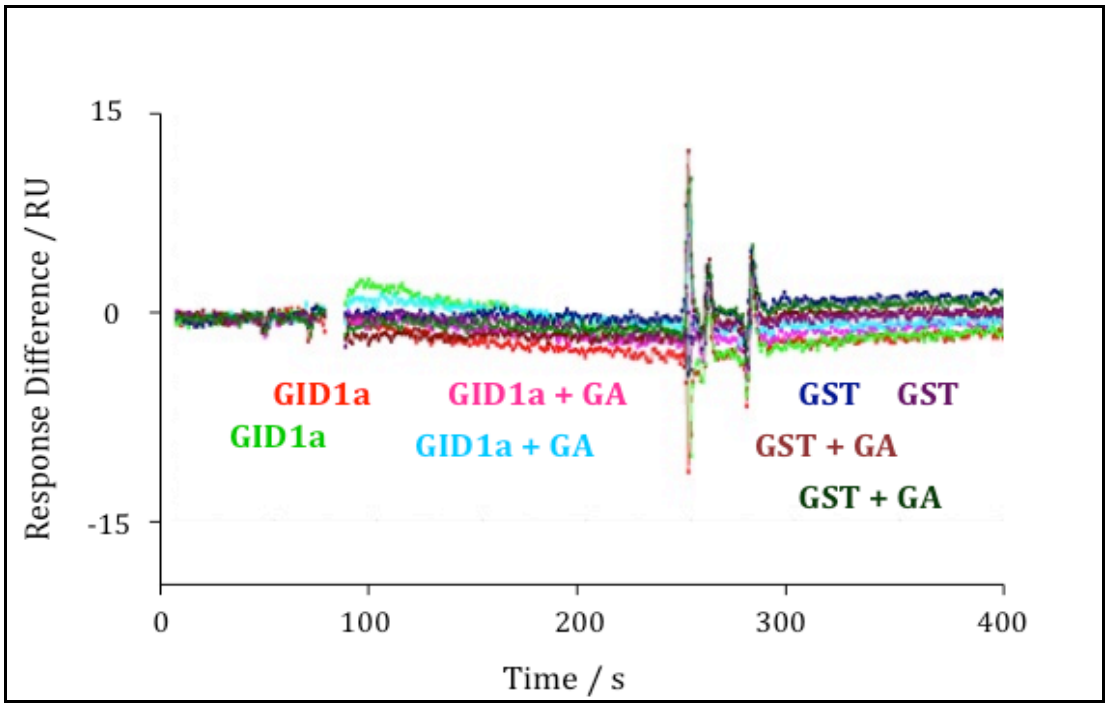

Figure 5-11 – SUMO1 is not a viable candidate as a ligand for SPR. GID1a and GST across SUMO1 bound to CM5 CHIP, in HBS-EP buffer +1mM dTT, with and without the presence of 100μM GA. 10mM Glycine-HCl pH2.2 was used for chip regeneration. Each sensorgram shows data for test channel subtracting ch1. Concentration of GID1a = 0.08mg/ml, concentration of GST= 0.093mg/ml.

From the results of this experiment (*Figure 5-11*), it is clear that there was little binding of GID1a or GST to SUMO1. As there was not binding, either specific or non-specific, and with or without presence of gibberellin, it is likely that SUMO1 is not a good candidate as a ligand for SPR.

5.4.5 Coupling to CHIP2

A new chip was prepared by coupling RGA, GID1a and GST as a control. A pH scout was carried out to find the optimal pH for binding of RGA to the CM5 CHIP (Figure 5-12).

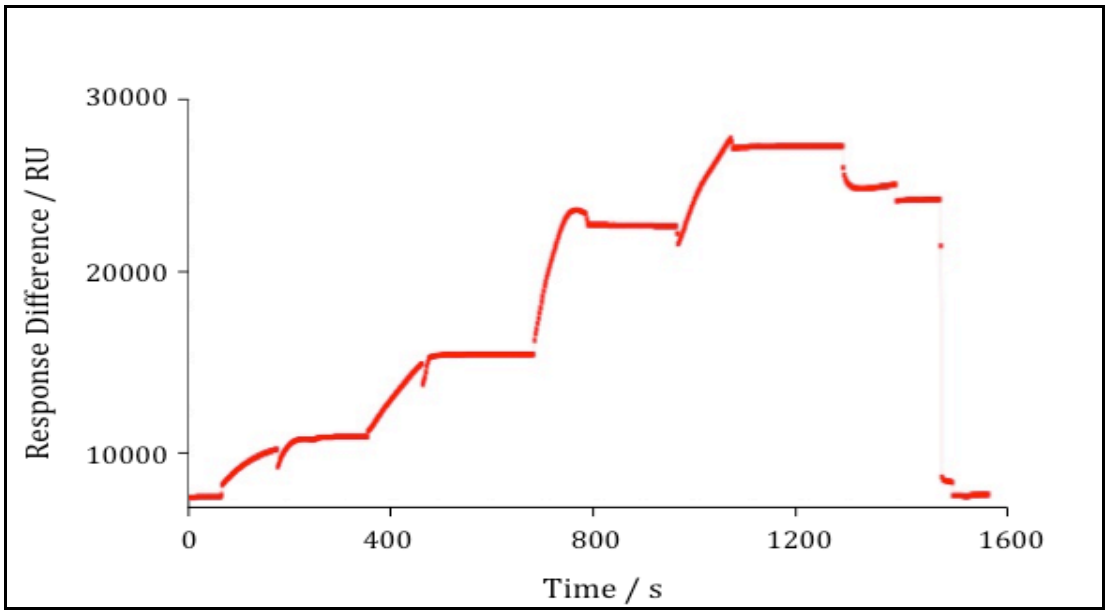

Figure 5-12 – RGA pH Scout on CM5 chip. RGA was diluted in 10mM sodium acetate buffers of pH3.5 to 5.5. 50mM NaOH pH 10 was used as the regeneration solution.

From the pH scout, RGA was found to have optimal association with the CHIP surface in a sodium acetate buffer pH4.5. RGA was then bound to the CHIP to a final level of ~526 resonance units, with the other proteins bound at ~1027 (GID1a) and ~405 (GST) units respectively (Figure 5-13).

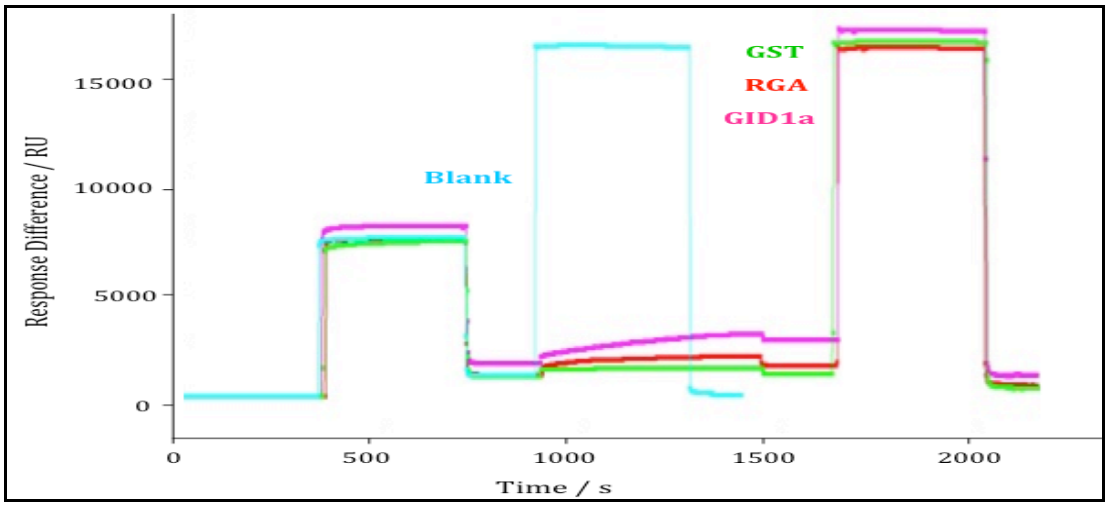

Figure 5-13 – RGA-His, GID1a-GST and GST coupling to a CM5 Chip. 10mM sodium acetate buffer pH4.5 (RGA) or pH5.5 (GID1a and GST), using reagents EDC and NHS, with Ethanolamine for blocking residual sites to terminate reactions. Resonance units bound onto the CHIP were ~526 for RGA (channel 2), ~1027 for GID1a (channel 3) and ~405 for GST (channel 4).

5.4.6 CHIP2 Binding Experiments

It was noted that the structural biology of SIM's had been investigated in a salt-free, 25mM phosphate pH7.0 (Conti *et al.*, 2008; Hecker *et al.*, 2006). Non-ionic detergent P20 was added for further SPR study. The next experiment used SUMO1 as the analyte over the ligands RGA, GID1a and GST, with variable dilutions of SUMO1, +/- gibberellin.

Figure 5-14c/d display the binding of SUMO1 to GID1a and GST. The sensorgram showing association between SUMO1 and GST (Figure 5-14d) shows no interaction between the proteins. This suggests that no binding of SUMO1 and GST occurs in a low salt buffer. In contrast, the sensorgram for SUMO1 and GID1a (Figure 5-14c) shows binding of the SUMO1 protein to GID1a and subsequent dissociation. The sensorgram has one trace that is slightly negative, which corresponds to a ⅛ dilution of SUMO1, and two traces that are horizontal, running along the baseline of the graph that are controls with no

SUMO1 protein in them. The rest of the traces had a curve, showing binding and dissociation as described. At a ¼ dilution of SUMO1, binding peaked at ~20 resonance units, and the two replicates of ½ dilution of SUMO1 peak at approximately 50 resonance units, demonstrating a weak, but clear concentration dependence to the association of SUMO1 to GID1a.

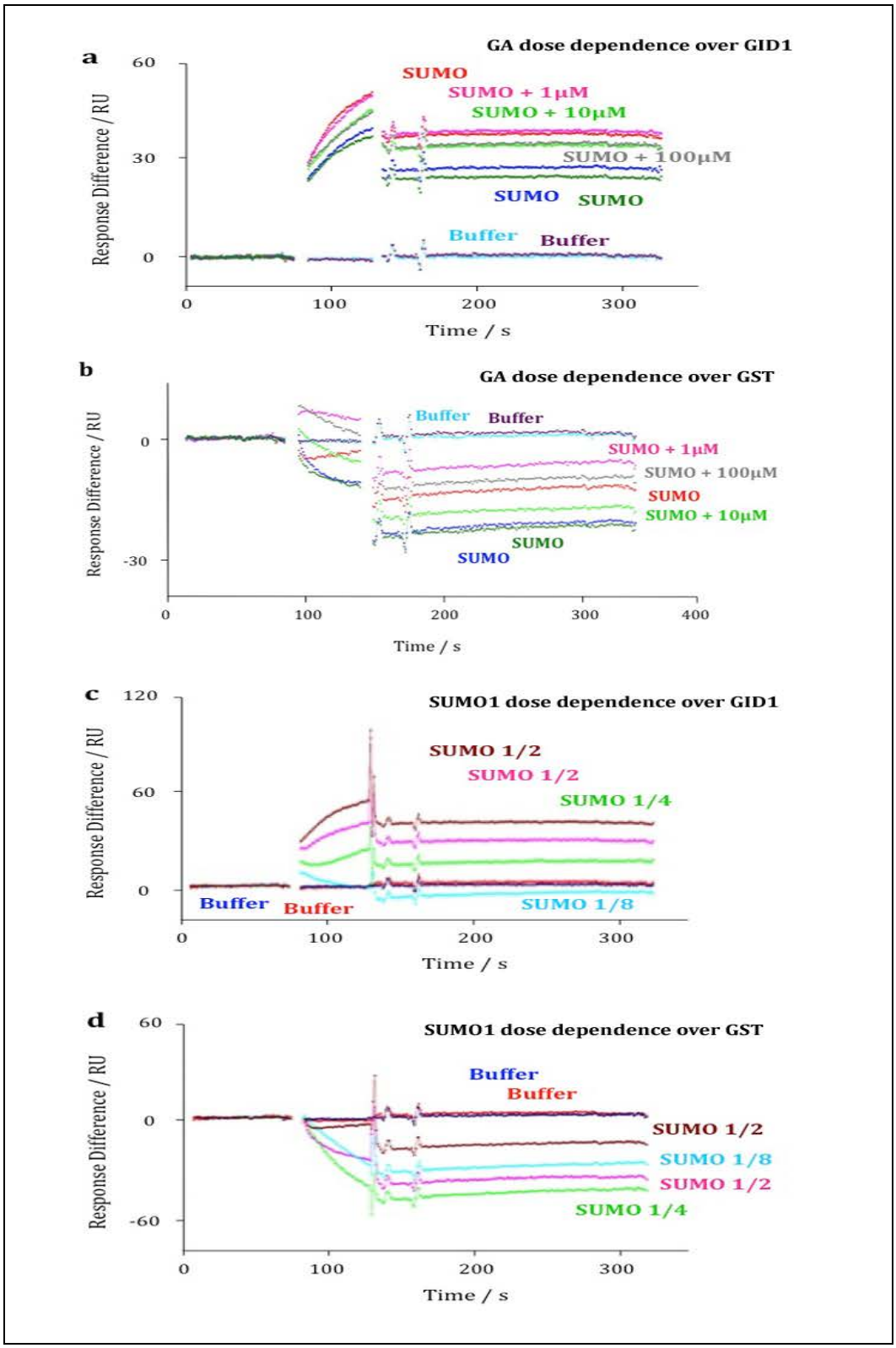

Figure 5-14 – SPR sensorgram traces showing SUMO1 protein binding to GID1a, not GST. All assays were done in 25mM phosphate buffer pH7 (+0.005% P20). Dilutions of SUMO1 and different concentrations of gibberellin were used as indicated: - SUMO1 (1/2) + 0, 1, 10 or 100µM GA or GID1a (a) or GST (b). SUMO1 (½, ¼ or ⅛) over GID1a (c) or GST (d). 10mM Glycine-HCl pH2.2 was used for chip regeneration. Each sensorgram shows data for test channel subtracting ch1. Concentration of SUMO1 (½) = 0.11mg/ml.

Having studied the interaction of the proteins at different quantities of SUMO1, gibberellin was introduced in order to see whether there was any level of GA dependence in this interaction. Figure 5-14b shows the interaction of SUMO1 with GST, at variable concentrations of GA from 0-100μM. The traces suggest no binding interaction between the proteins. By comparison, Figure 5-14a displays the interaction between SUMO1 and GID1a. As above (Figure 5-14c), the data all indicate binding between SUMO1 and GID1a, however no effect of GA can be discerned.

In order to test the effect was due to conditions, not variation in chip or proteins, the experiment was repeated to test the effect with low salt, phosphate buffer and with HBS-EP buffer. The results confirmed that the SUMO1-GID1a interaction was not supported in saline buffer.

Having also bound RGA onto the CM5 CHIP (Figure 5-13), we were able to test the interaction of RGA, as the ligand, with SUMO1 as analyte in low salt buffer.

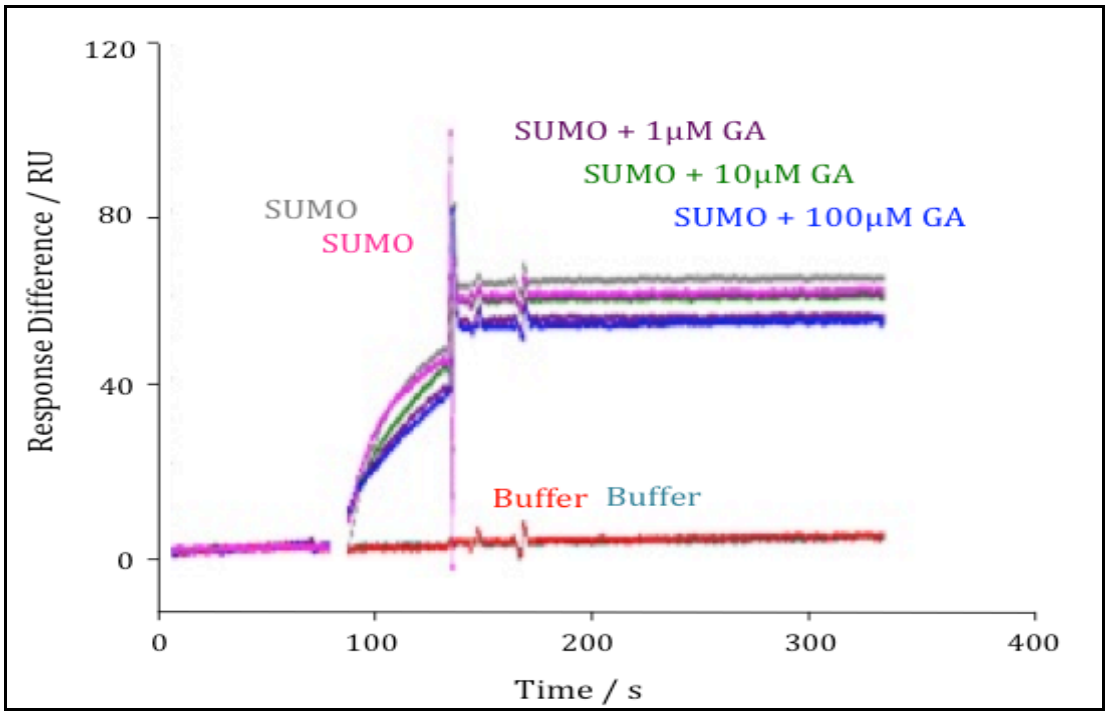

Figure 5-15 – No convincing interaction was found between SUMO1 and RGA. 25mM phosphate buffer pH7 (0.005% P20). Reactions took place in the absence or presence of gibberellin at 0, 1, 10 and 100µM. 10mM Glycine-HCl pH2.2 was used for chip regeneration. Each sensorgram shows data for test channel subtracting ch1. Concentration of SUMO1 = 0.11mg/ml.

The interaction of SUMO1 with RGA was investigated at a series of different gibberellin concentrations, and also in the absence of gibberellin (Figure 5-15). Apart from controls lacking proteins in the analyte, all traces had a characteristic shape, building up in a curve to a peak at approximately 50-60 resonance units, then a plateau. Clustered in this second set of traces are all of the samples with SUMO1 included, with or without gibberellin. There is no GA-dependence and less than 10 resonance units difference between the highest and lowest samples. This means that the association of all the SUMO1 samples, whether with or without gibberellin, is fairly comparable and the very long dissociation rates again suggest that RGA is a 'sticky' protein.

Despite the evidence to suggest RGA was sticky, the next step was to test RGA and GID1a. This interaction was assessed, again using a low salt 25mM phosphate buffer at pH7 (Figure 5-16).

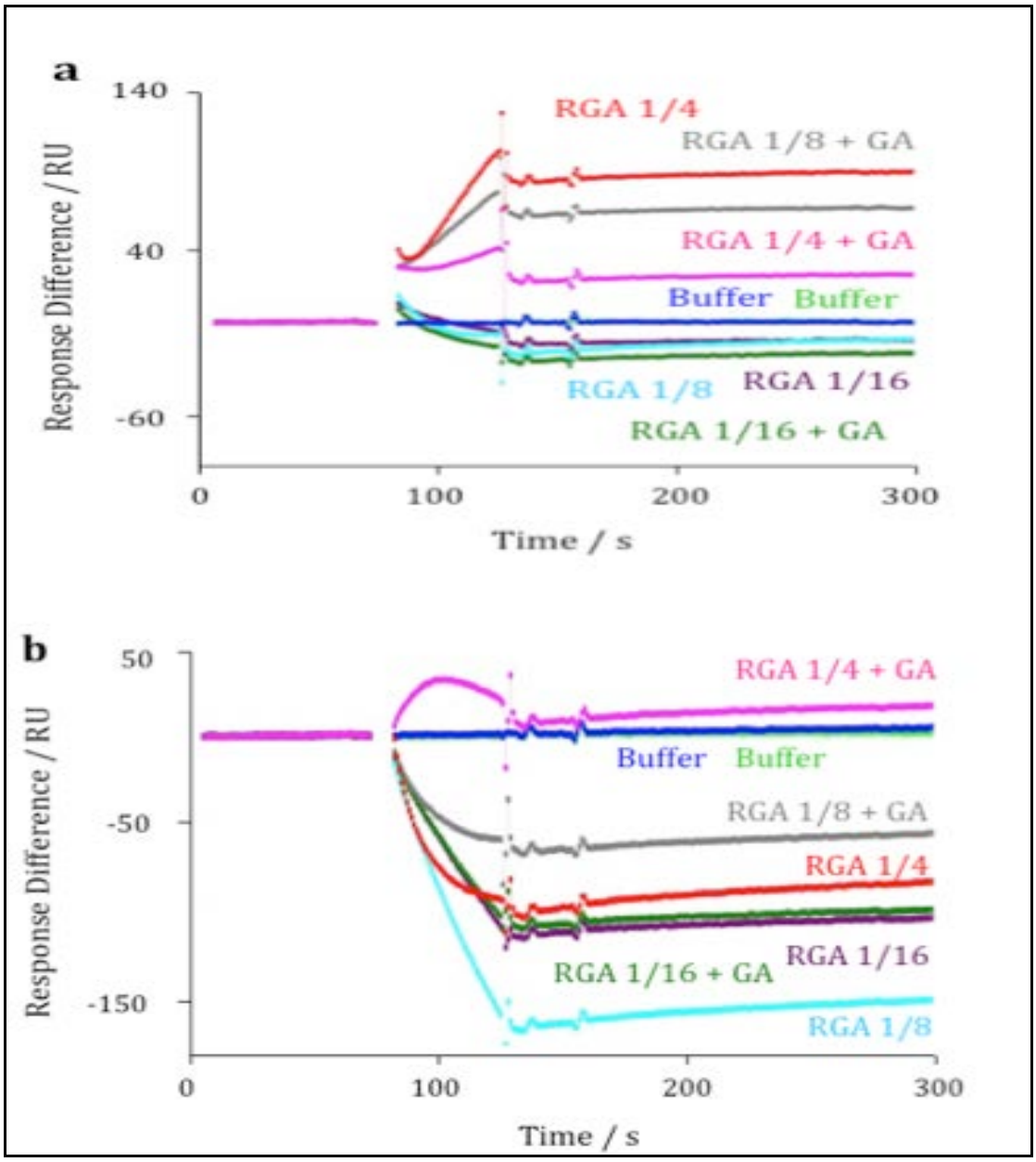

Figure 5-16 – RGA binds to GID1a, but fails to dissociate effectively. SPR sensorgram showing RGA binding to the ligands GID1a (a) and GST (b) in 25mM phosphate buffer pH7 (0.005% P20). Reactions took place in the absence or presence of 10μM gibberellin. 10mM Glycine-HCl pH2.2 was used for chip regeneration. Each sensorgram shows data for test channel subtracting ch1. Concentration of RGA (½) = 0.09mg/ml.

Figure 5-16b demonstrates that there is no interaction between RGA and GST. Figure 5-16a shows interaction of the ligand GID1a with a series of dilutions of RGA (¼, ⅛, and 1/16) in the presence and absence of 10μM GA. Three samples gave positive binding associations, building up in a curve to a peak, and then reaching a plateau. The lowest of these traces is the sample of RGA ¼ + GA, with a maximum reading in resonance units of around 40. The middle trace is the sample RGA 1/8 + GA, which peaks higher at a reading of 80 resonance units. The highest curve is that of RGA ¼ on GID1a, with resonance units of approximately 100 for the interaction. These results give a mixed message, in that there appears to be an interaction between RGA and GID1a, and this binding may have some GA dependency, but the data do not show classical binding curves and the dissociation is, again, very slow.

5.5 Discussion

5.5.1 Use of Different Components and Buffers

SPR often requires the consideration and use of numerous different buffers to try to reach an optimal result. In this case, HBS-EP buffer supported non-selective binding to GST as much as it supported interactions between test proteins. A low salt buffer was found to support more selective binding interactions, some of which are consistent with expectations from other biological experimentation.

Another important consideration in SPR is the proteins being used and which of the proteins used are bound to the CHIP as ligands, and which are used as

analytes. In this study, covalent coupling of SUMO1 supported no binding (Figure 5-11). We speculate that this is due to SUMO1 being small in size (~11kDa), and having 7 lysine residues. As lysine residues are the point of association of the ligand with the CHIP surface during amine coupling, it may be that association with the CHIP surface has lead to the SUMO1 molecule losing recognition sites or being coupled in an unfavourable orientation in terms of access to binding sites of SUMO1. This may be especially problematic as SUMO1 is such a small protein.

5.5.2 SUMO1 interaction with GID1a

Following a number of different experiments to assess the potential binding of SUMO1 to GID1a, both with HBS-EP buffer and later 25mM phosphate buffer, the data in low salt buffer (Figure 5-14a-d) seem to suggest several things. Firstly they demonstrate selective binding of SUMO1 to GID1a (Figure 5-14 c and d), as no binding to the negative control GST is notable. Secondly, no GA-dependence was found (Figure 5-14a-b). Addition of gibberellin at concentrations of 1, 3, 10, 30 and 100μM, did not lead to any increase in the binding of SUMO1 onto GID1a. Thirdly, this binding interaction did titrate with SUMO concentration. A concentration of around 0.11mg/ml of SUMO1 (approximately 6 μM) protein stimulates optimal binding suggesting the affinity of this interaction is sub-micromolar. There was no interaction between SUMO1 and the negative control GST within the same parameters.

5.5.3 SUMO1 interaction with RGA

As the association between SUMO1 and any DELLA protein is completely novel, and is yet to be demonstrated by any published data, any information that can be gained about association of SUMO with DELLA proteins and ultimately SUMOylation of RGA, is very useful to further understand these interactions. From the sensorgram in Figure 5-15, we have initial data showing binding of SUMO1 to RGA in a low salt buffer. However, the same figure also suggests that there is no GA dependence in this interaction, as all of the sensorgram traces are clustered together, whether the samples include gibberellin or not. The big reservation about these data is that the RGA was expressed and purified from E. coli and we do not have an *in vitro* activity assay. The 'stickyness' noted above might be the result of incorrect folding. If so, none of the binding data can be considered anything but preliminary, but this result definitely warrants further investigation.

5.5.4 RGA Interaction with GID1a

From the data shown in Figure 5-16, there may be a binding interaction between RGA and GID1a, but as above we must reserve judgement until we are able to show that the RGA protein is folded authentically. Nevertheless, when comparing the lack of any binding between RGA and GST (Figure 5-16b) and the apparent binding between RGA and GID1a (Figure 5-16a), there is a suggestion that this is specific binding between RGA and GID1a. This conclusion tallies with a great deal of work published regarding interaction between RGA and GID1a, but publications have also shown a requirement for GA (Conti *et al.*, 2009; Griffiths *et al.*, 2006). No dependency for gibberellin was found in this SPR

experiment (Figure 5-16a). It will be necessary to carry out further work, extending it to include a range of dilutions of RGA and GA to get a more accurate idea of what is required for the optimal binding of RGA and GID1a.

5.5.5 Future Work

Further work in this area will include, more SPR, in order to further analyse interaction between these proteins. This would start with more extensive experiments to confirm the interactions that have been recorded when using 25mM phosphate buffer pH7. Varying protein concentration of the ligand further may also maximise protein binding in this system. Further analysis may require expression of RGA from eukaryotic expression systems such as *Pichia pastoris* in yeast, or a plant-based system, rather than *E.coli*.

Another large-scale experiment to consider would be to design a competitive binding assay in order to test the affinity of both SUMO1 and RGA for the ligand GID1a.

Carrying out the same investigations using the GAI protein would confer whether interactions with this complex differ between RGA and GAI. Expressing and purifying some mutant versions of RGA and GAI, such as gai-1 (Xiong *et al.*, 2002; Koorneef *et al.*, 1985) and rga-Δ17 (Mahfouz *et al.*, 2006; Dill, Jung & Sun, 2001) missing protein functionality could give some interesting results in terms of how the DELLA, GID1 and SUMO1 proteins interact as a complex.

Further to the use of SPR, it would be worth using another technique to assess the binding interactions between this protein complex. One of the possibilities would be to use *in-vitro* binding assays, for which preliminary results have yielded some promising data.

6 The OTS1 SUMO protease and its relationship with Osmotic Stress

6.1 Introduction

6.1.1 SUMOylation

As one of several post-translational modifications in eukaryotes, SUMOylation is essential to many processes including chromosome segregation (Miura *et al.*, 2005; Watts, 2007), cancer and heart disease (Hanania *et al.*, 1999; Sarge & Park-Sarge, 2009) in humans, and cell growth and development in plants (Orth *et al.*, 2000; Miura & Hasegawa, 2010).

In plants, SUMOylation has a clear role in responses to biotic and abiotic stresses. In *Arabidopsis*, conjugation of AtSUMO1 and AtSUMO2 to target proteins is enhanced in response to abiotic stress, especially heat shock (Miura, Jin & Hasegawa, 2007; Kurepa *et al.*, 2003). The SUMO E3 ligase SIZ1 is implicated in gene regulation in reaction to drought stress (Dye & Schulman, 2007; Catala *et al.*, 2007; Mukhopadhyay & Dasso, 2007) and responses to phosphate deficiency (Miura, Jin & Hasegawa, 2007; Miura *et al.*, 2005). SUMOylation also has a function in the defence of plants from pathogens. Yeast-2-hybrid screens have shown that SUMO interacts with ETHYLENE-INDUCING XYLANASE (EIX), a protein that induces defence responses in tomato. The association of SUMO with EIX represses the induction of programmed cell death (Boggio & Chiocca, 2005; Hanania *et al.*, 1999). In addition, the avirulence gene AvrBsT from *Xanthomonas campestris* is anticipated to encode a SUMO-specific protease which is inserted into the host plant cell during the infection process (Johnson, 2004; Orth *et al.*, 2000).

6.1.2 SUMO Proteases

SUMO proteases (Ulp's) have peptidase activity (Lois, 2010; Miura, Jin & Hasegawa, 2007) to process precursor SUMO molecules (Conti *et al.*, 2008; Dye & Schulman, 2007; Mukhopadhyay & Dasso, 2007) and isopeptidase activity to recycle SUMO from substrates (Miura, Jin & Hasegawa, 2007). These combined together function as part of the SUMOylation process are illustrated in *Figure 6-1*.

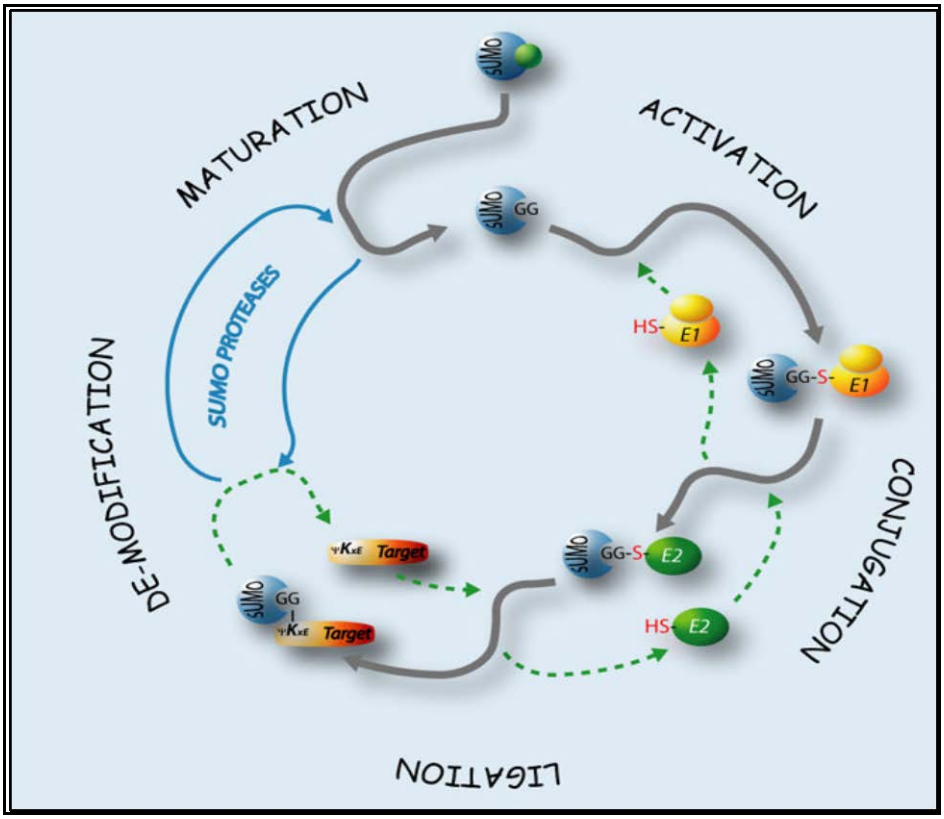

Figure 6-1 – The SUMOylation cycle is maintained by dual functions of SUMO protease as a peptidase for maturation of the SUMO protein and an isopeptidase for de-SUMOylation. Stages of SUMOylation processing (solid arrows) and recycling (dashed arrows) are shown. SUMO = Small Ubiquitin-Like Modifier, E1 = SUMO activating enzyme and E2 = SUMO conjugating enzyme. Taken from GAM1 and the SUMO pathway (Boggio & Chiocca, 2005).

Only a low number of protein substrates are ordinarily SUMOylated at any set time, suggesting that SUMO proteases have an essential regulatory role during

SUMOylation (Johnson, 2004). The overall function of these proteases is to regulate and maintain the cellular pool of SUMO available for protein modification (Lois, 2010), by controlling the equilibrium between the SUMOylated and deSUMOylated states of any given protein (Conti et al., 2008). This essential function in the SUMO cycle, requiring additional specificity, may be why there are a high number of Ulp's compared with SUMO E1 and E2 enzymes, suggesting a complex regulation of signalling at the level of deSUMOylation. Requirement for certain protease-substrate interactions or selectivity for different SUMO proteases for a particular SUMO isoform could be necessary (Conti et al., 2008). Significant *in-vitro* cleavage assays showed SUMO substrate preferences for *Arabidopsis* SUMO proteases, which in some cases were governed by the N-terminal domain of the protease (Chosed et al., 2006). Studies in the yeast species *Saccharomyces cerevisiae* show that the N-terminal domain modulates Ulp1 activity, target binding ability and localisation (Mossessova & Lima, 2000; Li & Hochstrasser, 2003). Evidence shows that distinction in the N-terminal domain may define the basis of specificity of particular SUMO proteases for certain signalling pathways in *Arabidopsis* (Conti et al., 2008).

SUMO proteases have been discovered in a number of eukaryotic species from humans and animals. In humans, SUMOylation is regulated by a family of sentrin/SUMO-specific proteases, termed SENP's. There are seven SENP's (SENP 1, 2, 3, 5, 6, 7, 8) identified in human species of which there has been variable characterisation, with SENP1 and SENP2 the best defined family members (Gong & Yeh, 2006). SENP1 and SENP2 are able to cleave SUMO from all SUMO-

modified proteins (Rajan et al., 2005), while SENP3 and SENP5 form a subfamily of SENP's that control formation of SUMO 2 and SUMO 3 conjugates, and in a lesser extent SUMO 1 modification (Gong & Yeh, 2006). SENP7 is found to be responsible for chromatin relaxation, with deSUMOylation by this protease necessary to uphold an appropriate chromatin environment for DNA repair (Garvin et al., 2013).

Homologous to the SENP's in humans are a group of SENP's/Ulp's in yeast, called Ulp1 and Ulp2 (Smt4) (Li & Hochstrasser, 1999; 2000). Ulp1 is a protein fundamental to yeast that co-localises with nuclear pore proteins. Deletion of *Ulp1* means yeast becomes non-viable. Ulp2 localises primarily to the nucleus and gene deletion of *Ulp2* leads to abnormal growth of yeast and hypersensitivity to DNA damage (Taylor et al., 2002).

There are also SUMO proteases found to be important in plant-pathogen interactions. Avirulence factors such as *Xanthomonas campertris* vesicatoria4 (AvrXV4) from the plant pathogenic bacterial species *X.campestris* can play a role as a SUMO protease. It appears to reduce SUMO conjugation onto target proteins in order to disrupt defence in host plant cells (Roden et al., 2004).

In *Arabidopsis thaliana* there have at least eight SUMO proteases identified, and some of these have been at least partially characterized. AtUlp1a, AtUlp1c, AtUlp1d and AtESD4 are reported to have a variable N-terminal domain and conserved C-terminal domain associated with catalytic activity (Kurepa et al., 2003; Chosed et al., 2006; Colby et al., 2006).

Ulp1a, also known as ESD-Like SUMO Protease 1 (ELS1) is the least well understood, with little information on its localization, phenotype, or any work done with knockout lines (Lois, 2010) until recent work found that although it is homologous to ESD4 in sequence they have very distinct functions. ELS1 is localised to the cytoplasm, potentially in association in endo-membranes, and is only very weakly detected in the nucleolus, but not other parts of the nucleus (Hermkes *et al.*, 2011). This is in contrast to the other plant SUMO proteases, which are all nuclear localised (Colby *et al.*, 2006). The ELS1 protease has also been reported to have an essential role in SUMO maturation (Li & Hochstrasser, 1999; Hermkes *et al.*, 2011).

Early in Short Days 4 (ESD4) is a far better characterised SUMO protease, which links together the role of SUMO metabolism and control of flowering time (Murtas et al., 2003). The mutation *esd4* was found to convey an extreme early-flowering phenotype in *Arabidopsis*, and an accelerated transition from vegetative growth to flowering, especially emphasised in short-day conditions which normally delays flowering (Reeves et al., 2002). The *esd4* mutant was restricted in regulation of SUMOylation, due to the absence of a functional SUMO protease and had further phenotypes including broadening of silique, alteration of phyllotaxy and dwarf appearance. It was also reported to be localised to the nuclear envelope of cells (Murtas et al., 2003).

The other two proteases, referred to as Ulp1c and Ulp1d, are also called OTS1 and OTS2, and are SUMO proteases involved in responses to high salinity (Conti et al., 2008). These two SUMO proteases will be focused on in section 6.1.3.

While there are more numerous, compared with other parts of SUMO machinery, the conservation in sequence among these proteases is much lower than other elements of this machinery. Sequence identity amongst SUMO proteases is between 12 and 44% for the four characterised isoforms that have been mentioned, making discovery of any further SUMO proteases in *Arabidopsis* challenging (Lois, 2010). These differences are due to a high degree of divergence in the Ulp N-terminal domain responsible for regulation. Even the two OTS SUMO proteases, which function redundantly, have only 25% N-terminal sequence identity compared with 70% identity in their catalytic domains (Mukhopadhyay & Dasso, 2007).

6.1.3 OTS1/2 SUMO Proteases

The *Arabidopsis* SUMO proteases OTS1 and OTS2 have been implicated in plant responses to high salinity. The *ots1 ots2* double mutant has increased salt sensitivity compared to single mutants or the wild-type (Conti et al., 2008), although plants look phenotypically comparable to the wild-type in non-salt conditions when assessing growth and development (Conti et al., 2009). SUMO-conjugated proteins collect at greater levels in *ots1* and *ots2* single mutants compared to the wild-type, and double mutants have a further increased level of SUMO conjugation to target proteins. Therefore, the conclusion is that OTS1 and OTS2 have a function in deSUMOylation of target proteins in non-stress

conditions (Conti et al., 2009). Salt-stress conditions leads to a rise in SUMO1/2-conjugated proteins in a dose-dependent manner in wild-type plants. The levels of these proteins are again enhanced in the *ots1 ots2* mutant. Overexpression of wild-type OTS1 leads to higher salt tolerance and a concurrent reduction in levels of SUMOylated proteins. Investigation in this chapter will centre on whether other stress conditions related to high salinity such as osmotic stress stimulate the same tolerance in OTS1 overexpressing lines.

It seems that OTS1 and OTS 2 are functionally redundant. Both proteins are nuclear localised and it has been demonstrated that salt stress directly affects OTS1 signalling by provoking its turnover (Conti et al., 2008). In addition it has been observed that overexpression of SUMO1 in the *ots1 ots2* double mutant dramatically decreases plant size in terms of rosette diameter, even under no abiotic stress, showing that the OTS proteases are essential as overSUMOylation of target proteins can have marked effects on plant growth (Conti et al., 2009)

6.2 Objectives

As the OTS SUMO proteases are integral in salt stress responses, and as stated above, other components of SUMO machinery have roles in abiotic stress responses, I set out to investigate whether the OTS proteases have a role in abiotic stresses other than high salinity, namely osmotic stress. This will be investigated with focus on the OTS1 protease, considering the functional redundancy between the two proteases. This may elucidate whether OTS1 may have interaction with other players known to be involved in osmotic stress

responses in *Arabidopsis* such as LOS6/ABA1 (Xiong et al., 2002), RAPTOR1 (Mahfouz et al., 2006) and SOS6/AtCSLD5 (Zhu et al., 2010).

The main objective of the chapter is to test whether the OTS1 SUMO protease has a role in osmotic stress, during seed germination or seedling establishment. This will be elucidated using independent transgenic lines overexpressing OTS1, compared with wild-type and vector only lines, along with the *ots1 ots2* double mutant line which is severely impaired in growth and development under high salinity.

Two different independent transgenic lines were used– 35S:NTAP-OTS1 1 and 35S:NTAP-OTS1 2. Within these independent lines, for the two separate experiments, some different derivative T4 lines from these two independent T3 lines were used, but these were used with correct controls, and the same lines were used for all replicates for the same experiment. Col-0 and NTAP 1 were used as controls. NTAP is a vector-only construct including the TAP tag. During this chapter there was not time to assess these lines genotypically to elucidate the gene and protein levels of the NTAP-OTS1 construct and fusion protein. However, the same independent transgenic lines were used for analysis of salt tolerance facilitated by OTS1 overexpression in *Arabidopsis* (Conti *et al.*, 2008), therefore the protein and construct expression levels had been confirmed in this previous work.

6.3 Strategy

The strategy used variable osmotic stress on the *Arabidopsis* lines: -

1. To test seed germination responses using polyethylene glycol 8000 to induce osmotic stress of between 0 and -0.8MPa
2. To test seedling establishment using mannitol between 0 and 600mM to create osmotic stress.

6.4 Results

6.4.1 Germination

Data for the germination phenotype of the OTS1 overexpressing lines was collected from an experiment designed to test germination of these lines under osmotic stress using polyethylene glycol at concentrations equivalent to osmotic pressure of 0, -0.2, -0.4, -0.6 and -0.8 megapascals.

6.4.1.1 Germination Experiment 1

Results in Figure 6-2 show germination responses to increases in concentration of polyethylene glycol and resultant osmotic stress. Without PEG and at low-level osmotic stress there is little difference in the germination rate, or final percentage germination (Figure 6-2a, b). As the osmotic pressure is increased the lines begin to diverge and greater differences in germination are visible. At -0.4MPa (Figure 6-2c) OTS1 2.2 has a similar pattern of germination to the control lines NTAP 1.2 and Col-0, while OTS1 1.3 has a lower rate of germination, with seeds of this line germinating more slowly, but reaching a comparable overall percentage germination after two days of delay in

germination. There are even greater differences at -0.6MPa, with the OTS lines only reaching a final germination of 75-80%, where the controls attained over 90% germination (Figure 6-2d). While OTS1 2.2 had a similar germination rate to the controls, but a lower final germination level, the OTS1 1.3 had a delay in germination by at least one day compared to the other lines, leading to a lower germination rate in addition to a lower final percentage germination compared to controls.

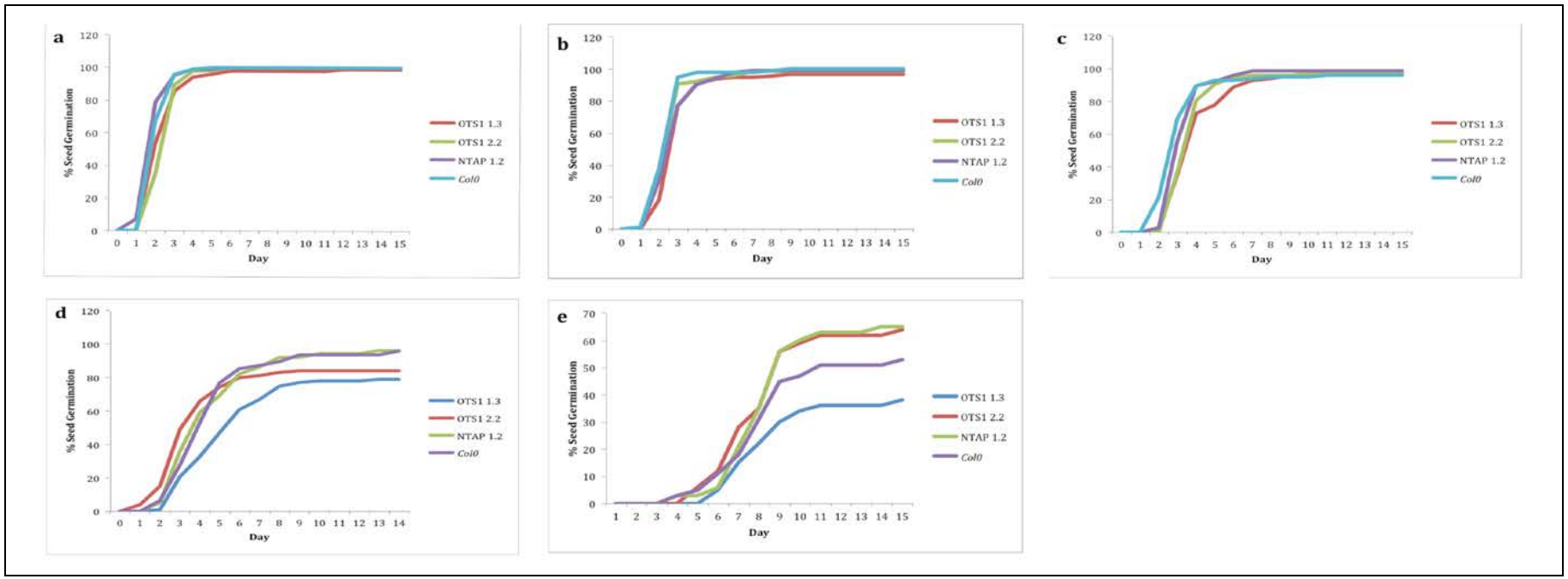

Figure 6-2 - Neither germination rate or level of germination are improved by overexpression of the OTS protease under osmotic stress. Percentage seed germination of four seed lines (p35S:NTAP-OTS1 1.3, p35S:NTAP-OTS1 2.2, p35S:NTAP 1.2, Columbia-0). Seeds were sterilised and vernalisation at 4°C for three days. germination at 15°C was monitored for 15 days in constant light. PEG8000 was used to create osmotic stresses equivalent to 0 MPa (a), -0.2 MPa (b), -0.4 MPa (c), -0.6 MPa (d) or -0.8MPa(e). For each seed line there were duplicate boxes for each of the five treatments (a-e). ANOVAs of each of the parameter values from the fitted Logistic equations showed no significant difference between treatments for different lines giving statistical values B (P=0.316), M (P=0.143), C (P=0.540), A+C (P=0.464). Germination was recorded as emergence of the radicle and germination data were normalised using the natural log. n = 11-50, for each of two technical replicates at each PEG concentration.

At -0.8MPa, the difference in final percentage germination is very clear (Figure 6-2e). Again, OTS1 1.3 is the last of the lines to begin germination on day 5, and has a lower rate of germination than other lines, with final germination on day 15 of 43%. The control Col-0 was earlier to begin germination on day 3, and exhibited a higher germination rate, but was the next lowest in final germination, at 53%. NTAP 1.2 begins germination a day earlier than OTS1 2.2 on day 3, but these lines have very similar germination rate, and final germination of 64 and 65% (OTS and NTAP). The *ots1 ots2* double knockout was not used for this experiment, as the germination rate of the seeds were exceptionally low, almost zero.

It seems that there is no improvement in germination under osmotic stress when *OTS1* is overexpressed in transgenic plants. However, while the OTS1 2.2 line does not show greater tolerance to stress than the NTAP line, it does have greater germination rate and final percentage of germination than the Col-0 control at high concentration of polyethylene glycol (high osmotic stress).

Statistical analysis was carried out to test the significance of the germination data. Using non-linear regression, germination curves for each of the seed lines were plotted for each treatment, with two experimental replicates for each treatment with each line. From each curve the values of A (the lower asymptote); BC/4 (the maximum germination rate), A+C (the upper asymptote) and M (time to reach 50% of maximum germination) (Appendices) were used to calculate C, A+C, B and M. These values were then used to run an ANOVA to calculate the significance of any difference in the curve parameters C, A+C, B and

M. No significance was found in any of these parameters when line and treatment were taken into account, but significance was noted in both line and treatment individually in most cases. The lines are significantly different from each other and osmotic treatment has a significant effect on each line but when the variables are combined there is no significance.

6.4.1.2 Germination Experiment 2

The experiment was replicated and the double mutant line was added to the analysis (Figure 6-3). As a clear response difference was only seen at higher osmotic stress, the replicate experiment included only three treatments – 0, -0.6 and -0.8MPa.

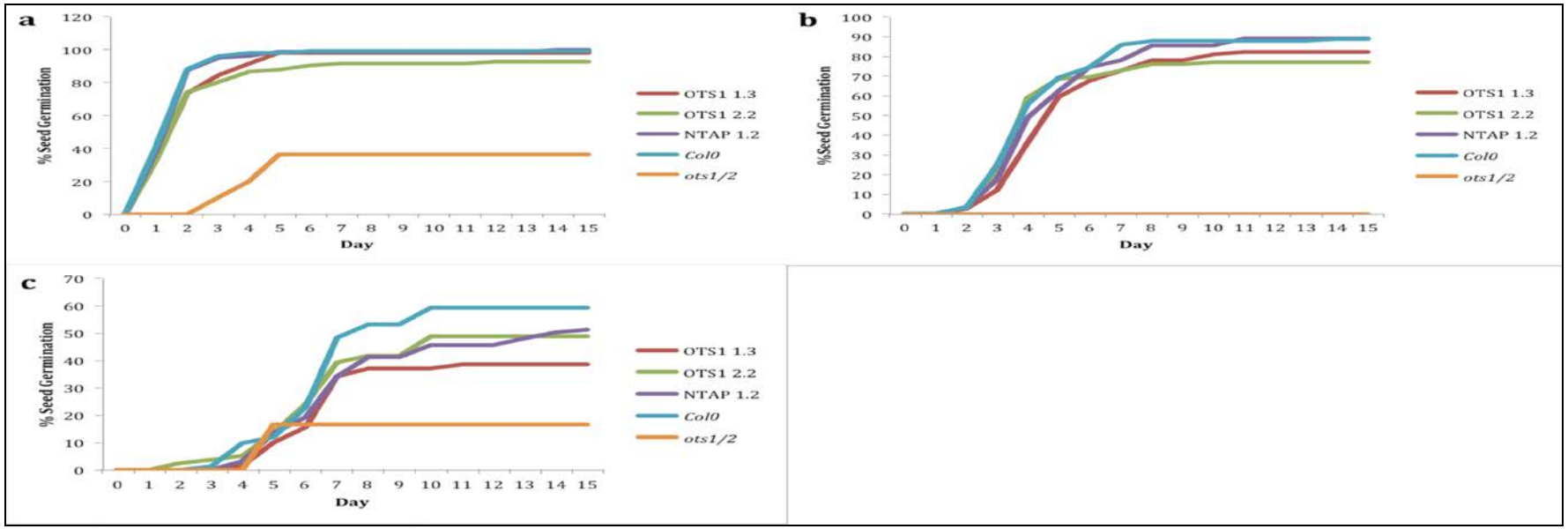

Figure 6-3 - Overexpression of the OTS1 protease does not enhance germination tolerance to osmotic stress in Arabidopsis thaliana. Percentage seed germination was recorded daily for five seed lines (p35S:NTAP-OTS1 1.3, p35S:NTAP-OTS1 2.2, p35S:NTAP 1.2, Columbia-0, ots1 ots2). Seeds were sterilised and vernalisation at 4°C for three days. germination at 15°C was monitored for 15 days in constant light. PEG8000 was used to create osmotic stresses equivalent to 0 MPa (a), -0.6 MPa (b), -0.8 MPa (c). For each seed line there were duplicate boxes for each treatment. ANOVAs of each of the parameter values from the fitted Logistic equations showed no significant difference between treatments for different lines giving statistical values B (P=0.316), M (P=0.143), C (P=0.540), A+C (P=0.464). Germination was recorded as emergence of the radicle and germination data were normalised using using the natural log. n = 5-50, for each of two technical replicates at each PEG concentration.

The *ots* double mutant line was two days later in germination than all other lines in the absence of osmotic stress, and only reached 36% germination. The rest of the lines achieved between 93 and 100% germination by day 15, and had fairly similar germination rates. On this occasion, the two 35S:OTS lines gave similar germination data, perhaps with a slightly longer lag into germination, and taking longer to reach their maximum germination level than Col-0 at moderate stress (Figure 6-3b). However, this characteristic is not extended by more severe stress (Figure 6-3c). The lowest germination level is with *ots1 ots2*, although it failed to germinate at all at moderate stress.

As in 6.4.1.1, non-linear regression analysis and ANOVA were used to assess significance. Again, based on treatment and factoring in the different transgenic lines, the results seen were not significant. Significance was seen individually with line or with treatment, but not combined.

Overall, the results of both experiments found no evidence that suggests the OTS protease is likely to influence osmotic stress tolerance during germination, although lack of OTS clearly impaired germination greatly.

6.4.2 Establishment

Having found that the OTS1 protease does not have much bearing on osmotic stress tolerance during germination, we endeavoured to test whether it had an influence at another stage of plant development, namely seedling establishment. Seeds were allowed to germinate on standard ½ MS media and then transferred

onto plates with mannitol concentrations between 0 and 600mM. Following growth on variable mannitol concentrations root growth data was collected using Image J.

Primary root growth is impaired by rising osmotic stress in all lines (Figure 6-4). Where there is no treatment, the highest primary root growth of 8.2cm was seen in the OTS1 2.1 line, to which Col-0 was very close in length. There is a noticeable drop in root length to NTAP 1.1, at 6.8cm. Below this, OTS1 1.1 and 1.2 are very similar with root length of 5.9 and 5.7cm respectively. The *ots1 ots2* line has the lowest root length of 4.4cm. A drop in root length of almost half the original length for most lines was evident with 100mM mannitol treatment, showing that even at this lower concentration, an osmotic stress effect is present. OTS1 2.1 has the highest primary root length with 3.77cm, however p35S:OTS lines perform fairly consistently and all lines are fairly similar in root length and above 3cm. At 200mM mannitol, a little more divergence in response to mannitol is clear. The two highest primary root lengths were derived from the same independent transgenic, OTS1 1.1 and 1.2 (3.16 and 2.90cm respectively). The NTAP 1.1 seems to be severely affected by the mannitol treatment, and root length is greatly reduced in this line from the 100mM treatment. Both the control lines Col-0 and *ots1 ots2* have lower primary root length than the OTS lines, with two of the lines overexpressing OTS showing lesser susceptibility to 200mM mannitol.

Higher mannitol concentration at 300mM leads to further decline in root lengths, other than for Col-0, which actually has an increase in primary root

length from the lower 200mM mannitol, against the hypothesis that osmotic stress would reduce plant root length in a dose-dependent manner. The rest of the lines have comparable root lengths, other than the NTAP 1.1 line, which is noticeably lower. At 400mM, the primary root length measurements were lower again, with the highest the Col-0 line. Increasing the mannitol concentration to 600mM leads to very minimal primary root growth, with all of the lines very close in root length between 0.25 and 0.45cm.

The part of the histogram that is most intriguing is the reaction of transgenic lines to no treatment compared with mannitol doses. At no treatment there is the highest difference in primary root growth between the OTS overexpressing lines and the *ots1 ots2* double knockout, and as the mannitol concentration increases, this divergence becomes far less. This suggests that the OTS protease does not have a direct effect on mediation of seedling establishment under osmotic stress, but does have a role in seedling establishment in non-stress conditions. Statistical analysis with an ANOVA found that the results of this experiment were significant for each line, and also accounting for the different mannitol treatments.

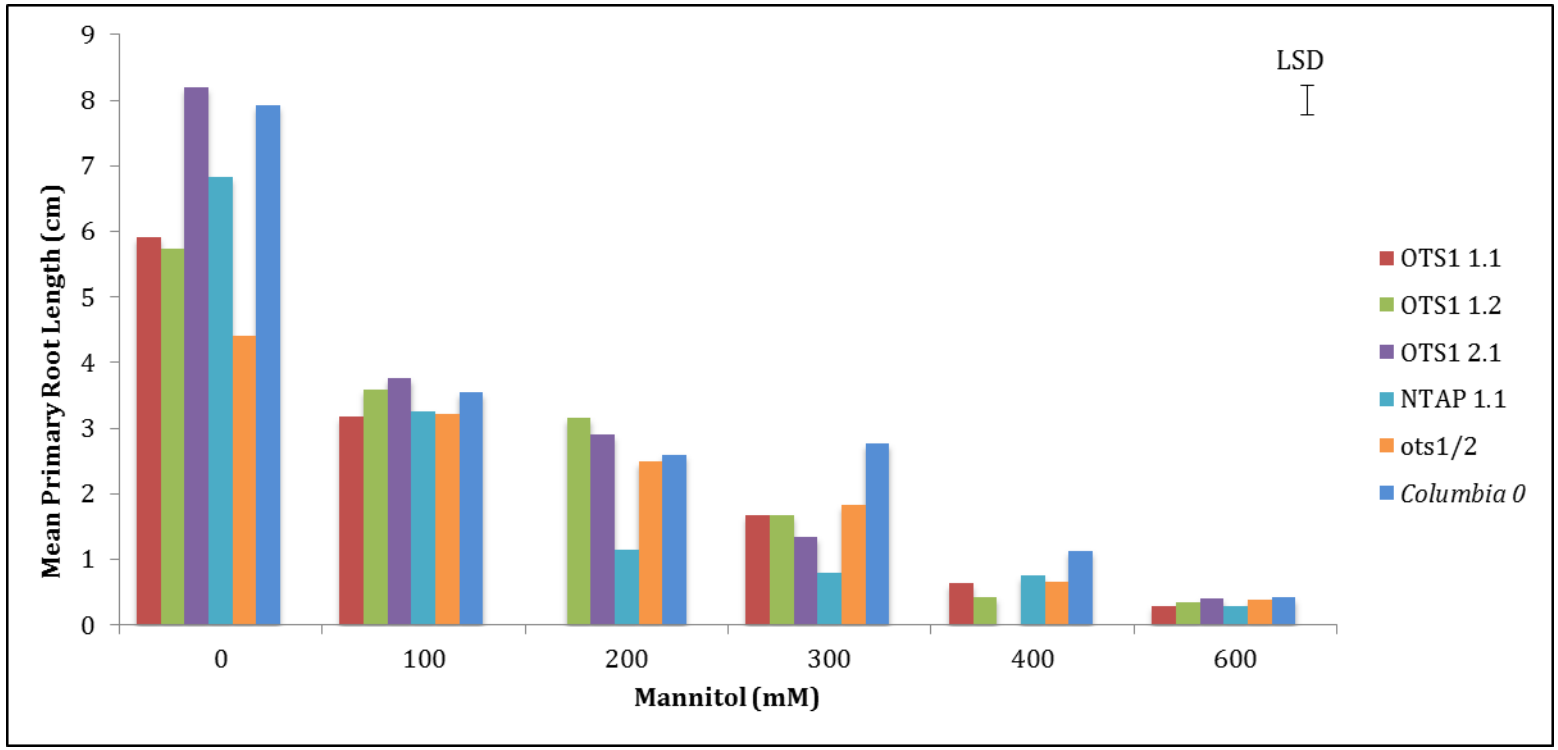

Figure 6-4 - OTS1 does not affect primary root growth inhibition at low levels of osmotic stress. Seeds from lines p35S:NTAP-OTS1 1.1, p35S:NTAP-OTS1 1.2, p35S:NTAP-OTS1 2.1, p35S:NTAP 1.1, ots1 ots 2 and Columbia-0 were applied to each ½ MS media plate, treated at 4°C for 2 days and allowed to germinate for 3 days in constant light. Seedlings were transferred onto plates of each treatment (0, 100, 200, 300, 400 and 600mM mannitol) and allowed to grow in constant light for a further 11 days prior to root measurements. There are no values for OTS1 1.1 at 200M and OTS1 2.1 at 400mM due to contamination of plates. Plates were scanned and primary root length measured with Image J software. General ANOVA found P<0.001, LSD (P<0.05) – 0.4366, d.f. - 779. n = 8-10, for each of two technical replicates at each mannitol concentration.

It is noted that the control of lateral root growth varies from primary root growth. For example, auxin inhibits primary root growth, but promotes laterals (Ivanchenko, Muday & Dubrovsky, 2008; Shi *et al.*, 2010), therefore, having assessed the relationship between OTS overexpression with primary root length in osmotic stress conditions, the same variables were used to examine the total lateral root length (Figure 6-5). The total lateral root length was the sum of the individual lateral root lengths on any one seedling, and was felt to be the most appropriate was to assess any phenotype associated with lateral roots.

For both 0mM mannitol and 100mM mannitol, the highest total lateral root length is for Col-0, with a root length of 12.5cm (0mM). At the other end of the spectrum *ots1 ots2* had shortest laterals with total lateral root length of 3.75cm (0mM). As above in regards to primary root length, increased osmotic stress reduced laterals in all lines. All values for the OTS overexpressors and NTAP controls are similar. At 200mM mannitol the highest total lateral root length is attributable to the OTS1 2.1 line, with the Col-0 line having a total lateral root length on average 1.1cm shorter than the OTS1 2.1 line, closely followed by the OTS 1 1.2 line. At higher mannitol concentration, lateral root length is impaired in all lines and the line, which performs the best under this osmotic stress looks to be Col-0.

As with Figure 6-4, the data forming these results was statistically analysed using ANOVA and the results of this experiment were found significant for each line, with each of the different mannitol treatments accounted for. The 35S:OTS lines do seem to behave quite similarly in conditions of osmotic stress, and

show consistency, but do not alleviate stress conditions, demonstrated by them not having longer total lateral root length. The ots double knockout is severely impaired in lateral root growth under mannitol application. Overall, taking into account that Col-0 has a better overall lateral root growth with osmotic stress, it seems that both overexpression and non-expression of the OTS proteases impair responses to osmotic stress.

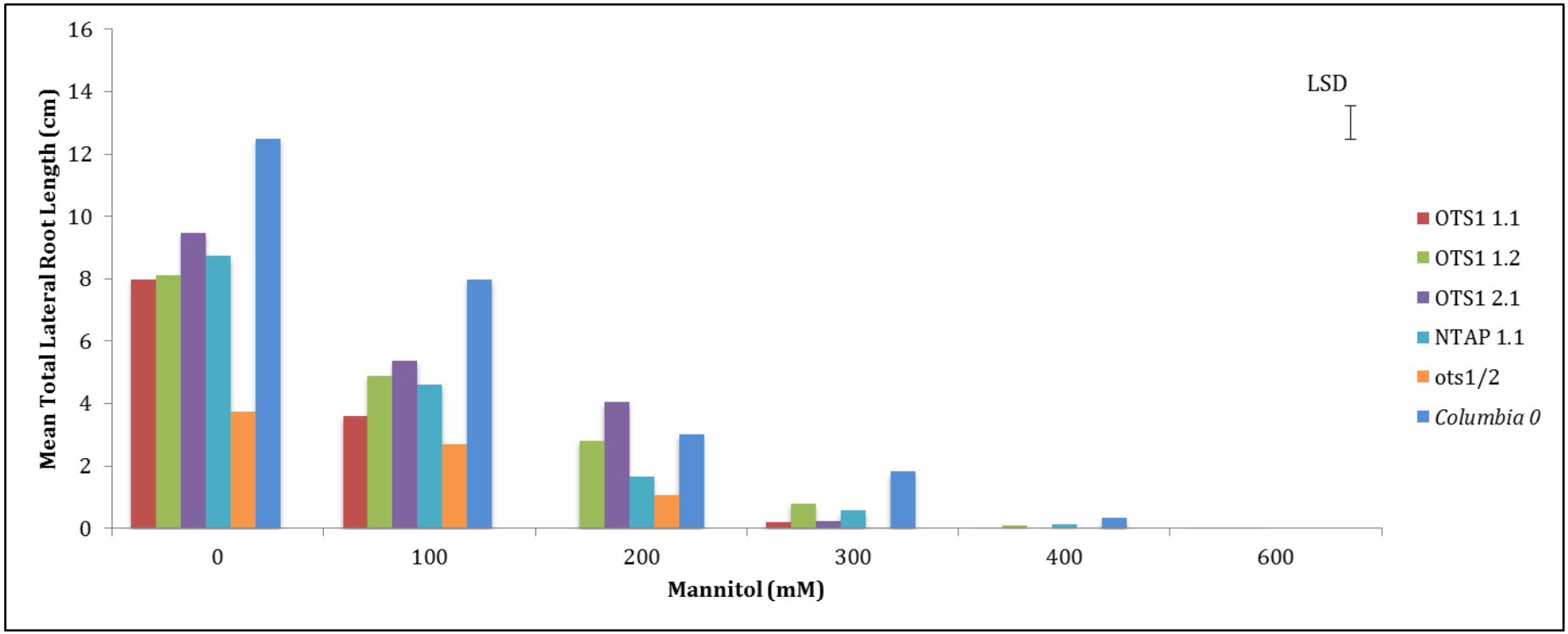

Figure 6-5 – Independent OTS1 overexpressing lines show no increased tolerance to osmotic stress in terms of summed lateral root growth. Seeds from lines p35S:NTAP-OTS1 1.1, p35S:NTAP-OTS1 1.2, p35S:NTAP-OTS1 2.1, p35S:NTAP 1.1, ots1 ots2 and Columbia-0 were applied to each ½ MS media plate, treated at 4°C for 2 days and allowed to germinate for 3 days in constant light. Seedlings were transferred onto the 6 treatments (0, 100, 200, 300, 400 and 600mM mannitol) and allowed to grow in constant light for a further 11 days prior to root measurements. There are no values for OTS1 1.1 at 200M and OTS1 2.1 at 400mM due to contamination of plates. Plates were scanned and primary root length measured with Image J software. General ANOVA found P<0.001, LSD (P<0.05) – 1.0673, d.f. – 779. n = 8-10, for each of two technical replicates at each mannitol concentration.

6.5 Discussion

From the results shown in Figure 6-2 and Figure 6-3 it is clear that overexpression of *OTS1* does not confer a great influence on osmotic stress responses during seed germination. The results of these experiments did not suggest that the lines overexpressing OTS1 had a greater final percentage of germination, or that the germination rate was quicker for these lines. This conclusion was reinforced by non-linear regression and ANOVA analyses, which did not find the data varied from one another significantly when including both the variables of transgenic line and treatment (PEG concentration). However, the inhibition of germination seen with the *ots* double mutant is a novel observation and suggests that there is a role for SUMOylation in this process. We speculate that deSUMOylation of proteins releases proteins necessary for seed germination, but that low levels of SUMO proteases are sufficient.

The conclusions reached were slightly different when analysing seedling establishment (Figure 6-4 and Figure 6-5). While there is no clear positive effect of the OTS protease in mediating osmotic stress across mannitol concentrations, it does seem to have an important role in emergence and seedling establishment through both data for primary and lateral root length. In both the primary root length data and total lateral root data, the best performing line under osmotic stress is Col-0. Analysing primary and lateral root data, OTS overexpressors are compromised in growth compared to Col-0. However, looking at primary root data they have notably longer primary roots when no treatment is applied

compared with the *ots* double knockout, and have longer total lateral root length in all treatments than *ots1 ots2*. This data shows that the OTS protease compromises primary root growth, both when overexpressed or absent, in osmotic stress conditions, and has a similar effect on lateral root growth, although perhaps through different means, since the ots knockout has reduced lateral root length in all treatments, compared with the OTS overexpressors, but is only impaired in primary root growth in the null treatment when reacted to the OTS lines. This could be due to divergent mechanisms controlling lateral and primary root growth governed by auxins (Ivanchenko, Muday & Dubrovsky, 2008; Shi *et al.*, 2010). However, these differences seen between plants overexpressing OTS1 and with both proteases knocked out show that the OTS does have a role in seedling emergence

These results are consistent with previous research of SUMO machinery in plants. The OTS1 protease has, so far, been implicated very specifically in stress responses following application of high salinity (Conti et al., 2008; 2009). OTS1 is not alone in having this specific role or function in *Arabidopsis* as part of plant development or response to stress conditions. For example, the ESD4 SUMO protease is known to be specifically required as a regulator of flowering time in *Arabidopsis* (Reeves et al., 2002; Murtas et al., 2003). In addition, another element of SUMO machinery the SUMO E3 ligase SIZ1 is responsible for management of salicylic-acid mediated innate immunity and regulation of cell growth and development through the same hormone in Arabidopsis (Watts, 2007; Lee *et al.*, 2007; Miura & Hasegawa, 2010). It also has roles in gene regulation following drought stress (Sarge & Park-Sarge, 2009; Catala *et al.*,

2007) and mediates phosphate deficiency responses (Miura & Hasegawa, 2010; Miura *et al.*, 2005).

By similar investigations, hopefully it will be possible to ascertain whether the SUMO proteases OTS1 and OTS2 play a role in stress responses other than high salinity and osmotic stress, including drought stress. The OTS protease, due its function in SUMOylation and previous data collected in regards to OTS and its relationship with salt stress (Kurepa *et al.*, 2003; Conti *et al.*, 2008; 2009), is likely to have wider developmental involvement in *Arabidopsis* which are yet discovered and may be integral to the plant in interaction with other proteins discovered to have involvement in osmotic stress such as LOS6/ABA1, RAPTOR1 and SOS6/AtCSLD5 (Catala *et al.*, 2007; Xiong *et al.*, 2002; Mahfouz *et al.*, 2006; Zhu *et al.*, 2010).

7 Discussion

Analysis and results within this thesis centres on the generation of two novel alleles of RGA and GAI ($RGA^{K/R}$ and $GAI^{K/R}$) based on an emerging protein modification system, SUMOylation. The $RGA^{K/R}$ and $GAI^{K/R}$ proteins have been recently demonstrated to be non-SUMOylatable (Conti *et al.*, 2014), and therefore the effect of these alleles on plant growth and development particularly during stress can provide new insights into the role of SUMOylation in plants. Binding interaction studies of the SUMO/GID1/GA/RGA complex using surface plasmon resonance, and records of transgenic lines overexpressing the SUMO protease OTS1 add further information about these important regulatory proteins.

The most significant finding is that the $GAI^{K/R}$-GFP protein does not confer a dwarf phenotype in plants, compared with its GAI^{K}-GFP counterpart and controls (Figure 3-6, Figure 3-7). In addition, transgenic lines overexpressing the $GAI^{K/R}$-GFP protein have fewer rosette leaves at the point of bolting than the GAI^{K}-GFP lines and controls (Figure 3-8). This is a completely novel observation and it demonstrates that SUMOylation of GAI is integral to the regular growth repressing function of GAI in *Arabidopsis*.

By contrast the results for RGA transgenic lines are not as clear. While the $RGA^{K/R}$-GFP mutation and its overexpression in *Arabidopsis* is a new mutant to be studied, overexpression of RGA^{K}-GFP has been analysed previously (Silverstone *et al.*, 2001). Generally, these lines have characteristic delay in

bolting, and greater number of rosette leaves at bolting and often a larger rosette at the point of bolting compared to controls. The RGA^{K}-GFP lines analysed here bolted at the same time as Col-0 and other controls (Figure 4-4). They did retain a larger rosette leaves (*Figure 4-5*) but lost these other key phenotypic features present associated with delayed bolting. Most surprising were the results for RGA$^{K/R}$-GFP, which were delayed in bolting, just the opposite phenotype to that conferred by $^{K/R}$ mutation in GAI. These results are a bit puzzling. One familiar effect of 35S-driven overexpression of cDNA's is co-suppression of both transgene and endogenous gene (Cogoni & Macino, 1999; Dalmay *et al.*, 2000; Thomas *et al.*, 2003; Catalanotto *et al.*, 2004). The RGA results cannot be explained by co-suppression, as protein is shown to be present on immunoblot with α-RGA (Figure 4-9). One explanation that seems viable is that the RGA^{K}-GFP transgene has picked up some unnoticed mutation rendering the protein less functional as a DELLA protein (relieving suppression of growth), but not leading to it being readily degraded. The transgenic lines were sequenced through CAPS marker analysis to confirm the presence of RGA transcript and of the $^{K/R}$ mutation (Figure 4-3), but full re-sequencing was not done given that the lines were provided to the project. There was a difference in level of SUMOylated RGA protein between the RGA^{K} and $^{K/R}$-GFP lines, evident after immunoprecipitation and a subsequent SUMOylation assay (Figure 4-10). Before further work is carried out using these RGA transgenic lines it would be advisable to have plasmids re-sequenced in order to account for any mutations in the full gene fragment.

In terms of the RGA$^{K/R}$-GFP transgenic line, the phenotype was found to be much as you might expect the RGA^{K}-GFP lines to be; with delayed bolting and growth repression phenotype compared to the control lines (Figure 4-4, *Figure 4-5*, Figure 4-6). We must assume that transgenic lines overexpressing the RGA$^{K/R}$-GFP fusion protein are active like non-mutated RGA. There is considerable protein expression of RGA$^{K/R}$ (Figure 4-9), and SUMOylation is demonstrated to be reduced compared with RGA^{K} (Figure 4-10), however knowing more information about the genotype, we cannot explain the phenotype by suggesting co-suppression. One option for analysing these transgenic lines further would be to transform the RGA^{K} and $^{K/R}$-GFP constructs into an *rga* mutant background conferring a null allele, such as *rga-24* (Dill & Sun, 2001; King, Moritz & Harberd, 2001) or *rga-22* (Dill *et al.*, 2004). This would allow further study of whether these overexpressing constructs in the ^{K} and $^{K/R}$ form are able to complement the function of the endogenous RGA missing from this background.

Figure 7-1 - *Figure showing the phenotype of T2 DELLA overexpression lines. Demonstration of bolting phenotype in (left to right) p35S:RGA$^{K/R}$-GFP, p35S:RGA^{K}-GFP, p35S:GAI$^{K/R}$-GFP and p35S:GFP control line.*

The alteration in phenotype due to the $^{K/R}$ mutation in RGA-GFP (Figure 7-1) and GAI-GFP (*Figure 7-2*) were investigated to ascertain how reduced SUMOylation was leading to such a phenotype. There have been cases in animal literature that SUMOylation induces recompartmentalisation of target proteins (Sachdev *et al.*, 2001; Geiss-Friedlander & Melchior, 2007). Analysis of RGA-GFP and GAI-GFP through confocal microscopy was carried out in order to see if there was any divergence of the position of GAI in the nucleus (Silverstone, Ciampaglio & Sun, 1998; Fleck & Harberd, 2002) due to the $^{K/R}$ mutation. No change in subcellular localisation of GAI$^{K/R}$-GFP was noted when compared with GAI^{K}-GFP (*Figure 3-14*). Both proteins were degraded in response to gibberellin treatment, and if the proteins were not fully degraded, nuclear localisation of GAI was still evident (*Figure 3-15*). By contrast, while RGA^{K} and $^{K/R}$-GFP were also both nuclear and both degraded upon GA treatment, this led to

disappearance of the nuclear GFP signal visible and a diffuse GFP signal throughout the cell. As previously discussed, a more quantifiable measure of presence and loss of nuclear expression in a time-course experiment would be the use of a nuclear stain such as DAPI.

The difference in the phenotype of the two DELLA$^{K/R}$ transgenic lines could be due to a number of factors. In *Arabidopsis* these proteins are known to have some divergent functions, with GAI being more common in root tissue (Busov *et al.*, 2006; Ubeda-Tomás *et al.*, 2008; 2009) and RGA associated with hypocotyl elongation (King, Moritz & Harberd, 2001) and not root extension or lateral root length, an observation supported by my data (Figure 3-9). As these proteins differ in function, perhaps they also have a different relationship with the SUMOylation process. For example, RGA and GAI, although similar in sequence, have different levels of homology to DELLA proteins outwith *Arabidopsis*, especially the crop species (Figure 1-6). Indeed, GAI has higher sequence similarity to the crop DELLA's such as Rht1, D8, SLR1 and SLN1 than RGA, suggesting that perhaps some of the functions of the two proteins and their mechanisms for interaction with SUMOylation have diverged. In addition, the SUMOylation motif sequence on the RGA protein is different to that of GAI and the crop DELLA species (Figure 1-6). This difference in the first amino acid in the motif from a hydrophobic leucine in RGA to an uncharged polar glutamine in GAI could be the key to differences in SUMOylation between the proteins.

As previously mentioned, GAI is reported to be more involved in root growth in *Arabidopsis* than RGA (King, Moritz & Harberd, 2001; Busov *et al.*, 2006; Ubeda-

Tomás *et al.*, 2008; 2009), and the data collected in this thesis reinforces this point. Comparisons of primary root growth in the GAI^{K} and $^{K/R}$-GFP lines shows that plants with and without capacity for SUMOylation of GAI have different responses to stress conditions such as high salinity or enhanced growth repression with paclobutrazol (Figure 3-9). Stress imposed by 100mM NaCl reduced primary root growth in the GAI^{K}-GFP line far more than in the GAI$^{K/R}$-GFP line. Addition of GA cancelled this effect. The GAI$^{K/R}$-GFP line response was similar to the control response in each case, suggesting that SUMOylation may protect the GAI protein from degradation induced by salt stress. As observed above, addition of GA induces GAI breakdown, relieving the suppression of growth from salt. Growth in PAC reinforces these observations. These data suggest that SUMOylation of GAI plays an important role in abiotic stress responses in *Arabidopsis thaliana*. This is consistent with a great deal of previous data linking SUMOylation to responses to both biotic and abiotic stress (Lois, Lima & Chua, 2003; Elrouby & Coupland, 2010; van den Burg *et al.*, 2010). Overexpression of RGA gave no apparent DELLA response in roots, so the affects of salt stress on RGA responses could not be evaluated.

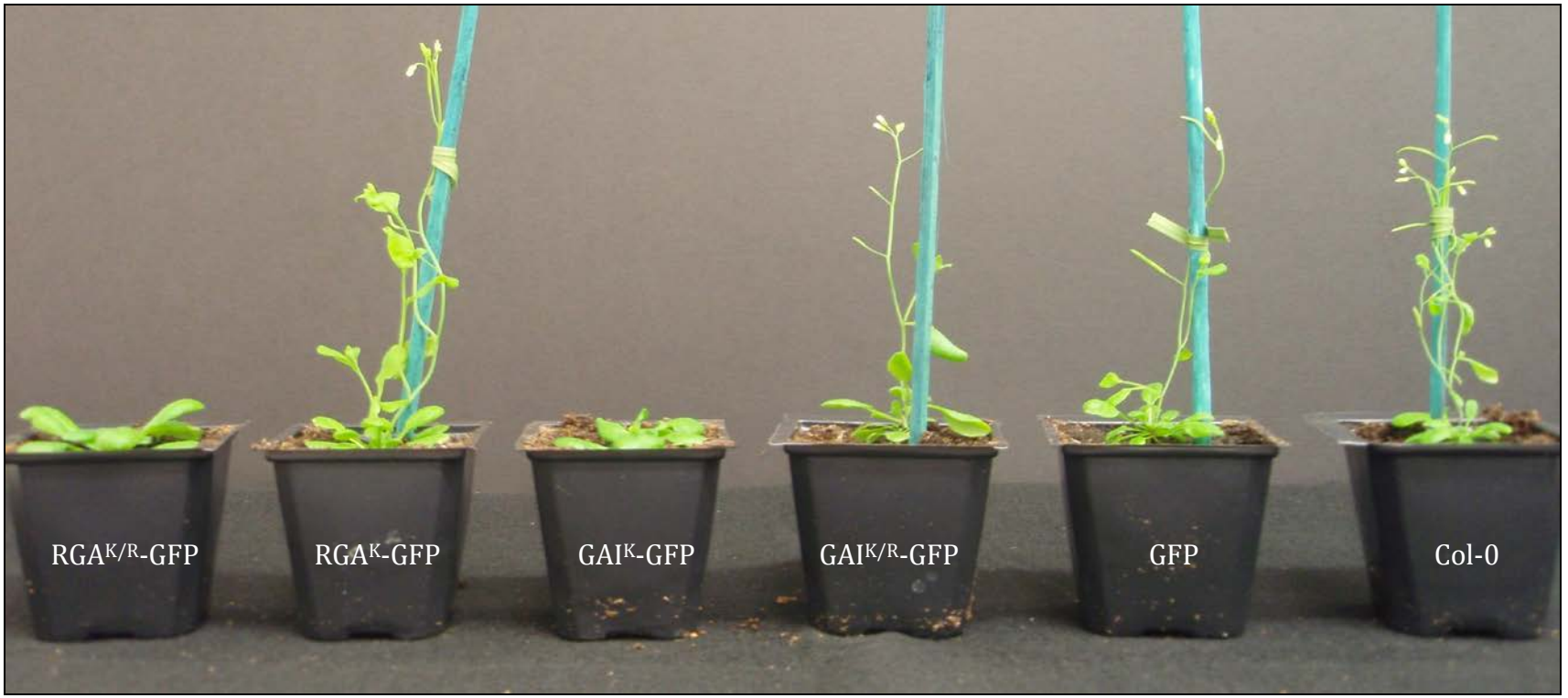

Figure 7-2 – The phenotype of T3 DELLA overexpression lines. Demonstration of bolting phenotype in (left to right) p35S:RGA$^{K/R}$-GFP, p35S:RGA^{K}-GFP, p35S:GAI^{K}-GFP, p35S:GAI$^{K/R}$-GFP, p35S:GFP and Columbia-0.

While we are unsure of the way that SUMO interacts with these two DELLA proteins, the SUMOylation assay (Figure 3-13, Figure 4-10) showed that RGA does become SUMOylated, although these assays require so much material and such care that it is likely that only very small pools of SUMOylation product exist. Indeed, it was hard to detect sufficient IP product from GAI (Figure 3-13). However, as well as SUMO ligation to target proteins it has become clear that a number of proteins carry SIMs, sites at which SUMO may interact non-covalently (Kerscher, 2007). Given that a SIM was identified on GID1 (Table 5-1), I decided to test the interaction of the GID1/DELLA/SUMO complex, along with Gibberellin. Novel data showing the non-covalent interaction of both GID1 and RGA with SUMO is demonstrated through initial SPR data (Figure 5-14, Figure 5-15). While this requires further investigation it does suggest that SUMO may affect DELLA protein availability through a mechanism that is not GA dependent, suggesting diverse interactions between SUMO and DELLA protein regulation. This is of course highly speculative at this point in data gathering.

The Sadanandom group has recently developed the hypothesis that the SUMO–SIM 'molecular glue' paradigm functions within plants to prevent ubiquitination of target proteins (i.e. by appropriating the GID1 receptor required for ubiquitination of its target protein DELLA). The SIM motif in GID1 that interacts with SUMO1 is situated in the N-terminal helical switch region known to bind VHYNP and LExLE motifs in DELLA proteins suggesting that SUMO1 may act as a physical antagonist against GID1 binding DELLAs. In addition, the SIM motif region in GID1 overlaps with the N-terminal 'lid' region that covering the GA docking pocket within the receptor. It is therefore tempting to speculate that

SUMOylation could also interfere with GA access to GID1 and as a result, affect binding to the DELLA motif (Conti *et al.*, 2014).

Study of mutants both overexpressing and with a knockout of the OTS proteases have also uncovered some interesting results. The OTS protease has previously been found to be integral to responses to high salinity in *Arabidopsis* (Conti *et al.*, 2008; 2009) and other stress conditions (Lee *et al.*, 2007; Miura *et al.*, 2011) The data in this thesis found that overexpression of the OTS1 protease did not improve plant responses to osmotic stress. This could be due to co-suppression of the OTS proteases and this possibility will require completion of transcript and protein analyses. However, what is evident from my results is that having no OTS protease (data for the *ots* double mutant) inhibits germination significantly under osmotic stress (Figure 6-3). This novel observation again indicates that there is a role for SUMOylation during germination and seedling establishment. Assuming that the 35S:OTS plants were not co-suppressed, it is clear that overexpression contributes no change in phenotype and that wild-type levels of OTS appear enough. Interestingly the *Arabidopsis* DELLA protein RGL2 has a prominent role in seed germination, so it would be interesting to carry out some crosses between OTS overexpressing lines and DELLA mutants to elucidate further interaction between SUMOylation and DELLA proteins (Lee *et al.*, 2002). During seedling establishment, differences between plants overexpressing OTS1 and *ots1 ots2* suggest mutants that OTS has a function in seedling emergence, during both primary and lateral root development (Figure 6-4, Figure 6-5).

Overall, the data collected in this thesis suggests that SUMOylation does play an important role in DELLA protein function and in abiotic stress responses. Given that the 35S:OTS lines and the *ots* mutant lines will affect the activities of many proteins, not just DELLAs it is likely that the data add weight to the argument that SUMO works both through DELLA proteins and by other mechanisms in Arabidopsis thaliana. The effects of SUMOylation seem to be particularly evident with GAI, and use of the GAI^{K} and $^{K/R}$-GFP lines has allowed me to focus on the role of SUMOylation on DELLAs. While we know that SUMOylation does play a role we are yet to elucidate exactly how this role manifests. We know that SUMOylation does not alter the subcellular localisation of DELLA proteins and does not prevent their degradation noticeably in the experiments carried out. The next stage in this project will be to investigate how SUMOylation interacts with DELLA proteins more specifically to have an effect in plant growth regulation. Following these steps, it may be possible to translate the knowledge we have gained from *Arabidopsis* into plants of economic and social importance such as crop species.

8 References

Achard, P., Cheng, H., De Grauwe, L., Decat, J., Schoutteten, H., Moritz, T., Van Der Straeten, D., Peng, J. & Harberd, N.P. (2006) Integration of plant responses to environmentally activated phytohormonal signals. *Science*. 311 (5757), pp. 91–94.

Achard, P., Gong, F., Cheminant, S., Alioua, M., Hedden, P. & Genschik, P. (2008a) The cold-inducible CBF1 factor-dependent signaling pathway modulates the accumulation of the growth-repressing DELLA proteins via its effect on gibberellin metabolism. *The Plant cell*. 20 (8), pp. 2117–2129.

Achard, P.P., Renou, J.-P.J., Berthomé, R.R., Harberd, N.P.N. & Genschik, P.P. (2008b) Plant DELLAs Restrain Growth and Promote Survival of Adversity by Reducing the Levels of Reactive Oxygen Species. *Current Biology*. 18 (9), pp. 5–5.

Ariizumi, T., Murase, K., Sun, T.-P. & Steber, C.M. (2008) Proteolysis-independent downregulation of DELLA repression in Arabidopsis by the gibberellin receptor GIBBERELLIN INSENSITIVE DWARF1. *The Plant cell*. 20 (9), pp. 2447–2459.

Bayer, P., Arndt, A., Metzger, S., Mahajan, R., Melchior, F., Jaenicke, R. & Becker, J. (1998) Structure determination of the small ubiquitin-related modifier SUMO-1. *Journal of molecular biology*. 280 (2), pp. 275–286.

Boggio, R. & Chiocca, S. (2005) Gam1 and the SUMO pathway. *Cell cycle (Georgetown, Tex.)*. 4 (4), pp. 533–535.

Bolle, C.C. (2004) The role of GRAS proteins in plant signal transduction and development. *Planta*. 218 (5), pp. 683–692.

Bonifacino, J.S.J. & Weissman, A.M.A. (1998) Ubiquitin and the control of protein fate in the secretory and endocytic pathways. *Annual review of cell and developmental biology*. 14pp. 19–57.

Boss, P.K.P. & Thomas, M.R.M. (2002) Association of dwarfism and floral induction with a grape 'green revolution' mutation. *Nature*. 416 (6883), pp. 847–850.

Börner, A., Plaschke, J., Korzun, V. & Worland, A.J. (1996) The relationships between the dwarfing genes of wheat and rye. *Euphytica*.

Brian, P.W. & Hemming, H.G. (1955) The Effect of Gibberellic Acid on Shoot Growth of Pea Seedlings. *Physiologia Plantarum*. 8 (3), pp. 669–681.

Budhiraja, R., Hermkes, R., Muller, S., Schmidt, J., Colby, T., Panigrahi, K., Coupland, G. & Bachmair, A. (2009) Substrates related to chromatin and to RNA-dependent processes are modified by Arabidopsis SUMO isoforms that differ in a conserved residue with influence on desumoylation. *Plant*

Physiology. 149 (3), pp. 1529–1540.

Busov, V.V., Meilan, R.R., Pearce, D.W.D., Rood, S.B.S., Ma, C.C., Tschaplinski, T.J.T. & Strauss, S.H.S. (2006) Transgenic modification of gai or rgl1 causes dwarfing and alters gibberellins, root growth, and metabolite profiles in Populus. *Planta*. 224 (2), pp. 288–299.

Castaño-Miquel, L., Seguí, J. & Lois, L.M. (2011) Distinctive properties of Arabidopsis SUMO paralogues support the in vivo predominant role of AtSUMO1/2 isoforms. *The Biochemical journal*. 436 (3), pp. 581–590.

Catala, R., Ouyang, J., Abreu, I.A., Hu, Y., Seo, H., Zhang, X. & Chua, N.-H. (2007) The Arabidopsis E3 SUMO ligase SIZ1 regulates plant growth and drought responses. *The Plant cell*. 19 (9), pp. 2952–2966.

Catalanotto, C.C., Pallotta, M.M., ReFalo, P.P., Sachs, M.S.M., Vayssie, L.L., Macino, G.G. & Cogoni, C.C. (2004) Redundancy of the two dicer genes in transgene-induced posttranscriptional gene silencing in Neurospora crassa. *Molecular and cellular biology*. 24 (6), pp. 2536–2545.

Chandler, P.M.P., Marion-Poll, A.A., Ellis, M.M. & Gubler, F.F. (2002) Mutants at the Slender1 locus of barley cv Himalaya. Molecular and physiological characterization. *Plant Physiology*. 129 (1), pp. 181–190.

ChandlerRobertson (1999) Gibberellin dose-response curves and the characterization of dwarf mutants of barley. *Plant Physiology*. 120 (2), pp. 623–632.

Cheng, H.H., Qin, L.L., Lee, S.S., Fu, X.X., Richards, D.E.D., Cao, D.D., Da D Luo, Harberd, N.P.N. & Peng, J.J. (2004) Gibberellin regulates Arabidopsis floral development via suppression of DELLA protein function. *Development*. 131 (5), pp. 1055–1064.

Chiang, H.H., Hwang, I. & Goodman, H.M. (1995) Isolation of the Arabidopsis GA4 locus. *The Plant cell*. 7 (2), pp. 195–201.

Chosed, R., Mukherjee, S., Lois, L.M. & Orth, K. (2006) Evolution of a signalling system that incorporates both redundancy and diversity: Arabidopsis SUMOylation. *The Biochemical journal*. 398 (3), pp. 521–529.

Cimarosti, H., Ashikaga, E., Jaafari, N., Dearden, L., Rubin, P., Wilkinson, K.A. & Henley, J.M. (2012) Enhanced SUMOylation and SENP-1 protein levels following oxygen and glucose deprivation in neurones. *Journal of cerebral blood flow and metabolism : official journal of the International Society of Cerebral Blood Flow and Metabolism*. 32 (1), pp. 17–22.

Clough, S.J. & Bent, A.F. (1998) Floral dip: a simplified method for Agrobacterium-mediated transformation of Arabidopsis thaliana. *The Plant journal : for cell and molecular biology*. 16 (6), pp. 735–743.

Cogoni, C.C. & Macino, G.G. (1999) Gene silencing in Neurospora crassa requires

a protein homologous to RNA-dependent RNA polymerase. *Nature*. 399 (6732), pp. 166–169.

Colby, T.T., Matthäi, A.A., Boeckelmann, A.A. & Stuible, H.-P.H. (2006) SUMO-conjugating and SUMO-deconjugating enzymes from Arabidopsis. *Plant Physiology*. 142 (1), pp. 318–332.

Conti, L., Kioumourtzoglou, D., O'Donnell, E., Dominy, P. & Sadanandom, A. (2009) OTS1 and OTS2 SUMO proteases link plant development and survival under salt stress. *Plant signaling & behavior*. 4 (3), pp. 225–227.

Conti, L., Nelis, S., Zhang, C., Woodcock, A., Swarup, R., Galbiati, M., Tonelli, C., Napier, R., Hedden, P., Bennett, M. & Sadanandom, A. (2014) Small Ubiquitin-like Modifier Protein SUMO Enables Plants to Control Growth Independently of the Phytohormone Gibberellin. *Developmental Cell*. 28 (1), pp. 102–110.

Conti, L., Price, G., O'Donnell, E., Schwessinger, B., Dominy, P. & Sadanandom, A. (2008) Small ubiquitin-like modifier proteases OVERLY TOLERANT TO SALT1 and -2 regulate salt stress responses in Arabidopsis. *The Plant cell*. 20 (10), pp. 2894–2908.

Conway, G. (1998) *The Doubly Green Revolution*. Cornell University Press.

Dalmay, T.T., Hamilton, A.A., Rudd, S.S., Angell, S.S. & Baulcombe, D.C.D. (2000) An RNA-Dependent RNA Polymerase Gene in Arabidopsis Is Required for Posttranscriptional Gene Silencing Mediated by a Transgene but Not by a Virus. *Cell*. 101 (5), pp. 11–11.

Davies, P.J. (2004) *Plant Hormones*. Springer.

Derkx, M., Vermeer, E. & Karssen, C.M. (1994) Gibberellins in seeds of Arabidopsis thaliana: biological activities, identification and effects of light and chilling on endogenous levels. *Plant Growth Regulation*.

Dill, A. & Sun, T. (2001) Synergistic derepression of gibberellin signaling by removing RGA and GAI function in Arabidopsis thaliana. *Genetics*. 159 (2), pp. 777–785.

Dill, A., Jung, H.S. & Sun, T.P. (2001) The DELLA motif is essential for gibberellin-induced degradation of RGA. *Proceedings of the National Academy of Sciences of the United States of America*. 98 (24), pp. 14162–14167.

Dill, A., Thomas, S.G., Hu, J., Steber, C.M. & Sun, T.-P. (2004) The Arabidopsis F-box protein SLEEPY1 targets gibberellin signaling repressors for gibberellin-induced degradation. *The Plant cell*. 16 (6), pp. 1392–1405.

Dye, B.T. & Schulman, B.A. (2007) Structural mechanisms underlying posttranslational modification by ubiquitin-like proteins. *Annual review of biophysics and biomolecular structure*. 36pp. 131–150.

Dyson, T. (1996) *Population and Food*. Routledge.

Eckardt, N.A. (2002) *Foolish Seedlings and DELLA Regulators The Functions of Rice SLR1 and Arabidopsis RGL1 in GA Signal Transduction*.

Ellis, M.H.M., Rebetzke, G.J.G., Azanza, F.F., Richards, R.A.R. & Spielmeyer, W.W. (2005) Molecular mapping of gibberellin-responsive dwarfing genes in bread wheat. *Theoretical and Applied Genetics*. 111 (3), pp. 423–430.

Elrouby, N. & Coupland, G. (2010) Proteome-wide screens for small ubiquitin-like modifier (SUMO) substrates identify Arabidopsis proteins implicated in diverse biological processes. *Proceedings of the National Academy of Sciences of the United States of America*. 107 (40), pp. 17415–17420.

Evans, L.T. (1996) *Crop Evolution, Adaptation and Yield*. Cambridge University Press.

Fivash, M., Towler, E.M. & Fisher, R.J. (1998) BIAcore for macromolecular interaction. *Current opinion in biotechnology*.

Fleck, B. & Harberd, N.P. (2002) Evidence that the Arabidopsis nuclear gibberellin signalling protein GAI is not destabilised by gibberellin. *The Plant journal : for cell and molecular biology*. 32 (6), pp. 935–947.

Fu, X., Richards, D.E., Ait-Ali, T., Hynes, L.W., Ougham, H., Peng, J. & Harberd, N.P. (2002) Gibberellin-mediated proteasome-dependent degradation of the barley DELLA protein SLN1 repressor. *The Plant cell*. 14 (12), pp. 3191–3200.

Fu, X., Sudhakar, D., Peng, J., Richards, D.E., Christou, P. & Harberd, N.P. (2001) Expression of Arabidopsis GAI in Transgenic Rice Represses Multiple Gibberellin Responses. *The Plant cell*. 13 (8), pp. 1791–1802.

Fujioka, S.S., Yamane, H.H., Spray, C.R.C., Katsumi, M.M., Phinney, B.O.B., Gaskin, P.P., Macmillan, J.J. & Takahashi, N.N. (1988) The dominant non-gibberellin-responding dwarf mutant (D8) of maize accumulates native gibberellins. *Proceedings of the National Academy of Sciences of the United States of America*. 85 (23), pp. 9031–9035.

Gale, M.D. & Marshall, G.A. (1976) The chromosomal location of Gai1 and Rht1, genes for gibberellin insensitivity and semi-dwarfism, in a derivative of Norin 10 wheat. *Heredity*.

Gale, M.D., Youssefian, S. & Russell, G.E. (1985) Dwarfing genes in wheat. *Progress in plant breeding-1*.

Garvin, A.J., Densham, R.M., Blair-Reid, S.A., Pratt, K.M., Stone, H.R., Weekes, D., Lawrence, K.J. & Morris, J.R. (2013) The deSUMOylase SENP7 promotes chromatin relaxation for homologous recombination DNA repair. *EMBO Reports*.

Geiss-Friedlander, R. & Melchior, F. (2007) Concepts in sumoylation: a decade on. *Nature Reviews: Molecular Cell Biology*. 8 (12), pp. 947–956.

Gill, G.G. (2005) Something about SUMO inhibits transcription. *Current Opinion in Genetics & Development*. 15 (5), pp. 6–6.

Gong, L. & Yeh, E.T.H. (2006) Characterization of a Family of Nucleolar SUMO-specific Proteases with Preference for SUMO-2 or SUMO-3. *Journal of Biological Chemistry*.

Goujon, M., McWilliam, H., Li, W., Valentin, F., Squizzato, S., Paern, J. & Lopez, R. (2010) A new bioinformatics analysis tools framework at EMBL-EBI. *Nucleic acids research*. 38 (Web Server issue), pp. W695–W699.

Griffiths, J., Murase, K., Rieu, I., Zentella, R., Zhang, Z.-L., Powers, S.J., Gong, F., Phillips, A.L., Hedden, P., Sun, T.-P. & Thomas, S.G. (2006) Genetic characterization and functional analysis of the GID1 gibberellin receptors in Arabidopsis. *The Plant cell*. 18 (12), pp. 3399–3414.

Gubler, F.F., Chandler, P.M.P., White, R.G.R., Llewellyn, D.J.D. & Jacobsen, J.V.J. (2002) Gibberellin signaling in barley aleurone cells. Control of SLN1 and GAMYB expression. *Plant Physiology*. 129 (1), pp. 191–200.

Hanania, U., Furman-Matarasso, N., Ron, M. & Avni, A. (1999) Isolation of a novel SUMO protein from tomato that suppresses EIX-induced cell death. *The Plant journal : for cell and molecular biology*. 19 (5), pp. 533–541.

Hannich, J.T., Lewis, A., Kroetz, M.B., Li, S.-J., Heide, H., Emili, A. & Hochstrasser, M. (2005) Defining the SUMO-modified proteome by multiple approaches in Saccharomyces cerevisiae. *The Journal of biological chemistry*. 280 (6), pp. 4102–4110.

Harberd, N.P. (2003) Botany. Relieving DELLA restraint. *Science*. 299 (5614), pp. 1853–1854.

Harberd, N.P., King, K.E., Carol, P., Cowling, R.J., Peng, J. & Richards, D.E. (1998) Gibberellin: inhibitor of an inhibitor of...? *BioEssays : news and reviews in molecular, cellular and developmental biology*. 20 (12), pp. 1001–1008.

Hart, G.W., Haltiwanger, R.S., Holt, G.D. & Kelly, W.G. (1989) Glycosylation in the nucleus and cytoplasm. *Annual review of biochemistry*. 58pp. 841–874.

Hart, G.W.G. (1997) Dynamic O-linked glycosylation of nuclear and cytoskeletal proteins. *Biochemistry*. 66pp. 315–335.

Hecker, C.-M., Rabiller, M., Haglund, K., Bayer, P. & Dikic, I. (2006) Specification of SUMO1- and SUMO2-interacting motifs. *The Journal of biological chemistry*. 281 (23), pp. 16117–16127.

Hedden, P. (2003) The genes of the Green Revolution. *Trends in Genetics*. 19 (1), pp. 5–9.

Hedden, P. & Kamiya, Y. (1997) GIBBERELLIN BIOSYNTHESIS: Enzymes, Genes and Their Regulation. *Plant Physiology and Plant Molecular Biology*. 48pp. 431–460.

Hellens, R.P., Edwards, E.A., Leyland, N.R., Bean, S. & Mullineaux, P.M. (2000) pGreen: a versatile and flexible binary Ti vector for Agrobacterium-mediated plant transformation. *Plant molecular biology*. 42 (6), pp. 819–832.

Hermkes, R., Fu, Y.-F., Nürrenberg, K., Budhiraja, R., Schmelzer, E., Elrouby, N., Dohmen, R.J., Bachmair, A. & Coupland, G. (2011) Distinct roles for Arabidopsis SUMO protease ESD4 and its closest homolog ELS1. *Planta*. 233 (1), pp. 63–73.

Hershko, A. & Ciechanover, A. (1998) The ubiquitin system. *Biochemistry*. 67pp. 425–479.

Hipp, M.S., Raasi, S., Groettrup, M. & Schmidtke, G. (2004) NEDD8 ultimate buster-1L interacts with the ubiquitin-like protein FAT10 and accelerates its degradation. *Journal of Biological Chemistry*. 279 (16), pp. 16503–16510.

Hochstrasser, M. (2009) Origin and function of ubiquitin-like proteins. *Nature*. 458 (7237), pp. 422–429.

Hochstrasser, M.M. (2000) Evolution and function of ubiquitin-like protein-conjugation systems. *Nature Cell Biology*. 2 (8), pp. E153–E157.

Hochstrasser, M.M. (2006) Lingering Mysteries of Ubiquitin-Chain Assembly. *Cell*. 124 (1), pp. 8–8.

Hooley, R. (1994) Gibberellins: perception, transduction and responses. *Plant molecular biology*. 26 (5), pp. 1529–1555.

Hussain, A. & Peng, J. (2003) DELLA Proteins and GA Signalling in Arabidopsis. *Journal of plant growth regulation*. 22 (2), pp. 134–140.

Ikeda, A., Ueguchi-Tanaka, M., Sonoda, Y., Kitano, H., Koshioka, M., Futsuhara, Y., Matsuoka, M. & Yamaguchi, J. (2001) slender Rice, a Constitutive Gibberellin Response Mutant, Is Caused by a Null Mutation of the SLR1 Gene, an Ortholog of the Height-Regulating Gene GAI/RGA/RHT/D8. *The Plant cell*. 13 (5), pp. 999–1010.

Ileperuma, N.R., Marshall, S.D.G., Squire, C.J., Baker, H.M., Oakeshott, J.G., Russell, R.J., Plummer, K.M., Newcomb, R.D. & Baker, E.N. (2007) High-resolution crystal structure of plant carboxylesterase AeCXE1, from Actinidia eriantha, and its complex with a high-affinity inhibitor paraoxon. *Biochemistry*. 46 (7), pp. 1851–1859.

Itoh, H.H., Ueguchi-Tanaka, M.M. & Matsuoka, M.M. (2008) Molecular biology of gibberellins signaling in higher plants. *International Review of Cell and Molecular Biology*. 268pp. 191–221.

Itoh, H.H., Ueguchi-Tanaka, M.M., Sato, Y.Y., Ashikari, M.M. & Matsuoka, M.M. (2002) The gibberellin signaling pathway is regulated by the appearance and disappearance of SLENDER RICE1 in nuclei. *The Plant cell*. 14 (1), pp. 57–70.

Ivanchenko, M.G., Muday, G.K. & Dubrovsky, J.G. (2008) Ethylene-auxin interactions regulate lateral root initiation and emergence in Arabidopsis thaliana. *The Plant journal : for cell and molecular biology*. 55 (2), pp. 335–347.

Jacobsen, S.E., Binkowski, K.A. & Olszewski, N.E. (1996) SPINDLY, a tetratricopeptide repeat protein involved in gibberellin signal transduction in Arabidopsis. *Proceedings of the National Academy of Sciences of the United States of America*. 93 (17), pp. 9292–9296.

Jacobsen, S.E.S. & Olszewski, N.E.N. (1993) Mutations at the SPINDLY locus of Arabidopsis alter gibberellin signal transduction. *The Plant cell*. 5 (8), pp. 887–896.

Johnson, E.S. (2004) Protein modification by SUMO. *Annual review of biochemistry*. 73pp. 355–382.

Kerscher, O. (2007) SUMO junction-what's your function? New insights through SUMO-interacting motifs. *EMBO Reports*. 8 (6), pp. 550–555.

Kerscher, O., Felberbaum, R. & Hochstrasser, M. (2006) Modification of Proteins by Ubiquitin and Ubiquitin-Like Proteins. *Annual review of cell and developmental biology*. 22 (1), pp. 159–180.

King, K.E.K., Moritz, T.T. & Harberd, N.P.N. (2001) Gibberellins are not required for normal stem growth in Arabidopsis thaliana in the absence of GAI and RGA. *Genetics*. 159 (2), pp. 767–776.

Konstantinova, I.M., Tsimokha, A.S. & Mittenberg, A.G. (2008) Role of proteasomes in cellular regulation. *International Review of Cell and Molecular Biology*. 267pp. 59–124.

Koorneef, M., Elgersma, A., Hanhart, C.J., Loenen-Martinet, E.P., Rijn, L. & Zeevaart, J.A.D. (1985) A gibberellin insensitive mutant of Arabidopsis thaliana. *Physiologia Plantarum*. 65 (1), pp. 33–39.

Koornneef, M. & Veen, J.H. (1980) Induction and analysis of gibberellin sensitive mutants in Arabidopsis thaliana (L.) heynh. *Theoretical and Applied Genetics*. 58 (6), pp. 257–263.

Kreppel, L.K.L., Blomberg, M.A.M. & Hart, G.W.G. (1997) Dynamic glycosylation of nuclear and cytosolic proteins. Cloning and characterization of a unique O-GlcNAc transferase with multiple tetratricopeptide repeats. *Journal of Biological Chemistry*. 272 (14), pp. 9308–9315.

Kurepa, J.J., Walker, J.M.J., Smalle, J.J., Gosink, M.M.M., Davis, S.J.S., Durham, T.L.T.,

Sung, D.-Y.D. & Vierstra, R.D.R. (2003) The small ubiquitin-like modifier (SUMO) protein modification system in Arabidopsis. Accumulation of SUMO1 and -2 conjugates is increased by stress. *The Journal of biological chemistry*. 278 (9), pp. 6862–6872.

Kurosawa, E. (1926) Experimental studies on the nature of the substance secreted by the‘ bakanae’ fungus. *Nat Hist Soc Formosa*.

Langridge, J. (1957) Effect of Day-length and Gibberellic Acid on the Flowering of Arabidopsis. *Nature*. 180 (4575), pp. 36–37.

Lee, J., Nam, J., Park, H.C., Na, G., Miura, K., Jin, J.B., Yoo, C.Y., Baek, D., Kim, D.H., Jeong, J.C., Kim, D., Lee, S.Y., Salt, D.E., Mengiste, T., et al. (2007) Salicylic acid-mediated innate immunity in Arabidopsis is regulated by SIZ1 SUMO E3 ligase. *The Plant journal : for cell and molecular biology*. 49 (1), pp. 79–90.

Lee, S., Cheng, H., King, K.E., Wang, W., He, Y., Hussain, A., Lo, J., Harberd, N.P. & Peng, J. (2002) Gibberellin regulates Arabidopsis seed germination via RGL2, a GAI/RGA-like gene whose expression is up-regulated following imbibition. *Genes & Development*. 16 (5), pp. 646–658.

Li, S.-J. & Hochstrasser, M. (2003) The Ulp1 SUMO isopeptidase: distinct domains required for viability, nuclear envelope localization, and substrate specificity. *The Journal of cell biology*. 160 (7), pp. 1069–1081.

Li, S.J. & Hochstrasser, M. (1999) A new protease required for cell-cycle progression in yeast. *Nature*. 398 (6724), pp. 246–251.

Li, S.J.S. & Hochstrasser, M.M. (2000) The yeast ULP2 (SMT4) gene encodes a novel protease specific for the ubiquitin-like Smt3 protein. *Molecular and cellular biology*. 20 (7), pp. 2367–2377.

Lois, L.M. (2010) Diversity of the SUMOylation machinery in plants. *Biochemical Society Transactions*. 38 (Pt 1), pp. 60–64.

Lois, L.M.L., Lima, C.D.C. & Chua, N.-H.N. (2003) Small ubiquitin-like modifier modulates abscisic acid signaling in Arabidopsis. *The Plant cell*. 15 (6), pp. 1347–1359.

MacMillan, J. (2001) Occurrence of gibberellins in vascular plants, fungi, and bacteria. *Journal of plant growth regulation*.

Mahfouz, M.M.M., Kim, S.S., Delauney, A.J.A. & Verma, D.P.S.D. (2006) Arabidopsis TARGET OF RAPAMYCIN interacts with RAPTOR, which regulates the activity of S6 kinase in response to osmotic stress signals. *The Plant cell*. 18 (2), pp. 477–490.

McGinnis, K.M., Thomas, S.G., Soule, J.D., Strader, L.C., Zale, J.M., Sun, T.-P. & Steber, C.M. (2003) The Arabidopsis SLEEPY1 gene encodes a putative F-box subunit of an SCF E3 ubiquitin ligase. *The Plant cell*. 15 (5), pp. 1120–1130.

McMillan, L.E.L., Brown, J.T.J., Henley, J.M.J. & Cimarosti, H.H. (2011) Profiles of SUMO and ubiquitin conjugation in an Alzheimer's disease model. *Neuroscience Letters*. 502 (3), pp. 201–208.

Melchior, F. (2000) SUMO--nonclassical ubiquitin. *Annual review of cell and developmental biology*. 16pp. 591–626.

Meulmeester, E., Kunze, M., Hsiao, H.H., Urlaub, H. & Melchior, F. (2008) Mechanism and consequences for paralog-specific sumoylation of ubiquitin-specific protease 25. *Molecular cell*. 30 (5), pp. 610–619.

Michel, B.E.B. (1983) Evaluation of the water potentials of solutions of polyethylene glycol 8000 both in the absence and presence of other solutes. *Plant Physiology*. 72 (1), pp. 66–70.

Minty, A., Dumont, X., Kaghad, M. & Caput, D. (2000) Covalent modification of p73alpha by SUMO-1. Two-hybrid screening with p73 identifies novel SUMO-1-interacting proteins and a SUMO-1 interaction motif. *The Journal of biological chemistry*. 275 (46), pp. 36316–36323.

Miura, K. & Hasegawa, P.M. (2010) Sumoylation and other ubiquitin-like post-translational modifications in plants. *Trends in Cell Biology*. 20 (4), pp. 10–10.

Miura, K., Jin, J.B. & Hasegawa, P.M. (2007) Sumoylation, a post-translational regulatory process in plants. *Current Opinion in Plant Biology*. 10 (5), pp. 495–502.

Miura, K., Rus, A., Sharkhuu, A., Yokoi, S., Karthikeyan, A.S., Raghothama, K.G., Baek, D., Koo, Y.D., Jin, J.B., Bressan, R.A., Yun, D.-J. & Hasegawa, P.M. (2005) The Arabidopsis SUMO E3 ligase SIZ1 controls phosphate deficiency responses. *Proceedings of the National Academy of Sciences of the United States of America*. 102 (21), pp. 7760–7765.

Miura, K.K., Jin, J.B.J., Lee, J.J., Yoo, C.Y.C., Stirm, V.V., Miura, T.T., Ashworth, E.N.E., Bressan, R.A.R., Yun, D.-J.D. & Hasegawa, P.M.P. (2007) SIZ1-mediated sumoylation of ICE1 controls CBF3/DREB1A expression and freezing tolerance in Arabidopsis. *The Plant cell*. 19 (4), pp. 1403–1414.

Miura, K.K., Lee, J.J., Gong, Q.Q., Ma, S.S., Jin, J.B.J., Yoo, C.Y.C., Miura, T.T., Sato, A.A., Bohnert, H.J.H. & Hasegawa, P.M.P. (2011) SIZ1 regulation of phosphate starvation-induced root architecture remodeling involves the control of auxin accumulation. *Plant Physiology*. 155 (2), pp. 1000–1012.

Morris, J.R., Boutell, C., Keppler, M., Densham, R., Weekes, D., Alamshah, A., Butler, L., Galanty, Y., Pangon, L., Kiuchi, T., Ng, T. & Solomon, E. (2009) The SUMO modification pathway is involved in the BRCA1 response to genotoxic stress. *Nature*. 462 (7275), pp. 886–890.

Mossessova, E. & Lima, C.D. (2000) Ulp1-SUMO crystal structure and genetic

analysis reveal conserved interactions and a regulatory element essential for cell growth in yeast. *Molecular cell*. 5 (5), pp. 865–876.

Mukhopadhyay, D. & Dasso, M. (2007) Modification in reverse: the SUMO proteases. *Trends in biochemical sciences*. 32 (6), pp. 286–295.

Murase, K., Hirano, Y., Sun, T.-P. & Hakoshima, T. (2008) Gibberellin-induced DELLA recognition by the gibberellin receptor GID1. *Nature*. 456 (7221), pp. 459–463.

Murtas, G., Reeves, P.H., Fu, Y.-F., Bancroft, I., Dean, C. & Coupland, G. (2003) A nuclear protease required for flowering-time regulation in Arabidopsis reduces the abundance of SMALL UBIQUITIN-RELATED MODIFIER conjugates. *The Plant cell*. 15 (10), pp. 2308–2319.

Müller, K.K., Tintelnot, S.S. & Leubner-Metzger, G.G. (2006) Endosperm-limited Brassicaceae seed germination: abscisic acid inhibits embryo-induced endosperm weakening of Lepidium sativum (cress) and endosperm rupture of cress and Arabidopsis thaliana. *Plant and Cell Physiology*. 47 (7), pp. 864–877.

Müller, S.S., Hoege, C.C., Pyrowolakis, G.G. & Jentsch, S.S. (2001) SUMO, ubiquitin's mysterious cousin. *Nature Reviews: Molecular Cell Biology*. 2 (3), pp. 202–210.

Nakajima, M., Shimada, A., Takashi, Y., Kim, Y.-C., Park, S.-H., Ueguchi-Tanaka, M., Suzuki, H., Katoh, E., Iuchi, S., Kobayashi, M., Maeda, T., Matsuoka, M. & Yamaguchi, I. (2006) Identification and characterization of Arabidopsis gibberellin receptors. *The Plant journal : for cell and molecular biology*. 46 (5), pp. 880–889.

Navarro, L.L., Bari, R.R., Achard, P.P., Lisón, P.P., Nemri, A.A., Harberd, N.P.N. & Jones, J.D.G.J. (2008) DELLAs Control Plant Immune Responses by Modulating the Balance of Jasmonic Acid and Salicylic Acid Signaling. *Current Biology*. 18 (9), pp. 6–6.

Niu, S., Li, Z., Yuan, H., Fang, P., Chen, X. & Li, W. (2013) Proper gibberellin localization in vascular tissue is required to regulate adventitious root development in tobacco. *Journal of Experimental Botany*. 64 (11), pp. 3411–3424.

Okada, S., Nagabuchi, M., Takamura, Y., Nakagawa, T., Shinmyozu, K., Nakayama, J.-I. & Tanaka, K. (2009) Reconstitution of Arabidopsis thaliana SUMO pathways in E. coli: functional evaluation of SUMO machinery proteins and mapping of SUMOylation sites by mass spectrometry. *Plant and Cell Physiology*. 50 (6), pp. 1049–1061.

Orth, K., Xu, Z., Mudgett, M.B., Bao, Z.Q., Palmer, L.E., Bliska, J.B., Mangel, W.F., Staskawicz, B. & Dixon, J.E. (2000) Disruption of signaling by Yersinia effector YopJ, a ubiquitin-like protein protease. *Science*. 290 (5496), pp.

1594–1597.

Payne, R.W., Harding, S.A. & Murray, D.A. (2008) Genstat release 11 reference manual, Part 2 directives. *VSN International*.

Peng, J. & Harberd, N.P. (1993) Derivative Alleles of the Arabidopsis Gibberellin-Insensitive (gai) Mutation Confer a Wild-Type Phenotype. *The Plant cell*. 5 (3), pp. 351–360.

Peng, J. & Harberd, N.P. (2002) The role of GA-mediated signalling in the control of seed germination. *Current Opinion in Plant Biology*. 5 (5), pp. 376–381.

Peng, J.J., Carol, P.P., Richards, D.E.D., King, K.E.K., Cowling, R.J.R., Murphy, G.P.G. & Harberd, N.P.N. (1997) The Arabidopsis GAI gene defines a signaling pathway that negatively regulates gibberellin responses. *Genes & Development*. 11 (23), pp. 3194–3205.

Peng, J.J., Richards, D.E.D., Hartley, N.M.N., Murphy, G.P.G., Devos, K.M.K., Flintham, J.E.J., Beales, J.J., Fish, L.J.L., Worland, A.J.A., Pelica, F.F., Sudhakar, D.D., Christou, P.P., Snape, J.W.J., Gale, M.D.M., et al. (1999) 'Green revolution' genes encode mutant gibberellin response modulators. *Nature*. 400 (6741), pp. 256–261.

Peng, J.J., Schwartz, D.D., Elias, J.E.J., Thoreen, C.C.C., Cheng, D.D., Marsischky, G.G., Roelofs, J.J., Finley, D.D. & Gygi, S.P.S. (2003) A proteomics approach to understanding protein ubiquitination. *Nature Biotechnology*. 21 (8), pp. 921–926.

Pickart, C.M. & Fushman, D. (2004) Polyubiquitin chains: polymeric protein signals. *Current Opinion in Chemical Biology*. 8 (6), pp. 7–7.

Pickart, C.M.C. (2001) Mechanisms underlying ubiquitination. *Biochemistry*. 70pp. 503–533.

Pysh, L.D.L., Wysocka-Diller, J.W.J., Camilleri, C.C., Bouchez, D.D. & Benfey, P.N.P. (1999) The GRAS gene family in Arabidopsis: sequence characterization and basic expression analysis of the SCARECROW-LIKE genes. *The Plant journal : for cell and molecular biology*. 18 (1), pp. 111–119.

Rajan, S., Plant, L.D., Rabin, M.L., Butler, M.H. & Goldstein, S.A.N. (2005) Sumoylation Silences the Plasma Membrane Leak K^+ Channel K2P1. *Cell*. 121 (1), pp. 11–11.

Reeves, P.H., Murtas, G., Dash, S. & Coupland, G. (2002) early in short days 4, a mutation in Arabidopsis that causes early flowering and reduces the mRNA abundance of the floral repressor FLC. *Development*. 129 (23), pp. 5349–5361.

Richards, D.E., King, K.E., Ait-Ali, T. & Harberd, N.P. (2001) How Gibberellin Regulates Plant Growth and Development: A Molecular Genetic Analysis of Gibberellin Signaling. *Plant Physiology and Plant Molecular Biology*. 52 (1),

pp. 67–88.

Robertson, M., Swain, S.M., Chandler, P.M. & Olszewski, N.E. (1998) Identification of a negative regulator of gibberellin action, HvSPY, in barley. *The Plant cell*. 10 (6), pp. 995–1007.

Roden, J.J., Eardley, L.L., Hotson, A.A., Cao, Y.Y. & Mudgett, M.B.M. (2004) Characterization of the Xanthomonas AvrXv4 effector, a SUMO protease translocated into plant cells. *Molecular Plant-Microbe Interactions*. 17 (6), pp. 633–643.

Rohila, J.S., Chen, M., Cerny, R. & Fromm, M.E. (2004) Improved tandem affinity purification tag and methods for isolation of protein heterocomplexes from plants. *The Plant journal : for cell and molecular biology*. 38 (1), pp. 172–181.

Sachdev, S.S., Bruhn, L.L., Sieber, H.H., Pichler, A.A., Melchior, F.F. & Grosschedl, R.R. (2001) PIASy, a nuclear matrix-associated SUMO E3 ligase, represses LEF1 activity by sequestration into nuclear bodies. *Genes & Development*. 15 (23), pp. 3088–3103.

Saitoh, H. & Hinchey, J. (2000) Functional heterogeneity of small ubiquitin-related protein modifiers SUMO-1 versus SUMO-2/3. *Journal of Biological Chemistry*. 275 (9), pp. 6252–6258.

Saracco, S.A.S., Miller, M.J.M., Kurepa, J.J. & Vierstra, R.D.R. (2007) Genetic analysis of SUMOylation in Arabidopsis: conjugation of SUMO1 and SUMO2 to nuclear proteins is essential. *Plant Physiology*. 145 (1), pp. 119–134.

Sarge, K.D. & Park-Sarge, O.-K. (2009) Sumoylation and human disease pathogenesis. *Trends in biochemical sciences*. 34 (4), pp. 200–205.

Sasaki, A., Itoh, H., Gomi, K., Ueguchi-Tanaka, M., Ishiyama, K., Kobayashi, M., Jeong, D.-H., An, G., Kitano, H., Ashikari, M. & Matsuoka, M. (2003) Accumulation of phosphorylated repressor for gibberellin signaling in an F-box mutant. *Science*. 299 (5614), pp. 1896–1898.

Shani, E.E., Weinstain, R.R., Zhang, Y.Y., Castillejo, C.C., Kaiserli, E.E., Chory, J.J., Tsien, R.Y.R. & Estelle, M.M. (2013) Gibberellins accumulate in the elongating endodermal cells of Arabidopsis root. *Proceedings of the National Academy of Sciences of the United States of America*. 110 (12), pp. 4834–4839.

Shi, C.-L., Park, H.-B., Lee, J.S., Ryu, S. & Ryu, C.-M. (2010) Inhibition of primary roots and stimulation of lateral root development in Arabidopsis thaliana by the rhizobacterium Serratia marcescens 90-166 is through both auxin-dependent and -independent signaling pathways. *Molecules and Cells*. 29 (3), pp. 251–258.

Shimada, A., Ueguchi-Tanaka, M., Nakatsu, T., Nakajima, M., Naoe, Y., Ohmiya, H., Kato, H. & Matsuoka, M. (2008) Structural basis for gibberellin recognition

by its receptor GID1. *Nature*. 456 (7221), pp. 520–523.

Sievers, F.F., Wilm, A.A., Dineen, D.D., Gibson, T.J.T., Karplus, K.K., Li, W.W., Lopez, R.R., McWilliam, H.H., Remmert, M.M., Söding, J.J., Thompson, J.D.J. & Higgins, D.G.D. (2011) Fast, scalable generation of high-quality protein multiple sequence alignments using Clustal Omega. *Molecular Systems Biology*. 7pp. 539–539.

Silverstone, A.L., Jung, H.-S., Dill, A., Kawaide, H., Kamiya, Y. & Sun, T.-P. (2001) Repressing a Repressor: Gibberellin-Induced Rapid Reduction of the RGA Protein in Arabidopsis. *The Plant cell*. 13 (7), pp. 1555–1566.

Silverstone, A.L., Mak, P.Y., Martínez, E.C. & Sun, T.P. (1997) The new RGA locus encodes a negative regulator of gibberellin response in Arabidopsis thaliana. *Genetics*. 146 (3), pp. 1087–1099.

Silverstone, A.L.A., Ciampaglio, C.N.C. & Sun, T.T. (1998) The Arabidopsis RGA gene encodes a transcriptional regulator repressing the gibberellin signal transduction pathway. *The Plant cell*. 10 (2), pp. 155–169.

Song, J.J., Durrin, L.K.L., Wilkinson, T.A.T., Krontiris, T.G.T. & Chen, Y.Y. (2004) Identification of a SUMO-binding motif that recognizes SUMO-modified proteins. *Proceedings of the National Academy of Sciences of the United States of America*. 101 (40), pp. 14373–14378.

Spoel, S.H., Tada, Y. & Loake, G.J. (2010) Post-translational protein modification as a tool for transcription reprogramming. *New Phytologist*. 186 (2), pp. 333–339.

Steber, C.M.C., Cooney, S.E.S. & McCourt, P.P. (1998) Isolation of the GA-response mutant sly1 as a suppressor of ABI1-1 in Arabidopsis thaliana. *Genetics*. 149 (2), pp. 509–521.

Sun, GoodmanAusubel (1992) Cloning the Arabidopsis GA1 Locus by Genomic Subtraction. *The Plant cell*. 4 (2), pp. 119–128.

Sun, T.-P. (2010) Gibberellin-GID1-DELLA: a pivotal regulatory module for plant growth and development. *Plant Physiology*. 154 (2), pp. 567–570.

Sun, T.-P. & Gubler, F. (2004) Molecular mechanism of gibberellin signaling in plants. *Annual review of plant biology*. 55pp. 197–223.

Sun, T.P.T. & Kamiya, Y.Y. (1994) The Arabidopsis GA1 locus encodes the cyclase ent-kaurene synthetase A of gibberellin biosynthesis. *The Plant cell*. 6 (10), pp. 1509–1518.

Sun, X., Jones, W.T., Harvey, D., Edwards, P.J.B., Pascal, S.M., Kirk, C., Considine, T., Sheerin, D.J., Rakonjac, J., Oldfield, C.J., Xue, B., Dunker, A.K. & Uversky, V.N. (2010) N-terminal domains of DELLA proteins are intrinsically unstructured in the absence of interaction with GID1/gibberellic acid receptors. *The Journal of biological chemistry*. 285 (15), pp. 11557–11571.

Swanson, K.A., Kang, R.S., Stamenova, S.D., Hicke, L. & Radhakrishnan, I. (2003) Solution structure of Vps27 UIM-ubiquitin complex important for endosomal sorting and receptor downregulation. *EMBO Journal*. 22 (18), pp. 4597–4606.

Talon, M., Koornneef, M. & Zeevaart, J.A. (1990) Endogenous gibberellins in Arabidopsis thaliana and possible steps blocked in the biosynthetic pathways of the semidwarf ga4 and ga5 mutants. *Proceedings of the National Academy of Sciences of the United States of America*. 87 (20), pp. 7983–7987.

Tanaka, T.T., Kawashima, H.H., Yeh, E.T.H.E. & Kamitani, T.T. (2003) Regulation of the NEDD8 conjugation system by a splicing variant, NUB1L. *Journal of Biological Chemistry*. 278 (35), pp. 32905–32913.

Taylor, D.L., Ho, J.C.Y., Oliver, A. & Watts, F.Z. (2002) Cell-cycle-dependent localisation of Ulp1, a Schizosaccharomyces pombe Pmt3 (SUMO)-specific protease. *Journal of Cell Science*. 115 (Pt 6), pp. 1113–1122.

Thomas, C.L.C., Leh, V.V., Lederer, C.C. & Maule, A.J.A. (2003) Turnip crinkle virus coat protein mediates suppression of RNA silencing in nicotiana benthamiana. *Virology*. 306 (1), pp. 9–9.

Thomas, S.G.S. & Sun, T.-P.T. (2004) Update on gibberellin signaling. A tale of the tall and the short. *Plant Physiology*. 135 (2), pp. 668–676.

Thornton, T., Kreppel, L., Hart, G. & Olszewski, N. (1999) Genetic and Biochemical analysis of Arabidopsis SPY. In: *Current Plant Science and Biotechnology in Agriculture*. Current Plant Science and Biotechnology in Agriculture. Dordrecht: Springer Netherlands. pp. pp. 445–448. doi:10.1007/978-94-011-4661-6_100.

Tian, C.C., Wan, P.P., Sun, S.S., Li, J.J. & Chen, M.M. (2004) Genome-wide analysis of the GRAS gene family in rice and Arabidopsis. *Plant molecular biology*. 54 (4), pp. 519–532.

Tyler, L., Thomas, S.G., Hu, J., Dill, A., Alonso, J.M., Ecker, J.R. & Sun, T.-P. (2004a) Della proteins and gibberellin-regulated seed germination and floral development in Arabidopsis. *Plant Physiology*. 135 (2), pp. 1008–1019.

Tyler, L.L., Thomas, S.G.S., Hu, J.J., Dill, A.A., Alonso, J.M.J., Ecker, J.R.J. & Sun, T.-P.T. (2004b) Della proteins and gibberellin-regulated seed germination and floral development in Arabidopsis. *Plant Physiology*. 135 (2), pp. 1008–1019.

Ubeda-Tomás, S., Federici, F., Casimiro, I., Beemster, G.T., Bhalerao, R., Swarup, R., Doerner, P., Haseloff, J. & Bennett, M.J. (2009) Gibberellin Signaling in the Endodermis Controls Arabidopsis Root Meristem Size. *Current Biology*. 19 (14), pp. 6–6.

Ubeda-Tomás, S., Swarup, R., Coates, J., Swarup, K., Laplaze, L., Beemster, G.T.S., Hedden, P., Bhalerao, R. & Bennett, M.J. (2008) Root growth in Arabidopsis requires gibberellin/DELLA signalling in the endodermis. *Nature Cell Biology*. 10 (5), pp. 625–628.

Ueguchi-Tanaka, M., Ashikari, M., Nakajima, M., Itoh, H., Katoh, E., Kobayashi, M., Chow, T.-Y., Hsing, Y.-I.C., Kitano, H., Yamaguchi, I. & Matsuoka, M. (2005) GIBBERELLIN INSENSITIVE DWARF1 encodes a soluble receptor for gibberellin. *Nature*. 437 (7059), pp. 693–698.

Ueguchi-Tanaka, M., Hirano, K., Hasegawa, Y., Kitano, H. & Matsuoka, M. (2008) Release of the repressive activity of rice DELLA protein SLR1 by gibberellin does not require SLR1 degradation in the gid2 mutant. *The Plant cell*. 20 (9), pp. 2437–2446.

Ueguchi-Tanaka, M., Nakajima, M., Katoh, E., Ohmiya, H., Asano, K., Saji, S., Hongyu, X., Ashikari, M., Kitano, H., Yamaguchi, I. & Matsuoka, M. (2007a) Molecular interactions of a soluble gibberellin receptor, GID1, with a rice DELLA protein, SLR1, and gibberellin. *The Plant cell*. 19 (7), pp. 2140–2155.

Ueguchi-Tanaka, M., Nakajima, M., Motoyuki, A. & Matsuoka, M. (2007b) Gibberellin receptor and its role in gibberellin signaling in plants. *Annual review of plant biology*. 58pp. 183–198.

van den Burg, H.A., Kini, R.K., Schuurink, R.C. & Takken, F.L.W. (2010) Arabidopsis small ubiquitin-like modifier paralogs have distinct functions in development and defense. *The Plant cell*. 22 (6), pp. 1998–2016.

Vlitos, A.J. & Meudt, W. (1957) Relationship between Shoot Apex and Effect of Gibberellic Acid on Elongation of Pea Stems. *Nature*. 180 (4580), pp. 284–284.

Watts, F.Z. (2007) The role of SUMO in chromosome segregation. *Chromosoma*. 116 (1), pp. 15–20.

Wen, C.-K. & Chang, C. (2002) Arabidopsis RGL1 encodes a negative regulator of gibberellin responses. *The Plant cell*. 14 (1), pp. 87–100.

Willige, B.C.B., Ghosh, S.S., Nill, C.C., Zourelidou, M.M., Dohmann, E.M.N.E., Maier, A.A. & Schwechheimer, C.C. (2007) The DELLA domain of GA INSENSITIVE mediates the interaction with the GA INSENSITIVE DWARF1A gibberellin receptor of Arabidopsis. *The Plant cell*. 19 (4), pp. 1209–1220.

Wilson, R.N. & Somerville, C.R. (1995) Phenotypic Suppression of the Gibberellin-Insensitive Mutant (gai) of Arabidopsis. *Plant Physiology*. 108 (2), pp. 495–502.

Wilson, R.N., Heckman, J.W. & Somerville, C.R. (1992) Gibberellin is required for flowering in Arabidopsis thaliana under short days. *Plant Physiology*.

Xiong, L., Lee, H., Ishitani, M. & Zhu, J.-K. (2002) Regulation of osmotic stress-

responsive gene expression by the LOS6/ABA1 locus in Arabidopsis. *Journal of Biological Chemistry*. 277 (10), pp. 8588–8596.

Xue, Y., Zhou, F., Fu, C., Xu, Y. & Yao, X. (2006) SUMOsp: a web server for sumoylation site prediction. *Nucleic acids research*. 34 (Web Server issue), pp. W254–W257.

Yabuta, T. (1938) On the crystal of gibberellin, a substance to promote plant growth. *J Agric Chem Soc Japan*.

Yamaguchi, S. (2008) Gibberellin metabolism and its regulation. *Annual review of plant biology*. 59pp. 225–251.

Yang, W., Sheng, H., Homi, H.M., Warner, D.S. & Paschen, W. (2008) Cerebral ischemia/stroke and small ubiquitin-like modifier (SUMO) conjugation--a new target for therapeutic intervention? *Journal of neurochemistry*. 106 (3), pp. 989–999.

Zeevaart, J. & Talon, M. (1992) Gibberellin mutants in Arabidopsis thaliana. *Progress in plant growth regulation*.

Zhong, S., Lin, Z., Fray, R.G. & Grierson, D. (2008) Improved plant transformation vectors for fluorescent protein tagging. *Transgenic research*. 17 (5), pp. 985–989.

Zhu, J., Lee, B.-H., Dellinger, M., Cui, X., Zhang, C., Wu, S., Nothnagel, E.A. & Zhu, J.-K. (2010) A cellulose synthase-like protein is required for osmotic stress tolerance in Arabidopsis. *The Plant journal : for cell and molecular biology*. 63 (1), pp. 128–140.

Zwar, J.A. & Chandler, P.M. (1995) α-Amylase production and leaf protein synthesis in a gibberellin-responsive dwarf mutant of 'Himalaya'barley (Hordeum vulgare L.). *Planta*.

9 Appendices

Appendix 1 - BASTA Testing

DELLA (T2)

Line	Number of Seeds			Ratio of Healthy : Sick	Homozygous/Heterozygous	Construct
	Healthy	Sick	Non-Germinant			
6-4	68	30	2	2.27:1	Heterozygous	p35S:RGA$^{K/R}$-GFP
6-6	251	72	0	3.49:1	Heterozygous	p35S:RGA$^{K/R}$-GFP
7-2	174	61	14	2.85:1	Heterozygous	p35S:RGA^{K}-GFP
7-6	291	91	0	3.2:1	Heterozygous	p35S:RGA^{K}-GFP
7-7	335	6	4	55.83:1	?	p35S:RGA^{K}-GFP
8-1	272	11	2	24.73:1	?	p35S:GAI^{K}-GFP
8-2	253	75	1	3.37:1	Heterozygous	p35S:GAI^{K}-GFP
9-1	Contaminated				Not Homozygous	p35S:GAI$^{K/R}$-GFP
9-2	247	58	1	4.26:1	Heterozygous	p35S:GAI$^{K/R}$-GFP
9-3	294	86	10	3.42:1	Heterozygous	p35S:GAI$^{K/R}$-GFP
10-2	269	7	0	38.42:1	?	p35S:GFP
10-4	218	62	1	3.52:1	Heterozygous	p35S:GFP
Col0	0	All	12	N/A	N/A	N/A

DELLA (T3)

Line	Healthy	Sick	Non-germinants	Homozygous	Line Reference
6-4X	7	0	10	✓	None
6-6D	65	0	21	✓	None
6-6O	54	0	12	✓	p35S:RGA$^{K/R}$-GFP 1.0
7-2E	63	0	16	✓	None
7-2P	96	0	12	✓	p35S:RGA^{K}-GFP 1.0
8-2R	25	0	10	✓	p35S:GAI^{K}-GFP 1.0
9-2T	57	0	4	✓	p35S:GAI$^{K/R}$-GFP 1.0
9-3I	61	0	12	✓	p35S:GAI$^{K/R}$-GFP 2.0
10-4B	78	0	12	✓	p35S:GFP 1.0
Col0A	0	176	4	Not applicable	Not applicable

Line	Healthy	Sick	Non-germinants	Homozygous	Line Reference
7-6I	33	0	13	✓	None
7-6J	101	0	15	✓	p35S:RGA^{K}-GFP 2.0
Col0A	0	96	4	Not applicable	Not applicable

OTS (T3)

	Seedlings			
Line	**Healthy**	**Sick**	**Non-Germinants**	**Ratio**
pLCG35S:NTAP-OTS1 (B2.A)	83	0	1	Homozygous
pLCG35S:NTAP-OTS1 (B2.C)	86	0	4	Homozygous
pLCG35S:NTAP-OTS1 (B2.D)	107	0	4	Homozygous
pLCG35S NTAP-OTS1 (C5.A)	46	12	2	3.8:1
pLCG35S:NTAP-OTS1 (C5.B)	52	15	1	3.5:1
pLCG35SNTAP (A)	67	0	2	Homozygous
pLCG35SNTAP (B)	77	0	1	Homozygous
Col0A	0	99	1	Not applicable

Appendix 2: Parameters for non-linear Regression analysis